Comparative analysis of Sonic Hedgehog signalling and the response to Sonic Hedgehog signalling in vertebrate forelimbs and hindlimbs

Martin David Carkett

Division of Developmental Biology,
MRC Francis Crick Institute, Mill Hill Laboratories
Mill Hill, London

UCL

Submitted in 2015 for the degree of doctor of philosophy

Declaration

I, Martin David Carkett, confirm that the work presented in this thesis is my own and was performed in the laboratory of Dr. Malcolm Logan at the MRC National Institute for Medical Research, the Francis Crick Institute Mill Hill Laboratories and King's College London. Where information or reagents have been derived from other sources, I confirm that this has been indicated in the thesis. This work has been submitted for the degree of doctor of philosophy.

Acknowledgments

First and foremost I would like to thank Malcolm for giving me the opportunity to study this project and for giving me both the freedom and support to complete it as best I could. It has been a great experience and I have learnt a lot. I would like to thank fellow Logan lab members Sorrel, Satoko, Ania, Sue, Vero, Natalie and Laurianne for their input, advice and friendship without which this would have been far more difficult and far less fun. Noriaki, James B, James T and Tim have given me valuable advice throughout, for which I thank them too. I would like to mention Alex E, Clem, Jimena, Andy, Manu, Charlie, Alex W and Aina who have been great friends and have made the last four years a far richer experience beyond the lab. Lastly, as ever, my family have offered perspective, support and guidance throughout which has been invaluable.

Abstract

The Sonic Hedgehog (Shh) morphogen is required to establish anteroposterior (AP) pattern in vertebrate limbs. Limb progenitors exposed to increasing levels or durations of Shh signalling ultimately give rise to progressively more posterior structures. However, how Shh specifies different digit identities at a molecular level is poorly understood and molecular markers of individual digits are yet to be determined. Shh also patterns the dorsoventral axis of the vertebrate neural tube, where desensitisation to Shh signalling via Patched-mediated negative feedback – termed temporal adaptation - is required for correct interpretation of the Shh morphogen gradient. To investigate how limb progenitors respond to, and integrate, different levels and durations of Shh signalling at a molecular level I have developed an *ex vivo* assay and used RNA-sequencing to examine the immediate transcriptional responses of chick limb progenitors exposed to defined concentrations of Shh over fixed periods of time. I observe that limb progenitors initially respond equivalently to different concentrations of Shh but establish a graded response over time through a variation of a temporal adaptation mechanism in which both signal desensitisation and signal accumulation are required to generate distinct transcriptional outputs. I demonstrate that signal desensitisation is mediated, at least in part, by Patched-mediated negative feedback, but that additional cell-autonomous and noncell-autonomous feedback mechanisms operating through Sufu/Gli and Disp1 also exist. I further use *in silico* analyses to identify candidate markers of digit identities that are induced by different levels of Shh signalling. I show a subset of candidate markers are expressed in intermediate AP domains, consistent with predictions, and may mark or specify middle digit identities. Finally, I have investigated differences in Shh signalling dynamics and the response to Shh signalling in chick forelimbs and hindlimbs and provide evidence that hindlimbs are patterned by Shh over a shorter period of time.

Table of contents

List of Figures

List of Tables

List of Abbreviations

LPM	Lateral Plate Mesoderm
ZPA	Zone of polarising Activity
AER	Apical Ectodermal Ridge
AP	Antero-posterior
PD	Proximo-Distal
DV	Dorso-Ventral
Shh	Sonic Hedgehog
qPCR	Quantitative Polymerase Chain Reaction
OPT	Optical Projection Topography
BMP	Bone Morphogenic Protein
FGF	Fibroblast Growth Factors
RA	Retinoic Acid
GNR	Gene Regulatory Network
ChIP	Chromatin Immuno-Precipitation
GBS	Gli Binding Site
GFP	Green Fluorescent Protein
RFP	Red Fluorescent Protein
CMV	Cytomegalovirus

Chapter 1: Introduction

1.1 The embryological origin and formation of vertebrate limbs

The skeletal structure of the vertebrate limb

Tetrapods have two sets of serially homologous, paired appendages, forelimbs and hindlimbs. These are formed along three axes: the proximodistal (PD) axis – shoulder (proximal) to finger (distal), the dorsoventral (DV) axis – back of the hand (dorsal) to the palm of the hand (ventral), and the anteroposterior (AP) axis – thumb (anterior) to little finger (posterior) (Fig. 1).

Although great diversity in the morphologies of limbs has evolved among species, all vertebrate forelimbs and hindlimbs share the same basic elements of their skeletal structure. The skeletal structures of forelimbs and hindlimbs are divided into three anatomical sections: the stylopod, the zeugopod and the autopod (Fig. 1). The stylopod, the most proximal section, is comprised of a single bone, the humerus/femur (forelimb/hindlimb), the zeugopod of two bones, the radius/tibia and ulna/fibular, whilst the autopod includes the wrist/ankle elements, the carpals/tarsals and the metacarpals/metatarsals and phalanges, which comprise the remainder of the hand/footplate and the digits (Fig. 1).

Interestingly, despite being controlled by conserved genetic regulatory networks, the number of digits within respective limbs can vary both between species and within a species. Humans have five digits in both forelimbs and hindlimbs, numbered 1-5 from anterior to posterior, but the chicken –the model organism used in this body of work– has three digits in the forelimb and four digits in the hindlimb, which are numbered 1-3 and 1-4 respectively from anterior to posterior (Fig. 1) (Tamura et al., 2011; Towers et al., 2011).

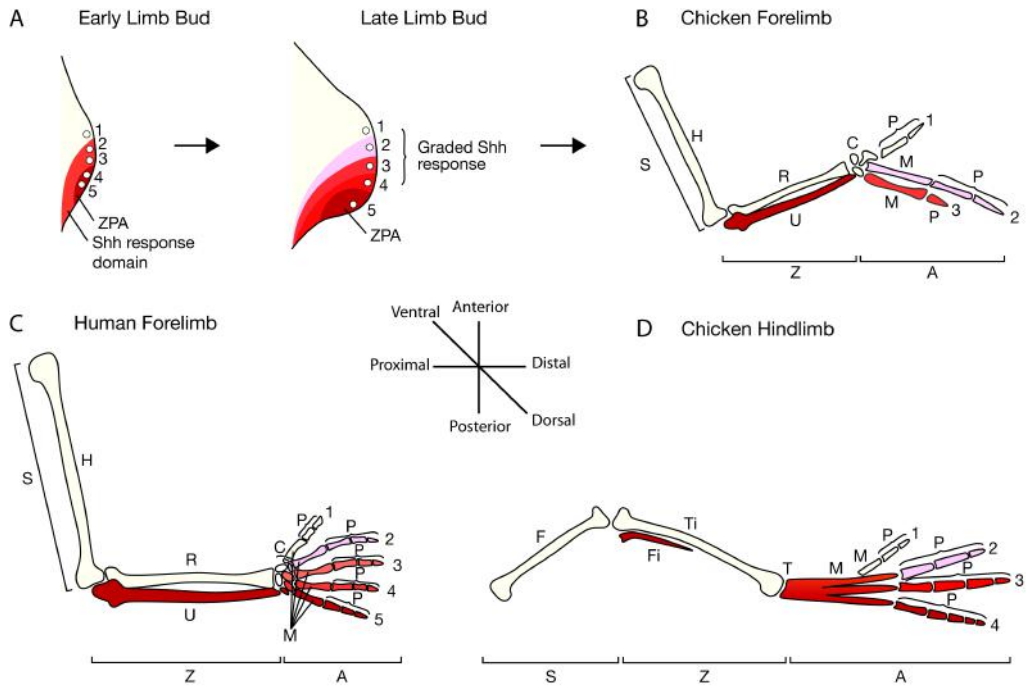

Figure 1| Overview of limb skeletal structures and the role of Shh in establishing anteroposterior polarity. The three axes of the limb: proximodistal (PD), dorsoventral (DV) and anteroposterior (AP). (A) Schematic diagram of graded Shh signalling across the AP axis of early and late forelimb buds. Cells comprising the Zone of Polarising Activity (ZPA) where the Sonic Hedgehog (Shh) morphogen is produced is shown in red. Different levels of Shh signalling experienced by cells are designated by colour, red (highest) to pink (lowest). Non-coloured sections represent areas not influenced by Shh signalling. Embryological positions (1-5) within the limb bud designate cells that will ultimately comprise digits of corresponding number in mature limbs (B-D). (B, D) Comparative schematic diagrams of the skeletal elements of the chicken forelimb and hindlimb. The bones of the forelimb (C): humerus (H), radius (R), ulna (U), carpals (C), metacarpals (M) and phalanges (P), and of the hindlimb (E): femur (F), tibia (T), fibular (F), tarsals (T), metatarsals (M) and phalanges (P) are labelled. The level of Shh signalling experienced by cells of the limb bud that comprise each digit is reflected by colour, red (highest) to non-coloured (no Shh signalling) corresponding to embryological positions in A. (C) Schematic diagram of a human forelimb showing the embryological origin of the digits as above. The digits of all limbs are numbered from 1, beginning with the anterior most. The three sections of the limb skeleton are shown, stylopod (S), zeugopod (Z) and autopod (A) (B-D).

Embryological origin of vertebrate limbs

The mature limb is a complex 3-dimensional structure comprised of multiple tissue types including: bone, connective tissue, tendons and ligaments, skeletal muscle, neuronal (axon extensions), vasculature, dermis and epidermis. These tissues predominantly originate from two distinct sources, the limb bud and the somites. Limb buds are initially comprised of mesodermal cells - originating from the Lateral Plate Mesoderm (LPM) - and over-lying ectodermal cells. Mesenchyme cells of the limb bud give rise to the skeletal structures, connective tissue fibroblasts, tendons, ligaments and dermis of the developed limb, whilst the surface ectoderm gives rise to the epidermis but also acts as an important signalling centre during development (Fernandez-Teran and Ros, 2008; Riddle et al., 1995). Skeletal muscle and some vasculature of the limb differentiate from mesodermal cells of the somites that migrate into the limb bud. In the chicken this occurs around Hamburger and Hamilton stage 20 of normal chicken development (Christ and Ordahl, 1995; Hamburger and Hamilton, 1951). Meanwhile, motor neuron axons innervate the limb bud at stage HH23-24 in the chicken (Lance-Jones and Landmesser, 1981).

Limb buds arise at fixed positions along the rostro-caudal axis of the body of the developing embryo (Duboc and Logan, 2011). In the chicken embryo, the forelimb bud first protrudes as a thickened ridge of the LPM at a level between somites 16-20, stage HH16 (Hamburger and Hamilton, 1951; Logan, 2003). The budding of the hindlimb bud is delayed relative to the forelimb bud, first emerging at the level of, and caudal to, somite 27, at stage HH17, approximately 3 hours later (Hamburger and Hamilton, 1951; Logan, 2003). In mammals, this heterochrony is more pronounced, with the mouse hindlimb bud emerging 12 hours later than the forelimb bud (Duboc and Logan, 2011).

Limb bud initiation

Limb bud initiation is dependent on establishing Fibroblast Growth Factor 10 (Fgf10) expression in the forelimb and hindlimb forming regions of the LPM. Fgf10 is both required and sufficient to initiate forelimb and hindlimb outgrowth. *Fgf10*$^{-/-}$ mice fail to form forelimb or hindlimb buds and show a complete absence of all limb skeletal elements except a rudimentary scapular and pelvis (Min et al., 1998; Sekine et al., 1999). Implantation of FGF soaked beads into the inter-limb region of the flank of pre-limb bud and early limb bud staged chicken embryos is sufficient to initiate growth of an ectopic limb (Cohn et al., 1995). Fgf10, secreted from mesenchymal cells of the LPM, signals to cells of the overlying ectoderm in the apical ectodermal ridge (AER) and induces *Fgf8* expression in the AER. In turn Fgf8, secreted back into the mesenchyme, positively regulates *Fgf10* expression in the LPM creating a positive feedback loop that is critical in driving limb outgrowth (Ohuchi et al., 1997; Xu et al., 1998).

Fgf10 activation is at least in part regulated by two paralogous T-Box transcription factors, Tbx5, which is expressed exclusively in the forelimb-forming region and Tbx4, which is expressed exclusively in the hindlimb-forming region (Gibson-Brown et al. 1996; Isaac et al. 1998; Lanctôt et al. 1999; Logan et al. 1998; Ohuchi et al. 1998). *Tbx5*$^{-/-}$ mice fail to form a forelimb bud and exhibit a complete absence of *Fgf10* expression (Agarwal et al., 2003; Rallis et al., 2003). *Tbx4*$^{-/-}$ mice however, are still able to form a hindlimb, though considerably reduced in size (Naiche and Papaioannou, 2003). In these mutants *Fgf10* expression is reduced but not entirely lost. Recent studies have demonstrated a paired-type homeodomain transcription factor, Pitx1, and a Lim-homeodomain transcription factor, Isl1, are also required for hindlimb outgrowth regulating both *Tbx4* and *Fgf10* directly (Logan & Tabin 1999; Kawakami et al. 2011; Duboc, Sulaiman and Logan Unpublished). Recently, it

has been demonstrated that *Tbx5* expression in the forelimb-forming region is controlled by a combinatorial *Hox* code (Nishimoto et al., 2014), but it is presently unclear what factors regulate *Tbx4, Pitx1* and *Isl1* expression in the hindlimb-forming region.

Finally, Retinoic Acid (RA) signalling from the flank has also been implicated in the initiation of both forelimbs and hindlimbs (Ang et al., 1996; Begemann et al., 2001; Grandel et al., 2002; Morriss-Kay and Sokolova, 1996; Murillo-Ferrol, 1965; Niederreither et al., 2002; Nishimoto et al., 2015; Stephens and McNulty, 1981; Sweeney and Watterson, 1969). Blocking RA signalling by placing a foil barrier between the somites and the LPM prevents forelimb and hindlimb initiation (Murillo-Ferrol, 1965; Stephens and McNulty, 1981; Sweeney and Watterson, 1969). This can be rescued by ectopic application of RA in the LPM, resulting in normal limbs (Nishimoto et al., 2015).

Organising centres within the limb

Once limb outgrowth has been initiated the growth and patterning of nascent limb buds is co-ordinated by three signalling centres: the Apical Ectodermal Ridge (AER), the dorsal/ventral ectoderm and the Zone of Polarising Activity (ZPA), contributing to the patterning of the PD, DV and AP axes respectively.

The AER is critical for maintaining limb outgrowth and, at least in part, responsible for patterning the PD axis by signalling to the underlying mesenchyme through Fgf4, Fgf8, Fgf9, Fgf17 and Wnts. Removal of the AER at successively earlier time points results in increasingly severe truncation of limbs which lack distal (and increasingly proximal) structures (Rowe and Fallon, 1982; Saunders, 1948; Summerbell, 1974). This led to the suggestion that the PD axis of the limb is specified in a proximodistal sequence by the AER as outgrowth occurs, and is

referred to as the progress zone model (Fernandez-Teran and Ros, 2008; Summerbell, 1974). A 2-signal model has also been proposed after demonstration that graded RA signalling from the flank is required for specifying the proximal limb (Cooper et al., 2011; Mercader et al., 2000; Rosello-Diez et al., 2011). Two recent papers have shown that cells exposed to both RA and Fgfs/Wnts remain in an undifferentiated state (Cooper et al., 2011; Rosello-Diez et al., 2011). As limb outgrowth occurs RA specifies the proximal limb but more distal cells become sufficiently distant from proximalising signals, allowing distalising signals from the AER to specify the intermediate and distal limb in a time dependent manner (Cooper et al., 2011; Rosello-Diez et al., 2011).

The dorsal limb is specified by the dorsal ectoderm, which signals to underlying mesoderm by secreting Wnt7a to induce expression of the LIM homeodomain transcription factor, *Lmx1* (Riddle *et al,* 1995). Ectopic expression of *Lmx1* in the ventral limb bud is sufficient to generate double-dorsal limbs (Riddle *et al,* 1995). *Engrailed-1,* expressed in the ventral ectoderm represses the expression of *Wnt7a* to prevent dorsalisation of the ventral limb (Chen and Johnson, 2002).

The antero-posterior axis of the limb is patterned by the polarising activity of the ZPA, which is mediated by the Sonic Hedgehog (Shh) morphogen – this activity is the major focus of this work. Shh is critical for establishing the number and identity of digits in the limb (Riddle et al., 1993). A thorough introduction of the role of Shh in patterning the AP axis of the limb is discussed (Introduction, 1.3).

Importantly, limb development is integrated by interactions between these signalling centres. A positive feedback loop exists between the AER and the ZPA. Shh signalling is required to maintain expression of FGFs in the AER, whilst *Fgf4* signals from the AER to ZPA cells to maintain *Shh* expression (Niswander *et al.*

1994). This feedback loop is also thought to include bone morphogenic protein (BMP) signalling. *Bmp2*, *Bmp4*, *Bmp7* and BMP antagonist *Gremlin1* (*Grem1)* are thought to be positively regulated by Shh. BMP signalling is required for AER maintenance and limb outgrowth, but at too high a level causes regression of the AER (Pizette and Niswander, 1999). Grem1, also regulated by Bmp2/4, is thought to limit Bmp4 signalling within the limb bud to an intermediate level that supports the AER and therefore indirectly the ZPA also (Bénazet et al., 2009; Zeller et al., 2009). Meanwhile, *Wnt7a* expression is also required for normal Shh expression and AP development. Mice lacking functional Wnt7a also lack posterior digits (Parr and McMahon, 1995).

1.2 The Sonic Hedgehog (Shh) signalling pathway

The Shh morphogen

Morphogens are defined as diffusible molecules that provide positional information to control the spatial arrangement of cellular differentiation (Gurdon and Bourillot, 2001; Wolpert, 1996). Morphogens were first described in concept by Turing, who proposed such molecules might act through a Turing Mechanism to provide positional information to cells (Turing, 1952). In contrast, Wolpert proposed that morphogens could act via a simple concentration gradient, whereby positional information is imparted by the concentration of morphogen that a cell is exposed to (Wolpert, 1969).

The Hedgehog (Hh) gene was first identified by genetic screens in *Drosophila Melanogaster* (Nüsslein-Volhard and Wieschaus, 1980). Sonic Hedgehog (Shh) is one of three mammalian orthologues of Hh, the others being Desert Hedgehog (Dhh) and Indian Hedgehog (Ihh) (Bitgood et al., 1996; Riddle et al., 1993;

Vortkamp et al., 1996). Ihh regulates the rate of chondrocyte differentiation in cartilage and bone development (Vortkamp et al., 1996), whilst Dhh is essential for germ cell development in the testis and peripheral nerve sheath formation (Bitgood et al., 1996). Shh is the broadest acting of the vertebrate Hh genes and mediates the polarising activity of the ZPA of the limb and patterns the DV axis of the developing neural tube (Briscoe and Thérond, 2013). It is further implicated in the growth and development of a number of other tissues and structures including: the kidneys, the fore-, mid- and hind-brain; the optic disc, stalk and retina of the eyes; the teeth and cranio-facial development (Dakubo et al., 2003; Dassule et al., 2000; Ho and Scott, 2002; Hu and Helms, 1999; Yu et al., 2002).

Shh synthesis and dispersion

Shh protein is synthesised as a 45kDa precursor, which is autoproteolyically cleaved, most probably within the endoplasmic reticulum (ER) (Chen et al., 2011a). This separates the amino- and carboxyl-terminals of the protein and further results in the covalent attachment of cholesterol to the N-terminal peptide at its new carboxyl-terminus (Mann and Beachy, 2004). The N-terminal peptide, which mediates all signalling activity, undergoes further post-translational modification by the attachment of an amide linked palmitic acid group to the most N-terminal Cys residue, by the acyltransferase, Skinny Hedgehog (Ski), to produce mature bi-lipidated Shh (Mann and Beachy, 2004). The C-terminal is rapidly degraded by the proteasome, but is required to recruit cholesterol to catalyse cleavage (Chen et al., 2011a; Mann and Beachy, 2004; Perler, 1998).

Bi-lipidated Shh is retained at the plasma membrane primarily through its cholesterol modification, though palmitic acid also promotes membrane association (Chen et al., 2004a; Rietveld et al., 1999). As a monomer, Shh is released

via the co-operative action of Dispatched (Disp1), a multipass transmembrane protein, and a vertebrate specific, secreted glycoprotein, Scube2 (Burke et al., 1999; Creanga et al., 2012; Johnson et al., 2012; Ma et al., 2002; Tian et al., 2005; Tukachinsky et al., 2012). Loss of *Disp1* results in the retention of cholesterol modified Hh at the plasma membrane (Burke et al., 1999), whilst loss of *Scube2* in conjunction with the loss of redundant family members *Scube1* and *Scube3*, results in a complete loss of Hh signalling (Johnson et al., 2012). Both Disp1 and Scube2 bind the cholesterol moiety at different parts of the molecule but only Scube2 stays bound as Shh is secreted. It is possible Disp1 transfers cholesterol-modified Shh to Scube2 at the plasma membrane in order to shield the cholesterol molecule from the aqueous extracellular environment, which thus permits the diffusion of Shh ligand (Briscoe and Thérond, 2013).

Shh can also be released in a diffusible multmeric form. Both lipid modifications and a highly conserved N-terminal region of Shh are required to form such multimers (Goetz et al., 2006). Multiple Hh molecules can be recruited into soluble lipoproteins and released at the membrane in *D. melanogaster*, although this has not been observed in vertebrates (Eugster et al., 2007; Panáková et al., 2005). It has been suggested that multiple Shh molecules may also be carried and diffused by exovesicles (Thérond, 2012). Most recently, it has been suggested filipodia-like cellular extensions, designated cytonemes, transport Shh to responding cells (Bischoff et al., 2013; Kornberg and Roy, 2014; Sanders et al., 2013). Punctae of Hh/Shh have been observed within or outside cytonemes in *D. melanogaster* and chicken limb bud cells, and graded target gene expression has been shown to correlate with both the maximum extension and the density of cytonemes in *D. melanogaster* (Bischoff et al., 2013; Sanders et al., 2013).

Shh signalling is mediated through Gli transcription factors

On reaching target cells, Shh binds to the multipass transmembrane receptor Ptch1, at the primary cilium, to initiate signal transduction (Rohatgi et al., 2007) (Fig. 2). The primary cilium itself is required for constitutive inactivation of Shh signalling and signal transduction in vertebrates (Goetz and Anderson, 2010). Binding of Shh to Ptch1 is facilitated by vertebrate co-receptors CAM-related/downregulated by oncogenes (Cdon), Brother of Cdon (Boc) and Growth Arrest Specific 1 (Gas1) (Allen et al., 2007; Allen et al., 2011; Tenzen et al., 2006). Cdon and Boc are single pass membrane proteins featuring Immunoglobulin and Fibronectin type one repeats whilst Gas1 is a GPI-linked protein (Allen et al., 2011; Izzi et al., 2011). All three bind Ptch1, to form multimolecular receptor complexes – though, it would appear in a separate and redundant fashion (Izzi et al., 2011). Only compound $Cdon^{-/-}/Boc^{-/-}/Gas1^{-/-}$ mutant mice demonstrate a complete lack of Shh signalling activity (Allen et al., 2011).

Ptch1 is a negative regulator of Shh signalling and active signalling is transduced by the activation of a transmembrane protein of the G-protein coupled receptor (GPCR) family, Smoothened (Smo) (van den Heuvel and Ingham, 1996a). In the absence of Shh, Ptch1 represses Smo through a mechanism that is unclear, although it appears to be non-stoichiometric (Ingham et al., 2000; Taipale et al., 2002). Ptch1 is structurally similar to resistance nodulation division (RND) transporter proteins and mutations in the RND domain of Ptch1 abolishes its ability to repress smoothened. This has led to the suggestion that Ptch1 may regulate Smo activity through the influx/efflux of a ligand (Taipale et al., 2002). Synthetic and naturally occurring small molecule agonists and antagonists of Smo have been identified, which bind to a membrane integrated domain within the protein (Mas and Ruiz i Altaba, 2010). Oxysterols including purmophamine and

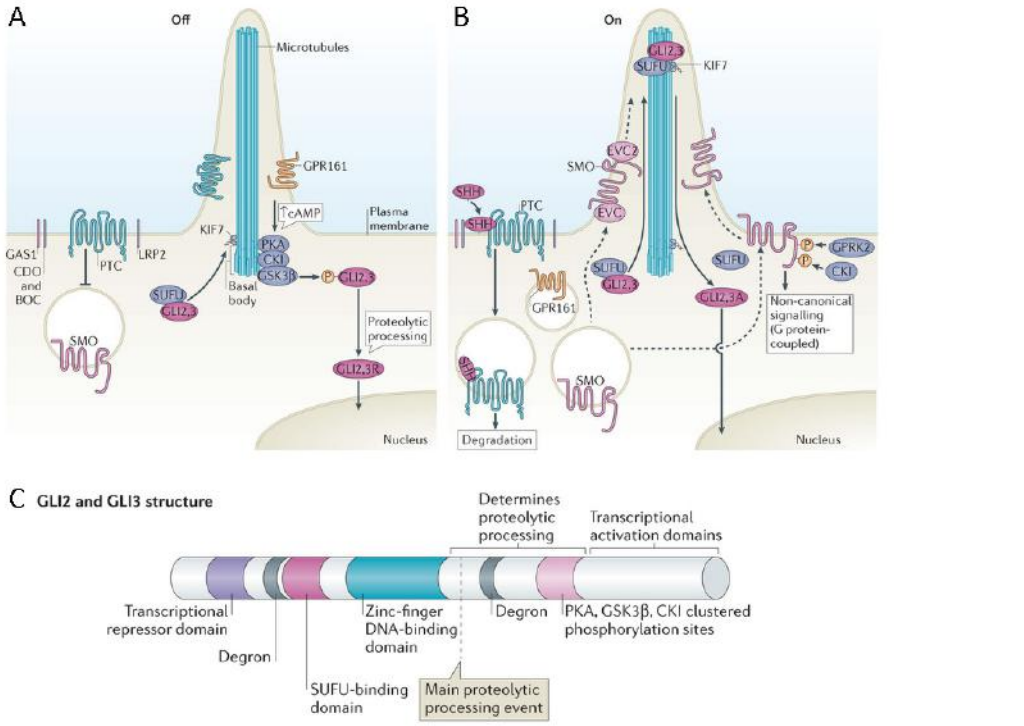

Figure 2 | Schematic of the Shh signalling pathway and structure of Gli proteins. (A) In the absence of Sonic hedgehog (Shh), Patched1 (Ptc/Ptch1) localises to the primary cilia and inhibits Smoothened (Smo). Suppressor of fused (Sufu) forms complexes with Gli2 and Gli3 in the cytoplasm. Sufu-Gli complexes shuttle through the primary cilium via Kinesin-like protein (Kif7) interactions. Gli2/3 proteins are sequentially phosphorylated by Protein kinase A (PKA), Glycogen synthase kinase 3 beta (Gsk3β) and Casein kinase I (Cki) which promotes their partial degradation by proteasomes at the base of the primary cilium into repressor forms $Gli2^R$ and $Gli3^R$ which then translocate to the nucleus to repress targets of Shh signalling. (B) Shh binds to Ptch1 and Ptch1 is internalised and degraded releasing Ptch1-mediated inhibition of Smo. Active Smo localises to the primary cilium and facilitates differential processing of Gli proteins. Sufu-Gli complexes concentrate in the primary cilium tip and Gli2/3 dissociate from Sufu and exit the primary cilium in full-length activator forms (GliA), bypassing proteasome partial degradation. $Gli2/3^A$ translocate to the nucleus to activate transcription of Shh targets. (C) Schematic of Gli2/3 structure. All Gli proteins (1-3) have a common zinc-finger DNA binding domain and a carboxyl end transcriptional activator domain. Gli2 and Gli3 have an additional amino end repressor domain that has been lost in Gli1. A Sufu binding site and phosphorylation sites are also conserved and are essential for processing full length Gli2/3 into repressor forms. Image adapted from Briscoe and Therond (Briscoe and Therond, 2013), permission obtained from Nature Publishing Group, License Number: 3693000798005.

smoothened agonist (SAG), bind directly to Smo and promote Shh signalling, whilst cyclopamine inhibits Shh signalling by binding directly to Smo (Chen et al., 2002; Corcoran and Scott, 2006; Dwyer et al., 2007; Nachtergaele et al., 2012). Ptch1 may regulate Smo by transporting such activating or inhibitory molecules, however this is yet to be demonstrated (Briscoe and Thérond, 2013).

Binding of Shh to Ptch1 causes it to become internalised and degraded, thus releasing Ptch1 mediated suppression of Smo. In the absence of Shh, Smo exists as a homodimer, in a closed conformation, localised to the cytoplasm in intracellular vesicles (Fig. 2A, B) (Wang et al., 2009). During active Shh signalling Smo is phosphorylated by Casein Kinase I Alpha (CKIα) and Gprc Kinase 2 (Gprk2) causing a conformational change to an open state (Chen et al., 2011b). This conformational change is required for Smo relocation and accumulation at the proximal plasma membrane of primary cilia and for signal transduction to occur (Chen et al., 2011b). Smo relocation is facilitated by β-arrestin and Kinesin like protein (Kif3a) (Chen et al., 2004b; Kovacs et al., 2008) (Fig. 2B).

Shh signalling is ultimately mediated through three transcriptional effectors in vertebrates, designated Glioma-associated Oncogene 1-3 (Gli1-3) (Bai et al., 2004; Hui and Angers, 2011; Kinzler and Vogelstein, 1990). Gli proteins are bi-functional and can act as activators or repressors of transcription, depending on their post-translational processing. All three Gli proteins have a similar zinc-finger DNA-binding domain and a C-terminal activator domain. Gli2 and Gli3 have an additional

N-terminal repressor domain, which has been lost in Gli1 (Fig. 2C) (Sasaki et al., 1999). Shh signalling alters the balance of intracellular levels of Gli activator and repressor forms by regulating their post-translational proteolytic processing (Pan and Wang, 2007). Gli2 acts as the principle activator of Shh signalling and Gli3 the

principle repressor. However, it is unclear whether this is due to differences in the strength of respective activator/repressor activities or whether Gli3 is more efficiently processed into a repressor form (Pan and Wang, 2007). Gli1 is dispensable for embryonic development, and appears to only serve as positive feedback to amplify Gli activator activity (Bai et al., 2002; Park et al., 2000).

In the absence of Shh, Gli2 and Gli3 are bound to cytoplasmic protein, Suppressor of Fused (Sufu), which acts as a negative regulator of Shh signalling (Dunaeva et al., 2003; Jia et al., 2009). Loss of Sufu reportedly results in constitutive activation of the Shh pathway, though a recent report has demonstrated that Sufu can also promote Shh signalling (Jia et al., 2009; Oh et al., 2015; Svärd et al., 2006). Although initially localised to the cytoplasm, Sufu-Gli complexes seem to transit through the primary cilium (Fig. 2A) (Humke et al., 2010; Kim et al., 2009; Tukachinsky et al., 2010; Wen et al., 2010). This flux, is dependent on Kinesin Like Protein, Kif7, and is essential for proteolytic processing of Gli2/3 into repressor forms (Kim et al., 2009; Liu et al., 2005). Kif7 thus acts as a negative regulator of the Hh pathway. Loss of Kif7 results in ectopic pathway activation (Cheung et al., 2009; Endoh-Yamagami et al., 2009; Liem et al., 2009; Putoux et al., 2011). Gli2/3 undergoes sequential phosphorylation at the basal body, by PKA, Glycogen Synthase Kinase 3 beta (Gsk3β) and Cki, at a conserved site (Fig. 2A) (Barzi et al., 2010; Fumoto et al., 2006; Sillibourne et al., 2002; Tuson et al., 2011). This results in ubiquitination by an E3 ubiquitin ligase complex containing β-TRCP, which targets Gli2/3 to proteasomes that are enriched at the base of the primary cilia, where the C-terminal activator domain is removed by partial degradation (Fig. 2A) (Jia et al., 2005). Due to the localisation of the PKA, Gsk3β, CKI and proteasomes at the basal body, it is thought that Gli proteins are processed as they exit the primary cilia

(Briscoe and Therond, 2013). The remaining Gli N-terminal repressor domain (GliR) translocates to the nucleus to repress the transcription of Shh targets.

Active Shh signalling increases the concentration of Sufu, Gli2, Gli3 and Kif7 in the primary cilium, particularly at the tip (Fig. 2B) (Chen et al., 2009; Kim et al., 2009; Maurya et al., 2013; Wen et al., 2010). Within the primary cilium, Sufu-Gli complexes dissociate and full length, activated Gli2 and Gli3 exit the primary cilium, bypassing proteolytic processing machinery and translocate to the nucleus to activate transcription of Shh targets (Fig. 2B) (Humke et al., 2010; Tukachinsky et al., 2010). Precisely how Sufu-Gli complexes are shuttled into the primary cilia and what occurs within the primary cilia to promote the release of full length Glis is not understood. However, Kif7 also appears to be implicated in this, and can thus also act as a positive regulator of Shh signalling (Maurya et al., 2013). Moreover, how this process is coupled to the activation and translocation of Smo to the primary cilia remains unclear (Briscoe and Thérond, 2013).

1.3 Sonic Hedgehog morphogen activity in vertebrate limbs

Classic embryological studies led to the discovery of the Antero-Posterior (AP) organising centre of the limb, the ZPA, located at the posterior margin of limb buds. Grafting mesenchyme cells from the posterior-distal margin of a wing bud to the anterior margin of a host wing bud induced mirror image duplication of digits (Fig. 2.1B) (Saunders and Gasseling, 1968; Tickle et al., 1975). A duplicate ulna can be induced in the anterior wing if ZPA cells are grafted sufficiently early, but not a second humerus, demonstrating the ZPA only controls asymmetry of the limb distal to the elbow (Saunders and Gasseling, 1968). Importantly, in these experiments ectopic wing elements in the host limb are formed from host cells, demonstrating

ZPA cells act as an instructive signal and do not form additional structures themselves.

Grafting ZPA cells to successive positions along the AP axis of a host limb bud also results in digit patterns consistent with a model in which the ZPA produces a diffusible morphogen, as digits are posteriorised by anterior and posterior to grafted ZPAs (Tickle et al., 1975).

RA was the first defined chemical that was able to mimic the polarising activity of the ZPA. RA-soaked beads implanted in the anterior margin of host wings induce digit duplications as observed in ZPA grafts (Tickle et al., 1982). However, subsequent experiments demonstrated the molecular basis of the ZPA's polarising activity is in fact the Shh morphogen (Riddle et al., 1993). *Shh* is expressed in the ZPA and ectopic application of Shh, by grafting *Shh* expressing cells or applying Shh-soaked beads to the anterior margin of wing buds is sufficient to induce full mirror image digit duplication (Riddle et al., 1993). Application of RA-soaked beads in the anterior margin of wing buds was shown to induce ectopic expression of *Shh* demonstrating the polarising activity of RA acts upstream of *Shh* (Riddle et al., 1993).

Consistent with the positional information model of morphogen patterning (Wolpert, 1969), Shh has been directly detected beyond the ZPA, throughout the posterior half of E10.5 mouse hindlimb buds and indirectly via *Ptch1* expression - a direct readout of Shh signalling - at an equivalent levels in chicken and mouse limb buds (Marigo et al., 1996a; Pearse et al., 2001). It has been proposed that an antero-posterior concentration gradient of Shh forms as Shh disperses across the limb bud which provides specific positional information to limb progenitors in a concentration dependent manner (Tickle, 1995). However, direct or indirect

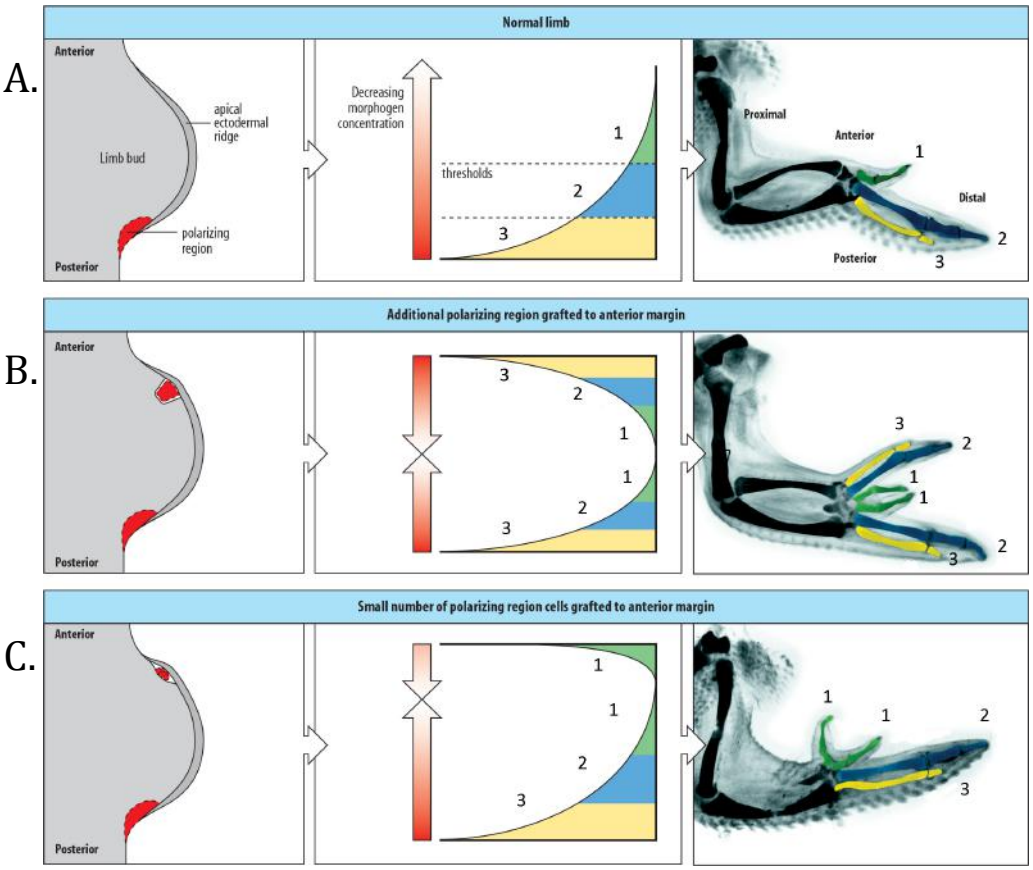

Figure 2.1 | The polarising activity of the posterior margin of the limb bud is concentration dependent. (A) Schematic of the Positional Information model in which a diffusible signal (morphogen) emanates from a group of mesenchymal cells at the posterior margin of the limb bud, designated the polarising region (Zone of Polarising Activity – ZPA) (Wolpert, 1969). Limb progenitors are assigned different antero-posterior fates (designated 1-3) by different concentrations of the diffusible signal they are exposed to. Progenitors increasingly close to the morphogen source are assigned increasingly posterior fates. (B) Classic embryological studies showed that grafting the posterior margin of a donor wing bud to the anterior margin of a host wing bud produces full mirror image digit duplication (3, 2, 1, 1, 2, 3), demonstrating the polarising activity of the ZPA (Saunders and Gasseling, 1968). (C) Grafting fewer polarising region cells however, produces fewer ectopic digits of less posterior fates, demonstrating the polarising activity of the ZPA is concentration dependent (1, 1, 2, 3) (Tickle, 1981). Image adapted from Wolpert, Tickle and Martinez-Arias (Wolpert, Tickle and Martinez-Arias, 2015), permission obtained from Oxford University Press.

measurement of Shh concentrations at different AP positions across the limb bud is yet to demonstrate this conclusively.

Shh is critical in establishing anteroposterior (AP) patterning and digit number in vertebrate forelimbs and hindlimbs (Riddle *et al*., 1993). *Shh*$^{-/-}$ mutant mice display a lack of anteroposterior patterning in skeletal structures distal to the elbow/knee joint and fail to form skeletal elements in the autopod, with the exception of a single digit 1 in mutant hindlimbs and a malformed digit 1 in forelimbs (Chiang et al., 1996). An equivalent phenotype is observed in naturally occurring *Oligozeugodactyly* (*Ozd)* chicken mutants, which do not express *Shh* in their limb buds (Ros et al., 2003). Meanwhile, *Talpid*^{3} mutant chicken and mice, which lack primary cilia and consequently display constitutive Shh pathway activation, exhibit severe polydactyly - a gain of digits (Bangs et al., 2011; Davey et al., 2006).

Shh acts to form a counter gradient of Gli3^{R} in the limb bud

Shh signalling is mediated by three bifunctional Gli transcriptions factors (Gli1-3) that are processed into repressor forms (Gli2-3^{R}) in the absence of Shh, but act as activators (Gli1-3^{A}) during active Shh signalling (Introduction, 1.2). However, Shh mediates its patterning activity in the limb primarily through regulation of Gli3. This has been demonstrated by generation of Gli1-3 mutants. *Gli1* null mice exhibit normally formed limbs (Park et al., 2000), whilst mice lacking functional Gli2 display slightly shortened, but normally patterned limbs (Mo et al., 1997). Compound *Gli1*$^{-/-}$; *Gli2*$^{-/-}$ mice show a similar limb phenotype to *Gli2*$^{-/-}$ limbs, though a small post-axial (additional posterior) nubbin is also observed in these mutants (Park et al., 2000).

In contrast, *Extra toes* mutants (*Xt/Xt),* which are *Gli3* null (hereafter *Gli3*$^{-/-}$), exhibit normal stylopods and zeugopods but show severe polydactyly in the autopod (Hui

and Joyner, 1993). *Gli3*$^{-/-}$ mutants reportedly exhibit a complete loss of wildtype digit identities, suggesting that Shh has no effect on skeletal patterning in the absence of Gli3 (Litingtung et al., 2002; te Welscher et al., 2002a). However, this interpretation has been challenged by the suggestion that posterior digits (3-5) can be identified in these mutants (Bowers et al., 2012). *Gli3*$^{-/-}$*; Shh*$^{-/-}$ mutants also exhibit polydactyly which more obviously lack wildtype digit identities. This reveals that additional digits in Gli3 mutants do not result from ectopic expression of *Shh,* as observed in *Alx-4*$^{-/-}$ mice, and that the autopod has an inherent polydactylous potential (Hui and Joyner, 1993; Litingtung et al., 2002; Qu et al., 1998; te Welscher et al., 2002a). This further demonstrates that *Gli3* and *Shh* are both dispensable for formation of the limb skeleton, but are required to impose a pentadactyl (5-digit) restraint on the polydactylous potential of the autopod and to specify digit identities (Litingtung et al., 2002; te Welscher et al., 2002a). Interestingly, *Gli3*$^{+/-}$; *Shh*$^{-/-}$ mice have 3-4 digits that are all identified as digit 1, demonstrating a correlation between levels of Gli3 and digit number, but also a requirement of Shh to pattern posterior digits. Therefore, regulation of digit number and specification of digit identities are separable processes that both depend on Gli3 (Litingtung et al., 2002).

It has been proposed that the role of Shh in specifying digit identities is to regulate the processing of Gli3 to form a counter gradient of Gli3^{R} across the AP axis (Litingtung et al., 2002; te Welscher et al., 2002a). Indeed, an anterior to posterior gradient of Gli3^{R} is detectable in wildtype limbs, but lost in Shh$^{-/-}$ limbs (Litingtung et al., 2002). However, *Gli1* and *Ptch1* are still expressed in a normal domain, though less strongly, in *Gli3* nulls, but are not detected in *Gli3*$^{-/-}$; *Shh*$^{-/-}$ mutants, suggesting a role for Gli2^{A} and to a lesser extent Gli3^{A} in regulating gene expression in the posterior of the limb bud. Two further studies have also implicated Gli2^{A} and

$Gli3^{A}$ in patterning posterior digits (Bowers et al., 2012; Wang et al., 2007). Digits in limbs lacking both Gli2 and Gli3 appear more malformed than those lacking Gli3 alone. This phenotype can be made less severe when a Gli^{A} is expressed under the influence of the Gli2 promoter (Bowers et al., 2012). However, it is difficult to judge whether the posterior digits of these mice are more patterned than the digits of *Gli2*$^{-/-}$;*Gli3*$^{-/-}$ or *Gli3*$^{-/-}$ mice. This highlights an inherent difficulty in interpreting cellular-level Shh signalling events by the effects on skeletal formation.

Shh signals in a dose and time dependant manner in vertebrate limbs

In contrast to a simple concentration gradient, the role of Shh in digit specification has been shown to be both concentration and time dependent. This was first shown in classic embryological studies, which demonstrated that the number of ZPA cells grafted to the anterior margin of a host wing, correlated to the identity of the resultant ectopic digit (Fig. 2.1C)(Tickle, 1981). As the number of ZPA cells (and therefore presumably the amount of secreted Shh) decreased, the ectopic digit they were capable of inducing became progressively more anterior (Fig. 2.1C) (Tickle, 1981). Similarly, the identity and number of additional digits produced by whole ZPA grafts is correlated to the amount of time a ZPA graft is left in place. Whole ZPA grafts left in place for 15 hours induce an additional digit 1, but induce an additional digit 2 after 17 hours and additional digits 1 and 2 after 24 hours (Smith, 1980).

Similar experiments using beads soaked in Shh protein directly demonstrated the effect of concentration and exposure time of Shh on digit identity. Beads soaked in increasingly higher concentrations of Shh are able to induce progressively more posterior digit(s) identities, when implanted into the anterior margins of wing buds (Yang et al., 1997). Meanwhile, removing beads soaked in a high

concentration of Shh after 16 hours induced an additional digit 1 only. Removal at progressively later time points up to 24 hours however resulted in additional digit(s) of increasingly posterior identity, revealing a temporal gradient to Shh digit specification (Yang et al., 1997).

Conversely, premature termination of Shh signalling by application of cyclopamine, a potent antagonist of Smoothened (Cooper et al., 1998; Incardona et al., 1998), in stage HH18 wing buds results in the loss of posterior digits, 2 and 3, with disruption to digit 1 reported in some cases (Scherz et al., 2007; Towers et al., 2011). Limbs administered with cyclopamine at developmentally later time points however, exhibit an increasingly less severe malformation and loss of structures in an anterior to posterior sequential fashion –digits 1 and 2 are formed normally in wing buds treated with cyclopamine at HH20, whilst limbs treated at HH22 develop digits 1-3 normally (Scherz et al., 2007; Towers et al., 2011). These data suggest digit identities in the chicken are specified in an anterior to posterior sequence and that progenitors are promoted to more posterior identities by either higher doses of Shh or by longer exposures to Shh signalling (Tickle, 1995). Shh also acts a mitogen in the chicken limb bud and is required for expansion of the AP axis which is critical for all digits of the chicken wing to form and has been proposed to be required for correct interpretation of the Shh morphogen gradient in the chicken limb. This has been termed the Growth/Morphogen model (Fig. 2.2C) (Towers et al., 2008).

The morphogenic activity of Shh in the mouse limb appears to be different to the chicken. Altering the levels of Shh signalling, but not the duration, only affects anterior digits in the mouse. Mice genetically engineered to produce lower than normal concentrations of Shh over a normal duration, reportedly lack digit 2 but maintain normal development of posterior digits (Scherz et al., 2007). Conversely,

mice engineered to produce normal levels of Shh but for a shorter than normal duration, reportedly lack digits 4 and 5 but develop normal anterior digits (Scherz et al., 2007). Meanwhile, mice defective in paracrine Shh signalling also reportedly lack a digit 2 (Harfe et al., 2004).

Fate mapping experiments have further revealed that the descendants of *Shh* expressing cells ultimately give rise to all cells in the posterior digits 4 and 5, and part of digit 3 in the mouse, suggesting that cells exposed to the highest levels of Shh signalling contribute to more than one digit identity and are therefore not specified by a simple concentration thresholds alone (Harfe et al., 2004). Interestingly, descendants of cells still expressing *Shh* at E10.5 only contribute to digits 4 and 5, whilst descendants of cells expressing *Shh* at E11.5 contribute only to digit 5 (Harfe et al., 2004). This suggests that cells exit the ZPA during patterning and that cells contribute to progressively more posterior digits the longer they remain in the ZPA – referred to as the Temporal Expansion model (Fig. 2.2A).

In the chicken, ZPA fate maps have revealed that ZPA cells and their descendants encompass all cells in the most posterior digit of the hindlimb and contribute to the soft tissues of the second most posterior digit. However, ZPA descendants of the forelimb only contribute to the soft tissues of the most posterior digit (Tamura et al., 2011; Towers et al., 2011). This has led to the proposal that the digits of the chicken hindlimb are equivalent to digits 1-4 in the mouse, but the digits of the chicken forelimb are equivalent to digits 1-3 in the mouse (Tamura et al., 2011; Towers et al., 2011).

Based on these data the Temporal Expansion model proposes that the anterior digits of the mouse (1-3) are specified by a morphogen gradient, dependent on Shh dispersion. Posterior digits (3-5) meanwhile are specified by a mechanism

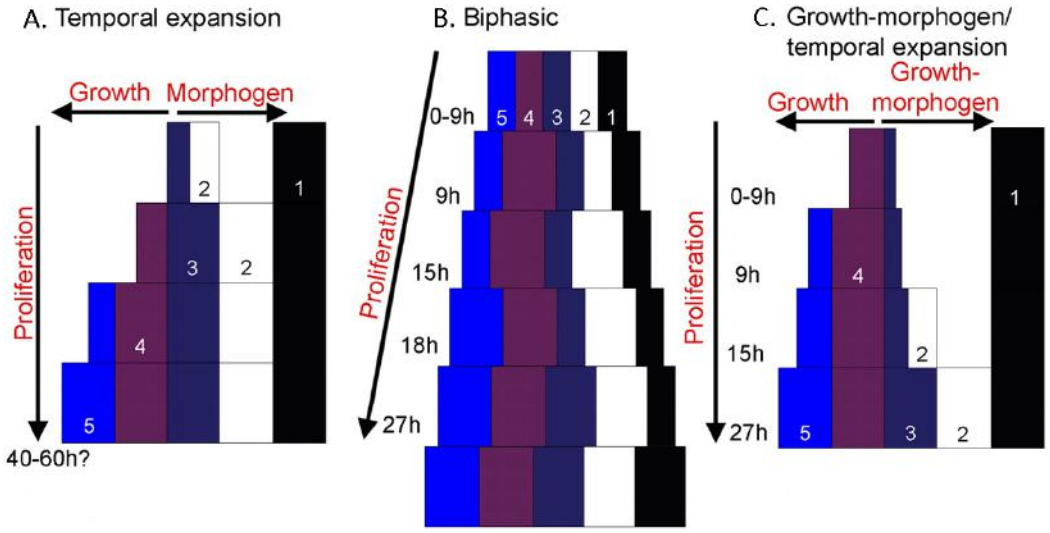

Figure 2.2 | Overview of different models of digit specification in vertebrate limbs by Shh signalling. A) The Temporal expansion model states that digit 1 arises independent of Shh signalling, digits 2-3 are specified on a Shh concentration gradient but digits 3-5 are specified by high concentrations of Shh and are differentiated by a temporal gradient (Harfe et al., 2004; Scherz et al., 2007). B) The Biphasic model states that Shh acts in two phases. It first specifies digit identities at an early stage and then acts in a mitogenic context to expand the digit forming field (Zhu et al. 2008). C) The Growth-morphogen model, similar to the temporal expansion model, but additionally states that the mitogenic activity of Shh is critical to expand the digit forming field and for consequently for correct digit patterning (Towers et al, 2008). The timing of digit specification is denoted in hours post the onset of Shh expression. Image adapted from Towers and Tickle (Towers and Tickle, 2009), permission obtained from the Company of Biologists, License Number: 3750270635424.

controlled by the length of cell exposure to autocrine Shh signalling (Harfe et al., 2004; Scherz et al., 2007). Thus, in specification of posterior digits, duration of Shh

signalling has been interpreted to be a more important parameter than a maximum threshold of Shh concentration. These data are consistent with a model in which digit identities are specified by cumulative levels of Gli activity, which are influenced by the level and duration of Shh signalling.

The Temporal Expansion model has been challenged however, by the Biphasic model, which primarily conflicts on the timing of digit specifications (Zhu and Mackem, 2011; Zhu et al., 2008). The Biphasic model proposes that Shh acts in two distinct phases: firstly, to specify digit identities at a very early stage, and then secondly as a growth promoting factor to drive proliferation and AP expansion (Fig. 2.2B) (Zhu and Mackem, 2011; Zhu et al., 2008). This is based on observations that seemingly conflict with a Temporal-Expansion model. Using a *Gli1* reporter, it was observed that posterior limb cells become less responsive to Shh signalling by E11.5 (Ahn and Joyner, 2004). This conflicts with a model in which continued Shh signalling is required to specify posterior digits.

Moreover, genetically removing Shh, using recombinases, at successively earlier stages reportedly resulted in digit losses in an unexpected order of: digit 3, digit 5, digit 2 and digit 4 (Zhu et al., 2008). This is also in conflict with previously reported loss of digits in antero-posterior order and, in particular, with observations that digits 4 and 5 are lost in mice with a shortened duration of Shh signalling (Scherz et al., 2007; Towers et al., 2008; Towers et al., 2011; Yang et al., 1997).

However, the morphologies of different mouse digits are similar and it can be difficult to interpret their identity, especially in mutants that have developed in abnormal contexts. This again illustrates the challenge of using the morphologies of

skeletal formations to deduce molecular and cellular interpretations of Shh signalling, particularly when they form many hours after the patterning event. It further highlights the need to uncover molecular markers of individual digit identities (if they exist) to aid the interpretation of patterning defects (Towers and Tickle, 2009).

An alternative model has proposed that digit patterning is not controlled by Shh but by a reaction-diffusion e-type mechanism. Indeed, Shh is not required for the formation of digits as demonstrated by the polydactylous limbs of *Gli3*$^{-/-}$*; Shh*$^{-/-}$ mice (Litingtung et al., 2002; te Welscher et al., 2002a). The reaction-diffusion mechanism model was originally proposed by Turing who demonstrated through mathematical modelling that periodic patterns of alternating stripes could be formed by the diffusion of interacting activators and inhibitors (Turing, 1952). Recent work combining experimental data with *in silico* modelling has led to a resurgence in this theory and Bmps, Sox9 and Wnts have recently been identified as putative molecules controlling a Turing network (Raspopovic et al., 2014; Sheth et al., 2012). In this model Bmps promote Sox9 but are self-inhibiting, whilst Sox9 inhibits both Bmps and Wnt and Wnt is inhibiting to itself and Sox9. In computer simulations this produces a pattern of alternating strips of Sox9 and Bmp/Wnt in a model limb, which ultimately gives rise to digital and inter-digital regions respectively that appear remarkably similar to actual digit patterns of the mouse (Raspopovic et al., 2014).

Experimentation has indirectly shown that Sox9 is observed out of phase with Bmps and Wnts but in phase with Bmp response, supporting this model. Moreover, perturbations to signalling in *in silico* models (such as termination of Bmp signalling) appears to accurately predict the digit patterns that are observed in limbs that are perturbed experimentally (Raspopovic et al., 2014). However, it is

yet to be directly demonstrated that Bmps/Wnt/Sox9 act as activators/repressors on one another or that Wnts are expressed in a periodic pattern as required by the model. Moreover, a critical requirement of reaction diffusion mechanisms is that activators and inhibitors must have different rates of diffusion, which has also yet to be determined. The role of a Turing-type mechanism in digit formation is an intriguing model, but cannot be conclusively defined without further supporting experimental data.

Whilst a Turing-type mechanism may control wavelengths of digital and inter-digital regions within developing limb buds, it unclear how such a model could specify different digit identities. It has recently been proposed that the seemingly conflicting positional information (Wolpert, 1969) and Turing mechanism models (Turing, 1952) could in fact be reconciled in a combined model where both mechanisms are required, and act co-operatively, to produce normally patterned limbs (Green and Sharpe, 2015). In this model it has been proposed that a Turing mechanism controls digital and inter-digital cell fates and a Shh morphogen gradient acts over this to specify digit identities in digit forming progenitors. Indeed, the digits of *Gli3*$^{-/-}$*; Shh*$^{-/-}$ mice lack all wildtype digit identities, demonstrating that the formation of digits and the patterning of digits are separable processes (Litingtung et al., 2002; te Welscher et al., 2002a). Moreover, *Gli3*$^{-/-}$mutants exhibit severe polydactyly similar to *Gli3*$^{-/-}$*; Shh*$^{-/-}$ mutants, but in contrast, display at least partially patterned posterior digits, highlighting the requirement of Shh to pattern posterior digits (Litingtung et al., 2002; te Welscher et al., 2002a).

Encoding digit identity

Whilst it has been demonstrated that altering either the level or duration of Shh signalling can ultimately specify different digit identities, it is still unclear how this is achieved at a transcriptional level. Moreover, though targets of Shh signalling have been identified in the limb, definitive molecular markers of individual digit identities remain elusive. Chromatin Immuno-precipitation (ChIP) and gene expression analysis experiments have begun to uncover downstream Gene Regulatory Networks (GRNs) of Shh signalling in limb progenitors (Bangs et al., 2010; McGlinn et al., 2005; Vokes et al., 2008).

A genome-wide analysis of Gli3 *Cis* regulatory sites in E11.5 mouse limb progenitors, genetically engineered to over-express $Gli3^{R}$, has been perhaps the most revealing of these studies (Vokes et al., 2008). Over 5000 high quality Gli binding sites and over 200 putative limb target genes were identified in this study. Of these, 23 posteriorly biased genes were closely associated with Gli Binding Regions (GBRs) including core Shh pathway components *Gli1*, *Ptch1* and *Ptch2.* The 5' *HoxA* and *HoxD* clusters, *Hand2*, *Sall1*, *Grem1*, *Bmp2,* and *Tbx2/3* were amongst a core subset of putative Shh targets in the posterior limb that have been directly implicated in normal limb development (Davenport et al., 2003; Fromental-Ramain et al., 1996; Khokha et al., 2003; McLeskey Kiefer et al., 2003; te Welscher et al., 2002b). *Dlk1* and the transcriptional repressor *Blimp1* were also named as prime posterior targets of Shh, though limb patterning is unperturbed in both *Dlk1* and *Blimp1* deficient embryos (Cheung et al., 2013; Vincent et al., 2005).

Anteriorly biased genes, *Pax1, Pax9, Alx-4, Dlx5, Irx3* and *Zic3* similarly associated with GBRs. *Dlx5* and *Alx-4* mutants also display limb abnormalities (Sowińska-Seidler et al., 2014; te Welscher et al., 2002a), whilst embryos lacking Gli3 do not

express *Alx-4* or *Pax9* in the anterior limb, demonstrating that binding of $Gli3^R$ can induce expression in certain contexts (te Welscher et al., 2002a). Several of the putative direct targets of Shh proposed in this study have recently been verified by whole mount *in situ* hybridisation analysis (Lewandowski et al., 2015).

This study categorised direct Shh targets in posterior, posterior-proximal, and middle AP territories, although functional analysis of these targets is yet to demonstrate whether they play a role in specifying digit identities.

Microarray analysis of the posterior and anterior thirds of wildtype and Talpid3 mutant chicken embryos also highlighted *HoxD13*, *Hand2, Sall1, Gi1*, *Ptch1* and *Bmp2* as downstream targets of Shh signalling (Bangs et al., 2010). Whilst, microarray analysis of $Gli3^{-/-}$ mutants in conjunction with whole mount *in situ* hybridisations demonstrated that Gli3 is required for *Pax9* to be expressed, and for the notch ligand receptor *Jagged1* (*Jag1)* to be repressed, in the anterior of mouse limbs (McGlinn et al., 2005). Interestingly, *Pax9* deficient mice exhibit an additional digit 1 in both forelimbs and hindlimbs (Peters et al., 1998). Homozygous mutations in *Jag1* are embryonic lethal, preventing diagnosis of potential limb defects, whilst heterozygotes appear normal (Xue et al., 1999).

Of the genes highlighted in these studies, *5'Hox* cluster and *Tbx2/3* have been proposed as transcription factors required to specify posterior digit identities. Successive loss of *HoxA13* and *HoxD13* alleles in mice results in progressively more severe autopod malformations (Fromental-Ramain et al., 1996). Loss of a single *HoxD13* allele results in a fusion of digits 2 and 3, whilst loss of a *HoxA13* and a *HoxD13* allele results in syndactyly in digits 2-4. $HoxA13^{+/-}$; $HoxD13^{-/-}$ and $HoxA13^{-/-}$; $HoxD13^{+/-}$ mice exhibit malformed and supernumerary digits that display distal

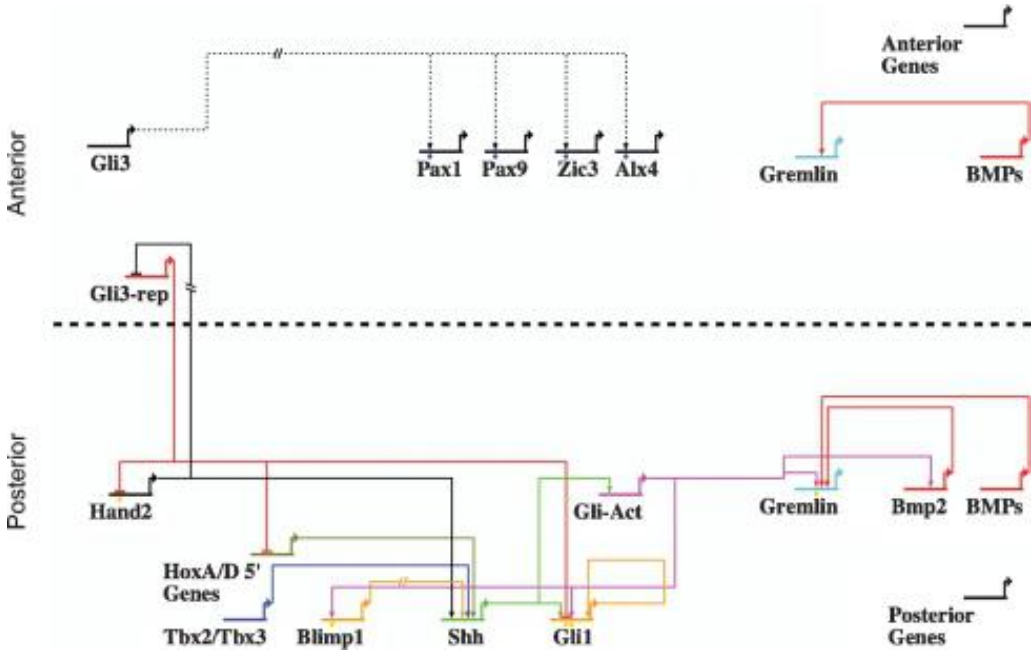

Figure 3 | Schematic of the proposed Gene Regulatory Network (GRN) downstream of Shh signalling in the limb. *Shh* expression is induced by *Hand2, Tbx2/3, 5'HoxA/D* and indirectly through the transcriptional repressor *Blimp1*. *Hand2* also represses $Gli3^R$ activity in the early posterior limb, whilst $Gli3^R$ antagonistically represses *Hand2* expression in the early anterior limb establishing an AP pre-pattern (Chiang et al., 2001). Shh signalling promotes processing of Gli^As and inhibits processing of $Gli3^Rs$. Gli^As positively regulate expression of *Gli1, Hand2, 5'Hox, Tbx2/3 and Blimp1* in a positive feed-forward loop, as well as *Grem1* and *Bmps* in the posterior and anterior limb bud. $Gli3^R$ negatively regulates *Hand2*, *Gli1* and *5'HoxA/D* and is indirectly required for *Pax1/9*, *Zic3* and *Alx-4* expression in the anterior limb bud. Image sourced from Vokes *et al.* (Vokes et al. 2008), permission obtained from Cold Spring Harbour Laboratory Press.

fusion. This phenotype appears more severe in *HoxA13*$^{+/-}$*; HoxD13*$^{-/-}$mutants (Fromental-Ramain et al., 1996). Mice completely lacking both *HoxA13* and *HoxD13* exhibit a complete loss of all autopod skeletal elements in both limbs (Fromental-Ramain et al., 1996). These data demonstrate *Hox13* is required for skeletal formation of the autopod and for constraining digit number. Conversely, ectopically expressing *HoxD11-13,* in the anterior of the early limb results in mirror image digit duplications comparable to those seen in ectopic Shh application (Zákány et al., 2004), leading to the suggestion that different levels of *HoxD11-13* levels across the antero-posterior axis specify different digit identities (Zakany and Duboule, 2007).

Tbx3$^{-/-}$ mice display skeletal abnormalities in the ulna and posterior digits of the forelimb and strikingly lack all skeletal elements of the hindlimb autopod except digit 1 (Davenport et al., 2003). Misexpression of *Tbx2/3* however, can reportedly transform digits 2 and 3 of the chicken hindlimb into more posterior fates leading to the suggestion that *Tbx3* and a combination of *Tbx2/3* specify chicken digits 3 and 4 respectively (Suzuki et al., 2004). However, both *Tbx2* and *Tbx3* are also expressed in anterior domains, which is conflicting with this model. Interestingly, recent studies have demonstrated that Tbx3 acts directly as a regulator of alternative RNA splicing, as well as a transcriptional repressor (Frank et al., 2013; Kumar et al., 2014).

Meanwhile, it has been proposed that *Zic3* and *Lhx9* expression may demarcate digit 1 of chicken forelimbs and hindlimbs (Carkett and Logan, 2011; Wang et al., 2011). Digit 1 progenitors of stage HH28 chicken limbs showed an enrichment of *Zic3* and *Lhx9* compared to progenitors of other digits via RNAseq analysis. Whilst these genes may mark particular digits, they are not necessarily direct targets of Shh signalling in specifying digit identities, as Shh is no longer expressed in stage HH28 limb buds.

It has also been suggested that BMP signalling from interdigital mesenchyme may play a role in defining identities of adjacent digits (Dahn and Fallon, 2000). Removal, of interdigit regions or application of beads soaked in BMP antagonist, Noggin, causes the loss of phalanxes in the adjacent digit, consistent with a more anterior identity, in chicken hindlimbs (Dahn and Fallon, 2000). In this model different levels of BMP signalling within each interdigit region (1-3), as measured by Smad activity, are thought to specify digit identities, with more posterior interdigit regions experiencing higher levels of Smad activity (Suzuki et al., 2008). However, genetic removal of BMPs expressed in limb development, singularly or in combination - *Bmp2*$^{c/c}$, *Bmp4*$^{c/c}$, *Bmp7*$^{-/-}$, *Bmp2*$^{c/c}$*; Bmp7*$^{-/-}$ or *Bmp2*$^{c/c}$*; Bmp4*$^{c/c}$ – produces limbs with no AP patterning defects although posterior digits are missing in *Bmp2*$^{c/c}$, *Bmp4*$^{c/c}$ mutants (Bandyopadhyay et al., 2006). It was also noted that a minimum amount of BMP signalling is required for the maintenance of chondrogenesis and some cartilaginous elements are missing from limbs lacking Bmp2 and Bmp4 (Bandyopadhyay et al., 2006).

1.4 Intra-cellular dynamics of Shh signalling: Insights from the neural tube

Shh interpretation by a temporal adaptation mechanism

A molecular understanding of the responses to Shh signalling has been well characterised in the vertebrate neural tube. Shh acts in a graded fashion to pattern the dorso-ventral axis of the neural tube via graded Gli activity (Ribes and Briscoe, 2009). This is a dynamic process in which different levels and durations of Shh signalling induce the expression of specific transcription factors to specify tightly controlled progenitor domains, which in turn give rise to distinct neuronal cell subtypes (Briscoe et al., 1999; Briscoe et al., 2000; Dessaud et al., 2007; Dessaud et al., 2010).

It has been demonstrated that negative feedback is critical for neural tube progenitors to correctly interpret graded Shh signalling, in a mechanism termed, Temporal Adaptation (Dessaud et al. 2007; Dessaud et al. 2010). Neural tube explants dosed with a range of exogenous Shh concentrations initially exhibit a similar level of response, measured by Gli activity, irrespective of the concentration of Shh they are dosed with. However, Gli activity decreases in explants over time, in an apparent desensitisation to Shh signalling (Dessaud et al., 2007). Interestingly, explants exposed to increasingly higher concentrations of Shh, begin to display desensitisation at an increasingly later time (Fig. 3A). Thus, cells exposed to higher concentrations of Shh experience longer durations of Gli activity. This converts extracellular concentrations of Shh into intra-cellular durations of Gli activity, integrating both the level (concentration) and duration of Shh signalling into a single output. This reconciles previous models of morphogen activity that have emphasised either concentration or time dependent mechanisms (Ribes and Briscoe, 2009).

Duration of Gli activity is critical in activating expression of *Olig2* and *Nkx2.2,* which are sequentially expressed and identify increasingly ventral fates (Briscoe *et al.*, 1999; Briscoe *et al.*, 2000, Dessaud *et al.*, 2007). Interestingly, assignment of positional identity in the neural tube is a dynamic process, whereby cells can revert to more dorsal fates upon premature termination of Shh signalling, demonstrating that cumulative Gli activity rather than maximal threshold levels are required to specify and maintain cell fates (Dessaud *et al.*, 2010). Thus, neural tube progenitors appear to be promoted to increasingly ventral fates by increasing levels of cumulative duration of Gli activity over time. Importantly, duration of Gli activity is limited in cells exposed to lower concentrations of Shh by an earlier onset of desensitisation.

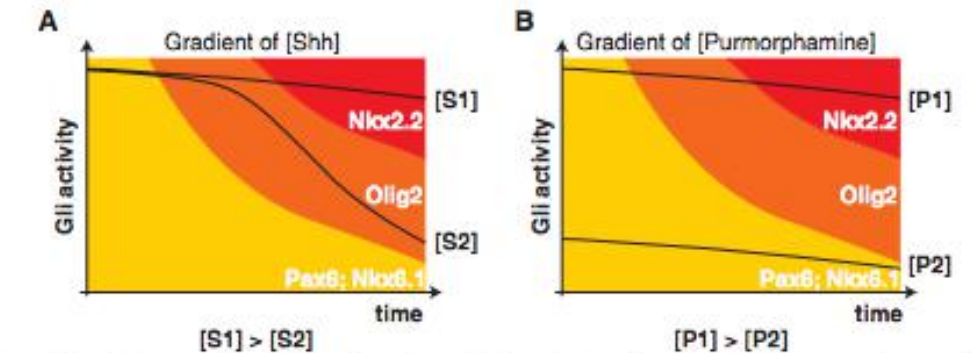

Figure 4| Schematic of the Temporal adaptation model. (A) Signal output of neural tube explants dosed with high concentrations of Shh ([S1]) and lower concentrations of Shh ([S2]), as measured by Gli activity over time. Initially, explants dosed with different concentrations of Shh exhibit a similar level of Gli activity. However, over time, explants become desensitised to Shh signalling at a rate that is inversely proportional to the concentration of Shh they are exposed to. Thus, cells exposed to lower concentrations of Shh experience a shorter duration of Gli activity. This temporal adaption mechanism is required for a graded response to Shh signalling and ultimately results in sequential expression of more ventral transcription factors designating more ventral progenitor pools (Dessaud et al., 2007). (B) In contrast, neural tube explants dosed with different concentrations of Smoothed (Smo) agonist purmorphamine ([P1], [P2]) display a similar, and more moderate, level of desensitisation irrespective of purmorphamine concentration. This suggests that desensitisation observed in explants dosed with Shh, is primarily controlled by events upstream of Smo activation, but that other forms of feedback inhibition may operate downstream of Smo activation. Image sourced from Ribes and Briscoe (Ribes and Briscoe, 2009), permission obtained from Cold Spring Harbour Laboratory Press.

Ligand dependent antagonism

Desensitisation to Shh is a result of negative feedback that inhibits Gli activity. Inhibition of Gli activity is at least in part mediated through upregulation of Shh receptors and a simultaneous downregulation of Shh co-receptors. The Shh receptors, Ptch1 and Ptch2, and Shh binding antagonist Hhip operate in a semi-redundant manner to limit the extent and level of Shh signalling (Coulombe et al., 2004; Goodrich et al., 1997; Holtz et al., 2013; Jeong and McMahon, 2005; Ochi et al., 2006; Taipale et al., 2002). Ptch1 and Ptch2, present at basal levels within the primary cilium, act to inhibit Smo activation in the absence of Shh ligand – known as Ligand Independent Antagonism (LIA) (Holtz et al., 2013; Ingham et al., 2000; Jeong and McMahon, 2005). Whilst Hhip is capable of limiting Shh signalling by sequestering Shh ligand, but has no influence on Smo (Coulombe et al., 2004; Ochi et al., 2006). Genetic removal of *Ptch1* results in almost complete ventralisation of the neural tube. However, mice genetically engineered to express low levels of *Ptch1* under a metallothionein promoter (*mtPtch1; Ptch1*$^{-/-}$) show a less severe ventralisation (Jeong and McMahon, 2005). Progressive removal of *Ptch1*, *Ptch2* and *Hhip* alleles on a *mtPtch1* background results in successively more ventralised neural tubes demonstrating their collective role in negatively regulating Shh signalling (Holtz et al., 2013; Jeong and McMahon, 2005).

Upon pathway activation, *Ptch1*, *Ptch2* and *Hhip* are upregulated resulting in high levels of receptors in cells close to the source of Shh. This causes both noncell-autonomous and cell-autonomous feedback inhibition. In *D. melanogaster*, high levels of Ptc close to a Shh source has been shown to sequester Shh and limit the spread of ligand to cells more distal to the source (Chen and Struhl, 1996). Conversely, expression of Shh targets in the dorsal neural tube and an expansion of more ventral domains upon downregulation or removal of Ptch1, Ptch2 and/or

Hhip, suggest Shh is able to spread further than normal in this context (Jeong and McMahon, 2005). In *Smo*$^{-/-}$ mutants, Shh ligand can be directly detected at twice its normal distance from the neural tube floorplate (where Shh is produced), demonstrating the importance of response to Shh signalling in limiting the spread of Shh ligand (Chamberlain et al., 2008). Thus, the upregulation of receptors has a noncell-autonomous affect by limiting Shh spread, shaping the spatial gradient of Shh ligand.

Conversely, ectopic expression of *Ptch1* or *Hhip* in the chicken neural tube inhibits specification of ventral neural fates in a cell-autonomous manner (Briscoe et al., 2001; Stamataki et al., 2005). It is unclear whether this results from increased repression of Smo or through increased competition of 'non-productive' receptors that can sequester Shh ligand but do not interact with Smo to transduce Shh signalling (Holtz et al., 2013; Jeong and McMahon, 2005). Autonomous and noncell-autonomous feedback inhibition resulting from active Shh signalling has been collectively termed Ligand Dependent Antagonism (LDA) (Holtz et al., 2013; Jeong and McMahon, 2005).

Shh co-receptors Gas1, Cdon and Boc, positively regulate Shh signalling and are collectively required for normal neural tube patterning (Allen et al., 2007; Allen et al., 2011; Martinelli and Fan, 2007; Tenzen et al., 2006). Misexpression of *Gas1*, *Cdon* or *Boc* in the dorsal neural tube promotes ectopic, Shh dependent, expression of ventrally associated transcription factors in a cell-autonomous manner (Allen et al., 2007; Allen et al., 2011; Tenzen et al., 2006). Genetic removal of any one co-receptor has only a mild effect on neural tube patterning, but removal of any two causes phenotypes reminiscent of a decrease in Shh signalling (Allen et al., 2007; Allen et al., 2011; Ribes and Briscoe, 2009). Strikingly, *Gas1*$^{-/-}$; *Cdon*$^{-/-}$; *Boc*$^{-/-}$ compound mutant mice exhibit a complete loss of Shh dependent neural tube

progenitors, and display a phenotype similar to $Smo^{-/-}$ mutants (Allen et al., 2011). All three co-receptors have been shown to be downregulated by Shh, which, it has been proposed, also contributes to LDA and desensitisation to Shh signalling (Allen et al., 2011; Tenzen et al., 2006).

It has been directly demonstrated that Ptch1-mediated LDA contributes to Shh desensitisation that is required for correct gradient interpretation by the temporal adaption mechanism. Inhibiting *Ptch1* upregulation using RNAi in neural tube explants promotes expression of more ventrally associated transcription factors when exposed to low doses of Shh (Dessaud et al., 2007). Meanwhile, explants dosed with a Smo agonist, purmorphamine, fail to show a graded desensitisation to increasing levels of Smo activation, demonstrating that feedback inhibition affecting levels of Gli activity operates upstream of Smo activation (Fig. 3B) (Dessaud et al., 2007). However, the roles of Ptch2, Hhip and co-receptor mediated LDA in correct gradient interpretation has yet to demonstrated directly.

Nonetheless, collectively these data suggest a model in which LDA acting upstream of Smo activation is required to limit Shh signalling and impose a temporal adaption mechanism. This in turn is required for correct interpretation of the Shh morphogen gradient. However, it is currently unclear why cells exposed to lower concentrations of Shh should experience desensitisation soonest. Also, negative feedback downstream of Smo activation has also been reported, suggesting that temporal adaption may be influenced by other negative feedback mechanisms in addition to LDA (Cohen et al., 2015; Dessaud et al., 2007). Shh signalling can lead to downregulation of Gli2 protein in neural tube progenitors whilst *Gli3* is transcriptionally downregulated by Shh signalling in limb buds (Cohen et al., 2015; te Welscher et al., 2002a).

Intra-cellular dynamics of Shh signalling in limb progenitors is yet to be investigated. However, it has been demonstrated that increasingly posterior fates can be induced by increasing either levels or durations of Shh signalling (Harfe et al., 2004; Scherz et al., 2007; Towers et al., 2011; Yang et al., 1997). This is consistent with a model in which concentration and duration of Shh signalling is integrated into cumulative Gli activity, which designates positional information in limb progenitors. A role of negative feedback in influencing the duration of Gli activity and therefore gradient interpretation in the limb is also yet to be determined.

1.5 Differences in Shh signalling in vertebrate forelimbs and hindlimbs

Although forelimb and hindlimb buds both develop from equivalent mesodermal tissues under the control of conserved signalling centres, they go on to form distinct morphological outputs (Duboc and Logan, 2011). The development of forelimb and hindlimb-type morphologies is thus a useful paradigm to study how diversity of form can be generated through modulation of conserved gene regulatory networks (Duboc and Logan, 2011).

In the chicken, differences between the forelimbs and hindlimbs are particularly pronounced, with the most obvious differences observed in the skeletal structures that are patterned by Shh. The forelimb is comprised of 3 digits (1-3) whereas the hindlimb is comprised of 4 digits (1-4). The digits of the hindlimb are generally composed of more phalanges than those of the forelimb (2-2-1; 2-3-4-5) (Fig. 1) and the metatarsals are also longer than the metacarpals making the hindlimb autopod larger overall (Fig. 1B, D). Differences also exist in the zeugopod, with the

hindlimb again being considerably larger. The zeugopod of the forelimb is formed of a radius and an ulna of approximately equal size, whilst the hindlimb is comprised of a large tibia but a very small fibular (Fig. 1). These differences suggest there may be differences in the levels or durations of Shh signalling in the respective limbs or intrinsic differences in the response of forelimb and hindlimb cells to equivalent Shh signalling. Despite this, it is generally assumed that Shh acts equivalently in forelimb and hindlimb buds and potential differences in Shh signalling dynamics of the respective limb buds have yet to be investigated.

Interestingly, several studies have highlighted differences in the populations of cells that appear to be responding to Shh and the effects of altering Shh signalling in forelimbs and hindlimbs. *Oligozeugodactylyl* chicken mutants, in which *Shh* expression is absent in the limb, lack all forelimb digits but retain a single digit 1 in the hindlimb, suggesting digit 1 of the hindlimb, but not of the forelimb, forms independently of Shh signalling (Ros et al., 2003). *Shh*$^{-/-}$ mice display an equivalent phenotype (Chiang et al., 2001). Recently, comparative fate maps of stage HH20 chicken forelimb and hindlimb buds demonstrated that cells that give rise to digit 1 of the hindlimb originate from a more anterior position than cells that give rise to digit 1 of the forelimb (Nomura et al., 2014; Vargesson et al., 1997a). This further suggests that cells that give rise to digit 1 in the hindlimb, but not the forelimb, may be too distant from the ZPA to be influenced by Shh signalling.

Fate maps of ZPA cells in chicken forelimbs and hindlimbs have meanwhile demonstrated differences in the populations that comprise the posterior digits. Descendants of the hindlimb ZPA encompass all cells of the most posterior digit of the hindlimb (digit 4) and contribute to the soft tissues of digit 3. Conversely, descendants of the forelimb ZPA only contribute to the soft tissues of the most posterior digit (Tamura et al., 2011; Towers et al., 2011). This has led to the

proposal that the digits of the chicken forelimb are equivalent to digits 1-3 in the hindlimb and demonstrates an intrinsic difference in the propensity of respective ZPAs to form a digit. Whilst these data don't necessarily suggest differences in Shh signalling or response to Shh signalling between forelimb and hindlimb cells, they demonstrate differences in the populations of cells that give rise to the digits of respective limbs.

The time required for Shh to complete patterning of respective limbs also appears to be different. Reducing the duration of endogenous Shh signalling in chicken limb buds using Smo antagonist, cyclopamine, has a more potent effect on forelimbs. Forelimb buds exhibit a greater loss of digits and more severe malformations of digits, than hindlimb buds dosed with cyclopamine over an equivalent period. Moreover, hindlimbs display normal patterning at an earlier time than forelimbs in these experiments suggesting that hindlimbs are patterned by Shh over a shorter period (Scherz et al., 2007; Towers et al., 2011).

Finally, phenotypic differences exist between the forelimbs and hindlimbs of mutants that display lack $Gli3^{R}$. *Shh*$^{-/-}$*; Gli3*$^{-/-}$, *Gli3*$^{-/-}$ and *Talpid*^{3} mutants display severe polydactyly and have up to 9 unpatterned (in *Shh*$^{-/-}$*; Gli3*$^{-/-}$*)* digits in the forelimb whilst hindlimbs only exhibit an additional digit, though patterning is equally affected (Litingtung et al., 2002). This suggests that the forelimb bud has an inherent potential to form more digits than the hindlimb in the absence of Shh.

Collectively, these data suggest that differences may exist in the levels of Shh signalling experienced by cells that comprise the digits of the respective limbs. Differences in Shh signalling in forelimbs and hindlimbs may result from differences in Shh exposure: spatially, quantitatively or temporally; or from

differential responses to equivalent Shh signalling. At present it is unclear whether the nascent forelimb and hindlimb are subject to equal levels of Shh signalling.

1.6 Summary of aims

The aim of this work is to build on previous studies to define a better understanding of how Shh patterns vertebrate limbs at a molecular level. Although downstream GRNs have begun to be unravelled in the limb, the immediate molecular responses to Shh signalling and how this directs morphogenesis of the limb is yet to be fully understood. Moreover, attempts thus far have been unable to differentiate between genes that are optimally induced by different levels or durations of Shh signalling and molecular markers of individual digit identities remain elusive. How cells integrate different levels and durations of Shh signalling and whether a temporal adaptation mechanism is required for correct interpretation of the Shh morphogen gradient as observed in the neural tube has not been investigated in the limb. Finally, Shh is assumed to act equivalently in forelimbs and hindlimbs, despite considerable morphological differences in structures that are patterned by Shh in some species. Thus, differences in Shh signalling or in responses to Shh signalling may exist between respective limbs.

To address these overriding biological questions, my aims were:

1. To develop an assay to examine the immediate transcriptional responses of chicken forelimb and hindlimb cells to different levels and durations of Shh signalling, using RNAseq.
2. To attempt to define candidate markers of individual digit identities
3. To examine the role of negative feedback, at different levels, in correct morphogen gradient interpretation in limbs.

4. To investigate potential differences in Shh signalling dynamics between chicken forelimbs and hindlimbs, and potential differences in the response of forelimb and hindlimb progenitors to equivalent Shh signalling.

Chapter 2: Materials and Methods

2.1 Chick limb bud measurements

The length of the proximodistal (PD) axis of stage HH18, HH19, HH20, HH21, HH22, HH24 and HH26 chick forelimb and hindlimb buds, were measured from images captured using a Leica MZ7S microscope at a magnification of x3.2 and a Leica DFC 320 camera, at the widest point, using ImageJ64 software (Rasband, 2008). The anteroposterior (AP) axis was measured, as above, at the mid-point of the proximodistal axis of the Shh expressing domain of limb buds. The PD-AP area of limb buds were measured using ImageJ64 software (Rasband, 2008) on images of limb buds captured using a Leica MZ7S microscope at a magnification of x3.2 and a Leica DFC 320 camera. Mean lengths and areas ±SEM were determined from biological replicates (n=3) using Graphpad Prism software.

2.2 Quantifying limb bud cell numbers

Whole forelimb and hindlimb buds from stage HH17, HH18, HH19, HH21, HH22, and HH24 chicks were dissected in L-15 media (Gibco) and dissociated in 0.5% Trypsin-EDTA solution (Gibco) for 5 minutes at 37^{o}C. Trypsinisation was terminated via a 10-fold dilution of Trypsin-EDTA solution in Dulbecco's Modified Eagle's Medium/Nutrient F-12 Ham (1:1) media (hereafter DMEM:F-12) (Gibco) containing 10% Fetal Calf Serum (FCS) (Gibco). Dissociated cells were pelleted via centrifugation in a Eppendorf 5702R centrifuge at 3000rpm for 5 minutes and were resuspended in 1ml DMEM:F-12 (Gibco). 10µl of resuspended cells was pipetted onto a hemocytometer and covered with a glass cover slip. Cell counts from two hemocytometer grids, for each biological sample, were counted using a Radiance 2100 (BioRad) microscope and multiplied by 10^4 to estimate concentration of cell suspension, cells/ml and total cell number. Total cell numbers were used to estimate the number of cells per limb bud. Resuspended cells were further diluted if the concentration of resuspended cells was greater than an optimum

concentration of between 1-3 million cells per millilitre (approximately 50-150 cell per grid). Further dilutions were taken into account in subsequent calculations of cell number estimates. Mean cell number/limb bud estimates ±SEM was determined from biological replicates (n=3 biological replicates of 3 limbs each) using Graphpad Prism software.

2.3 Whole mount *in situ* hybridisations

In situ template plasmids for: chicken *Shh*, *Gli1* and *Ptch2* previously described (Marigo et al., 1996a; Marigo et al., 1996b); for: chick *Hst3st2*, *Mab21l1*, *Cntfr*, *Smoc1*, *Hapln1*, *Hmgn5*, *Lhx6*, *Tsku* and *Has2* (Image cDNA clones, Source Bioscience) and for: chick *Foxc2*, *FoxF1*, and *Foxo6* generated as described below, were used as templates to generate RNA *in situ* hybridisation probes for respective transcripts. Templates were linearised using appropriate restriction enzymes (New England Bioscience) according to the manufacturer's instructions, in a final volume of 20µl for 1 hour. Linearised DNA plasmids were extracted by adding 180µl of 10mM Tris pH7.5 and 200µl of phenol:chloroform (Sigma Aldrich) and vortexing vigorously before centrifugation at 14,000 rpm in a Thermo Scientific Heraeus Fresco 17 centrifuge for 3 minutes at 4°C to separate the aqueous phase. The aqueous phase (200µl) was extracted by pipette and DNA was precipitated by adding 20µl 3M Na-acetate, 600µl 100% ethanol (EtOH) and 1µl glycogen, as carrier, and incubating at -20°C for 30 minutes. DNA was pelleted by centrifugation as before but for 10 minutes and was washed in 500µl of 70% EtOH before being re-pelleted, as before but for 3 minutes. Purified DNA was resuspended in 10µl of 10mM Tris pH7.5.

Digoxigenin (DIG) labelled RNA probes were transcribed *in vitro* from linearised template plasmids using T7 or T3 Polymerase (New England Bioscience) and DIG RNA labelling mix (Roche) according to manufacturer's instrcutions, in a final volume of 20µl

for 2 hours. Successful transcription was visualised by running 1µl of transcription reaction mix on a 1% agrose gel. RNA probes were precipitated by adding 80µl 10mM Tris pH7.5, 10µl 4M LiCl, 300µl 100% EtOH and 1µl glycogen to transcription reaction mixes and incubating at -20°C for 30 minutes. RNA was pelleted by centrifugation at 14,000 rpm in a Thermo Scientific Heraeus Fresco 17 centrifuge for 10 minutes and was washed in 500µl of 70% EtOH before being re-pelleted as before for 3 minutes. RNA pellets were air-dried and resuspended in 50µl of Tris pH7.5 and 50µl of hybridisation buffer. 50µl of resuspended RNA probe was diluted 150-fold in hybridisation buffer to a working concentration for *in situ* hybridisation. All probes were stored at -20°C.

Whole mount *in situ* hybridisations were carried out as previously described (Riddle et al., 1993). Images of RNA expression patterns were photographed using a Leica MZ7S microscope and a Leica DFC 320 camera using Leica Firecam software.

2.4 Quantifying endogenous expression levels of *Shh, Ptch1* and *Gli1* in chick forelimbs and hindlimb buds

The posterior third of chick forelimb and hindlimb buds of stage HH17, HH18, HH19, HH20, HH21, HH22 and HH24 chicks were dissected in L-15 media (Gibco) before immediate purification of total RNA using an RNeasy mini-kit (Qiagen). Endogenous, relative expression levels of *Shh, Ptch1,* and *Gli1* were determined by quantitative PCR as described below using primers and qPCR programs stated (Table 1, 2). Mean relative expression ±SEM was determined from biological replicates (n=2 biological replicates of 3 explants each) using Graphpad Prism software.

2.5 Quantifying Shh expression and Shh response domains in chick limb buds

In situ hybridisation patterns of *Shh* and *Ptch2* in forelimb and hindlimb buds were captured using a Leica MZ7S microscope at a magnification of x3.2 and a Leica DFC 320 camera. Total AP-PD areas of limb buds were measured using ImageJ64 software as above. To measure the expression domains (AP-PD areas) of *Shh* and *Ptch2,* images were converted to 8-bit grey-scale and an individual threshold for each image was set to ensure the full extent of the expression domain was measured above threshold. A boundary was drawn around the posterior third of the limb and the number of pixels above threshold within this boundary was measured to give an estimation of expression domain size. Mean estimated areas ±SEM were determined from biological replicates (n=3) using Graphpad Prism software. Normalised *Shh* and *Ptch2* domain sizes were calculated as a percentage of total limb bud AP-PD area.

2.6 Dissociated cell culture

Fertilised chicken eggs (Needle's Farms, Winter's Farms) were incubated at 37°C and staged according to Hamburger and Hamilton (HH) staging of normal chick development (Hamburger and Hamilton, 1951). The anterior two thirds of stage HH18 chick forelimbs and hindlimbs were dissected in L-15 media (Gibco). Forelimb and hindlimb explants were pooled separately and dissociated in 0.5% Trypsin-EDTA solution (Gibco) for 5 minutes at 37°C. Trypsinisation was terminated via a 10-fold dilution of Trypsin-EDTA solution in DMEM:F-12 (Gibco) containing 10% FCS (Gibco). Dissociated cells were pelleted via centrifugation in a Eppendorf 5702R centrifuge at 3000rpm for 5 minutes and were resuspended in serum free conditions in DMEM:F-12 (Gibco) supplemented with 150ng/ml Fgf4, Mito Serum (BD) and Glutamax (Invitrogen). Dissociated cells were seeded onto Fibronectin coated wells in 96-well plates (Nunco) at

a concentration of $1.3x10^5$ cells/well. Fibronectin coating was achieved by applying 200µl of 20mg/ml Fibronectin solution from Bovine plasma (Sigma) directly to the bottom of wells for 5 minutes, at room temperature, before being aspirated. Cells were cultured in DMEM:F-12 (Gibco) supplemented with 50U/ml Penicillin, 50µg /ml Streptomycin, 150ng/ml Fgf4, Mito Serum (BD) and Glutamax (Invitrogen) for 3, 6, 15 or 20 hours in the presence of 0, 1, 2, 4 or 8nM recombinant mouse Sonic Hedgehog (Shh)-N protein (Hereon Shh-N). Shh-N protein was a kind gift from Dr. James Briscoe (The Francis Crick Institute).

2.7 Explant *ex vivo* culture

The anterior two thirds of forelimbs and hindlimbs were harvested from stage HH18 chicken embryos as previously described. Limb explants were cultured *ex vivo* following an adaptation of previous protocols (Dessaud et al., 2007; Dessaud et al., 2010), with thanks to Dr. Noriaki Sasai and Dr. James Briscoe (The Francis Crick Institute) for input into protocol adaptation. Limb explants (3 per biological sample) were embedded, intact, in 25µl of Bovine Collagen type I (Sigma-Aldrich) containing DMEM (Gibco) and 7.5µmol Na_2CO_3 (Sigma-Aldrich) in 48-well plates (Nunco). Collagen solutions containing limb explants were incubated at 37°C for 45 minutes to allow them to set and were subsequently immersed and cultured in DMEM:F-12 media supplemented with 50U/ml Penicillin, 50µg/ml Streptomycin, 150ng/ml Fgf4, Mito Serum (BD) and Glutamax (Invitrogen). Explants were cultured *ex vivo* for 6, 12, 16 or 20 hours in the presence of 0, 1, 2, 4, 8 or 16nM Shh-N. All explant data represent biological triplicates.

In separate experiments, limb explants were harvested and cultured as previously described for 6, 12 or 16 hours in the presence of 0, 0.2, 0.4, 1.5, 3 or 6µM purmorphamine (Sigma) dissolved in 100% dimethyl sulfoxide (DMSO) (Sigma).

Explants under all purmorphamine conditions were cultured at a final concentration of 3.2% DMSO. All purmophamine dosage data represent biological triplicates.

2.8 Quantitative PCR

Total RNA was purified from explants and dissociated cells immediately after culture, using an RNeasy mini-kit (Qiagen) according to the manufacturer's instructions. Total RNA was eluted in 50µl of RNAse-free water and was stored at -80°C. RNA concentrations and quality were determined using a NanoDrop 2000 (Thermo Scientific). cDNA was generated from 100ng of total RNA per sample using 150ng of random hexamers (Invitrogen) and Superscript III reverse transcriptase (Invitrogen) according to the manufacturer's instructions.

Quantitative PCRs (qPCRs) were carried out using Power SYBR Green reagents (Applied bioscience) according to manufacturers instructions on a 7900 HT-fast machine (Applied biosystems) or a ViiA™ 7 Real-Time PCR System, using standard run length at a final volume of 20µl/well in 96-well plates (MicroAmp) or 10µl/well in 384-well plates (MicroAmp). Standard curves were generated for each qPCR using a 4-step, 1:5 dilution series from cDNA isolated from whole stage HH20 chick embryos. Primers and PCR programs used are summarised in Table 1 and Table 2 respectively. All qPCRs were carried out in technical triplicate.

Levels of transcripts were determined using the relative standard curve analysis (Applied biosystems) and were normalised to levels of *Gapdh* transcripts using Microsoft Excel. Mean of relative expression ±SEM was determined from biological replicates only (n=2-3 biological samples of 3 explants per biological sample or 1 well of dissociated cells per biological sample) using Graphpad Prism software. Statistical analysis of qPCR data was performed using Graphpad Prism software.

2.9 RNA-sequencing

Total RNA from limb explants were purified and stored as above. cDNA libraries were prepared using TruSeq RNA Sample Prep Kit V2 (Illumina) according to the manufacturers low throughput protocol, from 500ng of total RNA per biological sample. The quality of libraries was determined by Qubit (Life Technologies) and Bioanalyser (Agilent) and sequenced on a HiSeq2500 sequencing machine (Illumina), at a 75bp read length, single end only. Alignment free quantification of previously annotated RNA isoforms (Galgal4 chicken transcriptome, UCSC), from raw sequence reads was performed using the Sailfish computational method (Patro et al., 2014) with the kind help of Dr. James Briscoe (The Francis Crick Institute, Mill Hill Laboratories). Read counts were normalised using total read count (TC) method (Anders and Huber, 2010; Dillies et al., 2013; Soneson and Delorenzi, 2013).

2.10 Generation of gene lists

Downstream analysis of raw read counts was performed using Microsoft Excel and R programming language and statistical package (R Development Core Team, 2011). The value 1 was added to all read counts to prevent anomalies resulting from numbers <1 in downstream analyses. Genes with a sum normalised read count across all conditions of <24 (the sum of *Shh* read counts, which is not expressed in the anterior two thirds of limb buds) were considered 'not expressed' and were eliminated from further analysis. Differentially expressed (DE) genes between explants dosed with 2, 4 or 8nM Shh compared to control explants (0nM) at 6, 12 or 16 hours were determined by one way ANOVA and Tukey's Post-hoc test using Microsoft Excel software. Genes with a P-value ≤ 0.05 were subsetted and listed in order of those exhibiting the greatest difference between explants dosed with 2, 4 or 8nM Shh and control explants at 6, 12 or 16 hours.

	Gene	Sequence	
qPCR Primers	*c.Gapdh*	Fwd	5' - tctctggcaaagtccaagtg - 3'
		Rev	5' - tgcccattgatcacaagttt - 3'
	c.Shh	Fwd	5' - ccccaaattacaaccctgac - 3'
		Rev	5' - cattcagcttgtccttgcag - 3'
	c.Gli1	Fwd	5' - tgcgccaaggagtttgac - 3'
		Rev	5' - tggatgtgctcgttgttgat - 3'
	c.Ptch1	Fwd	5' - tttttctttttcctgggcttactt - 3'
		Rev	5' - catctctacccgggtagttc - 3'
	c.Tbx5	Fwd	5' - cctggaagacatcagctgtaaca - 3'
		Rev	5' - atggcagacactgtgcaac - 3'
	c.Alx4	Fwd	5' - ccctgcaggtctcctgttac - 3'
		Rev	5' - ctttcactccagcctccttc - 3'
Cloning Primers	*c.Foxc2*	Fwd	5' - gcgggatcccttctaccgcgagaacaagc - 3'
		Rev	5' - gcgactagtggtcatgatgttctccacgc - 3'
	c.Foxf1	Fwd	5' - gcgggatccgcatgatgaacggccactta - 3'
		Rev	5' - gcgactagtataacgcacggcttgatgtc - 3'
	c.Foxo6	Fwd	5' - gcgggatccaagttcctgcgcatcaaagg - 3'
		Rev	5' - gcgactagtgagatggaggagagcaggtc - 3'
	c.Mlb	Fwd	5' - ggcggatccttggtcaatcaacagcgtgg - 3'
		Rev	5' - ggcactagtggcaactacggcatcttctg - 3'

Table 1| Primers used in qPCR and cloning. Cloning primers were used to isolate chick *Foxc2, Foxf1, Foxo6* and *Mlb1* from the cDNA of stage HH20 whole chick embryos. BamHI (green) and SpeI (blue) restriction sites and additional nucleotides (red) were added to forward and reverse primers to facilitate downstream cloning and restriction enzyme binding respectively.

Gene clusters based on transcriptional profiles were generated using R programming language and statistical environment (R Development Core Team, 2011). As before, genes with a sum read count across all conditions <24 were eliminated. Remaining genes were subsetted on the similarity of their transcriptional profiles (expression levels at all time points and concentrations of Shh dosage) to either: *Ptch1, Hoxd11, Smoc1, Foxc2, Grem1* or *Alx-4;* or according to the time or concentration at which a peak response was exhibited namely: No Shh, 6 hours and 2nM, 12 hours and 4nM or 16 hours and 8nM. Lists were ordered according to the greatest difference between the peak response and the minimum response.

Specifically, 'profiles' subsetted genes that complied with the following criteria: "ptch1_like_fl" coded for A) induction by Shh at all concentrations and times, B) graded response at 16hr, C) for there to be accumulation at 8nM and 4nM between 6hr and 16hr,D) For there to be a characteristic dip in 2nM between 12hr and 16hr, E) for partial gradation (8nM greater than 4nM or 2nM) by 12 hours and F) Ordered by greatest induction by 8nM at 16hr. "hoxd_like_fl" coded for A) induction by Shh at all concentrations and times, B) specifies 8nM is highest at 16 hours and C) ordered by greatest induction by 8nM at 16 hours.

"foxc2_like_fl" and "foxc2_like_hl" coded for A) induction by Shh at all concentrations and times, B) a graded response at 12 hours and 16 hours and C) 12 hours (2nM, 4nM and 8nM) are higher response than at 16 hours (2nM, 4nM and 8nM), D) ordered by greatest induction by 8nM at 12 hours."smoc1_like_fl" and "smoc1_like_hl" coded for codes for A) induction by Shh at all concentrations and times, B) 4nM shows the peak response at 12 hours and 16 hours C) ordered by greatest induction by 4nM at 16 hours.

"twonm_like_fl" coded for A) induction by Shh at all concentrations and times, B) 2nM highest at 12 hours and 16 hours C) ordered on greatest induction by 2nM at 16

hours."sixhour_like_fl" and "sixhour_like_hl" coded for for A) induction by Shh at all concentrations and times B) a graded response at 12 hours and 16 hours and C) 6 hours (2nM, 4nM and 8nM) are higher response than at 16 hours (2nM, 4nM and 8nM), D) ordered by greatest induction by 8nM at 6 hours. "twonm_like_hl" and "twonm_like_hl" coded for A) induction by Shh at all concentrations and times, B) 2nM highest at 12 hours and 16 hours C) ordered by greatest induction by 2nM at 16 hours."grem1_like_fl' and 'grem1_like_hl" coded for for A) 2nM highest at all time points B) ordered by greatest induction by 2nM at 12 hours. "alx4_like_fl" and "alx4_like_hl" coded for A) 0nM highest at 12 hours and 16 hours, B) that 2nM is second highest at 12 hours C) a reverse graded response at 16 hours D) ordered by greatest repression by 8nM at 16 hours.

"ptch1_like_hl" coded for A) induction by Shh at all concentrations and times, B) graded response at 16hr, C) for there to be accumulation at all concetrations between 6hr and 12 hrs D) for desensitisation between 12hr to 16hr in 2,4 and 8nM E) for partial gradation (8nM greater than 4nM or 2nM) by 12 hours and F) ordered on greatest induction by 8nM at 16 hours. "hoxd_like_hl" coded for A) induction by Shh at all concentrations and times. B) for a graded response at 16h C) for desensitisation in 2nM between 12 hours and 16 hours D) accumulation from 6 hours to 16 hours in 2nM and 4nM E) 8nM is highest at 12 hours F) ordered on greatest induction by 8nM at 16 hours.

2.11 Chick *in ovo* electroporation

Stage HH14 chick embryos were injected *in ovo* with 100mg/ml of RNA duplexes, targeting chick *Ptch1* mRNA and chick *Ptch2* mRNA, 1.25µg of pCMV-DsRed-Express vector (Clonetech) and 0.5µl of Fast Green FCF dye (Sigma), at a final volume of 4µl, targeting a cavity within the forelimb forming region. RNA duplexes were ordered in 2' deprotected, annealed and desalted form (Option A4, Dharmacon). The RNA duplexes in this study are: *cPtch1* as previously described (Dessaud et al., 2007) and *cPtch2* siRN

	Step	Temp (°C)	Time (Min:Sec)
qPCR	1	95	02:00
	2	95	00:30
	3	60	01:00
	4	72	01:00
	5	Go to Step 2	
	6	Cycle x30	
	7	72	10:00
c.Foxc2	1	95	02:00
	2	95	00:30
	3	59	00:30
	4	72	01:00
	5	Go to Step 2	
	6	Cycle x29	
	7	72	02:00
c.Foxf1	1	95	02:00
	2	95	00:30
	3	57	00:30
	4	72	01:00
	5	Go to Step 2	
	6	Cycle x29	
	7	72	02:00
c.Foxo6	1	95	02:00
	2	95	00:30
	3	60.5	00:30
	4	72	01:10
	5	Go to Step 2	
	6	Cycle x29	
	7	72	02:00

Table 2| PCR programs for qPCR and gene isolation.

sense 5'-UCAAGGAGCUGCUGGAUAAUU-3'. Embryos were immediately electroporated after injection, *in ovo,* using an Intracell TSS20 electroporator at 25V, with 3 pulses at a width of 50ms separated by gaps of 200ms. Eggs were resealed using clear tape (5 Star Office) to prevent infection and drying-out and were incubated again at 37°C. Successfully targeted limb buds were identified using an Olympus MVX10 microscope and an X-Cite series 120 fluorescent light source. The anterior two-thirds of successfully targeted forelimbs were harvested at stage HH18 (approximately 24 hours after electroporation) and were cultured in the presence of 0, 2 or 8nM Shh for 16 hours, as above. A Plasmid DNA MaxiPrep Kit (Qiagen) was used according to the manufacturer's instructions to obtain sufficient quantities and concentrations of plasmids for electroporation.

In the case of Smoc1 misexpression experiments, stage HH14 chick embryos were injected *in ovo* as stated above but with 7.5µg pCMV-(Mouse)Smoc1-Sport6 vector (Source Bioscience) in place of RNA duplexes. Embryos were immediately electroporated, *in ovo,* and re-incubated as above but embryos that had been successfully targeted were incubated until stage HH36 of development where possible.

2.12 Cloning of chick genes

Partial cDNA sequences of chick *Foxc2* and *Foxo6* were isolated via PCR using the primers and PCR programs summarised (Tables, 1-2). cDNA generated from stage HH20 whole chick embryos, was used as a template in all PCR reactions. All primers were designed to target cDNA sequences using Primer 3 program (Koressaar and Remm, 2007; Untergasser et al., 2012) and had BamH1 and Spe1 restriction sites added to the 5' ends of forward and reverse primers respectively, with an additional spacer sequence of GCG or GGC 5' of restriction sites. Individual

PCR protocols for each gene were designed using Optimase ProtocolWriter™ (Transgenomic) (Table 2).

PCR products were purified using QIAquick PCR Purification Kit (Qiagen) according to the manufacturer's instructions. Purified PCR products and pBlueScript II pSK (+) vector (Agilent) was digested using BamH1 and Spe1 restriction enzymes (New England Bioscience) according to the manufacturer's instructions. Digestion products were gel isolated by electrophoresis and extracted using QIAquick Gel Extraction Kit (Qiagen) according to the manufacturer's instructions. Digested PCR products were ligated into pBlueScript II pSK (+) vector overnight at 4°C using T4 DNA Ligase (New England Bioscience) at a 3:1 molar ends ratio (insert:vector) and a final volume of 10µl, according to the manufacturer's instructions. 5µl of ligation mix was added to 30µl of α-Select Gold Competent Cells (Bioline) and incubated on ice for 10 minutes. Cells were heated shocked at 42°C for 45 seconds before immediate to ice, to induce uptake of ligated plasmid. Cells were spread onto ampicillin agar plates and incubated at 37°C overnight. Individual clones were picked and grown overnight at 37 °C in 3.5mls of Lysogeny Broth (LB) (Sigma-Aldrich) containing ampicillin. Plasmids were isolated from cells using a QIAprep Spin Miniprep Kit (Qiagen) and sequenced using a SmartSeq Kit (Eurofins Genomics) according to the manufacturer's instructions. Maps for generated plasmids were created using PlasMapper (Dong et al., 2004).

.

Chapter 3: Temporal and quantitative analysis of Shh signalling and Shh response domains in chicken forelimb and hindlimb buds

The Shh morphogen is responsible for establishing digit identities and the number of digits in vertebrate forelimbs and hindlimbs (Towers and Tickle, 2009). However, it is not understood how the different morphologies of the forelimb and hindlimb (and in the chicken, the number of digits) arise from this common morphogenic input. It is possible that, differences in Shh signalling may exist between the respective limb buds and that these contribute to differences in morphological output. Hypothetical differences in Shh signalling in forelimb and hindlimb buds may arise from various sources. The simplest way this might be achieved would be through differences in levels of Shh morphogen produced in respective limb buds. However, differences in the size of limb buds, the range and rate of morphogen dispersion and the timing of morphogen production may also contribute to overall differences in Shh signalling dynamics. Moreover, intrinsic differences may exist in how forelimb and hindlimb cells respond to Shh signalling.

In this chapter, I have aimed to gain insight into these potential differences by investigating temporal, spatial and quantitative differences in Shh production, the response to Shh signalling and the size of respective morphogen fields. Whilst the methods I have used in this chapter have technical limitations and rely on certain assumptions, I have been able to demonstrate a temporal difference in *Shh* expression between the forelimb and hindlimb bud and apparent differences in the response of the respective limbs to Shh signalling. Whilst the size of Shh expression domains and the quantity of Shh produced in respective limbs appear to be remarkably similar during Shh patterning stages.

3.1 The size of the hindlimb bud morphogen field is larger than the forelimb bud throughout the period of Shh patterning activity

To begin to investigate differences in the expression of, and response to, Shh in chicken forelimb and hindlimb buds, I first compared the size of the respective limb buds. As

morphogen fields – the space over which a morphogen acts- differences in the respective sizes of forelimb and hindlimb buds during Shh patterning stages may be important in influencing the morphological outputs of Shh signalling. To begin to measure potential differences in the forelimb and hindlimb morphogen fields I focused on measuring the PD and AP axes of respective limbs. The Shh gradient is formed across the AP axis, whilst both the AP and PD axes grow considerably during Shh patterning. The DV axis, by comparison, is narrow and does not grow substantially during Shh patterning. It was thus considered negligible and was not considered in this initial analysis.

In chicken limb buds Shh patterning activity occurs over a 16-hour period (Scherz et al., 2007; Towers et al., 2011), which equates to a period ranging from stage HH18-HH22. Accordingly, I measured the proximal-distal (PD) axis, the anteroposterior (AP) axis and the AP-PD area – as an estimate measure of overall limb bud size - of forelimb and hindlimb buds from chicken embryos covering these stages and beyond up to stage HH26. I further attempted to measure the number of cells in respective limb buds at these stages to examine potential differences in the cellular density of morphogen fields, which may affect rates of morphogen dispersion.

As expected, the PD axis of forelimb and hindlimb buds, measured at the widest point, increased between stages HH18-HH26, from 400μM to 1750μM (Fig. 5A). The PD axis of hindlimbs was greater than that of forelimbs from stage HH19 onwards, although this was not pronounced until after Shh patterning stages (Fig. 5A). The AP axis of forelimb and hindlimb buds, at a central PD position, also increased between stages HH18-HH26, from approximately 900μM to 12000μM (Fig. 5B). The AP axis of limb buds showed small but continual growth during Shh patterning stages, before larger increases at stage HH26 as limb buds expanded to form hand/footplates (Fig. 5B). The AP axes of hindlimb buds were wider than in forelimb buds from stage HH20 onwards, as the

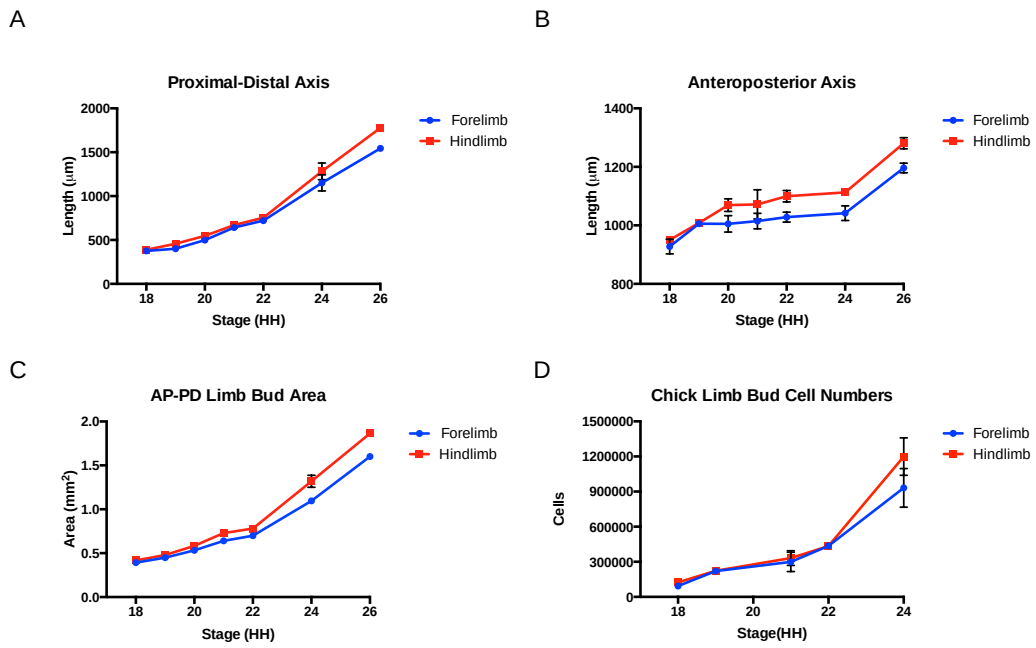

Figure 5 | Comparison of the size and cell number of chicken forelimb and hindlimb buds during Shh patterning stages. (A-B) Lengths of the proximo-distal (PD) (A) and antero-posterior (AP) (B) axes of chicken forelimb (blue) and hindlimb (red) buds at indicated Hamburger and Hamilton (HH) stages of development (Hamburger and Hamilton, 1953) , measured using ImageJ64 software (Rasband et al. 1997-2007) (n=3). (C) Antero-posterior-proximo-distal (AP-PD) areas of chicken forelimb(blue) and hindlimb (red) buds at indicated stages, measured using ImageJ64 software (n=3). (D) Number of cells in chicken forelimb (blue) and hindlimb (red) buds at indicated stages, as measured by hemocytometer (n=3 biological repeats of 6 limbs).

posterior margin of the hindlimb bud expanded more than the forelimb and the footplate became distinguished at an earlier stage than the handplate (Fig.5B, Fig.6). Again, substantial differences between limb buds were not observed until after Shh patterning stages.

Although the maximum extent of PD and AP axes were similar in forelimb and hindlimb buds during Shh patterning stages, it was possible the total AP-PD area showed a greater difference between respective limb buds. To estimate the total size of respective morphogen fields, I used ImageJ64 software to calculate the AP-PD area of images of chicken forelimb and hindlimb buds. As with individual PD and AP axes measurements, the total AP-PD area of hindlimb buds was slightly larger than that of forelimb buds from stage HH20 onwards, but this difference was minor during Shh patterning stages, before becoming more pronounced from stage HH24 (Fig. 5C).

The number of cells in forelimb and hindlimb buds also increased over time, from approximately $1.5x10^5$ cells in stage HH18 limb buds, to $1x10^6$ cells at stage HH24. Cell numbers were approximately equal in respective limbs between stages HH18-HH22, but hindlimbs exhibited a greater number of cells at stage HH24 (Fig. 5D). Collectively, these results demonstrate the hindlimb morphogen field is minimally, though reproducibly, larger than the forelimb during Shh patterning stages but only becomes considerably larger from stage HH24 onwards. The number of cells in forelimb and hindlimb buds was not detectably different during Shh patterning stages.

3.2 *Shh* is expressed for a shorter period of time in hindlimb buds than in forelimb buds

After establishing only minor differences exist in the size of the forelimb and hindlimb bud morphogen fields during Shh patterning stages, I next aimed to determine if

differences existed in the amount of Shh that is present in the respective limb buds. Currently, there is no reliable commercially available antibody that targets either chicken or mouse Shh, but mice have been generated that produce bioactive, fluorescently (GFP) labelled Shh from the endogenous locus (Chamberlain et al., 2008). However, fluorescent signal in the limbs of such mice was too weak to attempt to quantify (data not shown). Thus, to begin to analyse potential temporal and spatial differences in the production of Shh in forelimbs and hindlimbs, I used whole mount *in situ* hybridisation to examine the levels of *Shh* transcripts in respective limb buds of chicken embryos, which could directly affect levels of protein (Fig. 6). I examined *Shh* expression at a range of stages from HH18-HH26 covering the known period of *Shh* expression in chicken limb buds (Pearse et al., 2001; Riddle et al., 1993; Scherz et al., 2007; Towers et al., 2011). This analysis however is unable to identify any post-transcriptional differences that may exist.

Forelimb buds displayed an earlier onset of *Shh* expression, which was detectable at stage HH18 in forelimbs, but not until stage HH19 in hindlimb buds (Fig. 6). Although the initial outgrowth of the chicken hindlimb bud is slightly delayed compared to the forelimb, it is approximately equal in size by stage HH18 (Hamburger and Hamilton, 1951, Fig. 5C). Thus a delay in the onset of *Shh* expression in the chicken hindlimb exists that is not a direct consequence of the heterochrony in outgrowth. *Shh* expression also terminated sooner in chicken hindlimbs. At stage HH26, *Shh* expression was restricted to the most posterior edge of the hindlimb, but was still broadly expressed in the forelimb (Fig. 6).

To begin to examine potential temporal, spatial and quantitative differences in the response of limb progenitors to the Shh morphogen I also used whole mount *in situ* hybridisation to examine *Gli1* and *Ptch2* expression domains in the respective limb buds of chicken embryos (Fig. 6). This further served as a direct readout of active Shh protein

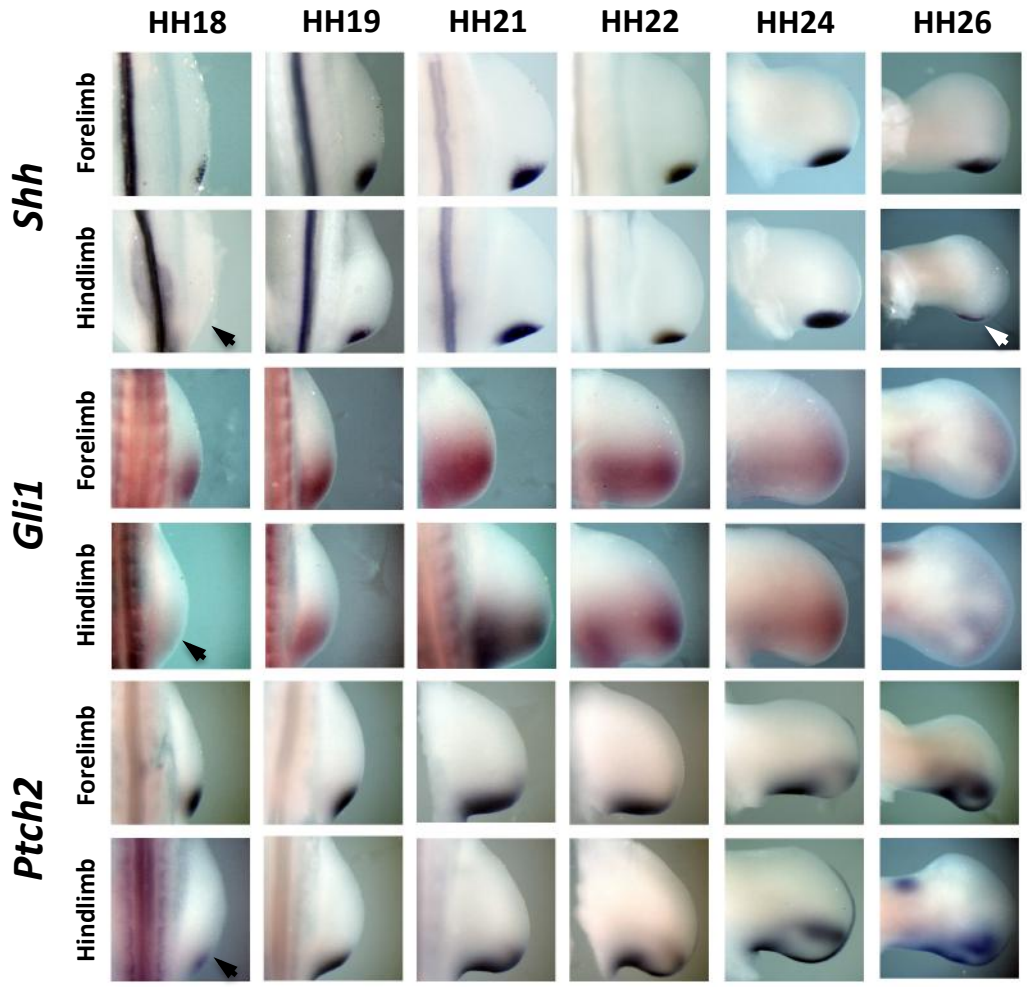

Figure 6| Temporal expression profiles of *Shh*, *Gli1* and *Ptch2* in chick forelimb and hindlimb buds. Whole mount *in situ* hybridisations of chicken forelimb and hindlimb buds at the indicated stages of development, targeting *Shh, Gli1* and *Ptch2.* Note the lack of *Shh, Gli1* and *Ptch2* expression in stage HH18 hindlimbs (black arrows) and earlier downregulation of *Shh* in stage HH26 hindlimbs (white arrow).

levels. *Gli1* and *Ptch2* expression was robust in stage HH18 forelimbs, but absent, or just beginning to be expressed in HH18 hindlimbs, consistent with a delay in the onset of *Shh* expression in hindlimb buds. *Gli1* and *Ptch2* expression also diminished sooner in chicken hindlimbs. At stage HH21-HH22, an area that lacked *Gli1,* and particularly *Ptch2,* expression was observed within the *Shh* expressing domain of chicken hindlimbs. This was increasingly digit-like in shape and may represent a condensation of cells forming the posterior most digit in these limb buds. Interestingly, such an area was not observed until stage HH24 in forelimbs. This may suggest the most posterior digit of the forelimb condenses later than that of the hindlimb, though further evidence is required to confirm the absence of *Gli1/Ptch2* expression coincides with a digit condensation.

3.3 Endogenous expression profiles of *Shh*, *Ptch1* and *Gli1* at stages HH17-HH24

Whole mount *in situ* hybridisation provided temporal and spatial data on the expression of *Shh* and transcriptional targets of Shh (Fig. 6). To gain insight into potential quantitative differences in the levels of *Shh* transcripts produced by limb buds I used quantitative PCR (qPCR) to determine the endogenous levels of *Shh*, *Gli1* and *Ptch1* transcripts in the posterior thirds of chicken forelimb and hindlimb buds, at all developmental stages between HH17-HH24 (Fig. 7A). The posterior third encompassed *Shh* expressing cells and cells adjacent to the Shh expressing domain (Fig. 7A).

Shh was not detected in stage HH17 limb buds, but was detected at constant levels during Shh patterning stages, HH18-HH22, in both forelimb and hindlimb buds, although there was a noticeable dip at stage HH19 in both limb buds (Fig. 7B). No significant difference in the levels of *Shh* was detected between respective limb buds at these stages (Fig. 7B). An apparent sharp increase in *Shh* expression was observed in

both forelimb and hindlimb buds at stage HH24, with hindlimb buds exhibiting a significantly higher level of expression compared to forelimbs (Fig. 7B). This analysis indicates that there is no difference in the levels of *Shh* transcripts between forelimb and hindlimb buds during patterning stages. To gain further insight into potential differences in the levels of Shh protein I again sought to determine the levels of direct transcriptional readouts, *Gli1* and *Ptch1.*

Basal expression of *Gli1* and *Ptch1* was detected in HH17 forelimbs and hindlimbs. HH18 forelimbs and hindlimbs showed a 3-fold increase in *Gli1* and *Ptch1* transcripts relative to expression in HH17 limbs, indicating a response to endogenous Shh expression (Fig. 7C,D). An apparent decrease in target transcripts was observed in HH19 forelimb and hindlimb buds compared to HH18 limb buds, consistent with an apparent dip in *Shh* expression at this stage. Unlike levels of *Shh,* which remained constant, levels of *Gli1* and *Ptch1* transcripts steadily increased in both limb types between stages HH19 and HH22, suggesting an accumulation of response to Shh signalling. Conversely, *Ptch1* and *Gli1* expression plateaued or dipped at the stage *Shh* expression peaked, suggesting a desensitisation to Shh signalling. *Ptch1* expression reached a peak in stage HH22 limb buds, representing a 4-fold increase in expression relative to stage HH17 limb buds, but decreased in stage HH24 limbs. *Gli1* expression continued to rise up to stage HH24, at which stage slightly higher levels were detected in hindlimb buds (Fig. 7C,D). Overall, detected levels of *Gli1* and *Ptch1* transcripts were not significantly different in forelimbs and hindlimbs at all stages measured, suggesting no detectable difference in the levels of endogenous response to Shh signalling in the respective limb buds during this period (Fig. 7C,D). This was consistent with data that suggests there is no difference in the level of *Shh* expression during this period (Fig. 7B).

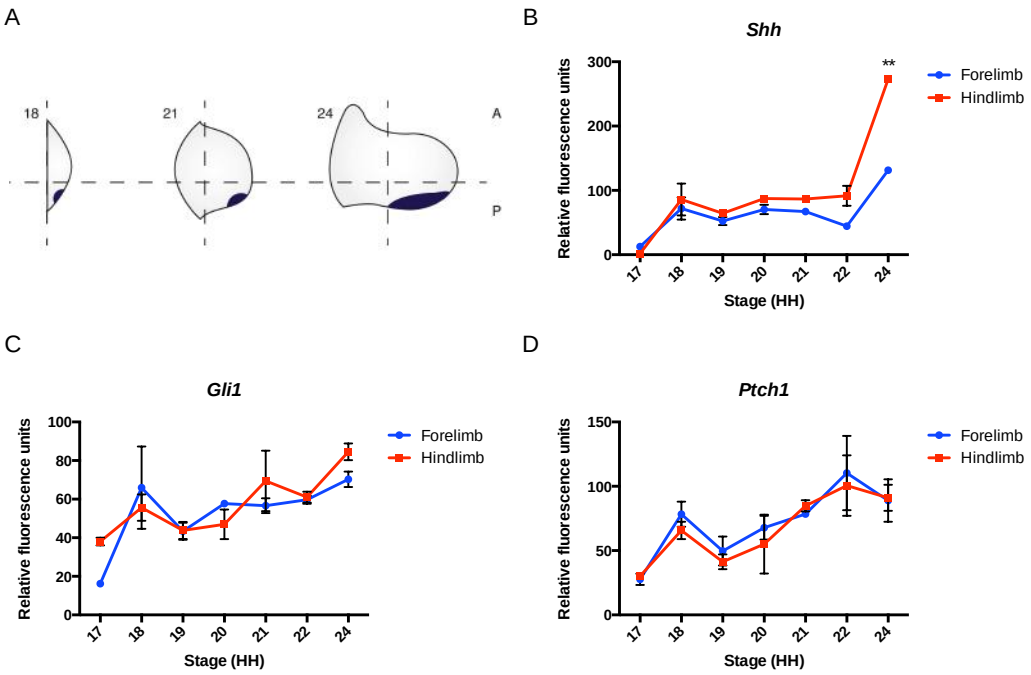

Figure 7| Comparison of endogenous expression profiles of *Shh*, *Ptch1* and *Gli1* in chicken forelimb and hindlimb buds (A) Schematic diagram. Posterior-distal thirds of limb buds harvested from chick embryos at various stages, during the period of endogenous *Shh* expression in limb buds. The domain of *Shh* expressing cells (blue) expands between HH18-HH24. Dotted lines represent approximate areas dissected for analysis. Numbers denote Hamburger and Hamilton stages (HH) of chicken development. (B-D) Temporal expression profiles of *Shh* (B), *Gli1*(C) and *Ptch1*(D) transcripts in the posterior thirds of chicken forelimb buds (blue) and hindlimb buds (red) at indicated stages, as measured by quantitative PCR analysis (Mean ±SEM, n=2 samples of 3 dissected limb buds). In all samples, levels of *Shh, Gli1* and *Ptch1* transcripts are normalised to levels of *Gapdh* transcripts.

3.4 The relative size of the *Shh* expressing domain of forelimb buds is larger than that of hindlimb buds during Shh patterning stages

To compliment the experiments described above, I also developed an alternative method of measuring potential spatial and quantitative differences in the expression of *Shh* and Shh transcriptional targets in chicken limb buds. I measured the AP-PD area of images of the *Shh* expressing domain of forelimb and hindlimb buds, using ImageJ64 (Rasband, 2008) to give an estimation of the number of cells expressing *Shh* in a limb bud (Fig.8 A). The number of cells expressing *Shh* may reflect the amount of Shh morphogen produced by respective limb buds. This method relies on assumptions, which are reviewed in discussion section 6.1.

The size of *Shh* expressing domains of both forelimb and hindlimb buds increased between stages HH18-HH21 (Fig. 8C). In forelimbs, the size of the *Shh* expressing domain remained consistent between stages HH21-HH26. In contrast, the *Shh* expressing domain of hindlimbs increased in stage HH24 hindlimb buds, before sharply decreasing in HH26 hindlimbs (Fig. 8C). There was no measurable difference in the size of the *Shh* expressing domain in forelimb and hindlimb buds between stages HH18-HH22. At stage HH24, the *Shh* expressing domain of hindlimb buds was greater than that of forelimbs, again consistent with qPCR analysis (Fig. 7), but this was reversed by stage HH26 as *Shh* expression is terminated sooner in hindlimb buds.

Differences in the size of the morphogen producing area between limb buds at different stages of development or between different limb-types may be consequent of differences in the overall size of limb buds and may not necessarily reflect differences in the levels of Shh signalling. To measure increases in the size of the *Shh* expressing domain relative to increases in size of the morphogen field – which may better reflect

differences in levels of Shh signalling - I normalised AP-PD areas of ZPAs to the overall AP-PD area of corresponding limb buds.

After the initial delay in onset of *Shh* expression in the hindlimb, normalised *Shh* domains in hindlimb buds were slightly smaller than in forelimb buds during patterning stages HH19-HH22. Normalised *Shh* domain sizes peaked at stage HH21 in both limbs, coinciding with the known period of Shh patterning activity in limb buds (Scherz et al., 2007; Towers et al., 2011). A gradual decrease in normalised *Shh* domain size was observed in forelimb and hindlimb buds between stages HH21-HH26. Interestingly, a decrease in the normalised *Shh* domain size was observed in stage HH19 forelimb and hindlimbs compared to limb buds at stage HH18. This was consistent with an apparent dip in *Shh, Gli1* and *Ptch1* expression measured at this stage by qPCR.

Collectively, these results suggest the level of Shh signalling experienced by the forelimb and hindlimb bud morphogen fields is maximal at stage HH21, and that a slightly greater proportion of forelimb progenitors may be exposed to Shh signalling than hindlimb progenitors. However, it is unclear if this would make a significant impact to subsequent morphologies.

3.5 The relative size of the Shh response domain of forelimb buds is larger than that of hindlimb buds during Shh patterning stages

It is uncertain how Shh is dispersed through the limb bud morphogen field (Briscoe & Thérond 2013, discussed in introduction section 1.2). However, it is possible to estimate the extent of Shh morphogen dispersion by measuring the expression of Shh transcriptional targets. *Gli1* and *Ptch2* are direct read outs of Shh signalling (Marigo et al., 1996a; Marigo et al., 1996b; Pearse et al., 2001). To begin to examine potential differences in the range of Shh morphogen dispersion between forelimb and

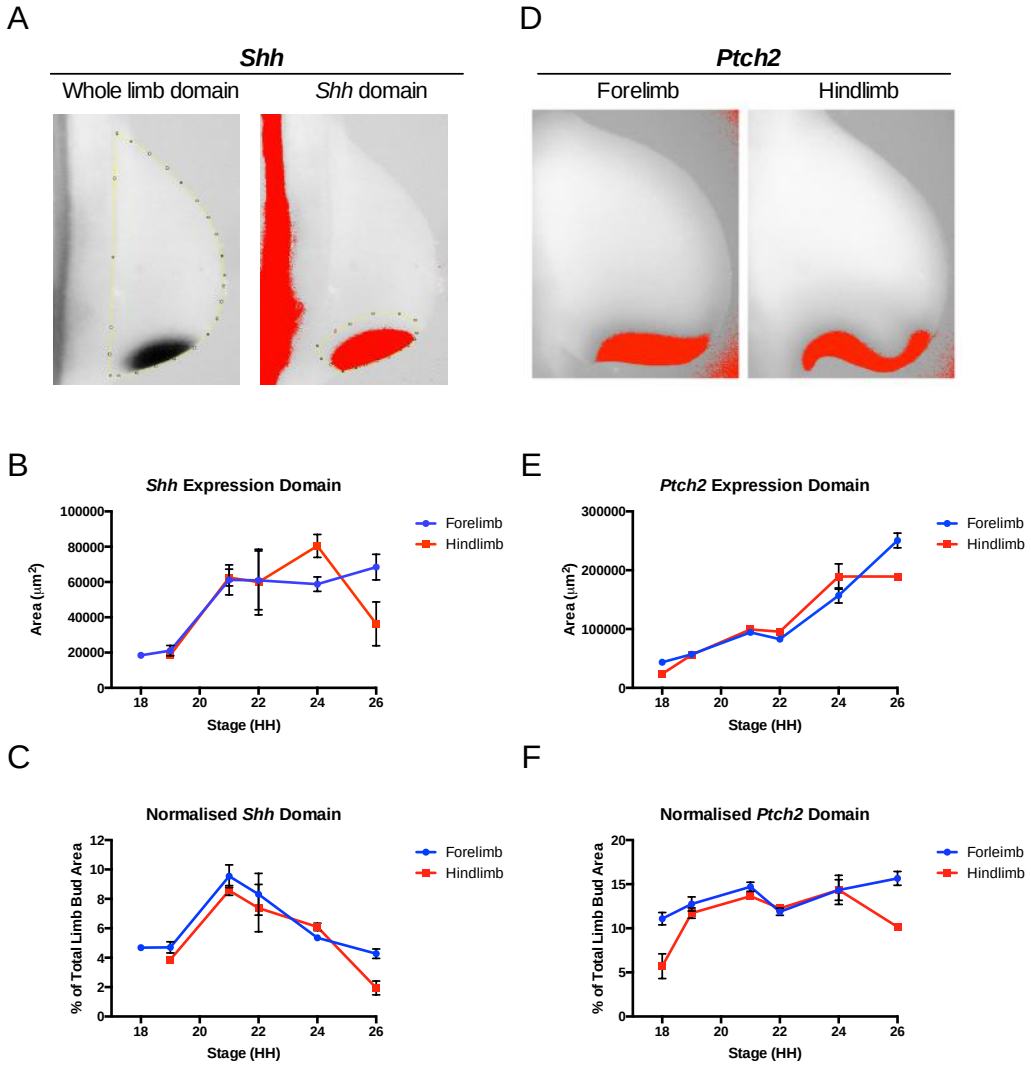

Figure 8 | Comparison of *Shh* and *Ptch2* expression domains in chicken forelimb and hindlimb buds. (A, D) Examples. Whole limb domains and *Shh* or *Ptch2* expressing domains were quantified using ImageJ64 (Rasband et al. 1997-2007). (B, E) Quantified *Shh* expression domains (B), and *Ptch2* expression domains (E), of chicken forelimb (blue) and hindlimb (red) buds at designated HH stages of development, as measured using ImajeJ64 (n=3). (C, F) Relative sizes of *Shh* expression domains (C) and *Ptch2* expression domains (F) in chicken forelimb (blue) and hindlimb (red) buds at designated stages as a proportion of whole limb buds (n=3).

hindlimb buds, I used *in situ* hybridisation to examine the expression domains of *Ptch2*, as this produced the clearest *in situ* patterns.

The size of the *Ptch2* expression domain increased in size between stages HH18-HH21, in both forelimbs and hindlimbs. Between stage HH21 and stage HH22, the *Ptch2* expression domain plateaued in both limb buds, before increasing again considerably at stages HH24-HH26. The size of the domain was larger in forelimb buds compared to hindlimb buds at stages HH18 and stage HH26, but similar in respective limb buds at all other stages measured. As with normalised *Shh* domains, normalised *Ptch2* expression domains occupied a slightly greater percentage of the forelimb bud than in hindlimb buds during Shh patterning stages (Fig. 8F). An initial peak in the normalised *Ptch2* expression domain was observed at stage HH21, before a second peak at stage HH26, in forelimb and stage HH24 hindlimb buds (Fig. 8F). This initial peak was consistent with a similar peak observed in the normalised *Shh* expression domain at this stage (Fig. 8C). Whilst *Ptch2* expression domains were similar between forelimb and hindlimb buds, the shape of the response domains were different, reflecting differences in the shape of the respective morphogen fields and possible early digit condensation in the hindlimb (Fig. 8D).

Taken together, the results in this chapter demonstrate that the hindlimb bud is slightly larger than the forelimb during Shh patterning stages but no detectable difference exists in the levels of *Shh, Gli1* and *Ptch1* transcripts, or the AP-PD area of *Shh* and *Ptch2* expression domains of forelimb and hindlimb buds during this period. Normalised *Shh* and *Pthc2* expression domains appear minimally larger in forelimbs reflecting the larger size of the hindlimb bud, but the equivalent size of *Shh* and *Ptch2* expression domains (Fig. 8C, F). A delay in the onset of *Shh* expression in the hindlimb is more clearly demonstrated and furthermore, a more

rapid termination of *Shh* expression (Fig. 6). Moreover, an earlier desensitisation to Shh is apparent in the hindlimb, as shown by the earlier condensation of a posterior digit, which indicates differential responses to equivalent Shh exposures may exist between forelimb and hindlimb buds (Fig. 6).

Chapter 4: Transcriptomic analysis of the response of limb progenitors to Shh signalling

Previous studies have demonstrated that exposing limb buds to different concentrations of Shh or durations of Shh signalling can alter the number and identity of digits that subsequently develop (Harfe et al., 2004; Scherz et al., 2007; Towers et al., 2011; Yang et al., 1997; Zhu et al., 2008). However, it is unclear how this is instructed at a molecular and cellular level during the relatively short period that Shh patterning activity has been shown to operate within (Scherz et al., 2007; Towers et al., 2011). In this chapter, I describe the development of an *ex vivo* assay – the first of such, to the authors knowledge, for culturing limb tissue (see Materials and Methods) - and use RNA sequencing (RNAseq) to investigate the immediate transcriptional response of limb bud cells to different Shh conditions. I show that limb progenitors initially respond equivalently to different concentrations of Shh but establish a non-linear graded response to Shh over time through a variation of a temporal adaptation mechanism. I provide evidence that this may be required for correct interpretation of graded Shh signalling. I further interrogate RNAseq results to uncover cell-autonomous and noncell-autonomous negative feedback mechanisms, which appear to contribute to signal desensitisation to Shh signalling that is observed in limb progenitors. Finally, the results of chapter 3 suggested there may be a difference in the response of forelimb and hindlimb cells to equivalent Shh signalling. I therefore also investigated how hindlimb explants respond to different Shh treatments to compare to the response of forelimb explants.

4.1 Dissociated limb bud cells exhibit a limited and inconsistent response to exogenous Shh

To investigate the immediate transcriptional responses of chicken forelimb and hindlimb cells to different levels of Shh signalling, I first attempted to establish an

in vitro assay. Limb progenitor cells were harvested from chicken forelimb and hindlimb buds and were dissociated and cultured *in vitro* with a range of recombinant Shh concentrations, for different lengths of time (Fig. 9A). To ensure cells had not been previously exposed to Shh but were competent to respond to Shh signalling – so called, Shh naïve - limb progenitors were harvested immediately prior to the onset of endogenous *Shh* expression at stage HH18 (Fig. 9A) (Riddle et al., 1993). To ensure progenitors would not express Shh themselves during the culture period, I harvested cells from the anterior two thirds of limb buds to avoid inclusion of cells from the ZPA (Fig. 9A). To avoid exposure to a complex mixture of signalling molecules present in serum, which may mask cell responses to Shh, dissociated limb cells were cultured in serum free conditions (see material and methods). Cells were seeded in a monolayer, to ensure all cells would be uniformly dosed with Shh.

To attempt to replicate physiologically relevant dosages of Shh, appropriate Shh concentrations and culture durations were deduced from previous studies. The endogenous concentration of Shh protein that is present in either limb bud has not been determined. For this series of experiments, I used a concentration range of 0-4nM Shh, as this range has been demonstrated to elicit the full range of dorsal-ventral (DV) cell fates in chicken neural tube explants (Dessaud et al., 2007). The affects of Shh on anteroposterior limb patterning are completed in an approximately 16-hour period, corresponding to stages HH18-22. When Shh signalling is totally inactivated by cyclopamine after 16 hours, a normally patterned, though smaller than normal, limb is formed (Scherz et al., 2007; Towers et al., 2011). Dissociated limb progenitors were therefore cultured in the presence of 0-4nM Shh for 3, 6 or 15 hours to reflect endogenous conditions of Shh signalling in developing limb buds (Fig. 10A).

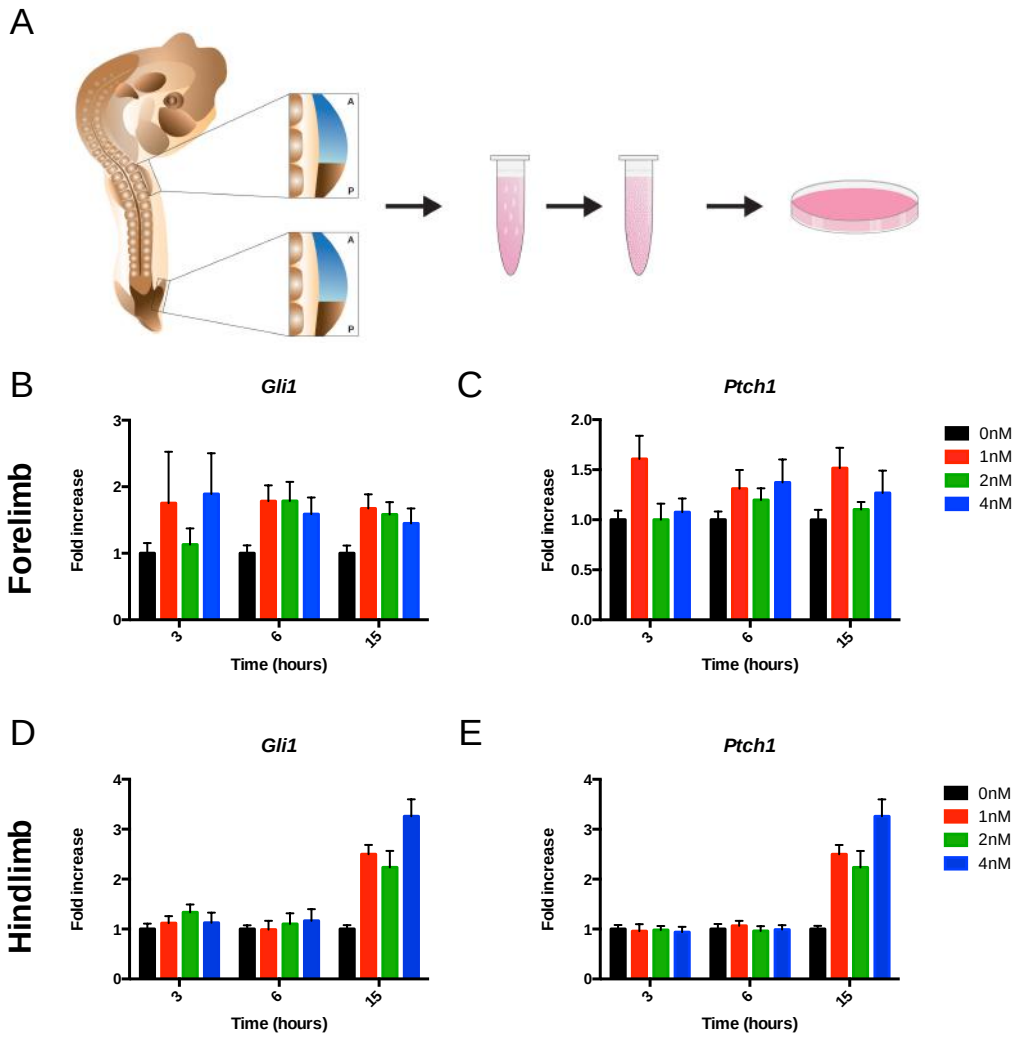

Figure 9| Dissociated forelimb and hindlimb progenitors exhibit a low level and inconsistent response to exogenous Shh (A) Experimental schematic. Anterior 2/3 of forelimb and hindlimb buds (blue) were dissected from stage HH18 chick embryos and pooled before being dissociated and cultured in monolayer in the presence of different concentrations of recombinant Shh for fixed periods of time. (B-E) Levels of *Gli1* and *Ptch1* transcripts in dissociated chick forelimb cells (B, C) and hindlimb cells (D, E) dosed with indicated Shh treatment as determined by quantitative PCR (relative *Gli1* and *Ptch1* expression n=3 ±SEM). In all samples, levels of *Gli1* and *Ptch1* transcripts are normalised to levels of *Gapdh and* levels of *Gli1* and *Ptch1* expression in untreated cells.

Gli1 and *Ptch1* are direct transcriptional read outs of Shh signalling (Marigo et al., 1996a; Marigo et al., 1996b). To measure the level of response of forelimb and hindlimb progenitors to different Shh conditions, I initially used qPCR to quantify the levels of *Gli1* and *Ptch1* relative to untreated cells. Forelimb cells dosed with 1, 2 or 4nM Shh exhibited no significant increases in the levels of *Gli1* or *Ptch1* transcripts after 3, 6 or 15 hours of exposure (Fig. 9B, C). There was no correlation between the levels of target transcripts and Shh concentration or between the levels of target transcripts and the duration of Shh exposure. Thus no concentration dependent or temporal trend was observed.

Hindlimb cells exposed to 1, 2 or 4nM Shh for 3 or 6 hours exhibited no significant increases in the levels of *Gli1* or *Ptch1* transcripts. Larger increases in *Gli1* and *Ptch1* transcripts were observed in hindlimb cells dosed with Shh for 15 hours, however, again, no correlation was observed between increases in transcription and Shh concentration (Fig. 9D, E). Taken together, forelimb and hindlimb cells treated with exogenous Shh showed no significant increases in levels of *Gli1* and *Ptch1* transcripts relative to cells under control conditions and failed to show any robust dose response or temporal trend in this system (Fig. 9B-E). A possible explanation for this is that cells were not dosed with enough recombinant Shh to induce a significant effect. Alternatively, dissociated cells may have lost their ability to respond normally to Shh in this assay.

4.2 Forelimb and hindlimb explants cultured *ex vivo* exhibit a robust and graded response to exogenous Shh

Tbx5 is a marker of early forelimb progenitors and is downregulated as cells differentiate (Gibson-Brown et al., 1996; Isaac et al., 1998; Logan et al., 1998;

Ohuchi et al., 1998). A downregulation in *Tbx5* expression may indicate that dissociated cells are differentiating in culture and may not be responding to Shh signalling as limb progenitors. To examine whether dissociated limb cells were expressing *Tbx5* at normal levels during culture, I quantified the amount of *Tbx5* transcripts in dissociated limb cells. For comparison, I also determined the levels of *Tbx5* from non-dissociated cells harvested from the anterior two thirds of HH18 forelimb buds and non-dissociated forelimb explants, cultured *ex vivo* for 16 hours.

Dissociated forelimb cells cultured for 15 hours showed a 4-fold reduction in *Tbx5* transcripts compared to that observed in undissociated cells harvested from stage HH18 forelimbs and a 6-fold reduction compared to explants that had been cultured *ex vivo* for 16 hours (Fig. 10A). To determine if an endogenous reduction of *Tbx5* over 15 hours was observed *in vivo*, I quantified levels of *Tbx5* transcripts from cells harvested from the anterior two thirds of stage HH22 chicken forelimbs, representing a 16-hour period of development *in vivo* from stage HH18. A 1.5-fold increase in *Tbx5* transcripts was observed in HH22 cells compared to HH18 cells, similar to the increase observed in explants cultured *ex vivo* (Fig. 10A). Dissociated cells therefore exhibited a lower than normal expression of *Tbx5,* which may indicate that dissociated cells have differentiated in culture and are unable to respond to Shh signalling as progenitors. Non-dissociated forelimb explants did not lose expression of *Tbx5* during *ex vivo* culture and therefore offer a potentially more robust system in which to continue this investigation.

To explore whether an *ex vivo* assay provided a more reliable system in which to investigate the response of limb bud explants to Shh signalling, I modified the above *in vitro* assay. Shh naïve cells from the anterior two thirds of forelimb and hindlimb buds were harvested as previously described, but were not dissociated.

Instead limb progenitors were cultured as explants, *ex vivo,* in the presence of defined concentrations of recombinant Shh, for fixed periods of time (Fig. 10B).

In a pilot experiment, forelimb explants were dosed with 0, 1, 2, 4 or 8nM Shh for 12 hours. In contrast to *in vitro* experiments, explants dosed with 1-8nM Shh showed a 4-6-fold increase in levels of *Gli1* and *Ptch1* expression, compared to explants not dosed with Shh (Fig. 10C, D). Significantly, a graded response was observed where increasing concentrations of Shh induced correspondingly higher levels of *Gli1* and *Ptch1* expression. Explants treated with 1nM Shh showed a 4-fold increase in *Ptch1* and *Gli1* transcripts, whilst explants treated with 4nM or 8nM Shh showed 5-fold and 6-fold increases in *Ptch1* and *Gli1* expression, respectively (Fig. 10C, D). An exception to this trend was seen in explants dosed with 2nM Shh, which exhibited disproportionally high levels of induced gene expression. A 5.5-fold increase in *Ptch1* transcripts and a 7.5-fold increase in *Gli1* transcripts was observed in these explants (Fig. 10D).

These data demonstrate that the range of Shh concentrations used was sufficient to induce graded target gene expression and that culturing explants *ex vivo* was a more reliable system in which to study responses to Shh signalling. A more extensive set of experiments was undertaken using this *ex vivo* approach. A broader range of Shh concentrations were used, 0-16nM, and culture periods were modified to 6, 12, 16 or 20 hours, as it was considered unlikely that explants would elicit a significant response to Shh signalling after only 3 hours of exposure.

After 6 hours of culture no difference was observed between forelimb or hindlimb explants dosed with different concentrations of Shh. Explants cultured with 2, 8 or 16nM Shh for 6 hours showed a 2-fold increase in *Gli1* and *Ptch1* transcripts compared to explants cultured without Shh over the same period (Fig. 10C, D).

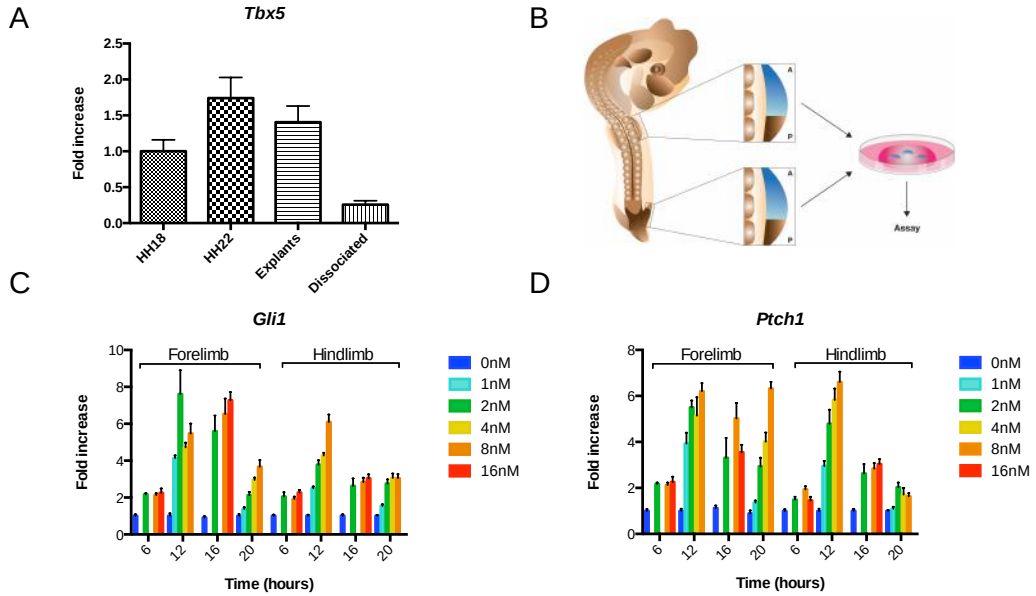

Figure 10 | Limb explants cultured *ex vivo* exhibit normal *Tbx5* transcriptional activity and a graded response to increasing concentrations of exogenous Shh. (A) Levels of *Tbx5* transcripts in explants taken directly from the anterior 2/3 of forelimbs from stage HH18 (HH18) and stage HH22 (HH22) chick embryos, in explants from anterior 2/3 of HH18 chick forelimb buds cultured *ex vivo* (Explants) and in dissociated limb cells from anterior 2/ 3 of HH18 forelimb buds (Dissociated) as determined by quantitative PCR (Relative *Tbx5* expression ±SEM, n=3 samples of 3 explants). In all samples levels of *Tbx5* transcripts are normalised to levels of *Gapdh* and to levels of *Tbx5* expression in HH18 samples. (B) Experimental schematic. Anterior 2/3 of forelimb and hindlimb buds (blue) were dissected from stage HH18 chick embryos and were embedded in type-I collagen (dark pink) before being cultured *ex vivo* in the presence of different concentrations of recombinant Shh for fixed periods of time. Levels of *Gli1* (C), and *Ptch1* (D) transcripts, in chick forelimb (FL) and hindlimb (HL) explants dosed with indicated Shh treatment as determined by quantitative PCR (Relative *Gli1* and *Ptch1* expression ±SEM, n=2-3 samples of 2 explants). In all samples levels of *Gli1* and *Ptch1* transcripts are normalised to levels of *Gapdh* and to levels of *Gli1* and *Ptch1* expression in untreated explants.

After 16 and 20 hours of culture, forelimb explants demonstrated a graded response of *Gli1* expression to increasing concentrations of Shh. Levels of *Gli1* transcripts were higher in explants cultured for 16 hours compared to those cultured for 12 hours at the same concentrations of Shh, but were lower in those cultured for 20 hours compared to those cultured for either 12 or 16 hours (Fig. 10C). This demonstrates that a temporal response gradient to Shh signalling exists but also that explants may become desensitised to Shh signalling over time.

Ptch1 expression in forelimb explants cultured for 16 or 20 hours was graded and at a similar level to that seen after 12 hours of culture (Fig. 10D). This represented a discrepancy with *Gli1* expression in these explants, which were expected to show a comparable temporal trend. Another notable discrepancy was the expression of *Ptch1* in forelimb explants treated with 16nM Shh for 16 hours, which was lower than that in explants dosed with 8nM over the same period, suggesting desensitisation to Shh signalling can also be induced by high concentrations of Shh (Fig. 10D). However, this was not supported by *Gli1* expression in these explants.

Hindlimb explants showed no substantial difference in expression of *Gli1* or *Ptch1* to different concentrations of Shh after 16 or 20 hours of culture (Fig. 10C, D). Strikingly, expression of both genes was much lower at these time points than observed after 12 hours of Shh treatment (Fig. 10C, D). This was in contrast to temporal trends observed in forelimb explants and suggested hindlimb explants may have already become desensitised to Shh signalling by 16 hours.

Collectively these data suggested that forelimb and hindlimb explants respond to Shh signalling in a binary fashion after 6 hours of exposure, eliciting the same low-level response when dosed with a range of Shh concentrations. After 12 hours, explants elicit a graded response to increases in Shh concentration, which is

maintained at 20 hours in forelimbs but is lost by 16 hours in hindlimbs. Data further suggested that explants may become desensitised to Shh over time and that this occurs at different rates in forelimb and hindlimb explants. Interestingly, explants exposed to lower concentrations of Shh showed a greater decrease in relative *Gli1* and *Ptch1* expression over time (Fig. 10C, D).

qPCR is limited by the number of reactions that can be performed in a single experiment. Consequently, results from several experiments had to be brought together to delineate temporal trends and compare forelimbs results to hindlimb results. Whilst I attempted to make results from different experiments comparable by presenting gene expression data as a fold change compared to controls, individual variations in experiments may still present themselves in data and cause inconsistencies in trends. Nonetheless, qPCR provided a useful initial insight into the questions raised in this chapter.

4.3 Forelimb bud explants exhibit a non-linear graded response to the Shh morphogen gradient through signal accumulation and signal desensitisation

In addition to the limitations mentioned above, qPCR can only measure the expression of selected genes that are known transcriptional targets. It is further an inefficient technique to measure the expression of many genes of such a large sample size. To circumvent these limitations and to find novel targets of Shh signalling I used seq to interrogate the full transcriptional responses of limb explants to defined Shh treatments.

I simplified my experimental approach to reduce the number of experimental conditions. I focused on 4 durations of culture: 0, 6, 12 and 16 hours and 4 concentrations of Shh: 0, 2, 4 and 8nM (Fig. 12A). Time points were based on previous qPCR results that suggested explants might have already started to become desensitised to Shh signalling by 20 hours (Fig. 10C, D). Concentrations were also based on qPCR results, which illustrated a 0-8nM range was sufficient to induce detectable differences in levels of target gene expression (Fig. 10C, D).

Before analysing the affects of Shh on transcriptional targets, I interrogated the data to confirm that experimental procedures had been performed accurately and that results could be reliably interpreted. Importantly, *Shh* expression was not detected in any samples via RNAseq analysis, confirming that affects on transcription resulted only from exposure to exogenous Shh (Fig. 11A). Expression of transcripts that were not expected to be differentially expressed (DE), were at similar levels in all samples, as exemplified by levels of *Smo* (Fig. 11B). This indicated that the normalisation strategy of raw readcounts was effective and secondly that levels of *Smo*, an important component of the Shh signalling pathway, were not affected by Shh exposure.

To confirm forelimb and hindlimb samples had been kept separate during experimental procedures, I examined the expression of established markers of limb identity. Tbx5, a transcription factor exclusively expressed in the developing forelimb (Gibson-Brown et al., 1996; Isaac et al., 1998; Logan et al., 1998; Ohuchi et al., 1998), was highly expressed in all forelimb samples but was not expressed in hindlimb samples (Fig. 11C). Conversely, *Tbx4*, a transcription factor expressed exclusively in the developing hindlimb (Gibson-Brown et al., 1996; Isaac et al., 1998; Logan et al., 1998; Ohuchi et al., 1998) was expressed at high levels in hindlimb samples, but was not expressed in forelimb samples (Fig. 11D).

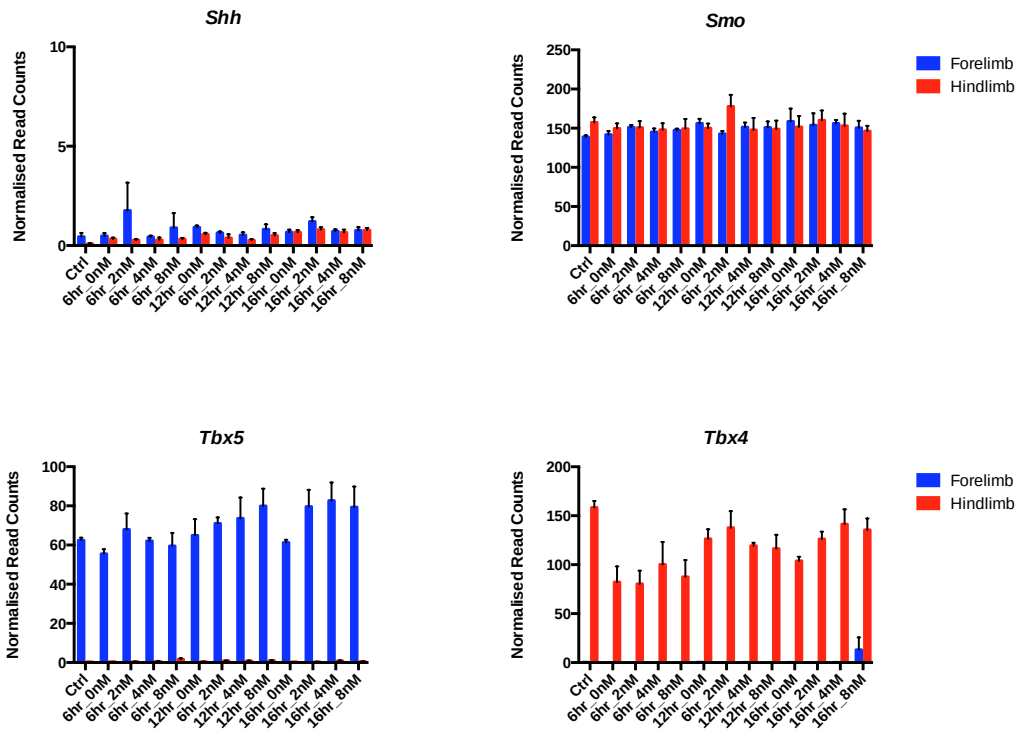

Figure 11| Cultured limb bud explants to not express endogenous *Shh* but express *Smo* consistently and express limb-type specific genes *Tbx5* and *Tbx4* in an exclusive manner. (A-D) Normalised read counts of *Shh* (A), *Smo* (B), *Tbx5* (C) and *Tbx4* (D) transcripts in forelimb (blue) and hindlimb (red) explants treated with Shh as designated, as determined by RNAseq analysis (n=3±SEM). All transcripts are normalised using the total count (TC) method of normalisation.

To begin to analyse the responses of limb explants to Shh via RNAseq, I first focused on the response of forelimb explants as determined by normalised read counts of *Gli1.* Consistent with qPCR results, forelimb explants dosed with all concentrations of Shh, at all time points, showed an increase in levels of *Gli1* transcripts compared to control explants, (Fig. 12B). After 6 hours of exposure, forelimb explants dosed with 2, 4 or 8nM Shh exhibited a 3.5-fold increase in levels of *Gli1* expression, compared to control explants, despite differences in Shh concentration (Fig. 12B). This was also consistent with qPCR results confirming explants respond equivalently to different Shh concentrations at this time point and that early response to Shh in limb progenitors is binary.

After 12 hours of Shh exposure a graded response was observed, in which explants exhibited increasing levels of *Gli1* expression in response to increasing concentrations of Shh and this response steepened in explants exposed to Shh for 16 hours (Fig. 12B). Interestingly, graded responses were achieved in a non-linear fashion by a combination of two related mechanisms first described in the neural tube: signal desensitisation and signal accumulation (Fig. 12C, D) (Dessaud et al., 2007).

Explants exposed to the lowest concentration of Shh (2nM) showed signal desensitisation, a relative decrease in *Gli1* expression over time from an initial response peak at 6 hours (Fig. 12B, D). *Gli1* expression in response to mid-dose Shh (4nM) remained constant over time whilst levels of *Gli1* continued to increase in explants treated with the highest concentration of Shh (8nM), signifying an accumulation of response to Shh signalling (Fig. 12B, C). These data are consistent with a variation of the temporal adaptation mechanism, which describes differential rates of signal desensitisation in neural tube progenitors which is required for correct interpretation of graded Shh signalling (Dessaud et al., 2007).

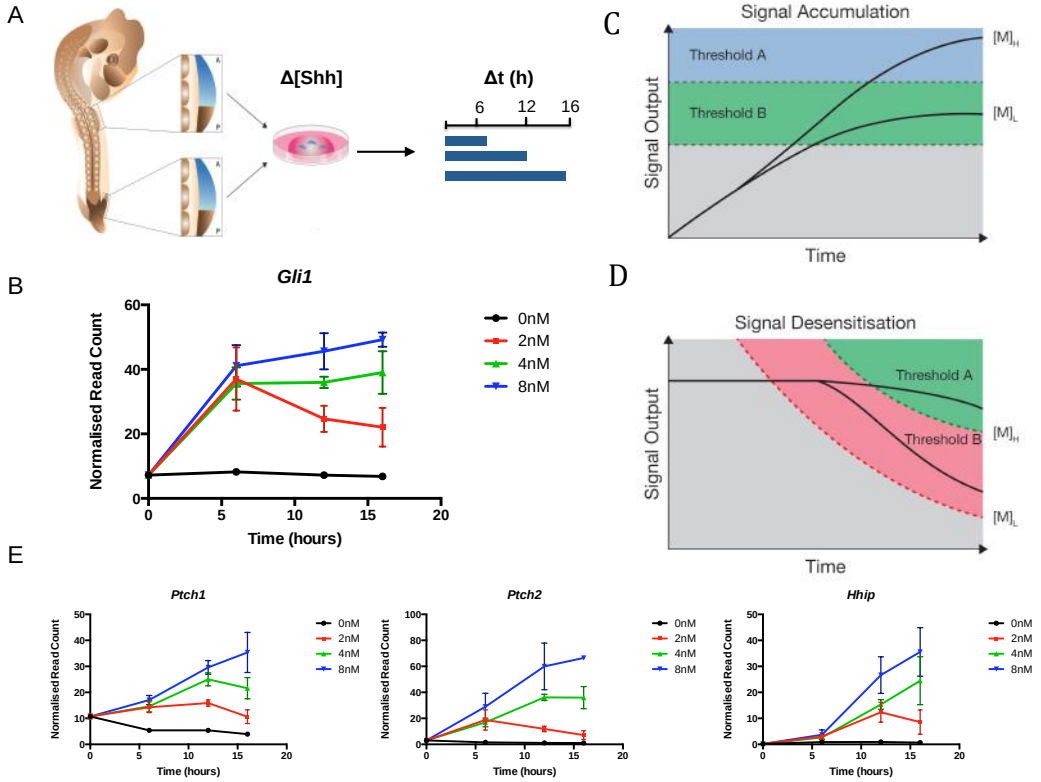

Figure 12 | Effects of concentration and duration of Shh exposure on the transcription of primary Shh targets in forelimb explants. (A) Experimental schematic. Anterior 2/3 of forelimb and hindlimb buds (Blue) were dissected from HH St.18 chick embryos and were embedded in type-I collagen (dark pink) before being cultured *ex vivo* in the presence of different concentrations of recombinant Shh-N. Explants were cultured for 0, 6, 12 or 16 hours before being assayed. (B, E) Normalised read counts of *Gli1*, *Ptch1*, *Ptch2* and *Hhip* transcripts in forelimb explants treated with the indicated concentrations of Shh for designated times, as determined by RNAseq analysis (n=3±SEM). Levels of all transcripts were normalised using the total count (TC) method of normalisation. (C, D), Model of neural tube progenitor specification resulting from different levels of signal accumulation or signal desensitisation in response to different concentrations of the Shh morphogen (Dessaud et al., 2007).

It has been widely reported that cells can become desensitised to a number of different signalling pathways. This is often achieved through negative feedback loops, whereby active signalling induces the expression of genes that code for proteins, which act to inhibit signal transduction. Desensitisation to the MAPK, EFG, PI3/AKT, JAK/STAT pathways, amongst others, have been well characterised (Avraham and Yarden, 2011; Carver et al., 2011; Nguyen and Kholodenko, 2015).

I next examined the response of other well-known Shh targets. The Shh receptors Ptch1 and Ptch2 and the Shh binding antagonist Hhip, are also targets of Shh signalling (Holtz et al., 2013; Jeong and McMahon, 2005; Marigo et al., 1996a; Vokes et al., 2007; Vokes et al., 2008). As with *Gli1* expression, levels of *Ptch1, Ptch2* and *Hhip* transcripts increased equivalently after 6 hours of Shh exposure, independent of Shh concentration, and continued to rise in explants dosed with 8nM Shh; but, characteristically plateaued or decreased in explants exposed to lower concentrations over time (Fig. 12E). Again, desensitisation to Shh signalling occurred earliest and to the greatest extent, in explants exposed to the lowest dose of Shh and therefore contributed to a steepened gradient that was observed at the assay end point.

A possible explanation for the decrease of target gene expression (desensitisation) in explants exposed to the lowest doses of Shh is that exogenous Shh degraded during culture. To test whether recombinant Shh was still biologically active after 16 hours, I cultured forelimb explants for 6 hours in media containing 2nM Shh that had previously been incubated for 16 hours. A 3.5-fold increase in *Gi1* transcripts was observed in explants treated with this conditioned medium compared to explants cultured without Shh for 6 hours (Fig. 13). This was not a significantly different increase to that exhibited by explants dosed with fresh 2nM Shh compared to control explants (Fig. 13).

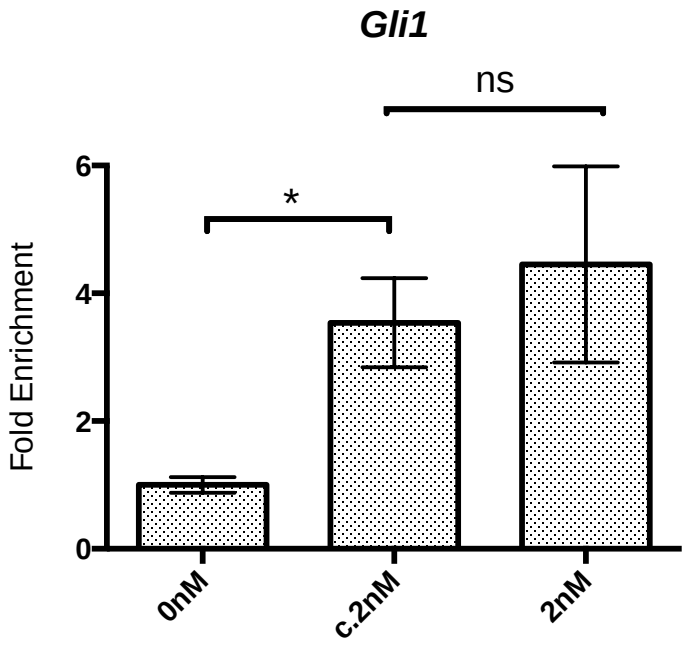

Figure 13 | Recombinant Shh remains biologically active after 16 hours of culture. Fold enrichment of *Gli1* transcripts in forelimb explants cultured for 6 hours with 2nM Shh or 2nM Shh previously incubated for 16 hours (c.2nM), compared to explants cultured without Shh, as determined by quantitative PCR (n=3±SEM). In all samples levels of *Gli1* transcripts are normalised to levels of *Gapdh* transcripts.

4.4 Signal desensitisation is mediated by a Ptch1/2 ligand dependent antagonism

Desensitisation to Shh signalling has previously been observed in the developing neural tube (Dessaud et al., 2007; Dessaud et al., 2010). Neural tube explants exposed to exogenous Shh show a decrease in signal output over time (Dessaud et al., 2007). Interestingly, the rate of desensitisation to Shh in neural tube explants is inversely correlated to the concentration of Shh explants are exposed to (Dessaud et al., 2007; Dessaud et al., 2010). This temporal adaption mechanism has been shown to be critical for the correct interpretation of the Shh morphogen gradient in the vertebrate neural tube (Dessaud et al., 2007; Ribes and Briscoe, 2009). Consistent with these data, the rate of signal desensitisation to Shh in limb explants, measured by decreases in *Gli1, Ptch1, Ptch2* and *Hhip* transcripts, was also inversely correlated to Shh concentration (Fig. 12B, D, E). Additionally however, in limb explants a simultaneous signal accumulation was also observed, which correlated to increasing Shh concentrations, when exposed to medium - high doses of Shh (Fig. 13B, C, E). This represented an interesting difference to the response of neural tube explants to Shh signalling.

Temporal adaptation in neural tube explants is caused, at least in part, by a cell-autonomous Ptch1-mediated inhibition (Dessaud et al., 2007). Ptch1 upregulation has been previously implicated in negative feedback to Shh signalling and this role has been termed Ligand Dependant Antagonism (LDA) (Jeong and McMahon, 2005). Roles for Ptch2 and Hhip mediated LDA have also been recently described in the neural tube (Holtz et al., 2013), and a downregulation of Shh co-receptors Gas1, Cdon and Boc by Shh is further thought to contribute to this mechanism (Allen et al., 2007; Allen et al., 2011; Holtz et al., 2013). Consistent with this model, limb

explants exhibited an upregulation of *Ptch1*, *Ptch2* and *Hhip* (Fig. 12E) and a downregulation of *Gas1* and *Cdon* in response to Shh, although levels of *Boc* remained appeared unaffected (Fig. 14C).

To directly determine if Ptch1 and Ptch2 contribute to a ligand dependent antagonism model in limb explants, I sought to determine if disrupting *Ptch1* and *Ptch2* upregulation in explants would inhibit signal desensitisation in response to Shh signalling. *Hhip* is not expressed in developing limb buds at detectable levels and *Hhip*$^{-/-}$ mice do not exhibit a limb phenotype and was therefore not targeted in this experiment (Aglyamova and Agarwala, 2007). Disruption was achieved by injecting siRNAs targeting *Ptch1* and *Ptch2* into a cavity adjacent to the forelimb-forming region of stage HH14 chicken embryos, followed by immediate electroporation (Fig. 14A). siRNAs were co-electroporated, with an RFP-expressing reporter construct, into progenitor cells that give rise to the forelimb bud. After 24 hours - for siRNAs to target *Ptch1* and *Ptch2* transcripts, limb explants were harvested from successfully targeted embryos at stage HH18 and cultured with 0, 2 or 8nM of Shh for 16 hours (Fig. 14A).

Explants electroporated with siRNAs and treated with 2 or 8nM Shh showed a binary 2-fold increase in *Gli1* transcripts compared to those not dosed with Shh. This was in contrast to control explants, which showed a graded response to increased Shh concentrations (Fig. 14B). Explants targeted with siRNAs and treated with 2nM Shh exhibited a significant increase in *Gli1* transcripts compared to those cultured without Shh and an increase in *Gli1* transcripts compared to control explants treated with 2nM Shh. Interestingly, explants targeted with siRNAs and treated with 0 or 8nM Shh exhibited a smaller increases in *Gli1* expression compared to control explants (Fig. 14B). This demonstrates that signal

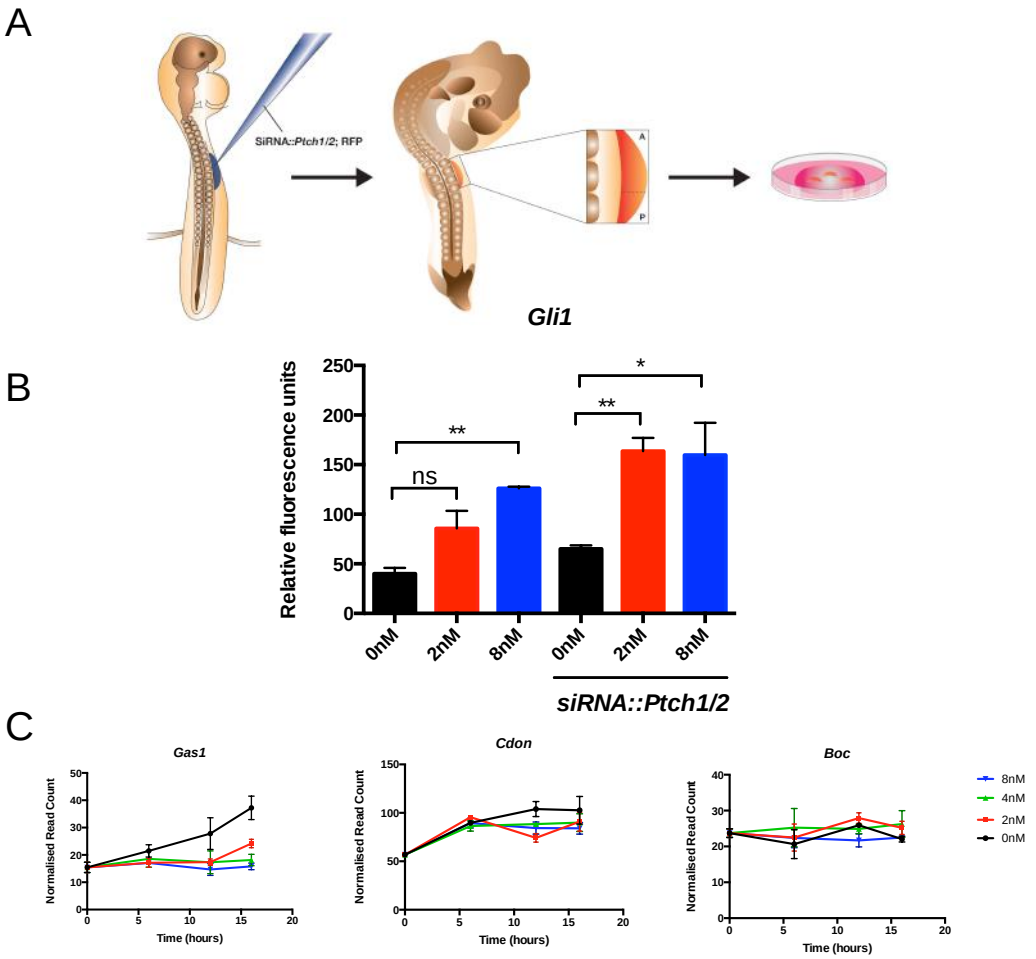

Figure 14 | Ligand dependent antagonism, mediated by *Ptch1/2,* causes desensitisation to Shh signalling in forelimb explants. (A) Experimental schematic. SiRNAs targeting *Ptch1* and *Ptch2* transcripts and a RFP reporter construct were electorporated into a cavity adjacent to the forelimb forming region at stage HH14. The anterior two thirds of RFP positive limbs were harvested at stage HH18 and cultured in the presence of Shh as previously described. (B) Relative expression (relative fluorescent units) of *Gli1* transcripts in forelimb explants cultured for 16 hours with indicated concentration of Shh, as determined by quantitative PCR (n=2-3 biological repeats of 3 explants per replicate ±SEM). Significance determined by paired T-tests, P-value = <0.01 (**), <0.05 (*), >0.05 (ns). Forelimb explants previously subject to 25 hours of siRNA treatment targeting *Ptch1* and *Ptch2* transcripts are denoted (siRNA). (C) Normalised read counts of Shh co-receptors *Gas1*, *Cdon* and *Boc* transcripts in forelimb explants treated with the indicated concentrations of Shh for designated times, as determined by RNAseq analysis (n=3±SEM). Levels of all transcripts were normalised using the total count (TC) method of normalisation.

desensitisation can be inhibited by disrupting the upregulation of *Ptch1* and *Ptch2* and has a more profound effect on explants exposed to lower doses of Shh.

Downstream signal transduction of the Shh pathway is mediated through activation of a 7-pass membrane protein Smoothened (Smo) (Alcedo et al., 1996; Ingham et al., 2000; van den Heuvel and Ingham, 1996b) (Fig. 2). To compliment siRNA experiments and gain further insight into whether Ptch1/2 mediated LDA is responsible for signal desensitisation in limb progenitors, I sought to determine the response of limb cells to direct Smo activation, bypassing any potential influence of Shh receptors. To do this, I exposed forelimb explants to equivalent doses of a smoothened agonist, purmorphamine, and measured the transcriptional responses of explants via qPCR analysis.

First, it was necessary to determine what concentration of purmorphamine would be equivalent to the concentrations of Shh used in previous experiments. In neural tube explants, a purmorphamine range of 0.025-2μM was shown to induce a full range of DV neuronal cell sub-types (Dessaud et al., 2007). Initially, I dosed forelimb explants with 0, 0.2, 0.4, 1.5, 3 or 6μM purmorphamine for 16 hours, to establish an appropriate dose range. Forelimb explants exhibited a graded response to purmorphamine whereby levels of *Gli1* transcripts increased in correlation with increased purmorphamine concentrations between 0.2 -3μM (Fig. 15A). Explants dosed with 0.4μM showed an approximately 2.5-fold increase in *Gli1* transcripts, whilst explants dosed with 3μM exhibited a 4-fold increase in *Gli1* transcripts (Fig. 15A). This was similar to the increases in *Gli1* transcripts induced by 2-8nM Shh. In subsequent experiments 0.4, 1.5 and 3μM were used as low, medium and high purmorphamine doses respectively.

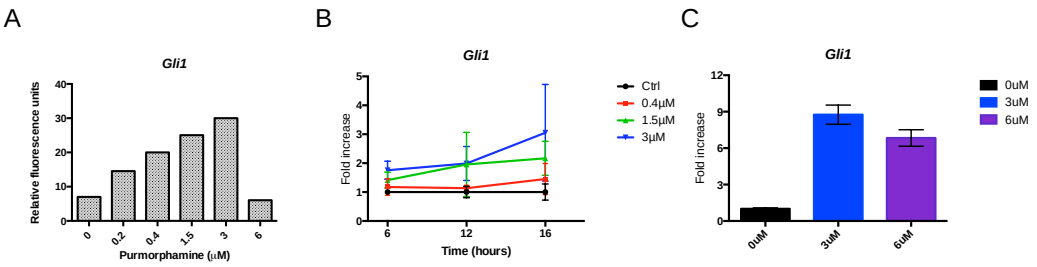

Figure 15| Effects of concentration and duration of purmorphamine exposure on the transcription of *Gli1* in forelimb explants. (A) Levels of *Gli1* transcripts in forelimb explants cultured with indicated concentrations of purmorphamine, for 16 hours, as determined by quantitative PCR (n=1). (B) Fold enrichment of *Gli1* transcripts in forelimb explants cultured with indicated concentrations of purmorphamine, for designated times, compared to vehicle controls, as determined by quantitative PCR (n=3±SEM). (C) Levels of *Gli1* transcripts in forelimb explants cultured with indicated concentrations of purmorphamine, for 16 hours, as determined by quantitative PCR (n=6±SEM). In all quantitative PCR samples levels of *Gli1* transcripts are normalised to levels of *Gapdh* transcripts.

To establish how limb progenitors respond to direct activation of Smo, forelimb explants were dosed with 0, 0.4, 1.5 or 3μM purmorphamine for 6, 12 or 16 hours. A graded response to increasing purmorphamine concentrations was seen at all time points (Fig. 15B). In contrast to explants dosed with Shh, explants exposed with equivalent doses of purmorphamine showed a continuous and linear increase in *Gli1* transcripts over time at low, medium and high doses (Fig. 15B). Desensitisation to Smo activation was not observed in explants dosed with lower doses of purmorphamine. This suggests that signal desensitisation, seen in explants treated with low doses of Shh, must be dependent upon a mechanism that acts upstream of Smo activation.

Surprisingly, in the pilot experiment, forelimb explants dosed with 6μM purmorphamine showed a relative decrease in *Gli1* transcripts compared to those dosed with 3μM (Fig. 16A). This suggests explants had become desensitised to Smo activation and could be indicative of another negative feedback mechanism downstream of Smo activation. To investigate if this was reproducible, I dosed forelimb explants with 0, 3 or 6μM for 16 hours (n=6) and measured levels of *Gli1* transcripts by qPCR. Although the effect was not as pronounced as previously observed, explants dosed with 6μM showed a 25% reduction in signal output as measured by *Gli1* expression (Fig. 15C). To investigate a possible negative feedback mechanism downstream of Smo activation, I used RNAseq to examine which genes were differently regulated in explants exposed to 0, 3 and 6μM of purmorphamine for 16 hours. Unfortunately, at the time of writing this report, I am still awaiting sequencing results.

4.5 *Sufu* is upregulated but *Gli2-3 and Disp1* are downregulated by Shh signalling

Negative feedback mechanisms are likely to impact components of the Shh signalling pathway. To investigate potential negative feedback mechanisms operating downstream of Smo activation via an alternative method, I interrogated the transcriptional response of key components of the Shh signalling pathway to different Shh treatments. The effect of Shh signalling on the transcription of Shh receptors and binding antagonists (Ptch1, Ptch2 and Hhip) and co-receptors (Gas1, Cdon and Boc) has been described (Fig. 12E; Fig. 14C). I also examined the expression of *Sufu, Kif7, Gli2, Gli3, Disp1* and *Scube2* in forelimb explants exposed to Shh. Sufu and Kif7 are involved in the intra-cellular transduction of Shh signalling and play a role in transporting Gli proteins through the primary cilia which is essential for their processing (Fig. 2, Introduction 1.2). Sufu and Kif7 also appear to be able to sequester Gli proteins in the cytoplasm. Sufu is a negative regulator Shh signalling whilst Kif7 has a more complex role and can act to promote or supress Shh signalling in different contexts promote Shh signalling (Jia et al., 2009; Kim et al., 2009; Maurya et al., 2013; Oh et al., 2015; Svärd et al., 2006; Tukachinsky et al., 2010; Wen et al., 2010) *Sufu* expression was upregulated in explants exposed to 4 or 8nM Shh only after 12 and 16 hours, but was unaffected by lower concentrations of Shh (Fig. 16A). Meanwhile, *Kif7* expression was unaffected by Shh signalling (Fig. 16A).

I next examined the response of transcriptional effectors of Shh signalling, *Gli1-3.* The transcriptional response of *Gli1* to Shh signalling has been described (Fig. 12). A reverse graded response to Shh signalling was observed in *Gli2* and *Gli3* expression, where increasing concentrations of Shh increasingly repressed *Gli2* and

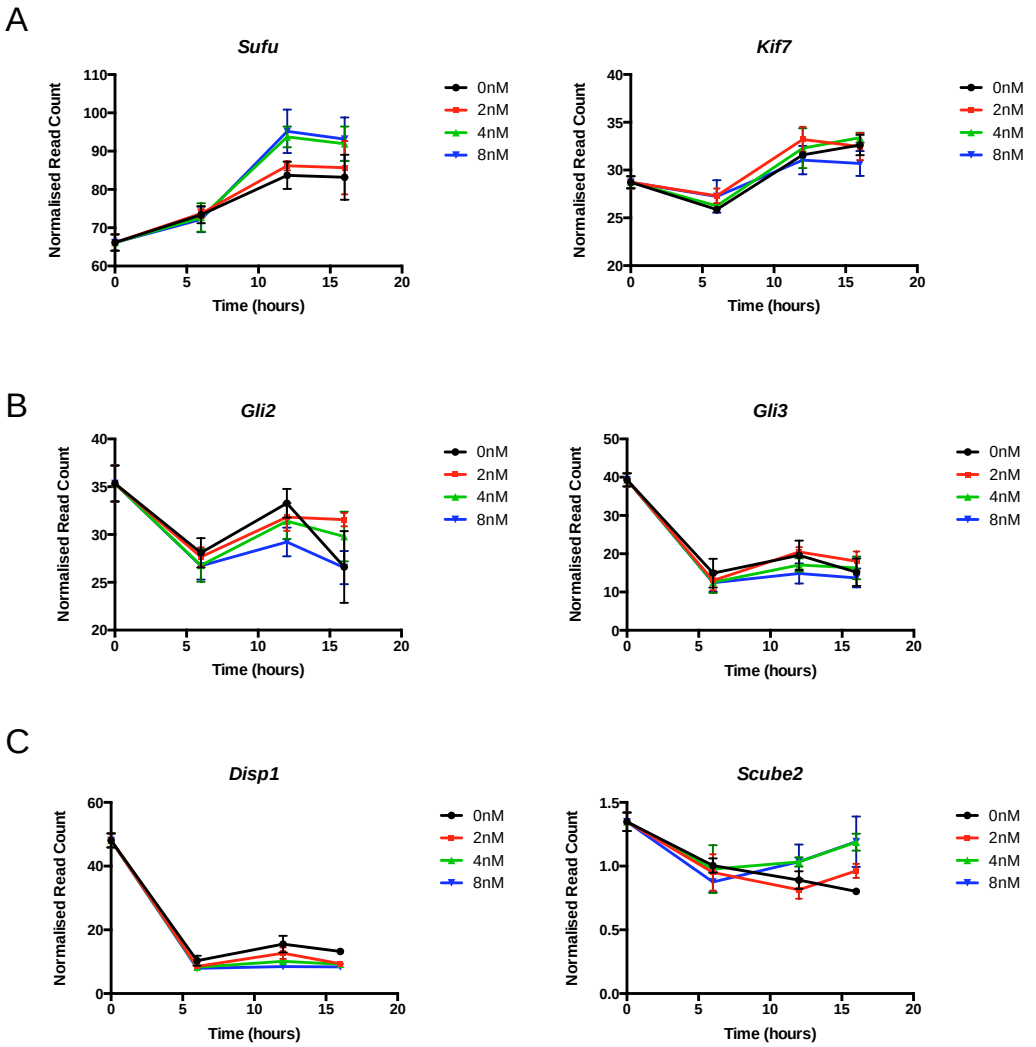

Figure 16 | Effects of Shh concentration and duration of Shh exposure on the transcription of components of hedgehog signalling in chick forelimb explants. Normalised read counts of components of intra-cellular Shh signal transduction (A), Shh transcriptional effectors (B) and components of Shh dispersion (C), in forelimb explants treated with the indicated concentrations of Shh for designated times, as determined by RNAseq analysis (n=3±SEM). All transcripts are normalised using the total count (TC) method of normalisation.

Gli3 expression after 6 and 12 hours. Intriguingly, after 16 hours, *Gli2* and *Gli3* expression was upregulated in explants exposed to low concentrations of Shh (2 and 4nM) compared to control explant, but explants exposed to 8nM Shh exhibited no difference in expression (Fig. 16B). Downregulation of *Gli2* and *Gli3* in response to Shh signalling was also observed in hindlimb explants which showed a reverse gradient at all time points, suggesting Shh signalling generally represses the expression of these genes (Data not shown).

Disp1, which is important for the release of Shh (Fig.2 Introduction 1.2), was also downregulated in response to Shh signalling after 12 and 16 hours (Fig. 16C). *Scube2*, which is also important for the release of Shh, was expressed at very low levels in all explants and was not significantly affected by Shh (Fig. 16C). Collectively, these results suggest that a downregulation of *Disp1* and an upregulation of *Sufu* may partly contribute to a transcriptional negative feedback loop to limit further Shh signalling.

Meanwhile, the downregulation of *Gli2* and *Gli3* may contribute to differences in the abundance of intra-cellular levels of GliA and GliR, and therefore may contribute to an overall downregulation of Shh signalling activity.

4.6 Genes implicated in anteroposterior (AP) identity exhibit a non-linear graded response to Shh in forelimb and hindlimb explants

A non-linear graded response to Shh signalling was observed in forelimb explants, as measured by the expression of *Gli1, Ptch1, Ptch2* and *Hhip.* These genes were used to measure levels of response to different levels of Shh signalling, but may not reflect different interpretations of Shh signalling in terms of specifying positional information. To determine if a non-linear graded response to Shh signalling was

important in establishing distinct anteroposterior (AP) positional domains in the developing limb bud, I examined the transcriptional response of genes that are known to play a role in limb development in forelimb explants dosed with Shh. In particular, I examined the expression profiles of genes known to have distinct endogenous AP expression patterns and genes previously described as targets of Shh Signalling.

The 5'HoxD cluster (*HoxD11-13*), *Bmp2*, *Tbx3* and *Hand2* are endogenously expressed posteriorly and are positively regulated by Shh signalling (Drossopoulou et al., 2000; Nelson et al., 1996; te Welscher et al., 2002b; Yamada et al., 2000). These genes have furthermore been implicated in specifying the identities of posterior digits (Drossopoulou et al., 2000; Suzuki et al., 2004; te Welscher et al., 2002b; Zákány et al., 2004). The transcriptional profiles of *Bmp2, Tbx3* and *HoxD13* were similar to that of *Gli1, Ptch1, Ptch2* and *Hhip*. After 6 hour of exposure, explants showed similar levels of expression regardless of the concentration of Shh they were exposed to (Fig. 17B). *Bmp2* and *Tbx3* showed a partially graded response after 12 hours, although similar levels of expression were observed between explants dosed with 4 and 8nM Shh (Fig. 17B).

Interestingly, the response of *HoxD13* expression remained binary after 12 hours of exposure, suggesting a possible time lag of *HoxD13* expression in response to Shh signalling compared to other targets. After 16 hours, a fully graded response of *Bmp2, Tbx3* and *HoxD13* expression was observed displaying both signal accumulation and signal desensitisation (Fig. 17B). HoxD12 and HoxD13 only showed any differential expression to different Shh concentrations after 16 hours, when signal accumulation was observed in explants treated with 8nM Shh (Fig. 17B). This again suggested that a transcriptional time lag might exist in the expression of the 5'HoxD cluster in response to Shh signalling. *Hand2* expression

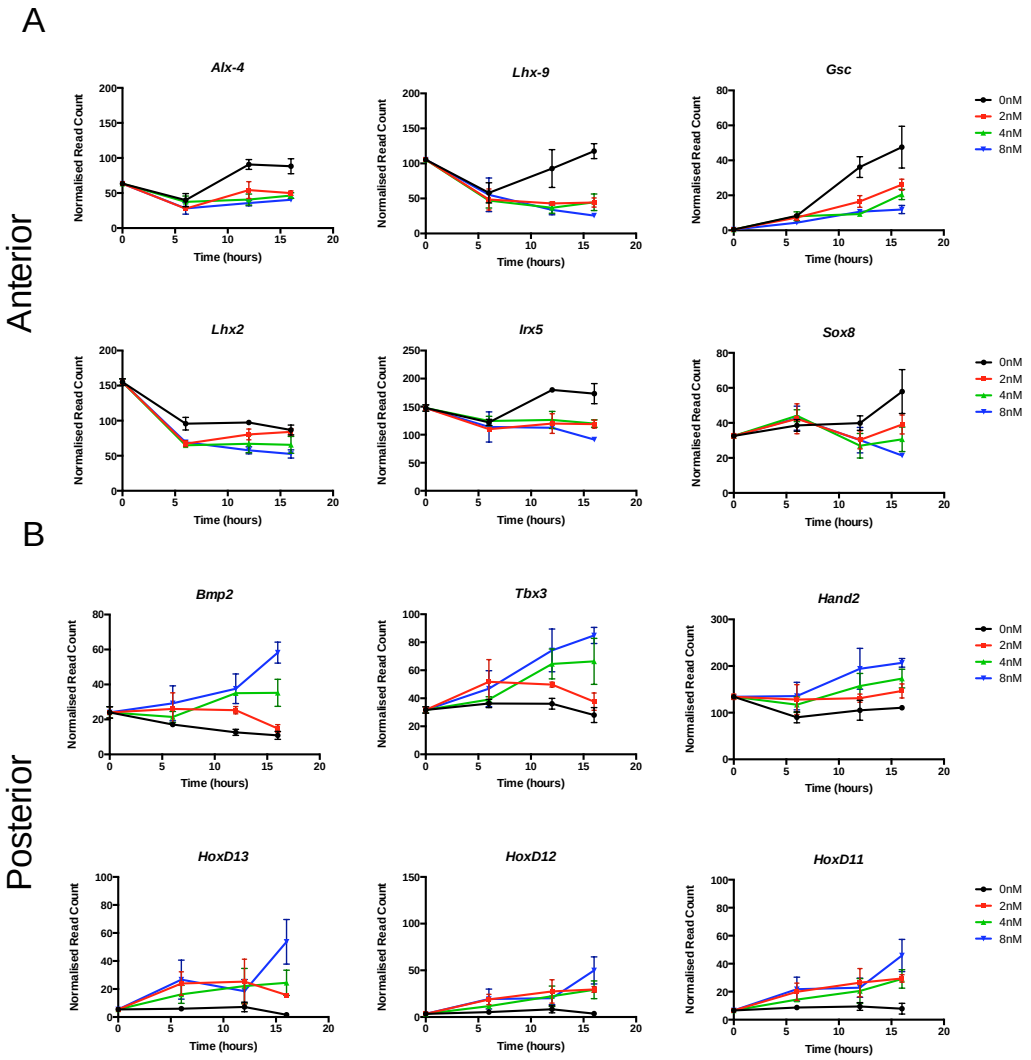

Figure 17| Effects of Shh concentration and duration of Shh exposure on the transcription of markers of anteroposterior (AP) identity in forelimb explants exhibit a non-linear. (A-B) Normalised read counts of transcripts that are endogenously anteriorly (A) and posteriorly (B) expressed limb buds, from forelimb explants treated with the indicated concentrations of Shh for designated times, as determined by RNAseq analysis (n=3±SEM). All transcripts are normalised using the total count (TC) method of normalisation.

showed a binary response after 6 hours and a graded response after 12 and 16 hours of Shh exposure (Fig.17B). However, there was no evidence of signal desensitisation measured by *Hand2* expression (Fig.17B).

I next examined the expression profiles of genes that are endogenously expressed anteriorly or have been reported to be negatively regulated by Shh, to examine whether a reverse graded response could be observed in the transcriptional profiles of these genes. This would provide further evidence that a non-linear graded response to Shh signalling is important in establishing distinct AP expression domains. Negatively regulated genes were expected to exhibit a continual fall in levels of transcription in explants exposed to the highest doses of Shh, reflecting continual repression by Shh. However, an increase in levels of transcription over time was expected in explants exposed to lower doses of Shh, as cells become desensitised to repression by Shh.

Alx-4, Lhx9, Lhx2, Irx5, Gsc and *Sox8* are expressed in the anterior half of developing limb buds during Shh patterning stages and may be implicated in specifying anterior digit identities (Bell et al., 2004; Bertuzzi et al., 1999; Heanue et al., 1997; Li et al., 2014a; Rodriguez-Esteban et al., 1998; te Welscher et al., 2002b). Explants not exposed to Shh showed a higher level of expression of all genes compared to those dosed with Shh. The expression profiles of negatively regulated genes also showed a reverse graded response to Shh; however, this was much tighter than the graded response observed in positively regulated genes (Fig. 17A). This suggests genes negatively regulated by Shh are more sensitive to Shh than those that are positively regulated. A partial or full graded response was also not clearly observed until after 16 hours of culture. Signal accumulation was most obviously observed in expression of *Lhx9*, *Lhx2*, *Irx5* and *Sox8*, in explants exposed to 8nM Shh, which exhibited the greatest continual decrease in levels of transcription over time (Fig.

17A). Signal desensitisation was also observed in *Sox8, Gsc* and *Lhx2* expression in explants exposed to 2nM Shh, which showed an increase in levels of transcripts after 16 hours of culture (Fig. 17A).

4.7 Hindlimb explants respond more rapidly than forelimb explants to Shh signalling

To determine if there were observable differences in the response of forelimb and hindlimb buds to Shh signalling, I examined the transcriptional profiles of select genes in hindlimb explants treated with Shh. Genes expressed endogenously in the posterior and anterior of developing limb buds were examined. A non-linear graded response to Shh signalling was observed in hindlimb explants, similar to that observed in forelimb explants. However, several interesting differences were seen.

Signal desensitisation was more clearly observed in *Hand2* and *HoxD11-13* in hindlimb explants dosed with 2nM Shh, compared to equivalent forelimb samples. Levels of *Hand2, HoxD11, HoxD12* and *HoxD13* showed a sharp decrease in hindlimb explants dosed with 2nM Shh for 16 hours (Fig. 18.2). This was not observed in equivalently dosed forelimb explants (Fig. 17B). Hindlimb explants exposed to both 4 and 8nM Shh exhibited an upregulation of *Hand2, HoxD11, HoxD12* and *HoxD13* after 16 hours, which resulted in a fully graded response in the expression of these genes (Fig. 18.2). Only explants exposed to 8nM Shh showed an increase in the transcription of these genes in forelimb explants and consequently only a partially graded response was observed (Fig. 17B).

Levels of *Bmp2* and *Gli1* transcripts also decreased in hindlimb explants exposed to 2nM Shh after 16 hours (Fig. 18.2). Interestingly, signal desensitisation was also

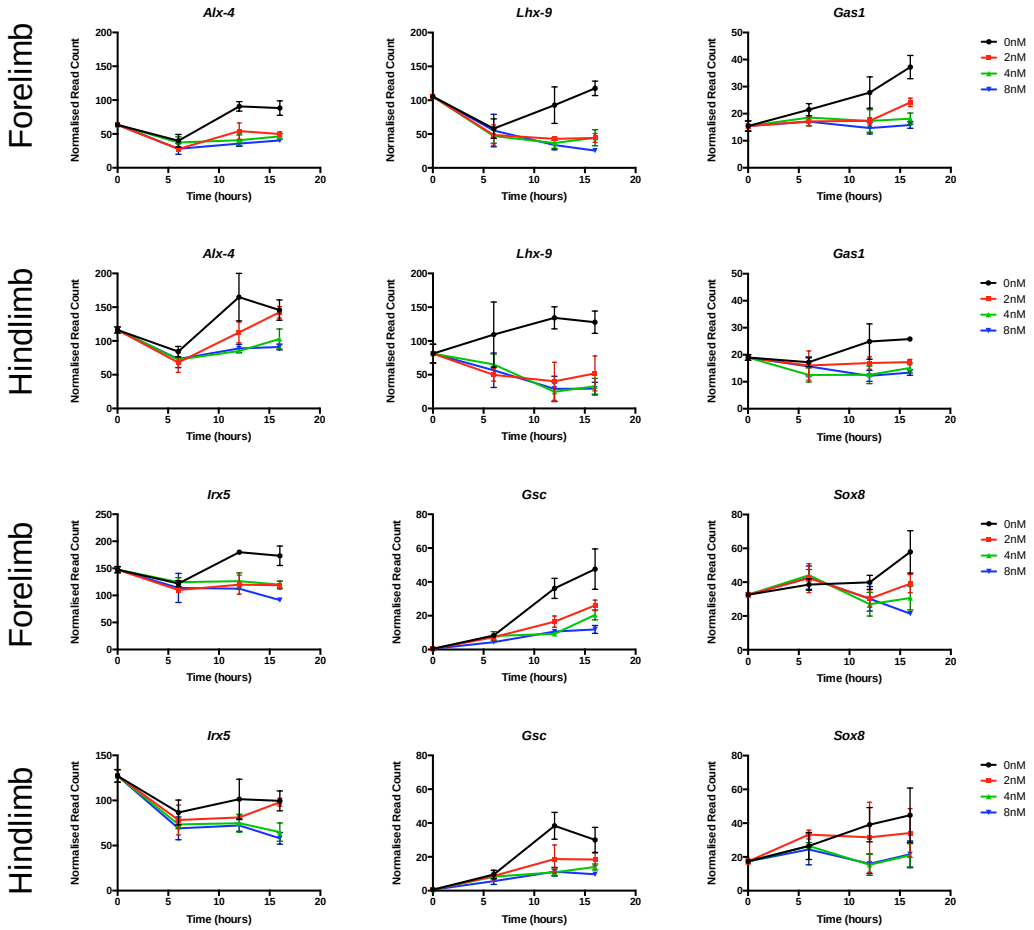

Figure 18 | A comparison of the effects of Shh concentration and duration of Shh exposure on the transcription of anterior markers in forelimb and hindlimb explants. Normalised read counts of transcripts negatively regulated by Shh, in forelimb and hindlimb explants treated with the indicated concentrations of Shh, for designated times, as determined by RNAseq analysis (n=3±SE). All transcripts are normalised using the total count (TC) method of normalisation.

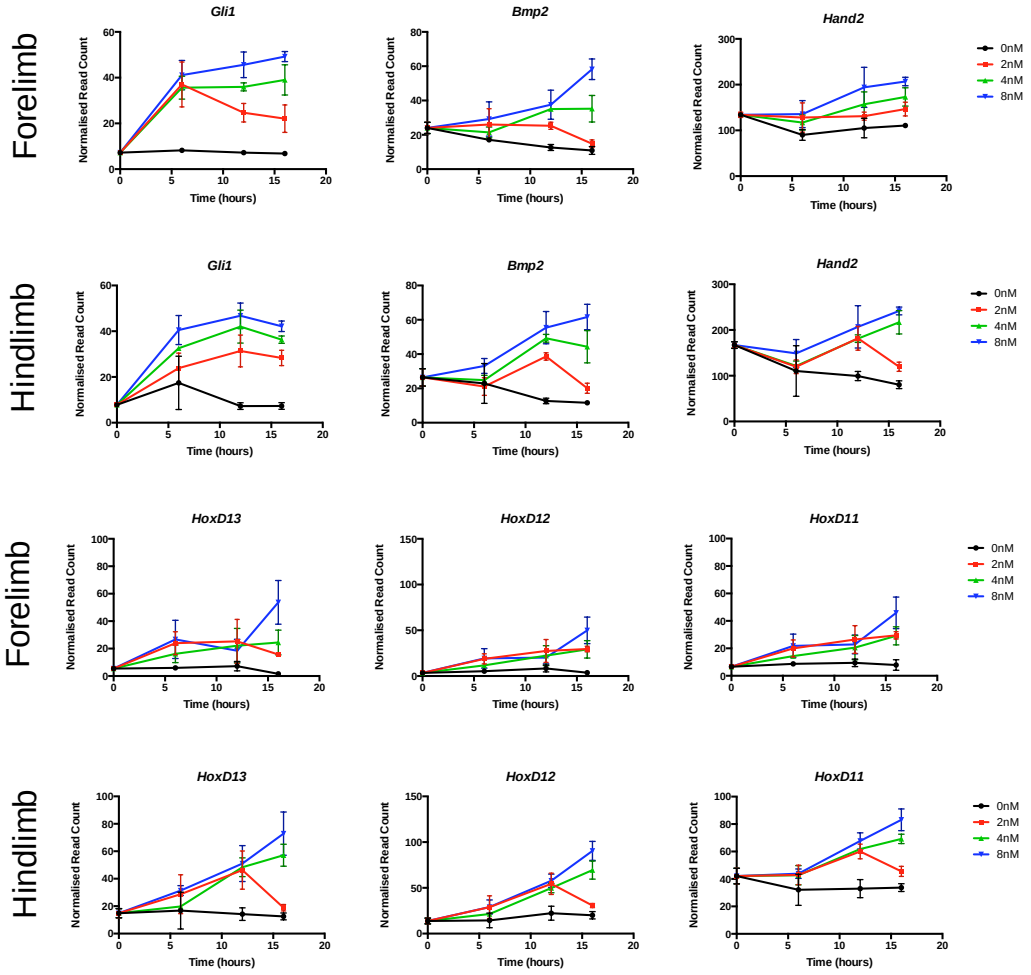

Figure 18.2 | A comparison of the effects of Shh concentration and duration of Shh exposure on the transcription of posterior markers in forelimb and hindlimb explants.

Normalised read counts of transcripts positively regulated by Shh, in forelimb and hindlimb explants treated with the indicated concentrations of Shh, for designated times, as determined by RNAseq analysis (n=3±SE). All transcripts are normalised using the total count (TC) method of normalisation.

observed in hindlimb explants exposed to 4 and 8nM Shh. *Bmp2* and *Gli1* expression showed a marked decrease in hindlimb explants exposed to 4nM Shh for 16 hours whilst explants exposed to 8nM Shh also showed a decrease or plateau in levels of *Gli1* transcripts at this time point (Fig. 18.2). This suggested that signal desensitisation had occurred in hindlimb explants exposed to the highest levels of Shh signalling by 16 hours and that a graded response was seen more rapidly in the expression of genes that show a delayed response to Shh. Thus, overall, both positive and negative responses to Shh signalling were observed more rapidly in hindlimb explants.

To further determine the response of hindlimb explants to Shh, I also examined the expression profiles of select genes that are endogenously expressed in the anterior of limb buds or are known to be negatively regulated by Shh signalling. This included *Alx-4, Lhx9, Gas1, Irx5, Gsc* and *Sox8.* As with forelimb explants, negatively regulated genes showed a tighter graded response than positively regulated genes in hindlimb explants (Fig. 18). However, graded responses were more evident in hindlimb explants. Signal desensitisation, demonstrated by an increase in the number of transcripts, was observed in the expression of *Alx-4, Lhx9, Irx5* and *Sox8,* after 16 hours in hindlimb explants dosed with 2nM Shh (Fig. 18). This was not observed in the expression of *Alx-4, Lhx9* and *Irx5* in equivalent forelimb samples (Fig. 17A). Signal desensitisation was also observed in the expression of *Sox8* in hindlimb explants exposed to both 4 and 8nM Shh after 16 hours (Fig. 18). The expression profiles of *Gsc* and *Gas1* were similar to that shown by equivalent forelimb samples (Fig. 18). These data are consistent with the proposal that hindlimb explants are at a more advanced stage of response to Shh signalling by 16 hours than forelimb explants.

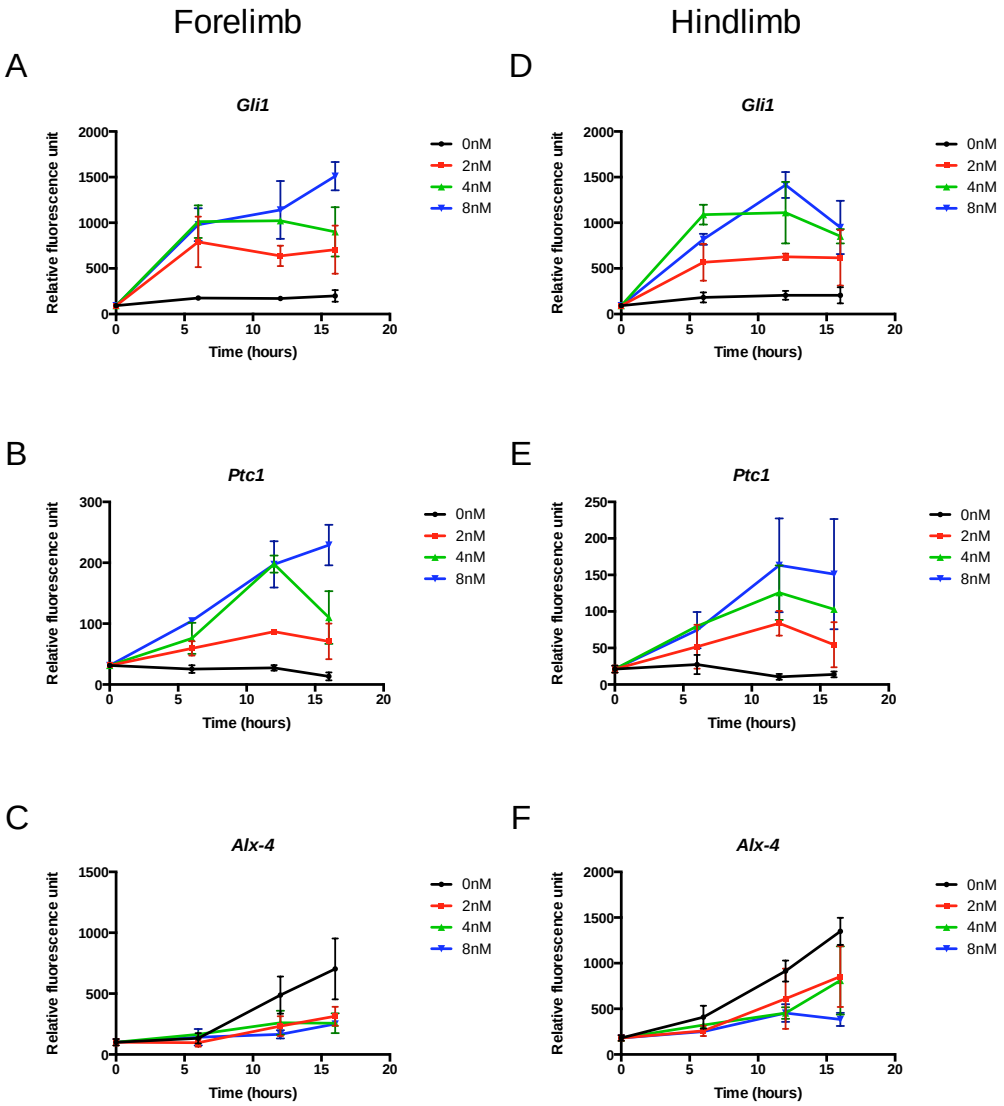

Figure 19| A non-linear graded response to Shh in limb explants is detected by quantitative PCR. Relative expression (relative fluorescent units) of *Gli1* (A, D), *Ptch1* (B, E) and *Alx-4* (C, F) transcripts in forelimb (A-C) and hindlimb (D-F) explants treated with the indicated concentrations of Shh for designated times as determined by quantitative PCR (n=3±SEM). In all samples levels of *Gli1*, *Ptch1* and *Alx-4* transcripts are normalised to levels of *Gapdh* transcripts.

For further confirmation of the transcriptional expression profiles observed by RNAseq, the transcriptional expression profiles of *Gli1, Ptch1* and *Alx-4* in forelimb and hindlimb explants were independently verified using qPCR analysis (Fig. 19 A-F). As seen using RNAseq, a non-linear graded response to Shh signalling was seen in forelimb and hindlimb explants, as determined by qPCR. Both signal accumulation and desensitisation were seen although the results of qPCR analyses were generally noisier (Fig. 19 A-F). The more rapid response of hindlimb explants to Shh signalling compared to forelimb explants was also detectable by qPCR (Fig. 19 A-F).

In this chapter I have investigated the transcriptional response of forelimb and hindlimb progenitors to different levels of Shh signalling using an *ex vivo* assay and RNAseq. I have described the development of this *ex vivo* assay and demonstrate that limb explants exhibit a graded response to increases in Shh signalling in this assay. Using RNAseq and qPCR I have demonstrated that limb explants establish a graded response to Shh signalling in a non-linear fashion through two related mechanisms: signal accumulation and signal desensitisation. I have further shown that desensitisation to Shh signalling is in part caused by a Ptch1/2 mediated feedback inhibition, but that upregulation of *Sufu,* and downregulation of *Gli2, Gli3, Disp1, Gas1* and *Cdon* may also contribute to negative feedback mechanisms. I have demonstrated that genes implicated in specifying different digit identities also show a non-linear graded response to Shh signalling which provides evidence that both signal accumulation and signal desensitisation are required for the correct interpretation of the Shh morphogen gradient in the limb. Lastly, I have described differences in the response of forelimb and hindlimb progenitors to equivalent Shh signalling, and have provided evidence that hindlimb progenitors show a complete

range of response to Shh signalling over a shorter period of time than forelimb progenitors.

Chapter 5: *In silico* and *in situ* analysis of the interpretation of graded Shh signalling in chicken forelimbs and hindlimbs

In the previous chapter I investigated how limb progenitors respond to different levels and durations of Shh signalling by examining the expression profiles of known Shh targets. In this chapter, I describe the use of an unbiased, *in silico* approach to uncover genes that have not been previously described as being regulated by Shh, RNAseq results. I identify genes that are differentially expressed (DE) in explants exposed to specific Shh treatments compared to control explants and identify candidate genes that may be expressed in specific domains across the AP axis based on their transcriptional response profiles. I have further screened a subset of candidate genes via whole mount *in situ* hybridisation and demonstrate that my *in silico* analyses can predict the expression domains of some genes. Finally, I have attempted to use electroporation to mis-express one of the most promising candidates, BMP antagonist *Smoc1,* in chicken forelimb buds to determine if it is sufficient to specify middle digits identities.

5.1 Genes implicated in limb development are differentially expressed in explants exposed to Shh

It has been demonstrated that graded Shh signalling can induce the expression of specific transcription factors, in restricted progenitor domains of the developing vertebrate neural tube. Expression of these transcription factors mark progenitors that give rise to distinct neuronal cell sub-types and may be implicated in specifying neuronal identities (Briscoe et al., 1999; Briscoe et al., 2000; Dessaud et al., 2007). To determine if a similar code of transcription factors is expressed in response to graded Shh signalling in the limb, I used *in silico* analyses to identify genes that are transcriptionally activated or repressed in response to specific concentrations and/or durations of Shh signalling.

To determine which genes are induced or repressed by specific levels or durations of Shh signalling in limb explants I used one-way ANOVA and Tukey's Post-hoc analysis to identify genes that were statistically differentially expressed (DE) in forelimb explants exposed to low, medium or high concentrations of Shh for 6, 12 or 16 hours, compared to control explants. I subsequently ordered genes by the difference in the level of expression in explants under a designated Shh treatment compared to control explants, to identify genes that were most induced or repressed by specific Shh treatments (Tables 3-4, Appendix 1-2, Materials and Methods 2.10). RNAseq analysis produces large quantities of data. In this report I have chosen to focus my analysis on the 50 most induced/repressed genes, with particular emphasis on transcription factors and genes implicated in major signalling pathways, as these are most likely to mark or specify different digit identities (Tables 3-6, Appendices 1-4).

In general, explants exposed to higher concentrations of Shh or for longer periods of time, exhibited a greater number of differentially expressed genes, including genes previously described as targets of Shh signalling in the limb. Forelimb explants dosed with 2, 4 or 8nM Shh for 6 hours showed differential expression of direct targets of Shh signalling, *Gli1* and *Ptch1,* and other genes of interest including Fork-head box transcription factors *Foxc2 and Foxo6, C-Fos Induced Growth Factor (Figf) (Vascular Endothelial Growth Factor D),* and *Ciliary Neurotrophic Factor Receptor* (*Cntfr*) (Table 3, Appendix 1). *LIM Homeobox 2* (*Lhx2*) was the only transcription factor downregulated at this time point (Table 4, Appendix 2). Consistently, *Figf* and *Cntfr* have previously been described as targets of Shh in the limb and neural tube respectively, whilst *Lhx2* is expressed in the anterior of the early limb bud, consistent with it being repressed by Shh signalling (Davey et al., 2007; Lewandowski et al., 2015; Rodriguez-Esteban et al., 1998).

6 hours						12 hours						16 hours					
2nM		4nM		8nM		2nM		4nM		8nM		2nM		4nM		8nM	
1	GLI1	1	FOXC2	1	GLI1	1	AMER2	1	AMER2	1	PTCH2	1	APOD	1	PTCH2	1	PTCH2
2	AMER2	2	PTCH1	2	HS3ST2	2	GLI1	2	CNTFR	2	HHIP	2	KIRREL3	2	AMER2	2	HHIP
3	FOXC2	3	CNTFR	3	FOXC2	3	PTCH1	3	GLI1	3	OSR1	3	FIGF	3	GLI1	3	HOXD13
4	NTN1	4	FOXO6	4	PTCH1	4	FIGF	4	LHX6	4	CNTFR	4	FGF10	4	CNTFR	4	HOXD12
5	PTCH1	5	STRA6	5	NTN1	5	TRIB1	5	PTCH1	5	GLI1	5	IRK1	5	FOXD1	5	OSR1
6	STRA6	6	TRIB1	6	CNTFR	6	RHOJ	6	HAPLN1	6	LHX6	6	VTN	6	SMOC1	6	PTCH1
7	CNTFR	7	FIGF	7	FIGF	7	CDK6	7	EFEMP1	7	AMER2	7	GREM1	7	KCNH5	7	AMER2
8	FIGF	8	CASS4	8	TRIB1	8	IRK1	8	FOXC2	8	PTCH1	8	SALL1	8	HAPLN1	8	GLI1
9	CASS4	9	P2RY1	9	STRA6	9	ASB9	9	KCNH5	9	HS3ST2	9	FSTL4	9	APOD	9	CNTFR
10	HAPLN1	10	TMEM106C	10	CASS4	10	TSKU	10	CNGA3	10	FOXC2	10	ADAM23	10	LHX6	10	EFEMP1
11	P2RY1	11	GRAMD1C	11	FOXO6	11	ENC1	11	TRIB1	11	EFEMP1	11	CMTM8	11	FOXC2	11	HOXD11
12	na	12	B4GALT3	12	P2RY1	12	ELMO1	12	KIRREL3	12	SPRY4	12	HOXA7	12	KIRREL3	12	LHX6
13	TMEM106C	13	SOX9	13	HOXA10	13	PTPRZ1	13	STRA6	13	SPRY4	13	PLCD1	13	BMP2	13	BMP2
14	IRK1	14	GDAP1L1	14	THBD	14	GNPDA1	14	FIGF	14	TRIB1	14	FAM49A	14	HAS2	14	KCNH5
15	na	15	HES4	15	MORN5	15	KBTBD11	15	BMP2	15	KCNH5	15	PLCG1	15	STRA6	15	FOXD1
16	RNF122	16	EYA1	16	CPLX2	16	SLC38A6	16	IRK1	16	CNGA3	16	MMP11	16	FIGF	16	FOXC2
17	PALM	17	RNF122	17	RNF122	17	FGF10	17	HAS2	17	BMP2	17	LPIN1	17	IRK1	17	HAPLN1
18	SOX9	18	CAPN5	18	EPHB1	18	RIC3	18	ADAMTS9	18	FIGF	18	EPHB3	18	VTN	18	TRIB1
19	GDAP1L1	19	na	19	PIM1	19	MAP4K4	19	TSKU	19	P2RY1	19	na	19	FGF10	19	FOXL1
20	RAB11FIP4	20	SCPEP1	20	TMEM106C	20	HPGDS	20	SPATA13	20	STRA6	20	DDX31	20	SPRY4	20	KIRREL3
21	HES4	21	NUDT19	21	IRK1	21	PDE5A	21	MORN5	21	RHOJ	21	DNM1	21	SPRY4	21	NANOS1
22	B4GALT3	22	CDC42EP1	22	IL11RA	22	CXCL12	22	RHOJ	22	MORN5	22	KCTD1	22	PAMR1	22	APOD
23	TLE3	23	FAM92A1	23	RHOJ	23	TLL1	23	TMEM132D	23	FOXO6	23	COMMD5	23	C1QTNF5	23	FIGF
24	na	24	TM2D3	24	HES4	24	CD69	24	PTGS1	24	PTGS1	24	40057	24	ELMO1	24	IRK1
25	PREP2	25	SCCPDH	25	TSPO	25	GJA1	25	FOXO6	25	TSKU	25	MED24	25	MORN5	25	RAMP1
26	PRICKLE2	26	SLC25A22	26	C16orf59	26	AGPAT5	26	CDK6	26	IRF10	26	na	26	CDK6	26	SPRY4
27	ZNF704	27	PLCG1	27	na	27	C11ORF24	27	ELMO1	27	IRK1			27	IRF10	27	SPRY4
28	SCPEP1	28	ACBD6	28	KLHL17	28	na	28	PIM1	28	PAX1			28	SALL1	28	P2RY1
29	CDC42EP1	29	MRPS17	29	GNPDA1	29	CPED1	29	ENC1	29	PIM1			29	TMEM132D	29	TBX3
30	PLCG1			30	PRICKLE2	30	na	30	KBTBD11	30	DUSP26			30	RHOJ	30	STRA6
31	APBB2			31	TLE3	31	TUB	31	PODXL	31	na			31	SLC25A22	31	HAS2
32	TM2D3			32	PARP16	32	CTSD	32	NDNF	32	ADAMTS9			32	FAR-1	32	FGF1
33	SLC25A22			33	B4GALT3	33	ABCC3	33	PAMR1	33	HS3ST3A1			33	PTGS1	33	VTN
34	SCCPDH			34	CDC42EP1	34	ZNF521	34	EPHB1	34	LMCD1			34	FZD10	34	FGF10
				35	GDAP1L1	35	APBB2	35	CAPN5	35	EPHB1			35	SORBS1	35	IGF2
				36	WDR83OS	36	38596	36	TLL2	36	ASB9			36	CPED1	36	MORN5
				37	PLCG1	37	NOTCH2	37	GNPDA1	37	LMO7			37	SLC38A6	37	RSPO3
				38	CYB5D2	38	PARP16	38	ASB9	38	LRRC32			38	PODXL	38	PODXL
				39	SCPEP1	39	C7H2orf69	39	MAP4K4	39	KBTBD11			39	EYA1	39	ELMO1
				40	AGPAT5	40	SCPEP1	40	GDAP1L1	40	ABCG4			40	SNED1	40	SALL1
				41	RAB11FIP4	41	ZNHIT6	41	RIC3	41	NPY			41	GRAMD1C	41	VSTM2L
				42	SLC25A22	42	MSI2	42	EYA1	42	na			42	SDK2	42	RHOJ
				43	PREP2	43	GPHN	43	PRKD1	43	GBX2			43	EPHB1	43	CDK6
				44	TM2D3	44	SETD7	44	SLC25A22	44	FGF10			44	COL4A2	44	na
				45	APBB2	45	PLCG1	45	GRAMD1C	45	na			45	PLEKHH2	45	CASS4
				46	CRYM	46	UBE4A	46	SEMA6A	46	ELMO1			46	SDC3	46	TSKU
				47	ZNF740	47	na	47	na	47	GNPDA1			47	CPLX2	47	PTGS1
				48	DUSP14	48	PWP1	48	VEGFA	48	TMEM200B			48	CAMK2D	48	IRF10
				49	PFDN1	49	LRP5	49	PIGA	49	ENC1			49	APBB2	49	ABCC3
						50	ASNS	50	ABCC3	50	CAPN5			50	TMTC2	50	SIX1

Table 3 | Genes significantly upregulated by different Shh treatments in forelimb explants. Genes that are positively, differentially expressed in forelimb explants dosed with designated concentration of Shh morphogen for designated period of time, compared to control explants, as measured by normalised read counts. Gene lists are ordered by greatest difference in normalised read counts between explants under designated treatment and control explants. Novel, unnamed genes are described as "na". Significance determined by one-way ANOVA and Tukey's post hoc test, p= <0.05.

6 hours						12 hours						16 hours					
2nM		4nM		8nM		2nM		4nM		8nM		2nM		4nM		8nM	
1	APOA1	1	MYLK	1	APOA1	1	GSC	1	GSC	1	GSC	1	DKK-1	1	LHX9	1	LHX9
2	KRT15	2	ST3GAL1	2	MYLK	2	PTX3	2	ALX-4	2	ALX-4	2	LHX9	2	RASL11B	2	GSC
3	TGFB2	3	LHX2	3	LGR5	3	IRX5	3	MSX1	3	PTX3	3	FILIP1L	3	GAS1	3	PTX3
4	COL12A1	4	GPR137C	4	ST3GAL1	4	P4HA3	4	PTX3	4	BARX2B	4	RASL11B	4	FILIP1L	4	SOX8
5	MYLK	5	PLEKHA1	5	LHX2	5	CDON	5	RASL11B	5	MSX2	5	CCK	5	MERTK	5	RASL11B
6	LHX2	6	HEG1	6	DCN	6	na	6	HS6ST1	6	MSX1	6	MSX2	6	ALX-4	6	GAS1
7	PLEKHA1	7	LSP1	7	TSHZ1	7	PRRX1	7	CD82	7	WNT7B	7	ALX-4	7	MSX2	7	TOX
8	ORC6	8	RAB30	8	LSP1	8	LPAR2	8	LGR5	8	TMEM108	8	MSX1	8	CD82	8	CCK
9	RAB30	9	TPM1	9	HNRNPD	9	THSD7B	9	ZIC2	9	RASL11B	9	CD82	9	MSX1	9	ALX-4
				10	KIF5C	10	SOSTDC1	10	PRRX1	10	CD82	10	GAS1	10	CCK	10	FILIP1L
				11	TPM1	11	HS6ST1	11	BARX2B	11	TFAP2B	11	S100A16	11	na	11	PKP2
				12	DNM1L	12	na	12	GLCCI1	12	VIT	12	IRX5	12	SGK1	12	MERTK
				13	GDI2	13	LMO4	13	na	13	LHX2	13	MERTK	13	S100A16	13	GAS1
				14	GSPT1			14	LMO4	14	PRRX1	14	PTRF	14	PRRX1	14	CD82
				15	ARF5			15	CCRN4L	15	HS6ST1	15	HS6ST1	15	HS6ST1	15	MSX1
				16	YWHAQ			16	COL24A1	16	LGR5	16	SCNM1	16	IRX5	16	MSX2
								17	ALDH18A1	17	DACT2	17	PSMB3	17	STX18	17	IRX5
								18	CEP76	18	IRX5	18	SPCS1	18	PTRF	18	HS6ST1
								19	BMP7	19	PAK1	19	FEZ1	19	FEZ1	19	TMEM108
								20	COG1	20	GLCCI1	20	na	20	LLPH	20	PRRX1
								21	MRPL15	21	SOSTDC1	21	MYL4	21	POLR1D	21	DISP1
										22	RSPO2	22	SPRYD3	22	ASPG	22	SH3D19
										23	TMEM200A	23	na	23	LMO4	23	SGK1
										24	TP63	24	CHSAP18	24	SPCS1	24	OLFM1
										25	SLC25A29	25	CHMP1A	25	RAB20	25	RAB4A
										26	THSD7B	26	RNF41	26	PSMB3	26	ANGPT1
										27	PPFIBP2	27	ZNF740	27	SYNGR2	27	S100A16
										28	CEP76	28	SMAP2	28	RPL29	28	ADAM33
										29	ITFG1	29	NUDCD3	29	na	29	BMP4
										30	CCNDBP1			30	DAD1	30	GLCCI1
										31	LMO4			31	na	31	FEZ1
										32	IRF6			32	RPB6	32	BLOC1S4
										33	APLP2			33	TMA7	33	STX18
										34	na			34	MON1A	34	COQ10B
										35	na			35	ZNF740	35	na
										36	FBLN2			36	MRPL30	36	OTUD3
										37	PRDM10			37	na	37	LMO4
										38	BMP7			38	RNF41	38	ASPG
										39	ABHD12			39	RPL21	39	na
										40	BAHD1			40	TXN2	40	SHROOM4
										41	ACADL			41	RPL27	41	RAB20
										42	na					42	PBX3
										43	ZADH2					43	C16ORF5
										44	TWF1					44	PTRF
										45	AKR1A1					45	SPOCK2
										46	COG1					46	KHDRBS3
										47	ZNF330					47	ACAD8
										48	AAGAB					48	SLC7A6OS
										49	ACAD9					49	SPCS1
										50	PAPSS1					50	na

Table 4| Genes significantly downregulated by different Shh treatments in forelimb explants. Genes that are negatively differentially expressed in forelimb explants dosed with designated concentration of Shh morphogen for designated period of time, compared to control explants, as measured by normalised read counts. Gene lists are ordered by greatest difference in normalised read counts between explants under designated treatment and control explants. Novel, unnamed genes are described as "na". Significance determined by one-way ANOVA and Tukey's post hoc test; p= <0.05.

Explants exposed to Shh for 12 hours also showed upregulation of *Gli1* and *Ptch1* as expected, and *Ptch2, Hhip* and *Bmp2,* in those exposed to 8nM Shh (Table 3, Appendix 1). Other potentially interesting genes upregulated included transcription factors: *Odd Skipped Related 1* (*Osr1*), *Foxc2, Foxo6* and *Lhx6*; negative regulator of Wnt signalling, *APC Membrane Recruitment Protein 2* (*Amer2*); inhibitor of the MAP kinase pathway *Sprouty4* (*Spry4);* proteoglycan *Tsukushi* (*Tsku*) - which can act as a BMP antagonist (Ohta et al., 2004) and heparan sulfate biosynthetic enzyme, *Heparan Sulfate (Glucosamine) 3-O-Sulfotransferase 2* (*Hs3st2*) (Table 3, Appendix 1). *Osr1* is expressed posteriorly, whilst Heparan Sulphate Proteoglycans (HSPGs) appear to be required for normal dispersion of Shh (Briscoe and Thérond, 2013; Stricker et al., 2006).

Genes that have been previously described as downregulated by Shh or are known to be expressed in the anterior of limb buds were shown to be statistically downregulated after 12 hours of Shh exposure. Homeobox transcription factors *Goosecoid (Gsc), Alx-4, Msh Homeobox 2* (*Msx2), Msx1* and *Iroquois Homeobox 5* (*Irx5*) were downregulated by Shh after 12 hours and are expressed anteriorly in early limb buds(Bell et al., 2004; Heanue et al., 1997; Li et al., 2014b; te Welscher et al., 2002b). Interestingly, *Bmp7* and heparan sulfate biosynthetic enzyme *Heparan Sulfate 6-O-Sulfotransferase 1* (*Hs6st1*) were also downregulated (Table 4, Appendix 2).

After 16 hours, explants exposed to 4 or 8nM Shh differentially expressed several genes associated downstream of Shh signalling including *Gli1, Ptch1, Ptch2, Hhip, Hoxd11-13*, *Bmp2*, *Tbx3, Sall1* and *Hand2.* Transcription factors *Foxc2, Foxd1, Foxl1, Six Homeobox 1* (*Six1*) were also upregulated, as well as, *EGF Containing Fibulin-Like Extracellular Matrix Protein 1* (*Efemp1*), *Fgf1, Fgf10,* cell cycle regulator *Cyclin Dependent Kinase 6* (Cdk6) and translational repressor *Nanos Homolog 1* (*Nanos1*).

6 hours						12 hours						16 hours					
2nM		4nM		8nM		2nM		4nM		8nM		2nM		4nM		8nM	
1	GPATCH3	1	MSC	1	SAMD11	1	SIX1	1	PTCH2	1	PTCH2	1	CNTFR	1	PTCH2	1	PTCH2
		2	MDM2	2	MAPK8IP2	2	ALDH1A2	2	GLI1	2	GLI1	2	GLI1	2	CNTFR	2	HHIP
		3	ZNF839	3	NRP1	3	BMP2	3	PTCH1	3	FOXF1	3	AMER2	3	HHIP	3	CNTFR
		4	EXD2	4	PRKD1	4	PIGG	4	BMP2	4	PTCH1	4	FIGF	4	OSR1	4	OSR1
		5	LSM14B	5	GAK	5	ADAMTS9	5	SIX1	5	HAPLN1	5	IRK1	5	FOXF1	5	EFEMP1
		6	ASXL1	6	PELO	6	FGFR4	6	DPYS	6	BMP2	6	STRA6	6	GLI1	6	HOXD13
		7	ODF2	7	F2RL2	7	PMP22	7	FIGF	7	FIGF	7	NGFR	7	HOXD13	7	FOXF1
		8	C5orf24	8	TSSC4	8	GRAMD1C	8	PODXL	8	SIX1	8	PTCH1	8	FIGF	8	PTCH1
				9	CNOT4	9	PKDCC	9	PAG1	9	IGF2	9	SCUBE3	9	BMP2	9	GLI1
				10	PTP4A3	10	MSANTD1	10	PIGG	10	ANO1	10	OPRM1	10	AMER2	10	BMP2
				11	SYT11	11	FZD10	11	NPR3	11	ALDH1A2	11	GDAP1L1	11	PTCH1	11	FIGF
				12	C5orf24	12	HOXD11	12	HAS2	12	PODXL	12	RASGEF1B	12	WT1	12	AMER2
						13	TBX3	13	SLC26A9	13	POSTN	13	PTPRU	13	HOXD12	13	HOXD12
						14	DNAJC12	14	GRAMD1C	14	HAS2	14	ELMO1	14	HAND2	14	FGF1
						15	KIAA1462	15	MSANTD1	15	LHX6	15	EYA1	15	LIX1	15	RASGEF1B
						16	TMEM106C	16	FRAS1	16	SLC26A9	16	RUNX1T1	16	CPXM2	16	na
						17	ZNF704	17	HOXA13	17	NPR3	17	na	17	PIGG	17	SIX1
						18	MANBA	18	P2RY1	18	PAG1	18	PODXL	18	FOXC2	18	SPRY4
						19	COL6A3	19	NCALD	19	TBX3	19	PTN	19	IRK1	19	SPRY4
						20	CD151	20	PLOD2	20	EMB	20	ASB9	20	VSTM2L	20	GJA4
						21	C10ORF11	21	HOXD11	21	GRAMD1C	21	LIMS1	21	HOXA13	21	HAND2
						22	na	22	DNAJC12	22	PIGG	22	na	22	TBX3	22	ENSGALG11911
						23	na	23	HES4	23	GDAP1L1	23	GRAMD1C	23	RASGEF1B	23	PIGG
						24	na	24	TLL2	24	ADAMTS9	24	COL4A2	24	PODXL	24	VTN
						25	PLOD2	25	TBX3	25	na	25	SLC38A6	25	RSPO3	25	TBX3
						26	NPNT	26	FABP5	26	VTN	26	TSKU	26	HOXD11	26	CPXM2
						27	SCPEP1	27	PKDCC	27	HOXD11	27	NEURL1B	27	GDAP1L1	27	HOXD11
						28	PIK3IP1	28	PDXK	28	HES4	28	CORTBP2	28	STRA6	28	HOXA13
						29	TOB	29	TMEM106C	29	MSANTD1	29	Unchar4	29	SCUBE3	29	VSTM2L
						30	ASB9	30	OLFM3	30	P2RY1	30	NR2F2	30	PDZRN4	30	ELMO1
						31	KIAA1715	31	GPRIN3	31	HOXA13	31	MSI1	31	TOX2	31	LMO1
						32	DEPDC1	32	KITLG	32	PLOD2	32	EPHB3	32	IRF10	32	ADAMTS9
						33	APP	33	PAWR	33	FGFR4	33	STXBP5	33	EYA1	33	KCNH5
						34	B4GALT3	34	ZNF704	34	PTGS1	34	SRR	34	RUNX1T1	34	PODXL
						35	AGA	35	SCPEP1	35	P4HA2	35	KLHL25	35	HEY1	35	IRK1
						36	RRAS2	36	PTGS1	36	NCALD	36	HOXA10	36	CYYR1	36	SCUBE3
						37	na	37	na	37	TLL2	37	ROR1	37	GRAMD1C	37	CASS4
						38	RAB11B	38	PIM1	38	TMEM200B	38	PCSK6	38	GNPDA1	38	EYA1
						39	KPNA2	39	SKAP2	39	PDXK	39	STRADB	39	SARM1	39	RSPO3
						40	RNF7	40	IGFBP2	40	DNAJC12	40	SCPEP1	40	SLC38A6	40	GDAP1L1
						41	PLK1	41	ASB9	41	HHIPL1	41	GPHN	41	FAM163A	41	SLC38A6
						42	CBX3	42	AP1S2	42	MORN5	42	DPYD	42	FAM101B	42	TOX2
						43	SAMM50	43	MTHFSD	43	SDK2	43	JDP2	43	ARAP3	43	IRF10
						44	ARPC1A	44	DCN	44	TMEM106C	44	AFAP1	44	FGF10	44	na
						45	BLCAP	45	TJP2	45	PPAPDC1A	45	LSM14B	45	NEURL1B	45	LIMS1
								46	GPSM1	46	ZNF704	46	MAP4K3	46	Unchar4	46	HAS2
								47	DEPDC1	47	PKDCC			47	LIMS1	47	GNPDA1
								48	PIK3IP1	48	OLFM3			48	HOXA11	48	IL13RA2
								49	CHST6	49	NELF			49	COL4A2	49	FGF10
								50	SNX6	50	SCPEP1			50	AGPAT5	50	PDZRN4

Table 5| Genes significantly upregulated by different Shh treatments in hindlimb explants. Genes that are positively, differentially expressed in hindlimb explants dosed with designated concentration of Shh morphogen for designated period of time, compared to control explants, as measured by normalised read counts. Gene lists are ordered by greatest difference in normalised read counts between explants under designated treatment and control explants. Novel, unnamed genes are described as "na". Significance determined by one-way ANOVA and Tukey's post hoc test; $p = <0.05$.

6 hours			12 hours						16 hours					
2nM	4nM	8nM	2nM		4nM		8nM		2nM		4nM		8nM	
<empty>	<empty>	<empty>	1	na	1	Unchar7	1	LHX9	1	PTX3	1	CRABP-I	1	GLIS1
			2	Unchar1	2	na	2	Unchar1	2	MSX1	2	FGFBP1	2	LHX9
			3	LHX9	3	Unchar1	3	na	3	MSX2	3	LHX9	3	ALX-4
			4	FILIP1L	4	LHX9	4	MSX1	4	MT1	4	CHST9	4	PTX3
			5	MSX1	5	na	5	LHX2	5	LAD1	5	PTX3	5	MSX1
			6	MSX2	6	MSX1	6	MSX2	6	LGR5	6	SOD3	6	NBL1
			7	na	7	MSX2	7	FILIP1L	7	ID1	7	GAS1	7	CD82
			8	na	8	FILIP1L	8	PCDH8	8	DISP1	8	GAS1	8	MERTK
			9	ZIC2	9	LHX2	9	ZIC2	9	na	9	CALML3	9	MSX2
			10	C1orf53	10	na	10	na	10	CALML3	10	SERPINB5	10	GSC
			11	HS6ST1	11	na	11	TNFRSF6B	11	ID2	11	SLC40A1	11	FGFBP1
			12	HPSE2	12	PCDH8	12	GLIS1	12	GAS1	12	LAMB3	12	KAT6B
			13	CRABP-I	13	ZIC2	13	SESN2	13	GLIS1	13	MSX2	13	PRRX1
			14	PHLDA2	14	TNFRSF6B	14	HS6ST1	14	MT4	14	ITGA4	14	HS6ST1
			15	BTBD6	15	CSRP2	15	TFAP2A	15	KIFAP3	15	NBL1	15	PRKCD
			16	COMTD1	16	SESN2	16	CNNM1	16	DDT	16	LAMC2	16	DISP1
			17	TRIM35	17	HS6ST1	17	HPSE2	17	TMSB4X	17	SDC1	17	KIFAP3
			18	SMTN	18	CNNM1	18	PRRX1	18	RARRES2	18	DISP1	18	GLCCI1
			19	SNRPA1	19	GLIS1	19	C1orf53	19	YWHAH	19	MVD	19	CRISPLD1
			20	ING2	20	TFAP2A	20	CBX4	20	PSMB7	20	ID2	20	SERPINB5
			21	SCP2	21	PRRX1	21	BTBD6	21	ARF1	21	KRT19	21	PDGFRL
			22	RWDD4	22	HPSE2	22	TRIM35	22	COPS2	22	RFTN2	22	SOCS4
					23	BTBD6	23	GSDMA			23	HS6ST1	23	CALML3
					24	RGS3	24	PHLDA2			24	PLCD3	24	GAS1
					25	C1orf53	25	CRHOB			25	ITGA6	25	GNAL
					26	SOCS4	26	OTUD3			26	C1orf53	26	GAS1
					27	IRF2BP2	27	COMTD1			27	LMO4	27	FNDC4
					28	PHLDA2	28	SMTN			28	PBX3	28	KRT19
					29	TRIM35	29	GNPNAT1			29	LTF	29	LY6E
					30	PQLC2	30	HPCAL1			30	MSX1	30	STX18
					31	SMTN	31	CCDC101			31	BASP1	31	SERPINF1
					32	CRHOB	32	BAZ2A			32	DGCR6	32	OTUD3
					33	BAZ2A					33	PRKCD	33	na
					34	PCCA					34	TMSB4X	34	S100A16
					35	HPCAL1					35	IMPA2	35	HSP70
					36	TACC1					36	SERPINF1	36	LAMB3
											37	PQLC2	37	SDC1
											38	na	38	na
											39	AMT	39	TOX
											40	YBX3	40	MYO1E
											41	PSPC1	41	NDRG1
											42	SOCS4	42	SLC40A1
											43	NEK7	43	PLCD3
											44	STX18	44	CARHSP1
											45	na	45	NR2F2
											46	FAM134A	46	IMPA2
											47	CACTIN	47	SAT1
											48	CAPZB	48	YBX3
											49	PRRX1	49	CACTIN
											50	GNAL	50	DGCR6

Table 6 | Genes significantly downregulated by different Shh treatments in hindlimb explants. Genes that are negatively differentially expressed in hindlimb explants dosed with designated concentration of Shh morphogen for designated period of time, compared to control explants, as measured by normalised read counts. Gene lists are ordered by greatest difference in normalised read counts between explants under designated treatment and control explants. Novel, unnamed genes are described as "na". Significance determined by one-way ANOVA and Tukey's post hoc test; p= <0.05.

Interestingly, only expression of *Grem1* and *Sall1* was significantly induced by low concentrations of Shh, with *Grem1* notably not differentially expressed in explants exposed to higher concentrations of Shh. BMP antagonist *Smoc1* meanwhile was only differentially expressed in explants exposed to 4nM Shh for 16 hours (Table 3, Appendix 1). In addition to genes of interest that are repressed after 12 hours of Shh exposure, *Sox8, Gas1* and *Bmp4* were also downregulated in explants dosed with Shh for 16 hours (Table 4, Appendix 2).

To investigate whether different genes are induced or repressed by Shh signalling in hindlimb buds compared to forelimb buds, I also examined which genes were differentially expressed in hindlimb explants exposed to different concentrations and durations of Shh (Tables 5-6, Appendices 3-4). Genes that were differentially expressed in hindlimb explants were largely similar to those in forelimb explants, though a few notable exceptions were observed. Most interestingly, *Hoxa10-13* were differentially expressed in hindlimb explants exposed to Shh for 12 and 16 hours but were not expressed at all in forelimb explants at any time point. This is consist with the *in situ* hybridisation expression pattern of *Hoxa13* which is more prominently expressed in the hindlimb during Shh patterning stages (Bell et al., 2004). *Limb expression 1* (*Lix1*) and *Scube3* - which plays a semi-redundant role with its paralog *Scube2* in releasing Shh from the cell membrane in zebrafish (Creanga et al., 2012) – were also differentially expressed in hindlimb explants (Table 5, Appendix 3).

Two genes of particular interest were differentially downregulated in hindlimbs but not in forelimb explants. *Glis Family Zinc Finger 1 (Glis1*) – a Gli-related transcription factor that can act to activate or repress targets in a similar manner to Gli transcription factors (Kim et al., 2002) – and *Neuroblastoma 1* (*Nbl1*) a DAN family BMP antagonist (Table 6, Appendix 4). Both are endogenously expressed in

both the anterior of fore- and hindlimb buds however (Gerlach-Bank et al., 2002; Kim et al., 2002).

The timing of differential expression was also different in some genes in hindlimb explants. This was most notable with the *Hoxd11* and *Six1,* which were both DE after 12 hours in hindlimb explants. *Six1* and interestingly *Eya1,* a transcriptional co-activator required by Six1, also showed higher levels of expression in hindlimb explants compared to forelimb explants (Tables, 5-6, Appendices, 3-4). This is reflected in *in situ* patterns of *Six1* but not *Hoxd11,* whilst the expression of *Eya1* remains to be defined in early limb buds (Bell et al., 2004).

5.2 *In silico* analyses can be used to predict specific AP expression patterns of Shh targets in chicken limb buds

This initial approach provided insight into which genes are induced and repressed by Shh signalling in limb progenitors, however, many genes were differentially expressed by different levels or durations of Shh making it difficult to uncover genes that may mark or specify different digit identities in response to different levels of Shh signalling. To further attempt to identify candidate genes that might be expressed in specific AP domains in response to distinct levels of Shh signalling, I clustered genes based on the similarity of their full transcriptional response profiles – the level of expression observed at each concentration and time point - to the profiles of genes that are known to be expressed at specific AP levels in limb buds.

Ptch1 is endogenously expressed in the posterior of limb buds and has a transcriptional response profile that shows a peak response (highest level of induced expression) to Shh signalling at the highest concentration (8nM) and

duration (16 hours) (Marigo *et al.,* 1996, Fig. 12). Its transcriptional profile also exhibits temporal adaptation, where explants exposed to the lowest concentration of Shh become desensitised to Shh signalling by 16 hours. To find genes that may be expressed in a posterior domain similar to *Ptch1*, I clustered genes that also showed a peak response to 8nM Shh after 16 hours, as well as temporal adaptation and designated this profile '*Ptch1*-like' (Fig. 20). I ordered the gene list generated by fold increase in expression at 8nM/16hour compared to controls to reveal genes that are most induced by high levels of Shh signalling (Fig. 20). I separately subsetted genes that showed a peak response to 8nM Shh after 16 hours, without specifying temporal adaptation as a required criteria, and designated this profile '*Hoxd13*-like' (Fig. 20). Genes within the '*Ptch1*-like' and '*Hoxd13*-like' clusters are predicted to be expressed in a posterior domain (Fig. 20, blue).

Conversely, *Alx-4* is expressed in the anterior of limb buds and exhibits a transcriptional profile in which the highest level of expression is observed in limb explants cultured without Shh. A reverse gradient is seen after 16 hours where increasing concentrations of Shh results in decreasing expression levels of *Alx-4.* Accordingly, I clustered genes that showed a similar transcriptional profile to *Alx-4* in an attempt to reveal genes that are expressed anteriorly and named this profile '*Alx4*-like' (Fig. 20).

I also sought to uncover genes that may be expressed at an intermediate AP level by clustering genes that showed a transcriptional profile where a peak response was exhibited by explants exposed to medium concentrations of Shh or to medium durations of Shh exposure. I subsetted genes that showed a peak response to 8nM Shh after 12 hours of exposure (Fig. 20, '*Foxc2*-like') or to 4nM Shh after either 12 or 16 hours (Fig. 20, '*Smoc1*-like') in an attempt to uncover genes that are expressed at an intermediate AP level directly anterior to the most posterior

domain – hereafter referred to as primary intermediate (Fig. 20, green). I further subsetted genes that showed a peak response to 8nm Shh after 6 hours (8nM_6hr) or to 2nM Shh after either 12 or 16 hours (Fig. 20, *'*Grem1-*like'*, 2nM_16hr) in an attempt to identify genes that are expressed at an intermediate AP level anterior to the primary intermediate domain, but posterior to the most anterior domain – hereon referred to as secondary intermediate (Fig. 20, Red).

As expected, in forelimb explants, several of the genes that were subsetted into '*Ptch1*-like' and '*Hoxd13*-like' profiles were also statistically differentially expressed in response to high concentrations of Shh (Table 3, Fig. 20, blue). Moreover, many of these genes are endogenously expressed in a posterior domain in chicken limbs (Fig. 20, bold) including established targets of Shh signalling: *Ptch1, Ptch2, Hhip, Gli1, Bmp2*, *Hoxd11-3* and *Tbx3,* which validated this approach. Transcription factors, *Foxf1, Foxl1, Lhx6 and Runt related transcription factor 2* (*Runx2*), *EGF-containing Extracellular Matrix Protein* (*Efemp1*) and *Hs3st2* – an enzyme involved in the synthesis of heparan sulphate chains on HSPGs - were also identified by this analysis and are predicted to be expressed posteriorly.

Similarly, several genes that were subsetted into the '*Alx-4*-like' profile are endogenously expressed in an anterior domain or are known to be repressed by Shh signalling, including: *Alx-4, Goosecoid* (*Gsc*)*, Gas1, Sox8, Sox6, Msx1, Msx2, Lhx2, Glis1 and Disp1* (Fig. 20, bold)*. Mab-21-like-1* and *Mab-21-like-2* - which are similar to a cell fate-determining gene found in *C. elegans, Mab-21* - *Hs6st1,* and interestingly, three BMP antagonists, *Nbl1, Noggin* (*Nog*) and *Von Willebrand Factor C Domain Containing 2* (*Vwc2*), were also highly ranked in this gene list and are predicted to be expressed anteriorly (Fig. 20, black). Mutations to *Mab-21* in *C. elegans* leads to homeotic transformations (Chow et al., 1995). Whilst BMPs play an

Figure 20 | Gene lists based on transcriptional profiles in forelimb explants. (A) Predicted AP expression domains of genes based on their transcriptional profile: posterior (blue), primary intermediate (green), secondary intermediate (red), anterior (black). (B) Lists of genes subsetted on the similarity of their transcriptional profiles to the transcriptional profiles of reference genes and/or on the duration or level of Shh signalling that induces a peak response using R language and statistical environment. Exemplary transcriptional profiles and reference genes/peak conditions are shown above gene lists. Genes that are known to be expressed in their predicted domain are shown in bold. Gene lists are ordered by greatest difference in normalised read counts between the Shh treatment that induces peak response and control - the top 40 ranked are shown. Ptch1_like conditions specify a peak response at 8nM Shh after 16 hours with temporal adaptation observed in explants dosed with 2nM Shh (*). Novel, unnamed genes are described as "na".

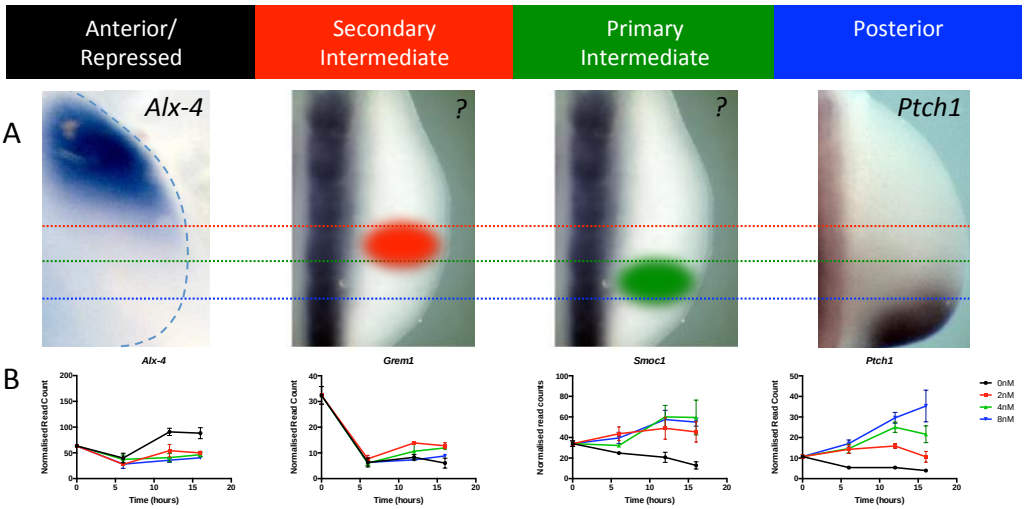

*Alx4*_like		6hr_Peak		*Grem1*_like		2nM_Peak		*Smoc1*_like		*Foxc2*_like		*Hoxd13*_like		*Ptch1*_like	
0nM_ Peak		8nM_6hr Peak		2nM_12hr Peak		2nM _16hr Peak		4nM_12/16hr Peak		8nM_12hr Peak		8nM_16hr Peak		8nM_16hr Peak*	
1	**GSC**	1	RADIL	1	AOX1	1	SULF1	1	SMOC1	1	OSR1	**1**	**PTCH2**	**1**	**PTCH2**
2	PTX3	2	KCNJ3	2	BSX	2	FANCC	2	CNGA3	2	FOXC2	**2**	**HHIP**	**2**	**HHIP**
3	MGMA	3	SASH3	3	SULF1	3	AMACR	3	HAPLN1	3	SPRY4	**3**	**HOXD13**	**3**	**OSR1**
4	MAB21L2	4	na	4	SLC22A23	4	CNTLN	4	ANO1	4	SPRY4	**4**	**HOXD12**	**4**	**PTCH1**
5	**SOX8**	5	na	**5**	**GREM1**	5	LRIG3	5	APOD	5	FGF1	**5**	**OSR1**	**5**	**GLI1**
6	MAB21L1	6	TMEM2..	6	DDX4	6	WDR36	6	NTN1	6	MORN5	**6**	**PTCH1**	**6**	**CNTFR**
7	RASL11B	7	SCNN1G	7	TRPA1	7	C9ORF3	7	HAS2	7	FOXO6	7	AMER2	7	EFEMP1
8	**GAS1**	8	DHX58	8	COL25A1	8	HOXA7	8	NRSN1	8	TSKU	**8**	**GLI1**	8	LHX6
9	**NBL1**	9	EPHB3	9	ABCG2	9	HEXB	9	DCDC2	9	RUNX2	**9**	**CNTFR**	9	FOXF1
10	**ALX-4**	10	na	10	SIX2	10	IDUA	10	PAMR1	10	SIAH3	10	EFEMP1	**10**	**BMP2**
11	VWC2	11	ARHGA..	11	FMN2	11	UGGT2	11	RUNX1T1	11	CNR1	**11**	**HOXD11**	**11**	**KCNH5**
12	PKP2	12	GNB1L	12	na	12	TBX18	12	SPATA13	12	ABCC3	12	LHX6	12	FOXC2
13	MERTK	13	PMP22	13	na	13	CYTL1	13	TMEM13..	13	SCPEP1	13	FOXF1	13	TRIB1
14	**GAS1**	14	NDUF..	14	SULT1E1	14	CD151	14	NGFR	14	PRICKLE2	**14**	**BMP2**	14	FOXL1
15	CD82	15	LRFN5	15	SLC1A4	15	ISOC1	15	APBB1IP	15	RAB38	**15**	**KCNH5**	**15**	**FIGF**
16	**MSX1**			16	MLB1	16	RBM43	16	GRIN3A	16	LAPTM4B	16	FOXC2	16	RAMP1
17	**MSX2**			17	FAM19..	17	ORC2L	17	GRAMD..	17	EXOC2	17	TRIB1	**17**	**TBX3**
18	CA10			18	DECR1	18	COMM..	18	EDIL3	18	FMNL2	18	FOXL1	18	FGF10
19	CRISPLD2			19	SLC7A11	19	MYOCD	19	PRKD1	19	ERCC6L2	19	KIRREL3	**19**	**RSPO3**
20	NOG			20	TAF4B	20	RAPGEF1	20	PRELP	20	LRFN5	20	HS3ST2	20	PLCXD3
21	FNDC4			21	ITPR2	21	TSEN2	21	HOXA4	21	CDC42EP1	21	SRRM3	21	RHOJ
22	ARHGAP..			22	na	22	KIF2A	22	MANBA	22	PELI2	**22**	**FIGF**	22	ABCC3
23	PALM2			23	SLA	23	MTX3	23	COL8A2	23	ARHGA..	23	IRK1	**23**	**SIX1**
24	HS6ST1			24	MYOCD	24	FAM17..	24	GDAP1L1	24	ZEB2	24	RAMP1	24	KBTBD11
25	**LHX2**			25	TDH	25	SLC25A12	25	PROM1	25	FAM116A	25	SPRY4	25	RUNX2
26	VIT			26	PCDH8	26	MRM1	26	KCNK5	26	NDUFA8	26	SPRY4	26	na
27	TMEM1..			27	LHX1	27	GLRA4	27	CCDC85A	27	AKAP10	27	P2RY1	27	SCNN1B
28	CA2			28	CASP3	28	ARL6	28	FBXL7	28	GNB1L	**28**	**TBX3**	28	RASGEF1B
29	GPR146			29	HARBI1	29	NUSAP1	29	SKAP2	29	na	29	STRA6	29	RGS6
30	RASSF9			30	TRAK2	30	GNA11	30	MATN2	30	na	30	FGF1	30	RFFL
31	PRRX1			31	SLC7A5	31	APBA2	31	PIGA	31	C11ORF82	31	VTN	31	PDZ_Unch
32	**SOX6**			32	TICRR	32	LMNB1	32	MAP4K4	32	ACTN4	32	FGF10	32	CNR1
33	PRDM16			33	VWA8	33	MED18	33	VILL	33	na	33	WNT9B	33	PDXK
34	**GLIS1**			34	SMYD3	34	CCDC171	34	SOX9	34	SGMS1	34	IGF2	34	SCPEP1
35	WNT7B			35	WIPI1	35	CENPL	35	LPIN1	35	TPI1	35	MORN5	35	MCC
36	**DISP1**			36	LACTBL1	36	ANKRD1	36	ACSL6	36	ADPRHL2	**36**	**RSPO3**	36	MSLN
37	PHLDA3			37	KIAA1958	37	na	37	WNT7A	37	NR3C2	37	PAPPA	37	STXBP5
38	KCNK1			38	KIAA1432	38	MTHFD2	38	PLCG1			38	PODXL	38	ACER3
39	NTS			39	TCEA3	39	AGGF1	39	PLXNA2			39	ELMO1	39	PRICKLE2
40	PODN			40	SLC7A5	40	na	40	TMEM13..			40	FHOD3	40	EXOC2

important role in limb development and *Hs6st1* encodes another enzyme involved in the synthesis of heparan sulphate chains on HSPGs.

Profiles that sought to identify genes that might be expressed at a primary intermediate AP level did not contain any genes that are known to be expressed at this level or that had previously been reported as being regulated by Shh signalling (Fig. 20, green). However, two BMP antagonists – *Smoc1* and *Tsku,* Fox transcription factors, *Foxc2* and *Foxo6,* and *Fgf1* were subsetted into these lists and are predicted to be expressed at a primary intermediate AP level (Fig. 20).

Meanwhile, BMP antagonist *Grem1* was the only gene previously described as targeted by Shh signalling in the limb present in profiles that sought to reveal genes expressed in a secondary intermediate AP domain (Fig. 20, red). *Grem1* is expressed in a domain consistent with this prediction and is required for normal limb development (Khokha et al., 2003). Intriguingly, the expression of *Sulfatase 1* (*Sulf1*) - a third enzyme I have identified that modifies the composition of heparan sulphate chains on HSPGs - was induced by low levels of Shh signalling ('*Grem1*-like') and is predicted to be expressed in a secondary intermediate AP domain. *Hs6st1* and *Hs3st2* are predicted to be expressed in anterior and posterior domains respectively, raising an interesting possibility that different levels of Shh signalling may regulate the spread of Shh ligand in different AP domains through inducing or repressing the expression of different genes involved in generating HSGPs. This would represent a novel noncell-autonomous feedback mechanism. *Brain specific homeobox* (*Bsx*), *Hoxa7*, *Six2*, *Lhx1* were the only transcription factors that clustered to these profiles and may be expressed in a similar domain to *Grem1*.

To further investigate whether different genes are induced or repressed by Shh signalling in hindlimb buds compared to forelimb buds, I also clustered genes

based on their transcriptional profile in hindlimb explants dosed with different Shh treatments, using the same methodology. Hindlimb explants show a full range of responses to Shh signalling over a shorter period of time (Fig. 18). Desensitisation to Shh signalling (as measured by *Ptch1* and *Gli1* expression) is already apparent in hindlimb explants dosed with 2, 4 or 8nM Shh after 16 hours. Of the genes that clustered with *Ptch1* in the hindlimb only *Gli1* was present in both forelimb and hindlimb '*Ptch1*-like' profiles, though, *Hoxa13, Eya1* and *Fgf10* also clustered to '*Ptch1*-like' in hindlimb explants (Fig. 21). However, many of the genes which clustered with '*Ptch1*-like' and *'Hoxd13*-like' forelimb profiles, also clustered with the hindlimb '*Hoxd13-like'* profile including *Ptch2, Hhip, Gli1, Bmp2, Figf, Hoxd11-13, Hoxa13, Hand2 and Tbx3* which are expressed posteriorly (Fig. 21). Genes predicted to be expressed in the posterior of the hindlimb were thus largely over-lapping with those of the forelimb, though *Fgf18* and *Hoxa9,* were notable additions to, and *Foxf1* and *Foxl1,* notable absences from, hindlimb lists. However, *Fgf18* is expressed in a broad intermediate domain in both forelimbs and hindlimbs, highlighting this analysis is not entirely free of false-positive or false-negative results.

Genes that were predicted to be expressed in a primary intermediate AP domain in the hindlimb were also similar to those predicted to be expressed at that level in the forelimb. Genes of particular interest were the transcription factors *Foxc2, Foxo6* and *Runx2*. Surprisingly, BMP antagonists *Smoc1* and *Tsku* were not clustered to these profiles. However, this was not reflected in the expression patterns of these genes (Fig. 22, Chapter V, 5.3). As with forelimb profiles, *Grem1* was the only gene known to be involved in limb development that was predicted to be expressed in a secondary intermediate domain. Interestingly, *Foxo6* was also predicted to be expressed in a secondary intermediate AP domain of hindlimbs.

Figure 21| Gene lists based on transcriptional profiles in hindlimb explants. (A) Predicted AP expression domains of genes based on their transcriptional profile: posterior (blue), primary intermediate (green), secondary intermediate (red), anterior (black). (B) Lists of genes subsetted on the similarity of their transcriptional profiles to the transcriptional profiles of reference genes and/or on the duration or level of Shh signalling that induces a peak response using R language and statistical environment. Exemplary transcriptional profiles and reference genes/peak conditions are shown above gene lists. Genes that are known to be expressed in their predicted domain are shown in bold. Gene lists are ordered by greatest difference in normalised read counts between the Shh treatment that induces peak response and control - the top 40 ranked are shown. Ptch1_like conditions specify a peak response at 8nM Shh after 16 hours with temporal adaptation observed in explants dosed with 2nM, 4nM and 8nM Shh (**). Hoxd13_like conditions specify a peak response at 8nM Shh after 16 hours with temporal adaptation observed in explants dosed with 2nM Shh (*). Novel, unnamed genes are described as "na".

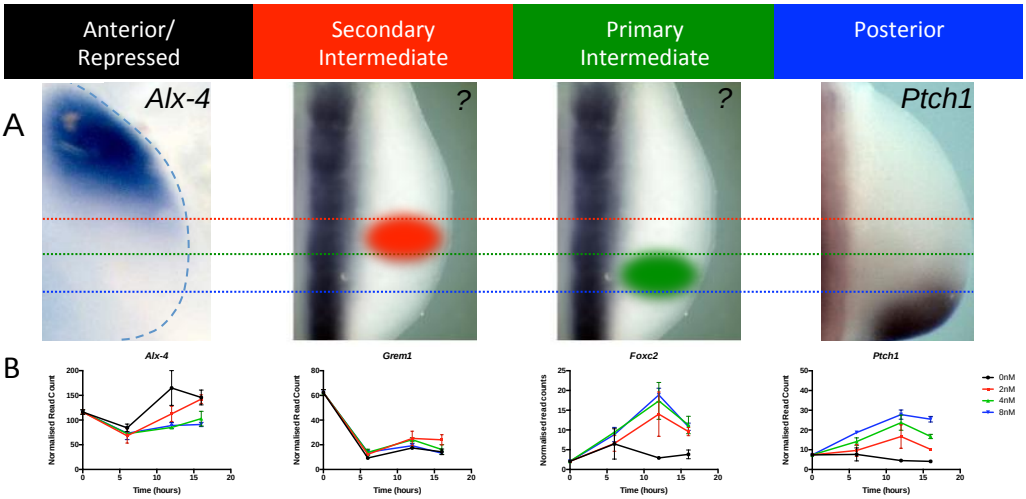

*Alx4*_like		2nM_Peak		*Grem1*_like		6hr_Peak		*Smoc1*_like		*Foxc2*_like		*Hoxd13*_like		*Ptch1*_like	
0nM_ Peak		2nM 16hr Peak		2nM 12/16hr Peak		8nM_6hr Peak		4nM_12/16hr Peak		8nM_12hr Peak		8nM_16hr Peak*		8nM_16hr Peak**	
1	**LHX9**	1	FOXO6	**1**	**GREM1**	1	NGFR	1	LIX1	1	GLI1	**1**	**PTCH2**	**1**	**PTCH1**
2	PTX3	2	FST	2	PITX2	2	NDNF	2	C1QTNF5	2	PTCH1	**2**	**HHIP**	**2**	**GLI1**
3	**GSC**	3	CYTL1	3	LITAF	3	na	3	SPATA13	3	AMER2	3	EFEMP1	3	AMER2
4	MAB21L1	4	RUNX2	4	PGF	4	CNGA3	4	IL1RL1	4	IGF2	**4**	**HOXD13**	**4**	**HOXA13**
5	**MSX2**	5	KIRREL3	5	MSI1	5	CORTBP2	5	KIAA0513	5	EYA1	**5**	**GLI1**	5	ADAMTS9
6	GDPD4	6	PIM1	6	na	6	KCNK5	6	GPRIN3	6	HAS2	**6**	**BMP2**	6	EYA1
7	ANTXR1	7	HES4	7	ARHGEF9	7	FBRSL1	7	PAMR1	7	RBPJL	**7**	**FIGF**	7	FGF10
8	LMO3	8	GNPDA1	8	CCDC19	8	MSI1	8	DNAJC6	8	GRAMD1C	8	AMER2	8	GRAMD1C
9	TOX	9	SIGMAR1	9	na	9	FBXL7	9	na	9	HES4	**9**	**HOXD12**	9	CPLX2
10	MERTK	10	AGPAT5	10	na	10	PLCG1	10	PODXL2	10	HOXA13	10	HS3ST2	10	MGAT4A
11	**GAS1**	11	WDY..	11	MANBA	11	AFAP1L1	11	RAC2	11	KIRREL3	**11**	**HAND2**	11	na
12	**DISP1**	12	MMP..	12	HSPA12A	12	SH3BP5	12	CALR3	12	CYTL1	12	FGF18	12	RBPJL
13	**GAS1**	13	ARHGA..	13	SLC45A3	13	ARHGE..	13	NRG1	13	FST	**13**	**TBX3**	13	RFFL
14	**GLIS1**	14	PFKFB3	14	CCDC164	14	CCDC19	14	C14ORF..	14	RFFL	**14**	**HOXD11**	14	SUPT3H
15	CD82	15	SV2B	15	TTC12	15	SH2B2	15	HMGB2	15	MORN5	**15**	**HOXA13**	15	COL13A1
16	**IRX5**	16	na	16	na	16	TMEM1..	16	C3H6ORF..	16	KCNJ3	16	NANOS1	16	SCPEP1
17	KAT6B			17	BRD3	17	na	17	PAWR	17	FOXO6	17	LMO1	17	SKAP2
18	EBF2			18	CAND2	18	TLE1	18	na	18	SDC3	18	ADAM..	18	MAN1A1
19	ADAMT..			19	ABTB2	19	TLL1	19	OLFM3	19	SCPEP1	19	FGF10	19	DEPDC1
20	**ZIC3**			20	LSM14B	20	ZNF521	20	na	20	MGAT4A	20	PDZRN4	20	ACER3
21	**ZIC3**			21	DTNBP1	21	GALK2	21	DHX58	21	na	21	FAM10..	21	HOXA9
22	PLCD3			22	TBC1D8	22	PTPN5	22	MPP6	22	ASB9	22	MGAT4A	22	VPS26A
23	PAK1			23	ADPRHL2	23	STRADB	23	DYX1C1	23	PIM1	23	RAMP1	23	ERCC6L2
24	**ALX-4**			24	NUDT13	24	MANBA	24	MLF1	24	SKAP2	24	SEMA6A	24	DINB1
25	FILIP1L			25	C10ORF12	25	TBC1D24	25	ALDOB	25	RUNX2	25	SLC25A22	25	KIAA1919
26	SRD5A3			26	SPSB4	26	HSPA12A	26	SRSF4	26	ABCC3	26	na	26	NR3C2
27	ARHGA..			27	CUEDC1	27	SLC45A3	27	SLC19A2	27	SUPT3H	27	PRSS23	27	CCDC102A
28	DACH1			28	TAF8	28	EXD2			28	na	28	TSPAN9	28	PDCL
29	PRRX1			29	NAIF1	29	WDR89			29	AGPAT5	29	REV3L		
30	PAK6			30	SLC44A1	30	SEMA3E			30	ERCC6L2	30	PDZ_Unch.		
31	SOX5			31	YEATS2	31	GBE1			31	GNPDA1	31	ACER3		
32	LY6E			32	STAT6	32	MATN4			32	SIGMAR1	32	HOXA9		
33	na			33	CCDC135	33	CCDC164			33	TPCN2	33	VPS26A		
34	PPP4R4			34	ZRANB3	34	na			34	WDYHV1	34	SCN8A		
35	TP63			35	C1H11OR..	35	na			35	COL13A1	35	DINB1		
36	GLIPR1			36	NEK8	36	AGL			36	MMP17	36	KIAA1919		
37	TIMP3			37	ACAA1	37	BTBD3			37	ARHGAP..	37	CCDC1..		
38	**SOX6**			38	ALKBH5	38	CAND2			38	GLT1D1	38	RNF19A		
39	WNK2			39	TPX2	39	JAK2			39	CSGALNA..	39	RGMB		
40	LINGO3			40	MAP4K4	40	METTL16			40	SV2B	40	DIAPH3		

Genes that clustered with the '*Alx-4*-like' profile and are predicted to be expressed in the anterior of the hindlimb were also largely overlapping with genes predicted to be expressed in the anterior of forelimbs. Notable additions to hindlimb lists included *Lhx9*, *Irx5* and *Zic3,* all of which are expressed posteriorly in both limb buds (Bertuzzi et al., 1999; Li et al., 2014a; Wang et al., 2011).

5.3 Candidate targets of Shh signalling are expressed in distinct AP domains in chicken limb buds consistent with predictions

To determine if genes are expressed in the domain that was predicted by *in silico* analysis I used whole mount *in situ* hybridisation to determine the endogenous expression domains of select genes of interest from gene lists. In particular I aimed to uncover genes not previously identified as being targets of Shh signalling that may have an undetermined role in marking or establishing different digit identities.

In this thesis I have focused my analysis on transcription factors and genes involved in major signalling pathways, as these are most likely to specify or mark individual digit identities. It has been proposed that different levels of Shh signalling specify different digit identities by instructing limb progenitors to differentiate into specific cell types (Wolpert, 1969). This is achieved by altering the transcriptional profiles and therefore behaviour and characteristics of cells, instructing them to become progenitors of specific digits. It is widely accepted that genes that will have the most profound effect on progenitors individual characteristics will be transcription factors and proteins involved in major signalling pathways. These proteins can regulate the transcription of many other genes and thus regulation of these genes represents the most efficient way to make global changes to a progenitor's transcriptional profile.

Of the genes predicted to be expressed in a posterior domain, *Foxf1* and *Lhx6* were the highest ranked transcription factors, not to have been previously reported to be expressed posteriorly. Interestingly, two other Fox transcription factors, *Foxc2* and *Foxo6* were the only transcription factors to show a peak response to intermediate levels of Shh signalling. A role for Fox family transcription factors in limb development has not previously been reported. Meanwhile, BMP antagonists *Smoc1* and *Tsku*, which show a peak response to intermediate levels of Shh signalling, are predicted to be expressed at a primary intermediate AP level within the limb. BMP antagonists are interesting candidate targets of Shh signalling given the essential role of BMPs and BMP antagonist *Grem1* in limb development.

Of the genes predicted to be expressed in an anterior domain *Mab21l1* and *Mab21l2* were the only homeotic genes or transcription factors that have not previously been implicated downstream of Shh signalling or in limb development. Finally, *Hs3st2*, predicted to have a posterior expression, also represented a potentially interesting line of investigation as the enzyme encoded by this gene generates a myriad of distinct heparan sulphate fine structures found on HSPGs. HSPGs are extracellular proteins capable of binding signalling molecules through heparan sulphate structures, thereby influencing signalling pathways. HSPGs are required for the spread of Shh through tissues (Bischoff et al., 2013; Briscoe and Thérond, 2013; Dreyfuss et al., 2009).

Accordingly I used *in situ* hybridisation to investigate the endogenous expression patterns of *Foxf1, Lhx6, Foxc2, Foxo6, Smoc1, Tsku, Mab21l1* and *Hs3st2* in chicken embryos at stages HH19, HH21 and HH22 – covering the period of Shh patterning activity. *In situ* hybridisation templates for *c.Foxc2, c.Foxf1* and c.*Foxo6* were not commercially available. To investigate the endogenous expression pattern of

c.Foxc2, c.Foxf1 and c.*Foxo6* I cloned a ~500bp region of the cDNA of each gene into a pBluescript II SK expression vector (Appendix 5-7).

Foxf1 expression was not detected in chicken forelimb and hindlimbs buds at stages HH19, HH21 or HH22 (Fig. 22). Strong expression in the gastro-intestinal tract was seen however, providing a positive control (Fig. 22). *Hs3st2* expression was not detected in stage HH19 limb buds but weak expression was observed at stage HH21 and HH22. Surprisingly, this was not in the most posterior portion of the limb bud as expected, but at an intermediate and more proximal region of the limb bud (Fig. 22). Interestingly, *Hs3st2* expression was broader in stage HH22 limb buds than it was in equivalent hindlimb buds (Fig. 22). Weak *Lhx6* expression was observed in the distal posterior of stage HH19 and HH21 limb buds and became more pronounced at stage HH22. However, high background staining was also observed in these embryos due to the long development time required (Fig. 22).

Tsku expression was observed in the posterior of stage HH19 forelimbs but was not detected in hindlimbs at this stage. In stage HH21 forelimb and hindlimb buds, *Tsku* expression was seen at the most distal margin of limb buds at an intermediate AP level, as predicted by *in silico* analysis. *Tsku* expression was not detected in the most posterior or the most anterior margins of limb buds at this stage (Fig. 22). Expression of *Tsku* was broader in stage HH22 limb buds, but maintained a distal-intermediate AP expression pattern (Fig. 22).

Smoc1 was robustly expressed in an intermediate AP domain in forelimbs and hindlimbs at stages HH19, HH21 and HH22, as predicted. As with *Tsku, Smoc1* expression was absent from the most posterior and most anterior portions of limb buds. Interestingly, a dorsal bias was observed in *Smoc1* expression in stage HH21 limb buds, which became less pronounced by HH22 (Fig. 22).

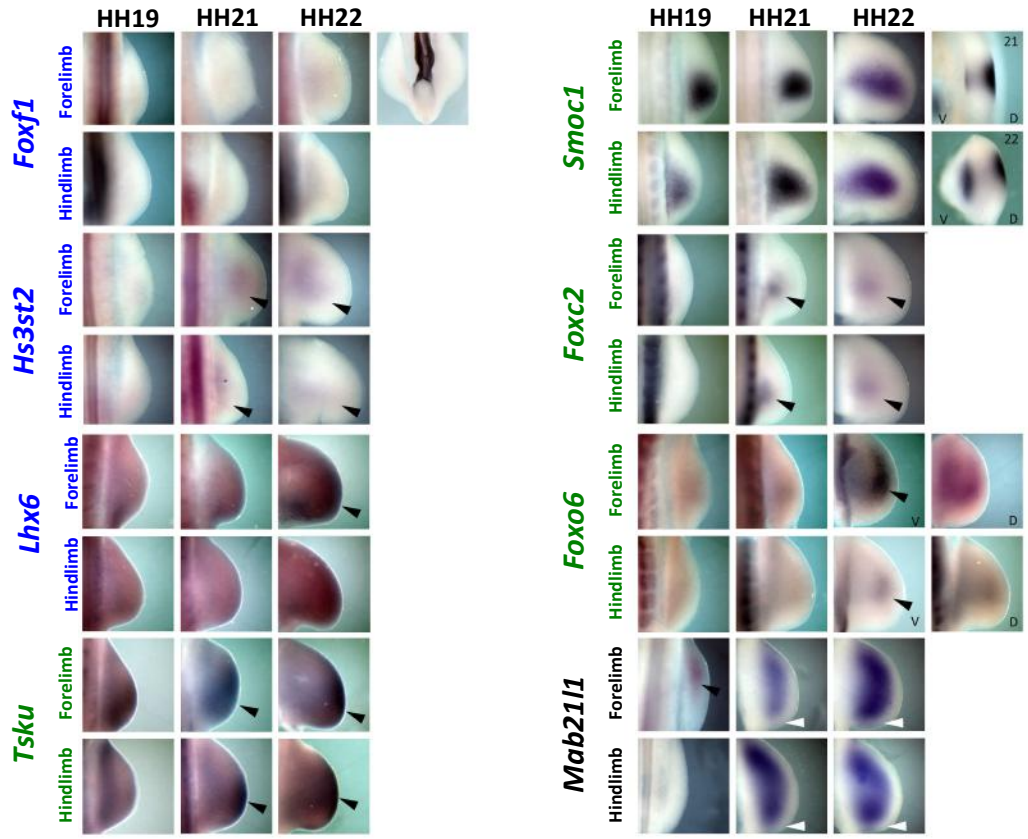

Figure 22 | *In situ* hybridisation expression patterns of genes predicted to be expressed indifferent AP domains, in chicken forelimb and hindlimb buds. Expression of chicken *Foxf1, Hs3st2, Lhx6, Tsku, Smoc1, Foxc2, Foxo6 and Mab21l1* in chicken forelimbs and hindlimbs at the designated Hamburger and Hamilton (HH) stages of normal chicken development, as determined by whole mount *in situ* hybridisation (n=3). Genes predicted by *in silico* analyses to be expressed posteriorly (blue), at an intermediate AP level (green) and anteriorly (black) are designated. Expression of genes (black arrows) and the absence of expression of genes (white arrows) is highlighted. Ventral (V) and dorsal (D) are denoted where applicable.

Foxc2 expression was not detected in either limb bud at stage HH19 but was expressed in a discrete domain that was proximal, but at an intermediate AP level, as predicted, at stages HH21 and HH22. *Foxo6* expression was not detected in stage HH19 or HH21 forelimb or hindlimb buds. However, expression was observed in stage HH22 limbs in a secondary intermediate-AP domain that was broader and more distal than the *Foxc2* domain and represented a distinct population of cells (Fig. 22). The expression pattern of *Foxo6* was similar to that of *Grem1.* Interestingly, *Foxo6* expression showed ventral bias and showed stronger expression in forelimb buds (Fig. 22).

As predicted, *Mab21l1* expression was observed in the anterior domain of stage HH19 forelimb buds, although was absent from hindlimb buds at this stage (Fig. 22). Unexpectedly, expression of *Mab21l1* expanded posteriorly across limb buds to occupy a broad expression domain at stages HH21 and HH22. Notably, expression was absent from the most posterior and the most distal margins of both forelimb and hindlimb buds at these stages (Fig. 22).

5.4 Attempt to mis-express *Smoc1* in the developing forelimb bud

Of the candidate genes lists, I was most interested in genes that were predicted to show a peak response to intermediate levels of Shh signalling as these genes may be involved in specifying middle digit identities, which has not been previously described. *Smoc1* showed the most robust intermediate AP expression of these genes via *in situ* hybridisation analysis and as a BMP antagonist could play an important role in limb development (Fig. 22).

The intermediate AP expression domain of *Smoc1* suggested that it could be implicated in specifying middle digit identities. Mutations in *Smoc1* have been

linked to patients with Waardenburg syndrome, who have abnormally developed middle digits and lack a second digit in their feet (Abouzeid et al., 2011; Okada et al., 2011; Rainger et al., 2011). *Smoc1* mutant mice also exhibit abnormal development of middle digits, which are less clearly patterned and lack either a digit 2 or a digit 3 in the hindlimbs (Okada et al., 2011). These data suggest that Smoc1 expression in response to medium levels of Shh signalling is required for the normal development of middle digits.

To attempt to determine if Smoc1 is sufficient to specify middle digits, I mis-expressed *Smoc1* in stage HH14 chicken forelimbs by electroporating a construct expressing *Smoc1,* CMV-*Smoc1*-Sport6 (Source Bioscience), into a cavity adjacent to the forelimb-forming region (Fig. 23A). CMV-*Smoc1*-Sport6 was co-electroporated with a construct expressing Red Fluorescent Protein (RFP), to identify successfully targeted forelimbs. Embryos were left to develop until stage HH36 where possible. Unfortunately, few embryos survived until a stage where potential limb phenotypes could be analysed.

Of the embryos successfully co-electroporated with CMV-*Smoc1*-Sport6, only three survived until stage HH25 or later and none beyond stage HH30. Of these, two embryos exhibited affected right (electroporated) forelimbs. In one embryo, a narrowing of the AP axis of the limb bud was observed compared to the left forelimb bud at stage HH25 (Fig. 23B). Conversely, a second embryo displayed a truncated 'hammer-head' shape, which featured narrow outgrowths at the anterior and posterior distal margins of the limb bud at stage HH30 (Fig. 23C). A third embryo exhibited a normally formed limb bud, but that had developed pointing dorsally. This appeared to be a side effect of electroporation rather than *Smoc1* mis-expression. Limbs electroporated with the reporter construct alone that developed until stage HH33 or beyond exhibited normal morphologies, although

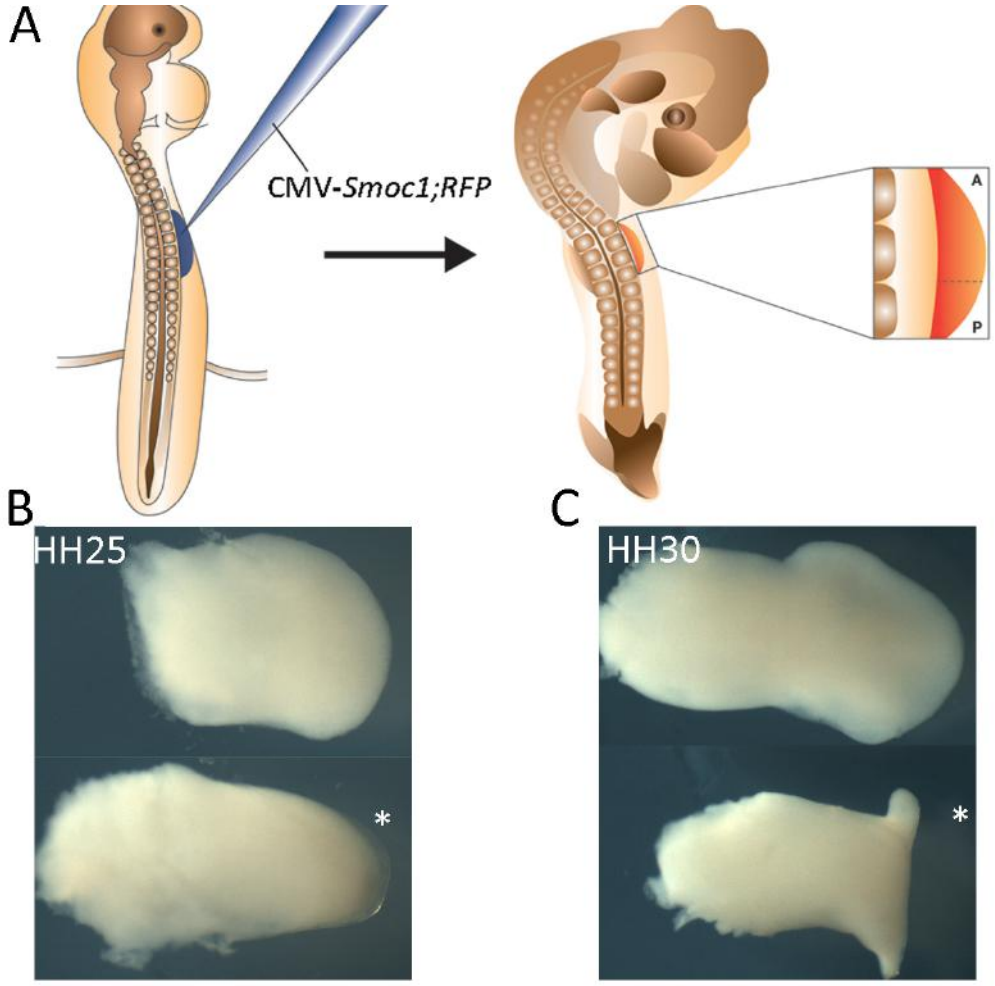

Figure 23| Affects of mis-expressing *Smoc1* in the chicken forelimb. (A) Experimental schematic. CMV_*Smoc1*_Sport6 plasmid was injected into a cavity adjacent to the forelimb forming region of stage HH14 chicken embryos and was co-electroporated into forelimb progenitors with a reporter construct expressing RFP. Successfully targeted limbs were identified by RFP expression (orange). (B) A normal, stage HH25 left wing bud and an affected right wing bud (*), following co-electroporation of *Smoc1* and *RFP* expressing constructs (n=1). (C) A normal, stage HH30 left wing bud and a differently affected right wing bud (*), following co-electroporation of *Smoc1* and *RFP* expressing constructs (n=1).

were truncated along the PD axis (n=2, data not shown). Given these difficulties I have begun to attempt to address this question using a transient transgenic mouse approach. Unfortunately, results are yet to be obtained from this is on-going study, but an overview of my strategy is discussed (Discussion 6.4).

5.5 Transcriptional targets of Shh signalling are expressed in the pharyngeal arches

Whilst examining the expression of predicted targets of Shh signalling by whole mount *in situ* hybridisation, it was apparent that several transcripts were expressed in the first and/or second pharyngeal arches as well as the limb buds. *Shh* is expressed in a distinct stripe at the posterior endodermal boarder of the second pharyngeal arch from stage HH15 onwards (Veitch et al., 1999; Wall and Hogan, 1995). However, downstream targets of Shh signalling in the pharyngeal arches have not been thoroughly investigated. To examine downstream targets of Shh signalling in the pharyngeal arches and to compare these to targets of Shh signalling in the limb I analysed *in situ* hybridisation patterns of stage HH19 chicken embryos, focusing on expression within the first and second pharyngeal arches.

As expected, direct readouts of Shh signalling, *Gli1, Ptch1* and *Ptch2* were expressed in a domain that coincided with the domain of *Shh* expression (Fig. 24A, and data not shown). *Foxo6* and *Tsku,* which were expressed at an intermediate AP level in limb buds, and *Has2*, which was predicted to be expressed at an intermediate AP level in limb buds, were also expressed in a domain consistent with *Shh* expression (Fig. 20, Fig. 24B). Conversely, *Foxc2* and *Smoc1,* which were also expressed at an intermediate AP level in limb buds, were expressed in the dorsal anterior of the second pharyngeal arch and adjacently in the dorsal posterior of the first

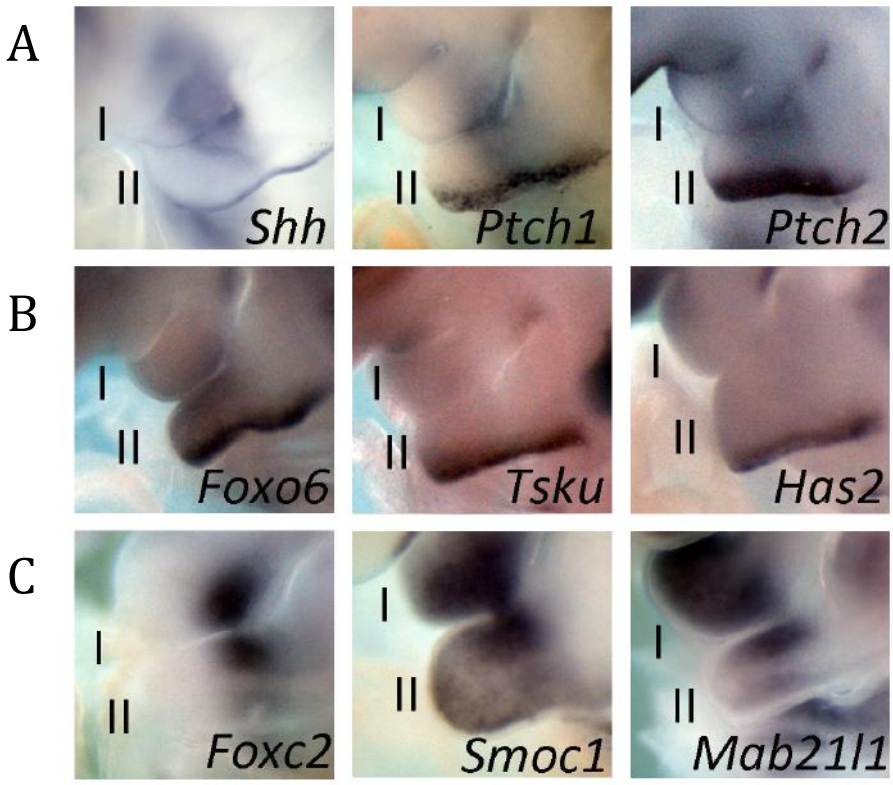

Figure 24| Common targets of Shh signalling in the limb and the pharyngeal arches. Expression of Shh transcriptional targets in the first (I) and second (II) pharyngeal arches of stage HH19 chicken embryos as determined by whole mount *in situ* hybridisations (n=3). (A) Expression pattern of *Shh* and direct targets of Shh signalling, *Ptch1* and *Ptch2.* (B) *Foxo6*, *Tsku* and *Has2*, which were predicted to be expressed at a intermediary AP level in the limb, were expressed in a similar domain to *Shh, Ptch1* and *Ptch2.* (C) *Foxc2*, *Smoc1* and *Mab21l1*, also predicted to be expressed at a intermediary AP or anterior level in the limb, are expressed in similar domains, anterior to that of *Shh, Ptch1* and *Ptch2.*

pharyngeal arch (Fig. 24C). Similarly, *Mab21l1*, which was expressed in the anterior of limb buds at stage HH18, was expressed in an area consistent with *Foxc2* and *Smoc1* expression, and also more broadly across the first pharyngeal arch (Fig. 24C).

Foxf1, Hs3st2 and *Cntfr* expression was not detected in the pharyngeal arches (data not shown). *Hmgn5* was broadly expressed throughout the first and second pharyngeal arches, consistent with its broad expression in limb buds, whilst *Lhx6* was not expressed in the pharyngeal arches, but was strongly expressed anterior to this (data not shown). These data suggest that Shh signalling induces the expression of common targets in different tissues and supports a model in which specific genes are expressed in response to different levels of Shh signalling.

In this chapter I have used different *in silico* analyses to identify candidate genes that are predicted to be expressed at specific AP levels based on their responses to different levels of Shh signalling. Of most interest, different *Fox* transcription factors, BMP antagonists and HSPG generating enzymes are predicted to be expressed in different AP domains in response to different levels of Shh signalling. Of these candidates, I have shown that *Smoc1, Foxc2, Foxo6* and *Tsku* are expressed at a primary intermediate AP level by *in situ* hybridisation, as predicted by *in silico* analysis. Unfortunately, attempts to determine the sufficiency of *Smoc1* to specify middle digits identities have been inconclusive.

Chapter 6: Discussion

6.1 Differences in Shh signalling between chicken forelimb and hindlimb buds

The forelimbs and hindlimbs of vertebrates arise from common mesodermal origins and are patterned by conserved signalling centres, yet, ultimately form distinct morphological structures. The clearest differences are seen in structures that are patterned by the Shh morphogen. This is particularly the case for the chicken, which features different numbers of digits in its respective limbs. To attempt to understand how different morphologies can arise from conserved genetic networks I investigated potential differences in the Shh signalling dynamics of chicken forelimb and hindlimb buds during Shh patterning stages including differences in the size of morphogen fields, morphogen production and range and the response of progenitors to Shh signalling.

Here, I report that chicken hindlimb buds are marginally, but reproducibly larger, than forelimb buds during Shh patterning stages and that this is predominantly the consequence of a broader AP axis that is observed in hindlimb buds (Fig. 5). However, more substantial differences in the size of the respective limbs buds do not become apparent until stage HH24 onwards (Fig. 5).

Using two measures, there was no apparent difference in the amount of Shh produced by respective limb buds during patterning stages. No significant difference in the levels of *Shh* transcripts between respective limbs was measurable by qPCR analysis (Fig. 7) and the size of *Shh* expression domains in forelimbs and hindlimbs are remarkably similar, suggesting an equivalent number of cells produce similar amounts of Shh in respective limb buds (Fig. 6, 8). Interestingly, *Shh* transcripts were observed at consistent levels from stages HH18-22 in both limbs by qPCR, suggesting that Shh is produced at a constant rate in both

limbs during patterning stages (Fig. 7). Whilst, temporal trends can be identified via qPCR, it may not be sensitive enough to distinguish differences in levels of *Shh* expression between limb types and this experiment is further subject to possible inaccuracies in dissections. Additionally, levels of transcripts may not reflect the concentrations of protein in respective limb buds. However, it is difficult to accurately measure the absolute concentrations of secreted proteins *in vivo*. To circumvent these problems I attempted to measure the levels of Shh targets by qPCR.

The expression levels of direct transcriptional read outs of Shh signalling *Ptch1* and *Gli,* as measured by qPCR (Fig. 7), and the sizes of *Ptch2* expression domains were also equivalent in forelimb and hindlimb buds during Shh patterning stages (Fig. 6, 8E). This supports the model that limb progenitors are subject to equivalent levels of Shh signalling during this period. Interestingly, in both limbs the levels of *Ptch1* and *Gli1* transcripts continued to rise over this period, despite *Shh* levels remaining constant. This suggests the transcriptional response to Shh accumulates with increased durations of Shh signalling.

Interestingly, *Shh* and *Ptch2* expression domains appeared to occupy a larger proportion of the total limb bud area (AP-PD) in forelimb buds than in hindlimb buds at Shh patterning stages – though, this was slight (Fig. 8C, F). This could suggest that a greater proportion of forelimb progenitors are subject to Shh signalling in chicken forelimb buds than in hindlimb buds. Consistently, all digits in the chicken forelimb are Shh dependent whereas digit 1 of the hindlimb forms independently of Shh signalling (Ros et al., 2003). Moreover, progenitors that give rise to digit 1 of the hindlimb originate from a relatively more anterior domain than progenitors which give rise to digit 1 of the chicken forelimb (Nomura et al., 2014; Vargesson et al., 1997b). It would be interesting to attempt to correlate Shh

response domains with fate maps of digit forming regions in respective limb buds (Vargesson et al., 1997b). Moreover, this raises an additional question on how the shape and size of a morphogen field may alter its ultimate morphological output when subject to equivalent levels of morphogen signalling.

However, the methods I have used are too limited to draw firm conclusions. Firstly, *in situ* hybridisation can only provide qualitative data on the presence of target transcripts and cannot accurately quantify the level of transcripts in cells nor account for post-transcriptional differences, which might alter amounts of protein. Moreover, determining the expression domains of transcripts is susceptible to the variations of the *in situ* hybridisation technique and is subject to arbitrary thresholds of what is considered signal above background. Despite these technical limitations, measurements were actually remarkably reproducible, in part due to the clear expression patterns of *Shh* and *Ptch2.* I have also, to an extent, circumvented these issues by indirectly measuring the amount of Shh protein through analysis of the expression of direct read outs of Shh signalling by qPCR and *in situ* hybridisation. Nonetheless, directly measuring the quantities of Shh and Gli proteins, would give a more insightful analysis into differences in Shh signalling between the limbs. This was not possible using Shh::GFP and Gli Binding Site (GBS)::GFP mice in the limb (Chamberlain et al. 2008; data not shown- see chapter 3.2), and will require reliable antibodies, which at present are not commercially available. Furthermore, to gain a full understanding, this should be measured across all three axes of limb buds using optical project tomography (Sharpe et al., 2002) or an alternative 3D imaging method.

The chicken hindlimb appears to be patterned faster than the forelimb

Here, I demonstrate that *Shh* is expressed for a shorter period of time in chicken hindlimb buds compared to forelimb buds (Fig. 6). Importantly, the onset of *Shh* expression is delayed in chicken hindlimbs by approximately 3 hours compared to forelimbs (Fig. 6). Despite this, the hindlimb is completely patterned sooner than the forelimb. Limb buds treated with the potent inhibitor of Shh signalling, cyclopamine, 15 hours after the onset of *Shh* expression display normally patterned hindlimbs but disrupted patterning in digit 3 of the forelimb (Scherz et al., 2007; Towers et al., 2011). Expression of *Shh* in chicken hindlimb buds also terminates sooner than in forelimbs though this occurs beyond the patterning phase of Shh activity (Fig, 6). These data demonstrate that fully patterned hindlimbs arise after a shorter duration of Shh signalling than forelimbs and suggests that chicken hindlimbs develop at a faster rate than forelimbs.

Consistently, the footplate is more easily distinguished at an earlier time point than the handplate, and an absence of *Gli1* and *Ptch2* expression in a digit-shaped domain - which may reflect a condensation of cells in an emerging digit which have begun to differentiate and have stopped responding to Shh signalling - is observed at an earlier time point in chicken hindlimb buds (Fig. 6). Interestingly, the first digit condensation in the mouse limb is more prominent in the hindlimb than the forelimb at E11.25 (Zhu et al., 2008). Moreover, RNAseq results I report here suggest that chicken hindlimb progenitors show a full range of transcriptional responses to Shh signalling over a shorter period of time, consistent with a model in which the chicken hindlimb is patterned and develops at a faster rate than the forelimb (Fig. 19, Discussion 6.5). To provide further evidence that chicken hindlimbs develop faster than forelimbs it would be useful to perform a

comparative time series on the emergence of digit condensations in respective limb buds using *Sox9* expression as a marker of chondrogenesis.

I demonstrate that the onset of *Shh* expression in chick hindlimbs is delayed relative to the forelimb. In this body of work I have not attempted to answer the question of why this is the case and whether *Shh* is regulated differently in hindlimbs compared to forelimbs. Expression of *Shh* in vertebrate limbs is controlled by a long range enhancer designated the ZRS (Lettice et al., 2003), though it is not clear what factors are required to occupy this enhancer to initiate *Shh* expression. Hand2 and retinoic acid have been proposed as factors required to initiate *Shh* expression, however no obvious difference in the timing of *Hand2* expression is observed between the forelimb and hindlimb of the chick or mouse (Bell et al., 2004; Chiang et al., 2001). Retinoic acid has been shown to induce *Shh* expression and it has been proposed that retinoic acid secreted from axial tissues is responsible for initiating *Shh* expression in the limbs and is required for forelimb and hindlimb outgrowth (Chinnaiya et al., 2014; Nishimoto et al., 2015; Riddle et al., 1993). It has been well characterised that axial tissues of vertebrates develop in a rostro to caudal sequence and it is thus possible that retinoic acid or other axial signals, are secreted at a developmentally later time point from more caudal axial tissues. This may account for the apparent delay in the onset of *Shh* expression in the chick hindlimb bud.

6.2 Establishing a graded response to the Shh morphogen gradient in vertebrate limbs

The Shh morphogen is traditionally thought to instruct positional information through a concentration gradient (Towers and Tickle, 2009; Wolpert, 1969).

However, neural tube progenitors express transcription factors associated with more ventral fates when exposed to either high concentrations of Shh or prolonged durations Shh signalling and require continued Shh signalling to maintain ventral fates (Dessaud et al., 2007; Dessaud et al., 2010). Meanwhile, limb progenitors form increasingly posterior structures when subject to either increasing concentrations of Shh or increasing durations of Shh signalling (Harfe et al., 2004; Scherz et al., 2007; Towers et al., 2011; Yang et al., 1997). However, it is poorly understood how limb progenitors integrate differences in the levels and durations of Shh signalling at a molecular level.

Here, I show that a simple concentration gradient is insufficient to induce distinct transcriptional outputs in limb explants and that time is required to establish a graded response to the Shh morphogen gradient. After 6 hours of exposure, limb explants dosed with different concentrations of Shh did not show a significant difference in the levels of direct transcriptional read outs of Shh signalling, including *Gli1*, *Ptch1/2* and *Hhip,* as measured by RNAseq. In contrast, after 12 and 16 hours of exposure, explants exposed to the same concentration range elicited a graded response to increasing concentrations of Shh. At 12 and 16 hours, the lowest dose of Shh (2nM) induces low level expression of *Gli1/Ptch1/2/Hhip* that is only marginally above basal expression levels, seen in control explants. I have further observed that similar levels of *Gli1* expression are also observed in explants dosed with lower concentrations of Shh: 1nM, 0.5nM and 0.25nM, for 6 hours, suggesting any concentration of Shh (presumably above a minimum threshold) will elicit a 'maximal' response at this time point. I propose this is because an insufficient time has passed for detectable differences in levels of response to become apparent.

Meanwhile, explants dosed with a higher concentration of Shh, 16nM, exhibit a smaller increase in the level of *Gli1* expression after 12-16 hours, suggesting this concentration is hitting the beginning of a plateau. Collectively these data demonstrate that the concentration range I have used is suitable and is likely to be physiologically relevant. It is interesting that the same concentration range produces different response curves at different time points. Namely, statistically indifferent responses after 6 hours, but a graded response after 12 or 16 hours of exposure. Here, I have termed this initial response after 6 hours as 'binary' to describe that progenitors experiencing different levels of Shh signalling are exhibiting the same or statistically indifferent levels of response. Based on this observation, I suggest that *in vivo*, progenitors (at the earliest stage of *Shh* expression) subject to different concentrations of Shh will also exhibit very similar levels of response and consequently will be initially assigned the same identity. As such in the early limb bud, I propose 2 populations of progenitors exist: progenitors exposed to any concentration of Shh (above a minimum threshold) and progenitors not exposed to Shh. Over time, as progenitors produce a graded response to different concentrations of Shh, more individual identities are specified (Fig. 25).

In neural tube progenitors, a temporal adaptation mechanism is required to produce a graded response to Shh signalling (Dessaud et al., 2007). In this model cells initially show a similar level of response to Shh but cells become desensitised to Shh signalling over time (decreasing levels of response) at a rate that is inversely proportional to the concentration of Shh they are exposed to (Fig. 3A) (Dessaud et al., 2007). Here, I demonstrate that a graded response to Shh signalling in limb progenitors is achieved by a variation of temporal adaptation. Limb progenitors exposed to lower concentrations of Shh exhibit signal desensitisation at a rate

inversely proportional to the Shh concentration they are exposed to (as per neural tube progenitors). However, Limb progenitors exposed to higher concentrations of Shh exhibit signal accumulation – the cumulative gain of signal output - at a rate proportional to the Shh concentration they are exposed to (Fig. 12, 25). Limb progenitors exposed to high concentrations of Shh are predicted to eventually become desensitised to Shh signalling. I demonstrate this effect occurs in hindlimb explants (Fig. 18). Importantly, as described in the neural tube, this signifies that cells experience a duration of active response to Shh (Gli activity) that is proportionate to the concentration of Shh they are exposed to. Thus, extracellular concentrations of Shh are translated into durations of intra-cellular Gli activity integrating levels and durations of Shh signalling into a single input. These results are also consistent with a model in which limb progenitors are promoted to increasingly posterior fates by continued Shh signalling as previously proposed (Scherz et al., 2007; Towers and Tickle, 2009; Towers et al., 2008; Yang et al., 1997) (Fig. 25).

There is some *in vivo* evidence that supports a model in which limb progenitors become desensitised to extended Shh signalling. *Gli1* expression, a direct read out of Shh signalling, decreases in the posterior margin of stage 22 chick limbs (Marigo, Johnson, et al. 1996; Marigo, Scott, et al. 1996, Fig.6). Expression of *Ptch1,* however is maintained suggesting progenitors are still responding to Shh signalling but *Gli1* expression has become repressed as progenitors become desensitised to extended Shh signalling. This is consistent with observations in the mouse that progenitors that ultimately comprise digit 5 also become desensitised to extended Shh signalling as shown via a Gli1-lacz reporter (Ahn and Joyner, 2004). However, *ex vivo* data suggests that cells that are exposed to the lowest concentrations of Shh become desensitised soonest, implying that progenitors that are more anterior

should become desensitised to Shh signalling first. This would be harder to observe, as it would be more difficult to distinguish between cells that have become desensitised to Shh signalling and cells that are out of range of Shh signalling. You could attempt to observe desensitisation *in vivo* by using *in situ* hybridisation to measure the expression domains of Shh targets such as *Gli1* over time. This domain would be expected to reduce along its AP axis (as a proportion of the whole limb, since this is continuously growing) if anterior progenitors were becoming desensitised to Shh signalling. However, *ex vivo* data suggests progenitors that become desensitised to Shh only reduce expression of Shh targets and do not switch off expression entirely. This may not be detectable by *in situ* hybridisation given it is a qualitative and not a quantitative technique. Nonetheless, the *in situ* expression domains of *Ptch2* and *Gli1,* as a proportion of whole limb buds, do appear to decrease after Stage 21, which also coincides with the end of the Shh patterning period (Fig. 6, 8) suggesting desensitisation could be occurring in anterior progenitors. Whilst the size of normalised *Ptch2* and *Gli1* expression domains increase again at stage 24, this is after the Shh patterning period and would not be expected to have an effect on digit specification.

Different levels of response to Shh (measured by Gli activity) induces the expression of specific transcription factors which demarcate distinct neuronal cell sub-types in the developing neural tube (Dessaud et al., 2007). There are no known molecular markers of individual digit identities in the limb at present, beyond what I describe here. Consequently, I was unable to determine whether different levels of response (measured by *Gli1* expression) specify different cell fates in limb progenitors. However, I demonstrate that genes that have been implicated in specifying different digit identities exhibit a non-linear graded transcriptional response to different levels of Shh signalling in limb explants (Fig. 17, 18). This

suggests temporal adaptation may be required for correct interpretation of the Shh morphogen in limb progenitors. Progenitor domains at different AP levels *in vivo* may exhibit different levels of these genes, which may be important in specifying the identity of the digit they ultimately give rise to. I have further used *in silico* analyses to uncover candidate genes that are expressed in response to different levels of Shh signalling and may be involved in specifying cell fates (Discussion 6.4, Tables 3-6, Fig. 20, 21). A gradient based on temporal adaptation would be steepened by the movement of cells away from the ZPA. As cells move away from the ZPA they would experience lower levels of Shh signalling and would therefore more rapidly display desensitisation to Shh signalling.

These data and the observation that posterior digits can be induced by either high concentrations of Shh or long durations of Shh signalling support a model in which cumulative Gli activity specifies digit identities in the vertebrate limb, as has been proposed in the vertebrate neural tube (Dessaud et al., 2010) (Fig. 25). This is consistent with the Temporal Expansion model of digit specification (Harfe et al., 2004; Scherz et al., 2007), in which anterior digits are specified by a Shh concentration gradient but different posterior digits are specified by different durations of high Shh signalling.

The temporal expansion model has been described as inconsistent with the biphasic model of Shh-mediated digit patterning (Introduction 1.3) (Towers and Tickle, 2009; Zhu et al., 2008). The biphasic model proposes that mouse digit identities are specified early in limb development, by 15 hours of Shh activity, and thereafter Shh acts solely as a mitogen to expand the digit-forming field (Zhu and Mackem, 2011; Zhu et al., 2008). The data I present here suggests that populations of progenitors that show distinct transcriptional outputs based on cumulative Gli activity can be achieved in chicken limb progenitors within a similar time frame

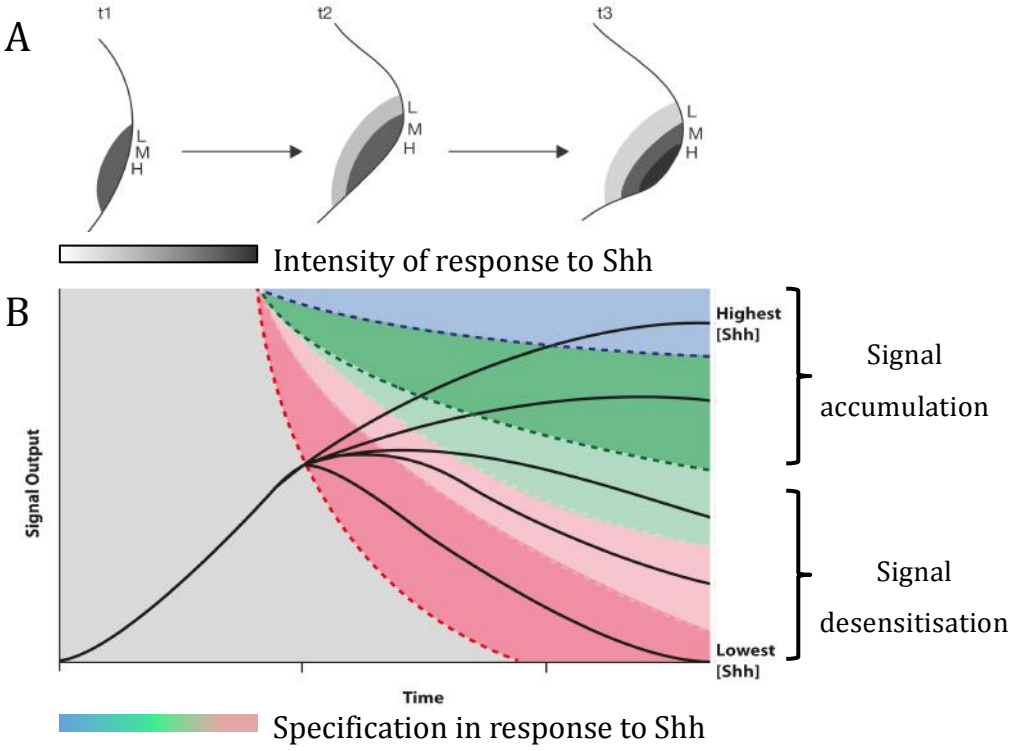

Figure 25 | Model of Shh morphogen gradient interpretation in the vertebrate limb. (A) Establishing populations of cells with distinct transcriptional outputs. At the earliest time point (t1), a binary response to Shh signalling is seen, cells respond equivalently to all concentrations of Shh (L=low [Shh], M=medium [Shh], H= high [Shh]) (grey) or are not exposed to Shh signalling (white). At time point 2 (t2), two distinct cellular populations, responding to Shh signalling are seen (light grey and grey). Signal desensitisation decreases signal output in cells exposed to the lowest concentration (L) of Shh (light grey). At time point 3 (t3) a graded response is seen, three distinct cellular populations have arisen as signal desensitisation continues to decreases signal output in cells exposed to the lowest concentration of Shh (L) (light grey) whilst signal accumulation has increased signal output in cells exposed to the highest concentrations of Shh (H) (dark grey). Cells exposed to medium concentrations of Shh (M) maintain a consistent level of signal output throughout (grey). Shh morphogen concentration is denoted as follows: L=low, M=medium, H= high, whilst intensity of response to Shh signalling is denoted in grey-scale. (B) Interpreting a graded response to Shh signalling. Different levels of signal output are achieved over time through a combination of signal accumulation in cells exposed to higher concentrations of Shh and signal desensitisation in those exposed to lower concentrations of Shh. Colours represent different anteroposterior (AP) cell fates (red-blue) that result from distinct levels of signal output. In this model cells are initially undifferentiated (grey) and are promoted to increasingly posterior fates over time in the presence of continued higher level Shh signalling.

(16 hours). Therefore it may be possible that Shh specifies digit identities within a 16-hour window through cumulative Shh signalling. This would reconcile the previously opposing models. Interestingly, the biphasic model also proposes that the mouse hindlimb is patterned by Shh after only 9 hours of Shh activity. Consistently, the data I present here also suggests that the hindlimb is patterned over a shorter period of time (12 hours) than the forelimb (Discussion 6.5).

6.3 The role of feedback mechanisms in correct morphogen gradient interpretation

Temporal adaptation by ligand dependent antagonism

A temporal adaptation mechanism is critical for correct interpretation of the Shh morphogen gradient in the neural tube (Dessaud et al., 2007). Temporal adaptation has been shown to be mediated, at least in part, by Ptch1 negative feedback, though Ptch2 and Hhip mediated negative feedback is also required for correct DV patterning of the neural tube (Dessaud et al., 2007; Holtz et al., 2013; Jeong and McMahon, 2005). Negative feedback through the downregulation of Shh co-receptors *Gas1, Cdon* and *Boc* is also required for correct DV patterning in the neural tube (Allen et al., 2007; Allen et al., 2011). Negative feedback resulting from the upregulation of *Ptch1, Ptch2* and *Hhip* and the downregulation of co-receptors *Gas1, Cdon* and *Boc* has been collectively termed Ligand Dependant Antagonism (LDA) (Holtz et al., 2013; Jeong and McMahon, 2005) (Fig. 26, Introduction 1.4).

Here, I show that a variation of temporal adaptation is required to establish a graded response to Shh signalling in limb progenitors (Fig. 12, Discussion 6.2). I further demonstrate that *Ptch1, Ptch2* and *Hhip* are strongly upregulated in limb explants exposed to recombinant Shh and could thus contribute to LDA and signal

desensitisation in limb progenitors (Fig. 12E, 20, 21). However, *Hhip*$^{-/-}$ mutants do not display a limb phenotype and *Hhip* transcripts are not detectable in chicken limb buds via whole mount *in situ* hybridisation (Aglyamova and Agarwala, 2007; Jeong and McMahon, 2005). Conversely, *Ptch1* and *Ptch2* are expressed posteriorly in limb bud and *Ptch1* and *Ptch2* hypomorphic mutants exhibit an expansion of *Gli1* and *Ptch1* expression domains in limb buds, which is an equivalent phenotype to the expansion of ventral domains in the neural tube observed in these mice (Butterfield et al., 2009; Holtz et al., 2013; Jeong and McMahon, 2005; Nieuwenhuis et al., 2006).

Moreover, I show that disrupting the upregulation of *Ptch1* and *Ptch2* using siRNAs, reduces signal desensitisation in limb explants dosed with Shh, confirming a role for *Ptch1/2*-mediated negative feedback in establishing temporal adaptation (Fig. 14B). I further demonstrate that limb explants dosed with the Smo antagonist, purmorphamine, did not exhibit signal desensitisation (Fig. 15B), demonstrating that the mechanism that controls signal desensitisation acts upstream of Smo activation. This provides further indirect evidence that Shh receptors and co-receptors are implicated in mediating the negative feedback that influences temporal adaptation. These results suggest Ptch1 and Ptch2, but not Hhip contribute to LDA and therefore adaptation, in the limb.

That *Hhip* expression is induced by Shh in *ex vivo* assays suggests that in an *in vivo* context an unknown factor may act to repress the upregulation of *Hhip.* Alternatively, *Hhip* expression in limb buds may be too low to detect by *in situ* hybridisation, whilst a potential role for Hhip in negative feedback may be masked by *Ptch1/2* compensation in *Hhip*$^{-/-}$ mutants. To more completely understand the individual contributions of Ptch1 and Ptch2, and to conclusively determine the involvement of Hhip in LDA in the limb a series of experiments comparing the

affects of siRNAs targeting *Ptch1, Ptch2* and *Hhip* individually and in combination on signalling output should be conducted. This however, was beyond the scope of this project. Such an experimental series would be more insightful if molecular markers of digit identities were discovered to clarify changes in morphogen interpretation.

Ptch1-2 and Hhip mediated negative feedback can act both cell-autonomously and noncell-autonomously (Ribes and Briscoe, 2009). However, precisely how these receptors act cell-autonomously is yet to be elucidated. It has been proposed that an abundance of Ptch1/2 and Hhip at the cell membrane, induced by Shh signalling, could increase competition between 'productive receptors' - that are actively inhibiting Smo, until bound by Shh - and 'non-productive' receptors - that do not actively inhibit Smo, but are capable of binding Shh (Holtz et al., 2013). In this model a decrease in signal output (desensitisation) arises from the binding of Shh to 'non-productive' receptors, which cannot transduce Shh signalling. However, whilst Hhip is capable of binding Shh ligand but is unable to repress Smo, direct evidence of the existence of 'non-productive' patched receptors is yet to be obtained. Moreover, why this should affect explants exposed to lower concentrations of Shh is unclear.

Alternatively, Ptch-mediated negative feedback may be directed through intra-cellular concentrations of small molecule ligands, such as oxysterols, which may be altered by the ratio of bound:unbound Ptch receptors. In this model the intra-cellular levels of such a ligand reaches a critical threshold, resulting in inhibition of Smo and termination of signal transduction. This model relies on Smo translocation and activation at the primary cilium being caused by a Ptch-mediated influx of small molecule ligands, which is yet to be directly demonstrated. The mechanism of

Patched-mediated negative feedback cannot be resolved until a better understanding of Patched-mediated repression of Smo is determined.

I also demonstrate that *Gas1* and *Cdon* are downregulated in response to Shh signalling in limb progenitors, but that *Boc* expression is unaffected. Interestingly, *Boc*$^{-/-}$, *Cdon*$^{-/-}$ and *Cdon*$^{-/-}$; *Boc*$^{-/-}$ mice display no limb phenotype whereas *Gas-1*$^{-/-}$ mice lack a digit 2 or digit 3. This is exacerbated in *Gas1*$^{-/-}$; *Boc*$^{-/-}$ mice, in which the remaining digit 2 or digit 3 has fused with digit 4, but *Gas1*$^{-/-}$; *Cdon*$^{-/-}$ mutants are phenotypically no different from *Gas-1*$^{-/-}$ mutants (Allen et al., 2007; Allen et al., 2011). This suggests that Gas1 plays an important role in Shh interpretation in the limb, and that Gas1 can compensate for a lack of Cdon or Boc in the limb. Cdon and Boc however cannot compensate for loss of Gas1, but Boc has a role in the absence of Gas1. These data suggest that downregulation of Gas1 by Shh provides the most profound contribution to LDA whilst Cdon may serve a redundant role and Boc, which is unaffected by Shh signalling, does not contribute to LDA in the limb.

Additional feedback mechanisms

Signal desensitisation is also observed in explants dosed with high levels of purmorphamine (Fig. 15A, C) (Cohen et al., 2015; Dessaud et al., 2007), suggesting that alternative negative feedback mechanisms may exist downstream of Smo activation. To identify such mechanisms I examined the effect of Shh signalling on key components of the Shh signalling pathway. Here, I demonstrate that expression of *Sufu* is induced, but *Disp1* is repressed, in limb explants exposed to medium and high concentrations of Shh after 12 and 16 hours (Fig. 16). Sufu is considered a negative regulator of Shh signalling (Chen et al., 2009; Jia et al., 2009), although recently it has been shown that it can also have a positive regulatory affect (Chen et al., 2009; Jia et al., 2009; Oh et al., 2015). Disp1 meanwhile is required for the

release of Shh ligand from morphogen producing cells (Burke et al., 1999; Ma et al., 2002; Tian et al., 2005; Tukachinsky et al., 2012). Downregulation of *Disp1 in vivo* may therefore reduce the amount of Shh ligand in the limb bud causing a decrease in responses to Shh in noncell-autonomous feedback mechanism (Fig. 26). Conversely, upregulation of *Sufu* is likely to have a cell-autonomous affect, decreasing response to Shh by sequestering Gli proteins in the cytoplasm (Jia et al., 2009) (Fig. 26).

I also show that Gli2 and Gli3 are downregulated by increasing levels of Shh signalling. This is consistent with previous reports that Gli2 protein expression is downregulated by Shh in the neural tube and *Gli3* is repressed by Shh in the limb (Cohen et al., 2015; te Welscher et al., 2002a; te Welscher et al., 2002b). Although bi-functional, during active Shh signalling Gli2 and Gli3 act as transcriptional activators (Gli^A). A transcriptional downregulation of Gli2 and Gli3 therefore is likely to lead to decreased levels of cytoplasmic $Gli2^A$ and $Gli3^A$ and consequently inhibit Shh signal transduction. Upregulation of *Gli1,* which can only act as a transcriptional activator of Shh targets, however will opposingly act to increase levels of cytoplasmic Gli^A and thus act to promote Shh signalling in a feed-forward loop (Fig. 26).

Lastly, I have identified another potential feedback mechanism that could operate through the regulation of Heparan Sulphate Proteoglycans (HSPGs). HSPGs are important for the spread of Hh proteins in tissues. Hh is unable to cross cells which are depleted in HSPGs in the imaginal discs of *D. melanogaster* (Bellaiche et al., 1998; Briscoe and Thérond, 2013; Han et al., 2004; Sanders et al., 2013), whilst defects in the synthesis of heparan sulphate chains on HSGPs or altering the sulphation-state of these chains can affect the spread and activity of Ihh and Shh in vertebrates

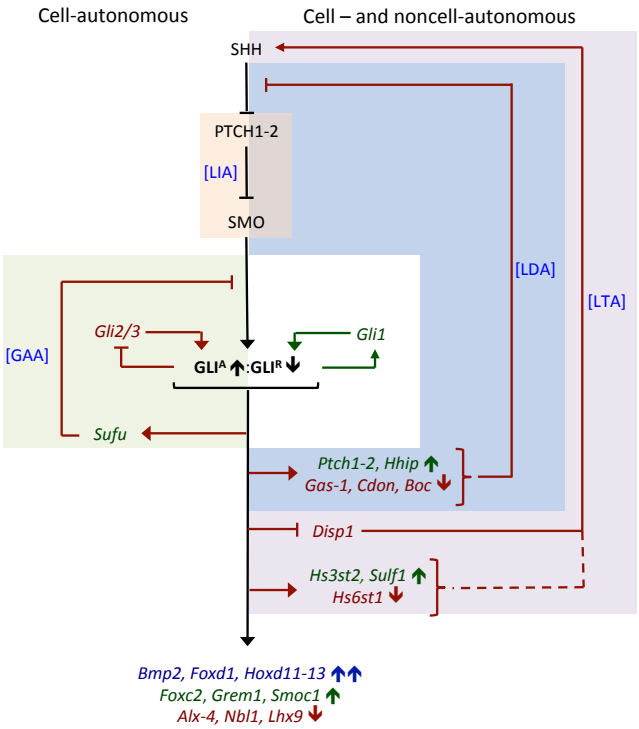

Figure 26| Flowchart of Shh signalling and feedback mechanisms. In the absence of Sonic Hedgehog ligand (SHH), Patched proteins (PTCH1-2) inhibit Smoothened (SMO) activation, termed Ligand Independent Antagonism (LIA) (orange box). Binding of SHH to PTCH1-2 releases Ptch1/2-mediated inhibition and SMO is activated which in turn promotes a shift in the balance of cytoplasmic bi-functional GLI transcription factors (GLI^A and GLI^R) in favour of GLI activators (GLI^A). This shift in balance promotes the transcription of positive Shh targets (upward arrows) and the repression of negative Shh targets (downwards arrows). Shh targets in the limb which show a peak response to high (blue) and medium (green) or are repressed (red) by Shh signalling are denoted. Shh signalling induces Shh receptors *Ptch1-2* and *Hhip,* and represses Shh co-receptors *Gas1, Cdon, Boc* which collectively inhibit Shh signal transduction in a mechanism termed Ligand Dependent Antagonism (LDA) (blue box). Downregulation of *Disp1* reduces levels of diffusible SHH ligand whilst regulation of *Hs3st2*, *Sulf1* and *Hs5st1* may inhibit the diffusion of SHH ligand noncell-autonomously, collectively termed here Ligand Transport Antagonism (LTA) (purple box). Downregulation of *Gli2/3* reduces GLI^A whilst an upregulation of *Sufu* inhibits GLI activity and together lead to cell-autonomous negative feedback termed here Gli Activator Antagonism (GAA) (green box). Upregulation of *Gli1,* which lacks repressor activity serves as a positive feedback loop to promote GLI^A. Positive feedback (green) and negative feedback (red) routes are distinguished. Cell-autonomous and noncell-autonomous negative feedback mechanisms that are shown on the left and right of the image respectively. Genes and transcripts (italics) and proteins (capitals) are distinguished. Potential feedback loops are denoted with dash lines.

and *D. melanogaster* (Briscoe and Thérond, 2013; Danesin et al., 2006; Koziel et al., 2004; Touahri et al., 2012; Wojcinski et al., 2011).

Here I show that three enzymes, involved in the synthesis or modulation of heparan sulphate chains on HSGPs are differentially expressed in explants exposed to Shh signalling. Hs3st2 and Hs6st1 generate a myriad of heparan sulphate fine structures, whilst Sulf1 selectively removes 6-O-sulphate groups from heparan sulphate chains. *Hs3st2* and *Sulf1* exhibit a peak induction by high and low levels of Shh signalling respectively, whilst *Hs6st1* is repressed by Shh signalling (Tables 3-6, Fig. 21, 22). This raises a interesting possibility that Shh signalling could promote or impede the spread and activity of Shh ligand in different AP domains by inducing or repressing different enzymes involved in the synthesis and modulation of heparan sulphate chains on HSPGs (Fig. 26). It is possible that Hs3st2 and Hs6st1 have antagonistic actions, with Hs6st1 promoting, but Hs3st2 impeding, Shh diffusion or activity. Contrary to *in silico* predictions*, Hs3st2* is detected weakly in an intermediate AP domain, though this does not preclude its involvement in HSPG-related feedback loops.

Taken together, cell-autonomous upregulation of *Sufu* and downregulation of *Gli2* and *Gli3* are the mechanisms most likely to induce signal desensitisation in neural tube and limb explants dosed with purmorphamine. However, to gain further insight into cell-autonomous negative feedback mechanisms I have begun to analyse the transcriptional responses of limb explants dosed with high concentrations of purmorphamine. Meanwhile, downregulation of *Disp1* and regulation of HSPGs may contribute to further noncell-autonomous feedback mechanisms.

The possible feedback loops described in this sub-chapter are stimulated by Shh ligand and should therefore come under the designation of LDA. However, it is useful to differentiate feedback mechanisms operating cell-autonomously and noncell-autonomously and I have further sought to distinguish LDA negative feedback mechanisms from novel potential noncell-autonomous feedback mechanisms. Subsequently, in this report I have termed feedback acting cell-autonomously through Sufu and Gli2/3 Gli Activator Antagonism (GAA) and noncell-autonomous feedback operating through Disp1 and potentially HSPGs as Ligand Transport Antagonism (LTA) (Fig. 26). Whether these additional feedback mechanisms are required for correct interpretation of Shh morphogen gradients, as temporal adaptation is, remains to be determined.

6.4 Targets of Shh signalling in the limb and encoding digit identity

Evaluation of *in silico* analyses

Different levels and durations of Shh signalling can specify different digit identities. However, how Shh signalling instructs this at a molecular level is poorly understood. Moreover, molecular markers of distinct digit identities remain elusive. Here, I identify genes that are statistically differentially expressed (DE) in limb explants cultured *ex vivo* in different concentrations of Shh for fixed periods of time and genes that cluster to specific transcriptional profiles to predict genes that may be expressed in different AP domains. I describe candidate genes that I predict are expressed at: posterior, primary intermediate, secondary intermediate and anterior AP levels and may mark or contribute to specifying different digit identities (Fig. 20, 21, 27).

An alternative method of identifying novel markers of digit identities would have been to measure the transcriptome of progenitors at different AP positions (at different developmental stages) and that ultimately give rise to different digits directly. Indeed, this would be a good approach to address this biological question, however, identifying novel markers of digit identities was not the initial aim of this project. This experiment would not be able to define which genes are induced/repressed by different levels of Shh in limb progenitors and would not allow direct comparison of the response of forelimb and hindlimb progenitors to equivalent Shh signalling as it is not known if respective limb buds are exposed to equivalent levels of Shh signalling *in vivo*. Lastly, it would be more difficult to maintain consistency with dissections and staging (especially between respective limb buds that develop at different rates) in this experiment.

Candidate gene lists featured a number of genes that are known targets of Shh signalling in the limb and that are expressed in the AP domains predicted by *in silico* analyses, validating this approach (Fig. 27, green). This was particularly the case for genes predicted to be expressed in either posterior or anterior domains, whilst *Grem1* was the only gene that featured in intermediate AP lists that is known to be expressed in an intermediate domain (Fig.27). Interestingly, genes not previously described as targets of Shh signalling, and with unknown expression patterns in the limb, also featured in gene lists and are predicted to be expressed in specific AP domains.

Here, I show that *Smoc1, Foxc2* and *Tsku* are expressed at a primary intermediate AP level and *Foxo6* is expressed at a primary and secondary intermediate AP level, consistent with *in silico* predictions, further validating this approach (Fig.22). I further show that *Mab21l1* is initially expressed in an anterior domain as predicted before expanding posteriorly expression domain, reminiscent of the expression

patterns of *Msx1* and *Msx2,* whilst *Lhx6* appears to be expressed weakly in a posterior domain (Fig.22).

However, I also show that some genes are not expressed in the domain that is predicted. *Foxf1,* which was predicted to be expressed posteriorly, is not detectable in the developing limb bud. Robust *Foxf1* expression was detected in the developing gut however demonstrating this probe is able to clearly detect *Foxf1* expression. Meanwhile, *Hs3st2,* which was also predicted to be expressed posteriorly, is weakly expressed in a primary intermediate domain. These data demonstrate that false positive results can arise using these prediction strategies. Genes that appear to be expressed in response to Shh signalling *ex vivo* but are not detected *in vivo* may be repressed by another factor *in vivo* that is absent in culture. Alternatively, expression of these genes may be very low making them hard to detect by *in situ* hybridisation. This may especially be the case for genes that exhibit low read-counts by RNAseq such as *Foxf1*.

Both clustering and statistically significant gene lists can also give rise to false negatives as demonstrated by the absence of *Lhx9* in the forelimb '*Alx-4-like'* cluster and the absence of *Mab21l1* in the list of genes repressed by 8nM Shh after 16 hours in forelimbs (Fig. 21, Table 4). False negatives (and false positives) in statistically DE gene lists could be negated by increasing the n number, though this was not feasible in the time scale of this project.

Meanwhile, clustering experiments are susceptible to false negative/positive results depending on the level of stringency that is set. Low stringency increases the likelihood of false positives whilst high stringency increases the likelihood of false negatives. These errors can also be avoided by increasing n numbers, but may also by reduced by coding for a degree of flexibility in gene clusters to account for

the margin of error in normalised read counts. Interestingly, genes that are repressed by Shh were more prone to false negative results in clustering gene lists as the expression levels of genes in explants exposed to different concentrations of Shh were often similar and over-lapping (Fig. 17, 18, 20, 21). This may indicate that genes that are repressed by Shh are generally more sensitive to Shh signalling.

Whilst all statistical and clustering analyses are prone to false positive/negative results, I have tried to circumvent errors by using two methodologies to produce gene lists and have cross-referenced gene lists to attempt to ascertain genes that are truly likely to be expressed at specific AP domains (Fig. 27).

Encoding posterior digit identities

Genes that feature in posterior, primary intermediate, secondary intermediate and anterior gene lists are predicted to be expressed in corresponding AP domains and may contribute to specifying the identities of digits that arise from these domains. Indeed, many of the genes that are predicted to be expressed in a posterior domain are expressed in this domain and are implicated in limb development (Fig. 27). *Hoxd11-13, Hoxa10-13, Hand2, Bmp2, Tbx3,* and *Sall1,* which feature in posterior gene lists, are expressed posteriorly and have been identified as direct targets of Gli transcription factors in mouse limbs (Vokes et al., 2008) (Fig.3). These therefore represent strong candidates of genes that are regulated by Shh to specify posterior digit identities and indeed have been implicated in the development of posterior digits (Davenport et al., 2003; Drossopoulou et al., 2000; McLeskey Kiefer et al., 2003; te Welscher et al., 2002b; Yang et al., 1997; Zákány et al., 2004) (Fig. 27). *Kchn5, Cntfr, Figf, Fgf18, Fgf10, Rspo3,* and *Six1* which also feature in posterior gene lists are also expressed in a posterior domain and may contribute to the

development of posterior digits (Bangs et al., 2010; Bell et al., 2004; Bonnin et al., 2005; Davey et al., 2007) (Fig. 27).

Conversely, I demonstrate *Foxf1* is unlikely to play a role in specifying posterior digit identities despite being in posterior gene lists, as its expression is not detectable in chicken limbs (Fig. 22). Similarly, *Lhx6* is only weakly expressed in chicken limbs making its importance unclear (Fig.22). *Blimp1* and *Jag1* meanwhile, which have also been reported as a direct target of Gli in limbs (McGlinn et al., 2005; Vokes et al., 2008) (Fig.3) do not feature in posterior gene list but did respond positively, though insignificantly, to Shh signalling and thus its role is also unclear (data not shown).

Of the remaining genes in this list, *Foxd1* and *Foxl1* represented the most interesting candidates as transcription factors with unknown roles in limb development. Constructs containing chicken *Fox* genes were not commercially available and consequently it was necessary to clone these genes from chicken cDNA. Unfortunately, I was unable to do this for *Foxd1* and *Foxl1* despite repeated attempts using different primers, template cDNA and PCR programs. I therefore have been unable to determine whether these genes are expressed posteriorly as predicted.

Encoding anterior digit identities

As with posterior gene lists, many of the genes that were predicted to be expressed in an anterior domain are expressed in this domain and several have been implicated in limb development, though they have not necessarily been previously described as being influenced by Shh signalling. *Lhx9/2, Gsc, Glis1, Alx-4, Sox8, Msx1/2, Gas1*, *Nbl1, Irx5* and *Zic3* are expressed anteriorly (Bell et al., 2004; Bertuzzi et al., 1999; Gerlach-Bank et al., 2002; Heanue et al., 1997; Li et al., 2014b;

Rodriguez-Esteban et al., 1998; te Welscher et al., 2002a; Wang et al., 2011). Of these, *Alx-4* and *Irx5* have been implicated in normal development of the anterior structures whilst it has been suggested that *Zic3* may mark digit 1 in chicken forelimbs and hindlimbs (Li et al., 2014b; te Welscher et al., 2002a; Wang et al., 2011). Here, I demonstrate that *Mab21l1* is also expressed in an anterior domain early in limb development, before expanding more posteriorly (Fig. 22).

These data suggest that Shh signalling is important in maintaining the expression of these genes -and potentially other genes within anterior gene lists presented here - in a distinct anterior domain. That many of them are transcription factors or have been previously described as homeotic genes suggests that they may play an important role in specifying anterior digit identities or that there absence is required for the formation of posterior digits. Moreover, BMP antagonists *Nbl1, Vwc2* and *Nog* may also play a role in limb development given the requirement of BMP antagonist Grem1 in normal limb development (Khokha et al., 2003). Indeed, *Nog*$^{-/-}$ mice develop 'club shaped limbs' that feature a normal number of digits but which are abnormally broad and lack all wildtype digit identities (McMahon et al., 1998; Wijgerde et al., 2005).

Conversely, *Pax1* and *Pax9* which have previously been reported as repressed by Shh signalling in mouse limbs (McGlinn et al., 2005; Vokes et al., 2008), were absent from anterior gene lists. *Pax1* and *Pax9* expression was not detected in limb explants and consequently it was not possible to detect any repression that may be mediated by Shh signalling. However, this does not preclude the possibility that Shh represses *Pax1* and *Pax9 in vivo* and suggests that an unknown factor absent from *ex vivo* culture is required for the endogenous induction of these genes.

Figure 27| Summary of targets of Shh signalling that are predicted to contribute to specifying different digit identities. Summary lists of genes predicted to be expressed in designated AP domains of chicken limb buds and may contribute to the specification of the digits that arise from these progenitor domains. Exemplary expression patterns are shown above corresponding list. Components of the Shh signalling pathway (purple, striped purple (tentative)), transcription factors (yellow) and genes implicated in signalling pathways (blue) are denoted. Genes implicated in the differentiation or maintenance of different tissues that comprise mature limbs (orange) are also denoted. Genes that are known to be expressed in the domains predicted by *in silico* analysis or are known to be repressed by Shh are highlighted (bold, green). Genes predicted to be involved specifically in chicken hindlimb patterning are designated (*).

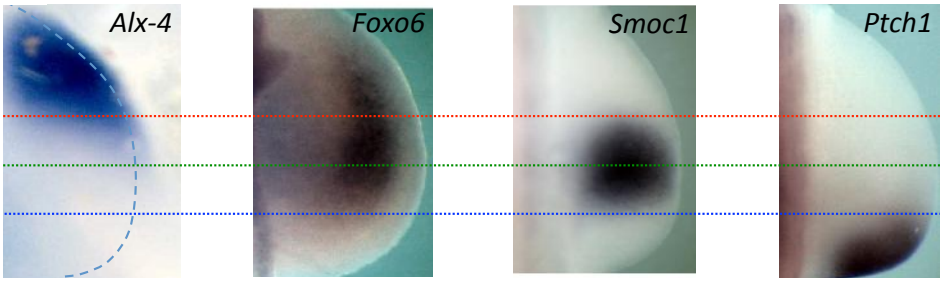

Anterior /Repressed			Secondary Intermediate			Primary Intermediate			Posterior		
		LHX9	Bone	BMP	**GREM1**	Bone	BMP	**SMOC1**			**PTCH2**
		GSC			AOX1	Lym		**FOXC2**			**HHIP**
		GLIS1*			BSX			CNGA3			**HOXD13**
		GLI3			SULF1			LIX1*			**HOXD12**
		GLI2			FOXO6		FGF	SPRY4			**OSR1**
		PTX3			KIRREL3	Tend		HAPLN1			**PTCH1**
		ALX-4			FANCC			ANO1			**GLI1**
		MGMA			RADIL			KIRREL3	Neur		**CNTFR**
		MAB21L2			KCNJ3			APOD		EGF	EFEMP1
		SOX8			AMACR			MORN5		WNT-	AMER2
Bone		**MSX1**			SLC22A23			NTN1			**HOXD11**
Bone	BMP	**NBL1**			CNTLN	Tend		HAS2			**HOXA13***
		MAB21L1			LRIG3			**FOXO6**	Bone	FGF	**FGF18***
		RASL11B			TMEM200B	Bone	BMP	**TSKU**			LHX6
		GAS1			DDX4			NRSN1			FOXF1
		CD82			WDR36			DCDC2	Bone	BMP	**BMP2**
		MERTK			SCNN1G			IL1RL1			**KCNH5**
Bone	BMP	VWC2			TRPA1			PAMR1			FOXD1
Bone		**MSX2**			C9ORF3			PODXL2	Vas	VEGF	**FIGF**
		PKP2			DHX58			PRICKLE2		GPRC	RAMP1
		KAT6B			EPHB3			TMEM132D			**TBX3**
		FGFBP1			COL25A1			NGFR		GPRC	TRIB1
		IRX5			HOXA7			NRG1			FOXL1
		DISP1			ABCG2			KCNJ3			HS3ST2
		ZIC3			SIX2			APBB1IP		FGF	**FGF10**
		HS6ST1			HEXB			LAPTM4B		WNT	RSPO3
		LHX2			ARHGAP26			EDIL3			PLCXD3
		FILIP1L			FMN2			EXOC2	Vas	VEGF	**RHOJ**
Bone	BMP	**BMP4**			IDUA			SDC3			ABCC3
		TMEM108			GNB1L			SCPEP1	Tend		**SIX1**
		CRISPLD1			TBX18			PIM1	Bone		RUNX2
		CRISPLD2			PITX2			PRKD1			IRK1
Bone	BMP	NOG			PMP22			FMNL2			PODXL
Neur		SOX6			CYTL1			PRELP			P2RY1
		PRRX1			NDUFA8			LRFN5			STRA6
Bone		SOX5			SULT1E1			MANBA		FGF	FGF1
		KCNK1			CD151			PELI2			**HAND2**
Bone	BMP	**BMP7**			ISOC1			ZEB2			**HOXA11***
		TOX			LHX1			PROM1			**HOXA10***
		GLCCI1			FAM190B			KCNK5			**SALL1**

Encoding intermediate digit identities

Of the genes that are predicted to be expressed in intermediate AP domains only BMP antagonist *Grem1* has previously been demonstrated to be expressed in such a domain (broadly across primary and secondary intermediate domains) and plays a crucial role in limb development. Mice lacking *Grem1* exhibit limbs with only 3 digits of unclear identity (Khokha et al., 2003). Here I demonstrate that two other BMP antagonists, *Smoc1* and *Tsku* are expressed in a primary intermediate domain, as predicted, and may play a similar role in inhibiting BMP signalling in the intermediate limb bud. Recently it has been reported that *Smoc1*$^{-/-}$ mice lack either a digit 2 or digit 3 and patterning of digits appears to be disrupted, although the authors do not emphasis this (Okada et al., 2011) – discussed below.

I further demonstrate transcription factors *Foxc2* and *Foxo6* are also expressed in primary and secondary intermediate domains respectively. These represent the only transcription factors that were predicted to be expressed intermediately and may mark or contribute to specifying middle digit identities. Intriguingly, *Smoc1, Foxc2, Tsku* and *Foxo6* are expressed by different progenitor populations within the primary and secondary intermediate AP domains, suggesting they may play distinct roles in limb development (Fig. 22).

The role of *Smoc1* in specifying and marking middle digit identities

I demonstrate that *Smoc1* expression exhibits a peak response to medium Shh concentrations and show that it is expressed in a primary intermediate AP domain consistent with *in silico* predictions. Smoc1 is a BMP antagonist and could have a role in inhibiting BMP signalling in limb development similar to Gremlin1 (Introduction 1.3). Moreover, its distinct expression pattern suggests it may be implicated in specifying middle digit identities. Indeed, mutations in *Smoc1* result

in the abnormal development of middle digits in humans and mice (Okada et al., 2011; Rainger et al., 2011), however its sufficiency to specify middle digit identities has not been previously investigated. Results reported in this study are unfortunately unable to provide conclusive evidence to address this question (Fig. 23). Chicken embryos that had been successfully electroporated with a *Smoc1* expressing construct unfortunately died before formation of skeletal structures in the limb had been completed (Fig 23). In some cases this was due to infection, but other embryos appeared to die from the effects of electroporation, illustrating an inherent problem with this technique.

Although, limb defects appeared to be apparent in early limb buds of two embryos the abnormalities observed were inconsistent (Fig. 23). Moreover, several control limbs, that were electroporated with an RFP-expressing construct only, also exhibited limb abnormalities. Distinguishing the effects of electroporation from the effects of *Smoc1* over-expression thus represents another difficulty in using this technique. To circumvent these issues this question could be addressed by a number of other methods, which unfortunately there was insufficient time to complete in this study. *Smoc1* could be ectopically expressed throughout early chick limb buds by injecting an avian specific Replication-Competent ASLV long terminal repeat (LTR) with a Splice acceptor (RCAS) viral vector engineered to constitutively express *Smoc1* into limb buds. Alternatively, this question could be addressed by generating a mouse that constitutively expresses *Smoc1* across the entire limb bud using the *Paired Related Homeobox 1* (*Prx1*) promoter, which is active in limb mesenchyme, and a *Cre-Lox* system (Logan et al., 2002; Sauer and Henderson, 1988). Similarly, a transient transgenic mouse with *Smoc1* directly under the control of the *Prx-1* promoter could be generated.

Fate-mapping cells that have expressed *Smoc1* using a *Cre-Lox* system would also be useful to determine if *Smoc1* positive progenitors ultimately give rise to middle digits and can be used as marker of middle digit identities. This would be useful in a number of limb studies in identifying digit identities in limbs in which patterning has been perturbed.

An overview of Shh targets in the limb

Many transcription factors and genes implicated in signalling pathways are predicted to be expressed in posterior and anterior domains (Fig. 27). Conversely, relatively few transcription factors and genes implicated in signalling pathways are predicted to be expressed in primary and secondary intermediate domains (Fig. 27). Moreover, many of the genes in anterior and posterior gene lists are expressed broadly across the either the anterior or posterior half of the limb buds. The digits arise from progenitors that constitute the posterior 50-60% of limb buds (Nomura et al., 2014; Vargesson et al., 1997b). This suggests there may not be a clear code of transcription factors that specify distinct progenitor identities as observed is in the neural tube. Indeed Shh is operating over a larger area to specify distinct 3-dimensional structures, which are comprised of many different cell types rather than distinct neuronal cell-subtypes of the neural tube. Different levels of posterior transcription factor activities (and the absence of anterior transcription factor activities), responding to different levels of Shh signalling in distinct AP domains may be sufficient to specify distinct digit identities. However, two notable exceptions present themselves from *in silico* analyses that represent the best candidates of code-like (Vargesson et al., 1997b) markers, or genes that are involved in the specification individual, of digit identities (Fig. 27).

Of particular interest is the *Fox* family of transcription factors and BMP signalling/antagonism. Although *Foxf1* appears not to play a role, both *Foxd1* and *Foxl1* are predicted to be expressed posteriorly and may have a role in specifying posterior digit identities. *Foxc2* and *Foxo6* meanwhile are expressed at primary and secondary intermediate AP levels respectively, raising the intriguing possibility that a code of *Fox* transcription factors may mark or contribute to specifying different digits identities across the AP axis.

In silico analyses indicate that Shh induces and represses the expression of different BMP signalling molecules and BMP antagonists at different AP levels. *Bmp2,* is induced posteriorly but *Bmp4* and *Bmp7* appear to be repressed by Shh signalling but are expressed in both anterior and posterior domains. Meanwhile BMP antagonists *Nbl1, Vwc2* and *Nog* appear to be repressed by Shh signalling which may restrict their expression anteriorly. Indeed, *Nbl1* is expressed anteriorly (Gerlach-Bank et al., 2002). However, BMP antagonist *Grem1* is expressed in a broad intermediate domain (Khokha et al., 2003) whilst *Smoc1* and *Tsku* are expressed in different primary intermediate domains (Fig. 22) (Okada et al., 2011). Different BMP antagonists, induced or repressed by different levels of Shh signalling may regulate BMP signalling to distinct levels in different AP domains. This may act to refine Shh patterning across the AP axis of the limb. Expression and functional analyses of these BMP antagonists and Fox transcription factors should be a priority.

Interestingly, many of the genes highlighted in both differentially expressed gene lists and clustered gene lists are reportedly implicated in the differentiation or maintenance of cell types/tissues that are in the mature limb including muscle, neuronal, bone, vasculature tissues as well as extracellular matrix proteins (Fig. 27, orange). This provides the beginning of an understanding of how Shh signalling

specifies different morphological structures comprised of these different tissues at a molecular level.

Finally, several genes that are expressed in posterior and primary intermediate AP domains in the limb in response to high and intermediate levels of Shh signalling respectively are also expressed in equivalent domains in the pharyngeal arches where Shh signalling is also active. Direct read outs of Shh signalling such as *Ptch1*, *Gli1* and *Ptch2* are co-expressed with *Shh,* whilst *Smoc1* and *Foxc2* were expressed in an intermediate domain and *Mab21l1* was expressed in an intermediate and anterior domain in the pharyngeal arches (Fig. 22, 24A, C). This supports a model in which different levels of Shh signalling induce the expression of different targets of Shh. However, a subset of genes that are expressed at an intermediate AP level in the limb are expressed in a posterior domain in the pharyngeal arches, including *Foxo6* and *Tsku* (Fig. 22, 24B). This suggests that either the level of Shh produced by cells is modulated in different tissues to induce the expression of specific genes in those tissues or that high levels of Shh can induce genes such as *Foxo6* but other factors (which may also be induced by Shh) supress the activation of *Foxo6* in the posterior limb bud. This raises an interesting possibility that the response of cells within a morphogen field may differ depending on the context of the environment they are in, as well as the level of signalling they are exposed to.

6.5 Differences in the response of forelimb and hindlimb progenitors to equivalent Shh signalling

In this report I provide evidence that chicken hindlimbs are patterned by Shh over a shorter period of time than forelimbs but that few genes appear to be differentially expressed between forelimb and hindlimb progenitors in response to

Shh signalling. The rate at which progenitors display desensitisation to Shh signalling is critical to the temporal adaptation model. This occurs at a rate inversely proportional to the concentration of Shh progenitors are exposed to (Dessaud et al., 2007). Subsequently, explants exposed to the highest doses of Shh should exhibit signal desensitisation last.

The results I present here suggest that hindlimb cells show a complete range of Shh responses over a shorter period of time (Fig. 18). Signal desensitisation is only observed in forelimb explants exposed to lower concentrations of Shh after 16 hours as judged direct readouts of Shh signalling, *Gli1* and *Ptch1,* but is observed in hindlimb explants exposed to all concentrations of Shh by this time.

Similarly, levels of *Hoxd11-13,* which do not demonstrate signal desensitisation in response to any concentration of Shh after 16 hours in forelimb explants have already begun to display desensitisation in hindlimb explants exposed to low concentrations of Shh by this time. Together these data suggest that hindlimb explants show temporal adaptation after a shorter duration of Shh signalling than forelimb progenitors. This is consistent with the observation that Shh is expressed for a shorter period of time in the hindlimb (Fig. 6) and that patterning is completed over a shorter period of time in chicken hindlimbs (Scherz et al., 2007; Towers et al., 2011).

Directly comparing forelimb and hindlimb gene lists can be misleading, as hindlimb explants appear to be at a more advanced stage of Shh response by 16 hours than forelimb explants. Whilst both differentially expressed gene lists and profiling gene lists feature different genes between forelimb and hindlimbs this appears to mostly represent a temporal differences. This is demonstrated in gene profiling lists where many of the genes that cluster with *Ptch1* in forelimb explants cluster with

Hoxd13 in hindlimb explants as the hindlimb *Ptch1* expression profile is at a more advanced stage of response.

However, almost all genes are predicted to be expressed in specific AP domains are present in both forelimb and hindlimb lists and moreover this is reflected in *in situ* hybridisations. The most notable exceptions to this was *Hoxa10-13,* which are induced by Shh signalling in hindlimb explants but are not expressed at all in forelimb explants in this assay. Consistently, *in situ* hybridisations demonstrate that *Hoxa10-13* is expressed during Shh patterning stages in the chicken hindlimb but not in the forelimb (Bell et al., 2004). Although *Hoxa* genes are expressed later in the forelimb, it would be interesting to determine the effect of precociously mis-expressing these genes on the morphology of chicken forelimbs.

Moreover, despite being induced in both limb buds, certain genes appear to be induced/repressed more robustly in response to Shh signalling in one limb than another. The two clearest examples of this are *Six1* and its co-activator *Eya1,* which are more strongly induced in hindlimb explants than forelimb explants and *Glis1,* which is more severely repressed in hindlimb explants. Interestingly, expression of *Six1* does appear to be more broadly expressed in hindlimbs in *in situ* hybridisations (Bell et al., 2004).

In conclusion, hindlimb progenitors appear to complete their response to Shh quicker than forelimb progenitors and the *Hoxa* cluster represents the strongest candidates of genes, which might confer different responses to equivalent Shh signalling between the respective limbs.

6.6 Summary and future directions

In the work presented in this report I have attempted to gain a molecular insight into how the Shh morphogen patterns vertebrate forelimbs and hindlimbs. To do this I have investigated potential differences in Shh signalling dynamics of the respective limb buds and have further investigated the transcriptional responses of forelimb and hindlimb progenitors to different levels of Shh signalling.

In the absence of more direct or rigorous techniques, I have attempted to gain insight into potential differences between Shh signalling dynamics of the chicken forelimb and hindlimb. Despite the limitations to the techniques I have used, I have been able to make some interesting observations. Firstly, that chicken the hindlimb bud is slightly larger than the forelimb bud during Shh patterning stages but that both limb buds appear to produce similar amount of Shh at a consistent rate from a similar number of cells. Subsequently, a greater proportion of forelimb bud progenitors maybe be subject to Shh signalling than the hindlimb bud. Secondly, that hindlimbs buds are exposed to Shh signalling for a shorter duration and appear to be completely patterned by Shh over a shorter period of time.

In a separate line of investigation I have used an *ex vivo* approach and RNAseq analysis to examine the immediate transcriptional responses of forelimb and hindlimb progenitors to different levels and durations of Shh signalling. I have demonstrated that chicken limb buds display a variation of a temporal adaptation mechanism which is required for graded expression of Shh targets implicated in specifying digit identities in response to graded Shh signalling. I have further demonstrated that signal desensitisation, a critical component of the temporal adaptation mechanism, is mediated by Ptch1-2 directed LDA.

I have also identified other potential negative feedback mechanisms. I have demonstrated that *Sufu,* a negative regulator of Shh signalling is upregulated by Shh, whilst *Gli2* and *Gli3* are downregulated by Shh. These mechanisms comprise a cell-autonomous negative feedback mechanism I have termed Gli Activator Antagonism (GAA). I have also shown that *Disp1,* required for the release of Shh ligand is downregulated by Shh and *HS3st2* and *Sulf1* - enzymes that synthesise and alter heparan sulphate chains on HSPGs – are upregulated whilst *Hs6st1,* another such enzyme, is downregulated by Shh. These responses may contribute to a noncell-autonomous negative feedback mechanism I have termed Ligand Transport Antagonism (LTA).

I have used *in silico* analysis to identify genes that are induced or repressed by different levels of Shh signalling and that are predicted to be expressed in specific AP domains. These genes may mark or specify different digit identities. Of particular interest, I have identified Fox transcription factors and BMP antagonists, which are expressed in different AP domains and may be implicated in marking or specifying middle digit identities.

Finally I have shown that many of the same genes are induced and repressed in hindlimb progenitors and forelimb progenitors in response to Shh signalling. However, *Hoxa10-13, Six1, Fgf18* and *Glis1* appear to be upregulated to a greater extent in hindlimb progenitors. Moreover, hindlimb progenitors display a complete range of Shh responses over a shorter period of time than forelimb progenitors.

Future lines of investigation

Future projects should focus on expression and functional analyses of candidate genes identified by *in silico* analyses. In particular to investigate the roles of BMP antagonists, *Smoc1, Tsku, Nbl1* and *Vwc2* and Fox transcription factors *Foxd1*, *Foxl1,*

Foxc2 and *Foxo6* in marking and specifying distinct digit identities. Investigations should first aim to determine the expression patterns of *Vwc2, Foxd1* and *Foxl1* to eliminate any further false positive results. The genetic tools of the mouse should be utilised to determine the requirement and sufficiency of these genes to specify distinct digit identities and to determine if they mark particular digits.

To determine if these genes are required to specify distinct digit identities a *Cre-lox* system and the *Prx1* promoter could be used to conditionally knock out genes of interest in limb mesenchyme (Logan et al., 2002). Conversely, to determine if these genes are sufficient to induce the formation of specific digit identities ectopically, a similar *Prx1* driven *Cre-lox* system could be used to constitutively express genes of interest throughout the limb mesenchyme. Alternatively, transient transgenic mice could be generated expressing genes of interest in limb mesenchyme directly from the *Prx1* promoter (Logan et al., 2002). Finally, to determine if these genes may demarcate individual digit identities fate-mapping analysis should be employed to determine the identity of digit(s) that ultimately arise from progenitors that express specific genes.

Alternative future projects should focus on identifying and characterising Shh signalling feedback mechanisms. To determine the roles of *Hs3st2, Sulf1* and *Hs6st1* in a potential noncell-autonomous negative feedback loop, gain-of-function and loss-of-function experiments in the neural tube could be used to determine how these genes influence the Shh morphogen gradient.

The neural tube is the best tissue to study general mechanics of Shh signalling as an established code of transcription factors gives a clear readout of morphogen interpretation, which gives greater insight into the effects of perturbing the morphogen gradient. Heterozygous and homozygous mutant mice could be

generated for loss of function studies, whilst the chicken neural tube could be used for ectopic expression via electroporation of constructs expressing *Hs3st2, Sulf1* or *Hs6st1.*

Finally, to identify further possible cell-autonomous negative feedback mechanisms, I have begun to use RNAseq analysis to determine genes that are differentially expressed in limb explants exposed to high concentrations of purmorphamine (which induces signal desensitisation), compared to explants dosed with lower concentrations of purmorphamine or with equivalent doses of Shh.

References

Abouzeid, H., Boisset, G., Favez, T., Youssef, M., Marzouk, I., Shakankiry, N., Bayoumi, N., Descombes, P., Agosti, C., Munier, F. L., et al. (2011). Mutations in the SPARC-related modular calcium-binding protein 1 gene, SMOC1, cause waardenburg anophthalmia syndrome. *Am. J. Hum. Genet.* **88**, 92–98.

Agarwal, P., Wylie, J. N., Galceran, J., Arkhitko, O., Li, C., Deng, C., Grosschedl, R. and Bruneau, B. G. (2003). Tbx5 is essential for forelimb bud initiation following patterning of the limb field in the mouse embryo. *Development* **130**, 623–633.

Aglyamova, G. V and Agarwala, S. (2007). Gene expression analysis of the hedgehog signaling cascade in the chick midbrain and spinal cord. *Dev. Dyn.* **236**, 1363–1373.

Ahn, S. and Joyner, A. L. (2004). Dynamic changes in the response of cells to positive hedgehog signaling during mouse limb patterning. *Cell* **118**, 505–516.

Alcedo, J., Ayzenzon, M., Von Ohlen, T., Noll, M. and Hooper, J. E. (1996). The Drosophila smoothened gene encodes a seven-pass membrane protein, a putative receptor for the hedgehog signal. *Cell* **86**, 221–232.

Allen, B. L., Tenzen, T. and McMahon, A. P. (2007). The Hedgehog-binding proteins Gas1 and Cdo cooperate to positively regulate Shh signaling during mouse development. *Genes Dev.* **21**, 1244–1257.

Allen, B. L., Song, J. Y., Izzi, L., Althaus, I. W., Kang, J. S., Charron, F., Krauss, R. S. and McMahon, A. P. (2011). Overlapping roles and collective requirement for the coreceptors GAS1, CDO, and BOC in SHH pathway function. *Dev. Cell* **20**, 775–787.

Anders, S. and Huber, W. (2010). Differential expression analysis for sequence count data. *Genome Biol.* **11**, R106.

Ang, H. L., Deltour, L., Hayamizu, T. F., Zgombić-Knight, M. and Duester, G. (1996). Retinoic acid synthesis in mouse embryos during gastrulation and craniofacial development linked to class IV alcohol dehydrogenase gene expression. *J. Biol. Chem.* **271**, 9526–9534.

Avraham, R. and Yarden, Y. (2011). Feedback regulation of EGFR signalling: decision making by early and delayed loops. *Nat. Rev. Mol. Cell Biol.* **12**, 104–17.

Bai, C. B., Auerbach, W., Lee, J. S., Stephen, D. and Joyner, A. L. (2002). Gli2, but not Gli1, is required for initial Shh signaling and ectopic activation of the Shh pathway. *Development* **129**, 4753–4761.

Bai, C. B., Stephen, D. and Joyner, A. L. (2004). All mouse ventral spinal cord patterning by Hedgehog is Gli dependent and involves an activator function of Gli3. *Dev. Cell* **6**, 103–115.

Bandyopadhyay, A., Tsuji, K., Cox, K., Harfe, B. D., Rosen, V. and Tabin, C. J. (2006). Genetic analysis of the roles of BMP2, BMP4, and BMP7 in limb patterning and skeletogenesis. *PLoS Genet.* **2**, 2116–2130.

Bangs, F., Welten, M., Davey, M. G., Fisher, M., Yin, Y., Downie, H., Paton, B., Baldock, R., Burt, D. W. and Tickle, C. (2010). Identification of genes downstream of the Shh signalling in the developing chick wing and syn-expressed with Hoxd13 using microarray and 3D computational analysis. *Mech. Dev.* **127**, 428–441.

Bangs, F., Antonio, N., Thongnuek, P., Welten, M., Davey, M. G., Briscoe, J. and Tickle, C. (2011). Generation of mice with functional inactivation of talpid3, a gene first identified in chicken. *Development* **138**, 3261–3272.

Barzi, M., Berenguer, J., Menendez, A., Alvarez-Rodriguez, R. and Pons, S. (2010). Sonic-hedgehog-mediated proliferation requires the localization of PKA to the cilium base. *J. Cell Sci.* **123**, 62–69.

Begemann, G., Schilling, T. F., Rauch, G. J., Geisler, R. and Ingham, P. W. (2001). The zebrafish neckless mutation reveals a requirement for raldh2 in mesodermal signals that pattern the hindbrain. *Development* **128**, 3081–3094.

Bell, G. W., Yatskievych, T. A. and Antin, P. B. (2004). GEISHA, a Whole-Mount in Situ Hybridization Gene Expression Screen in Chicken Embryos. *Dev. Dyn.* **229**, 677–687.

Bellaiche, Y., The, I. and Perrimon, N. (1998). Tout-velu is a Drosophila homologue of the putative tumour suppressor EXT-1 and is needed for Hh diffusion. *Nature* **394**, 85–88.

Bénazet, J.-D., Bischofberger, M., Tiecke, E., Gonçalves, A., Martin, J. F., Zuniga, A., Naef, F. and Zeller, R. (2009). A self-regulatory system of interlinked signaling feedback loops controls mouse limb patterning. *Science* **323**, 1050–1053.

Bertuzzi, S., Porter, F. D., Pitts, A., Kumar, M., Agulnick, A., Wassif, C. and Westphal, H. (1999). Characterization of Lhx9, a novel LIM/homeobox gene expressed by the pioneer neurons in the mouse cerebral cortex. *Mech. Dev.* **81**, 193–198.

Bischoff, M., Gradilla, A.-C., Seijo, I., Andrés, G., Rodríguez-Navas, C., González-Méndez, L. and Guerrero, I. (2013). Cytonemes are required for the establishment of a normal Hedgehog morphogen gradient in Drosophila

epithelia. *Nat. Cell Biol.* **15**, 1269–81.

Bitgood, M. J., Shen, L. and McMahon, A. P. (1996). Sertoli cell signaling by Desert hedgehog regulates the male germline. *Curr. Biol.* **6**, 298–304.

Bonnin, M. A., Laclef, C., Blaise, R., Eloy-Trinquet, S., Relaix, F., Maire, P. and Duprez, D. (2005). Six1 is not involved in limb tendon development, but is expressed in limb connective tissue under Shh regulation. *Mech. Dev.* **122**, 573–585.

Bowers, M., Eng, L., Lao, Z., Turnbull, R. K., Bao, X., Riedel, E., Mackem, S. and Joyner, A. L. (2012). Limb anterior-posterior polarity integrates activator and repressor functions of GLI2 as well as GLI3. *Dev. Biol.* **370**, 110–124.

Briscoe, J. and Thérond, P. P. (2013). The mechanisms of Hedgehog signalling and its roles in development and disease. *Nat. Rev. Mol. Cell Biol.* **14**, 416–29.

Briscoe, J., Sussel, L., Serup, P., Hartigan-O'Connor, D., Jessell, T. M., Rubenstein, J. L. and Ericson, J. (1999). Homeobox gene Nkx2.2 and specification of neuronal identity by graded Sonic hedgehog signalling [In Process Citation]. *Nature* **398**, 622–627.

Briscoe, J., Pierani, A., Jessell, T. M. and Ericson, J. (2000). A homeodomain protein code specifies progenitor cell identity and neuronal fate in the ventral neural tube. *Cell* **101**, 435–445.

Briscoe, J., Chen, Y., Jessell, T. M. and Struhl, G. (2001). A hedgehog-insensitive form of Patched provides evidence for direct long-range morphogen activity of Sonic hedgehog in the neural tube. *Mol. Cell* **7**, 1279–1291.

Burke, R., Nellen, D., Bellotto, M., Hafen, E., Senti, K. A., Dickson, B. J. and Basler, K. (1999). Dispatched, a novel sterol-sensing domain protein dedicated to the release of cholesterol-modified hedgehog from signaling cells. *Cell* **99**, 803–815.

Butterfield, N. C., Metzis, V., McGlinn, E., Bruce, S. J., Wainwright, B. J. and Wicking, C. (2009). Patched 1 is a crucial determinant of asymmetry and digit number in the vertebrate limb. *Development* **136**, 3515–3524.

Carkett, M. D. and Logan, M. P. O. (2011). 1 , 2 , 3 : Counting the fingers on a chicken wing. **4**, 10–12.

Carver, B. S., Chapinski, C., Wongvipat, J., Hieronymus, H., Chen, Y., Chandarlapaty, S., Arora, V. K., Le, C., Koutcher, J., Scher, H., et al. (2011). Reciprocal Feedback Regulation of PI3K and Androgen Receptor Signaling in PTEN-Deficient Prostate Cancer. *Cancer Cell* **19**, 575–586.

Chamberlain, C. E., Jeong, J., Guo, C., Allen, B. L. and McMahon, A. P. (2008). Notochord-derived Shh concentrates in close association with the apically positioned basal body in neural target cells and forms a dynamic gradient during neural patterning. *Development* **135**, 1097–1106.

Chen, Y. and Struhl, G. (1996). Dual roles for patched in sequestering and transducing Hedgehog. *Cell* **87**, 553–563.

Chen, J. K., Taipale, J., Cooper, M. K. and Beachy, P. A. (2002). Inhibition of Hedgehog signaling by direct binding of cyclopamine to Smoothened. *Genes Dev.* **16**, 2743–2748.

Chen, M. H., Li, Y. J., Kawakami, T., Xu, S. M. and Chuang, P. T. (2004a). Palmitoylation is required for the production of a soluble multimeric Hedgehog protein complex and long-range signaling in vertebrates. *Genes Dev.* **18**, 641–659.

Chen, W., Ren, X.-R., Nelson, C. D., Barak, L. S., Chen, J. K., Beachy, P. A., de Sauvage, F. and Lefkowitz, R. J. (2004b). Activity-dependent internalization of smoothened mediated by beta-arrestin 2 and GRK2. *Science* **306**, 2257–2260.

Chen, M. H., Wilson, C. W., Li, Y. J., Law, K. K. Lo, Lu, C. S., Gacayan, R., Zhang, X., Hui, C. C. and Chuang, P. T. (2009). Cilium-independent regulation of Gli protein function by Sufu in Hedgehog signaling is evolutionarily conserved. *Genes Dev.* **23**, 1910–1928.

Chen, X., Tukachinsky, H., Huang, C. H., Jao, C., Chu, Y. R., Tang, H. Y., Mueller, B., Schulman, S., Rapoport, T. A. and Salic, A. (2011a). Processing and turnover of the Hedgehog protein in the endoplasmic reticulum. *J. Cell Biol.* **192**, 825–838.

Chen, Y., Sasai, N., Ma, G., Yue, T., Jia, J., Briscoe, J. and Jiang, J. (2011b). Sonic Hedgehog dependent Phosphorylation by CK1?? and GRK2 is required for Ciliary Accumulation and Activation of Smoothened. *PLoS Biol.* **9**,.

Cheung, H. O.-L., Zhang, X., Ribeiro, A., Mo, R., Makino, S., Puviindran, V., Law, K. K. L., Briscoe, J. and Hui, C.-C. (2009). The kinesin protein Kif7 is a critical regulator of Gli transcription factors in mammalian hedgehog signaling. *Sci. Signal.* **2**, ra29.

Cheung, L. Y. M., Rizzoti, K., Lovell-Badge, R. and Le Tissier, P. R. (2013). Pituitary Phenotypes of Mice Lacking the Notch Signalling Ligand Delta-Like 1 Homologue. *J. Neuroendocrinol.* **25**, 391–401.

Chiang, C., Litingtung, Y., Lee, E., Young, K. E., Corden, J. L., Westphal, H. and Beachy, P. A. (1996). Cyclopia and defective axial patterning in mice lacking

Sonic hedgehog gene function. *Nature* **383**, 407–413.

Chiang, C., Litingtung, Y., Harris, M. P., Simandl, B. K., Li, Y., Beachy, P. a and Fallon, J. F. (2001). Manifestation of the limb prepattern: limb development in the absence of sonic hedgehog function. *Dev. Biol.* **236**, 421–435.

Chinnaiya, K., Tickle, C. and Towers, M. (2014). Sonic hedgehog-expressing cells in the developing limb measure time by an intrinsic cell cycle clock. *Nat. Commun.* **5**, 4230.

Chow, K. L., Hall, D. H. and Emmons, S. W. (1995). The mab-21 gene of Caenorhabditis elegans encodes a novel protein required for choice of alternate cell fates. *Development* **121**, 3615–3626.

Christ, B. and Ordahl, C. P. (1995). Early stages of chick somite development. *Anat. Embryol. (Berl).* **191**, 381–396.

Cohen, M., Kicheva, A., Ribeiro, A., Blassberg, R., Page, K. M., Barnes, C. P. and Briscoe, J. (2015). Ptch1 and Gli regulate Shh signalling dynamics via multiple mechanisms. *Nat. Commun.* **6**, 1–12.

Cohn, M. J., Izpisúa-Belmonte, J. C., Abud, H., Heath, J. K. and Tickle, C. (1995). Fibroblast growth factors induce additional limb development from the flank of chick embryos. *Cell* **80**, 739–746.

Cooper, M. K., Porter, J. A., Young, K. E. and Beachy, P. A. (1998). Teratogen-mediated inhibition of target tissue response to Shh signaling. *Science* **280**, 1603–1607.

Cooper, K. L., Hu, J. K.-H., ten Berge, D., Fernandez-Teran, M., Ros, M. a and Tabin, C. J. (2011). Initiation of proximal-distal patterning in the vertebrate limb by signals and growth. *Science* **332**, 1083–1086.

Corcoran, R. B. and Scott, M. P. (2006). Oxysterols stimulate Sonic hedgehog signal transduction and proliferation of medulloblastoma cells. *Proc. Natl. Acad. Sci. U. S. A.* **103**, 8408–8413.

Coulombe, J., Traiffort, E., Loulier, K., Faure, H. and Ruat, M. (2004). Hedgehog interacting protein in the mature brain: Membrane-associated and soluble forms. *Mol. Cell. Neurosci.* **25**, 323–333.

Creanga, A., Glenn, T. D., Mann, R. K., Saunders, A. M., Talbot, W. S. and Beachy, P. a. (2012). Scube/You activity mediates release of dually lipid-modified Hedgehog signal in soluble form. *Genes Dev.* **26**, 1312–1325.

Dahn, R. D. and Fallon, J. F. (2000). Interdigital regulation of digit identity and homeotic transformation by modulated BMP signaling. *Science* **289**, 438–441.

Dakubo, G. D., Wang, Y. P., Mazerolle, C., Campsall, K., McMahon, A. P. and Wallace, V. A. (2003). Retinal ganglion cell-derived sonic hedgehog signaling is required for optic disc and stalk neuroepithelial cell development. *Development* **130**, 2967–2980.

Danesin, C., Agius, E., Escalas, N., Ai, X., Emerson, C., Cochard, P. and Soula, C. (2006). Ventral neural progenitors switch toward an oligodendroglial fate in response to increased Sonic hedgehog (Shh) activity: involvement of Sulfatase 1 in modulating Shh signaling in the ventral spinal cord. *J. Neurosci.* **26**, 5037–5048.

Dassule, H. R., Lewis, P., Bei, M., Maas, R. and McMahon, a P. (2000). Sonic hedgehog regulates growth and morphogenesis of the tooth. *Development* **127**, 4775–4785.

Davenport, T. G., Jerome-Majewska, L. A. and Papaioannou, V. E. (2003). Mammary gland, limb and yolk sac defects in mice lacking Tbx3, the gene mutated in human ulnar mammary syndrome. *Development* **130**, 2263–2273.

Davey, M. G., Paton, I. R., Yin, Y., Schmidt, M., Bangs, F. K., Morrice, D. R., Smith, T. G., Buxton, P., Stamataki, D., Tanaka, M., et al. (2006). The chicken talpid3 gene encodes a novel protein essential for Hedgehog signaling. *Genes Dev.* **20**, 1365–1377.

Davey, M. G., James, J., Paton, I. R., Burt, D. W. and Tickle, C. (2007). Analysis of talpid3 and wild-type chicken embryos reveals roles for Hedgehog signalling in development of the limb bud vasculature. *Dev. Biol.* **301**, 155–165.

Dessaud, E., Yang, L. L., Hill, K., Cox, B., Ulloa, F., Ribeiro, A., Mynett, A., Novitch, B. G. and Briscoe, J. (2007). Interpretation of the sonic hedgehog morphogen gradient by a temporal adaptation mechanism. *Nature* **450**, 717–720.

Dessaud, E., Ribes, V., Balaskas, N., Yang, L. L., Pierani, A., Kicheva, A., Novitch, B. G., Briscoe, J. and Sasai, N. (2010). Dynamic assignment and maintenance of positional identity in the ventral neural tube by the morphogen sonic hedgehog. *PLoS Biol.* **8**,.

Dillies, M. A., Rau, A., Aubert, J., Hennequet-Antier, C., Jeanmougin, M., Servant, N., Keime, C., Marot, N. S., Castel, D., Estelle, J., et al. (2013). A comprehensive evaluation of normalization methods for Illumina high-throughput RNA sequencing data analysis. *Brief. Bioinform.* **14**, 671–683.

Dong, X., Stothard, P., Forsythe, I. J. and Wishart, D. S. (2004). PlasMapper: A web server for drawing and auto-annotating plasmid maps. *Nucleic Acids Res.* **32**,.

Dreyfuss, J. L., Regatieri, C. V., Jarrouge, T. R., Cavalheiro, R. P., Sampaio, L. O.

and Nader, H. B. (2009). Heparan sulfate proteoglycans: structure, protein interactions and cell signaling. *An. Acad. Bras. Cienc.* **81**, 409–429.

Drossopoulou, G., Lewis, K. E., Sanz-Ezquerro, J. J., Nikbakht, N., McMahon, A. P., Hofmann, C. and Tickle, C. (2000). A model for anteroposterior patterning of the vertebrate limb based on sequential long- and short-range Shh signalling and Bmp signalling. *Development* **127**, 1337–1348.

Duboc, V. and Logan, M. P. O. (2011). Regulation of limb bud initiation and limb-type morphology. *Dev. Dyn.* **240**, 1017–1027.

Dunaeva, M., Michelson, P., Kogerman, P. and Toftgard, R. (2003). Characterization of the physical interaction of Gli proteins with SUFU proteins. *J. Biol. Chem.* **278**, 5116–5122.

Dwyer, J. R., Sever, N., Carlson, M., Nelson, S. F., Beachy, P. A. and Parhami, F. (2007). Oxysterols are novel activators of the hedgehog signaling pathway in pluripotent mesenchymal cells. *J. Biol. Chem.* **282**, 8959–8968.

Endoh-Yamagami, S., Evangelista, M., Wilson, D., Wen, X., Theunissen, J. W., Phamluong, K., Davis, M., Scales, S. J., Solloway, M. J., de Sauvage, F. J., et al. (2009). The Mammalian Cos2 Homolog Kif7 Plays an Essential Role in Modulating Hh Signal Transduction during Development. *Curr. Biol.* **19**, 1320–1326.

Eugster, C., Panáková, D., Mahmoud, A. and Eaton, S. (2007). Lipoprotein-Heparan Sulfate Interactions in the Hh Pathway. *Dev. Cell* **13**, 57–71.

Fernandez-Teran, M. and Ros, M. a. (2008). The Apical Ectodermal Ridge: Morphological aspects and signaling pathways. *Int. J. Dev. Biol.* **52**, 857–871.

Frank, D. U., Emechebe, U., Thomas, K. R. and Moon, A. M. (2013). Mouse Tbx3 Mutants Suggest Novel Molecular Mechanisms for Ulnar-Mammary Syndrome. *PLoS One* **8**,.

Fromental-Ramain, C., Warot, X., Messadecq, N., LeMeur, M., Dollé, P. and Chambon, P. (1996). Hoxa-13 and Hoxd-13 play a crucial role in the patterning of the limb autopod. *Development* **122**, 2997–3011.

Fumoto, K., Hoogenraad, C. C. and Kikuchi, A. (2006). GSK-3 b -regulated interaction of BICD with dynein is involved in microtubule anchorage at centrosome. **25**, 5670–5682.

Gerlach-Bank, L. M., Ellis, A. D., Noonen, B. and Barald, K. F. (2002). Cloning and expression analysis of the chick DAN gene, an antagonist of the BMP family of growth factors. *Dev. Dyn.* **224**, 109–115.

Gibson-Brown, J. J., Agulnik, S. I., Chapman, D. L., Alexiou, M., Garvey, N., Silver, L. M. and Papaioannou, V. E. (1996). Evidence of a role for T-box genes in the evolution of limb morphogenesis and the specification of forelimb/hindlimb identity. *Mech. Dev.* **56**, 93–101.

Goetz, S. C. and Anderson, K. V (2010). The primary cilium: a signalling centre during vertebrate development. *Nat. Rev. Genet.* **11**, 331–344.

Goetz, J. A., Singh, S., Suber, L. M., Kull, F. J. and Robbins, D. J. (2006). A highly conserved amino-terminal region of Sonic Hedgehog is required for the formation of its freely diffusible multimeric form. *J. Biol. Chem.* **281**, 4087–4093.

Goodrich, L. V, Milenković, L., Higgins, K. M. and Scott, M. P. (1997). Altered neural cell fates and medulloblastoma in mouse patched mutants. *Science* **277**, 1109–1113.

Grandel, H., Lun, K., Rauch, G.-J., Rhinn, M., Piotrowski, T., Houart, C., Sordino, P., Kuchler, A. M., Schulte-Merker, S., Geisler, R., et al. (2002). Retinoic acid signalling in the zebrafish embryo is necessary during pre-segmentation stages to pattern the anterior-posterior axis of the CNS and to induce a pectoral fin bud. *Development* **129**, 2851–2865.

Green, J. B. a. and Sharpe, J. (2015). Positional information and reaction-diffusion: two big ideas in developmental biology combine. *Development* **142**, 1203–1211.

Gritli-Linde, a, Lewis, P., McMahon, a P. and Linde, a (2001). The whereabouts of a morphogen: direct evidence for short- and graded long-range activity of hedgehog signaling peptides. *Dev. Biol.* **236**, 364–386.

Gurdon, J. B. and Bourillot, P. Y. (2001). Morphogen gradient interpretation. *Nature* **413**, 797–803.

Hamburger, V. and Hamilton, H. L. (1951). A series of normal stages in the development of the chick embryo. *J. Morphol.* **88**, 49–92.

Han, C., Belenkaya, T. Y., Wang, B. and Lin, X. (2004). Drosophila glypicans control the cell-to-cell movement of Hedgehog by a dynamin-independent process. *Development* **131**, 601–611.

Harfe, B. D., Scherz, P. J., Nissim, S., Tian, H., McMahon, A. P. and Tabin, C. J. (2004). Evidence for an expansion-based temporal Shh gradient in specifying vertebrate digit identities. *Cell* **118**, 517–528.

Heanue, T. A., Johnson, R. L., Izpisua-Belmonte, J. C., Stern, C. D., De Robertis, E. M. and Tabin, C. J. (1997). Goosecoid misexpression alters the morphology

and Hox gene expression of the developing chick limb bud. *Mech. Dev.* **69**, 31–37.

Ho, K. S. and Scott, M. P. (2002). Sonic hedgehog in the nervous system: Functions, modifications and mechanisms. *Curr. Opin. Neurobiol.* **12**, 57–63.

Holtz, A. M., Peterson, K. a, Nishi, Y., Morin, S., Song, J. Y., Charron, F., McMahon, A. P. and Allen, B. L. (2013). Essential role for ligand-dependent feedback antagonism of vertebrate hedgehog signaling by PTCH1, PTCH2 and HHIP1 during neural patterning. *Development* **140**, 3423–34.

Hu, D. and Helms, J. a (1999). The role of sonic hedgehog in normal and abnormal craniofacial morphogenesis. *Development* **126**, 4873–4884.

Hui, C. and Angers, S. (2011). Gli Proteins in Development and Disease. *Annu. Rev. Cell Dev. Biol.* **27**, 513–537.

Hui, C. C. and Joyner, A. L. (1993). A mouse model of greig cephalopolysyndactyly syndrome: the extra-toesJ mutation contains an intragenic deletion of the Gli3 gene. *Nat. Genet.* **3**, 241–246.

Humke, E. W., Dorn, K. V., Milenkovic, L., Scott, M. P. and Rohatgi, R. (2010). The output of Hedgehog signaling is controlled by the dynamic association between Suppressor of Fused and the Gli proteins. *Genes Dev.* **24**, 670–682.

Incardona, J. P., Gaffield, W., Kapur, R. P. and Roelink, H. (1998). The teratogenic Veratrum alkaloid cyclopamine inhibits sonic hedgehog signal transduction. *Development* **125**, 3553–3562.

Ingham, P. W., Nystedt, S., Nakano, Y., Brown, W., Stark, D., Van den Heuvel, M. and Taylor, A. M. (2000). Patched represses the Hedgehog signalling pathway by promoting modification of the Smoothened protein. *Curr. Biol.* **10**, 1315–1318.

Isaac, A., Rodriguez-Esteban, C., Ryan, A., Altabef, M., Tsukui, T., Patel, K., Tickle, C. and Izpisúa-Belmonte, J. C. (1998). Tbx genes and limb identity in chick embryo development. *Development* **125**, 1867–1875.

Izzi, L., Lévesque, M., Morin, S., Laniel, D., Wilkes, B. C., Mille, F., Krauss, R. S., McMahon, A. P., Allen, B. L. and Charron, F. (2011). Boc and gas1 each form distinct shh receptor complexes with ptch1 and are required for shh-mediated cell proliferation. *Dev. Cell* **20**, 788–801.

Jeong, J. and McMahon, A. P. (2005). Growth and pattern of the mammalian neural tube are governed by partially overlapping feedback activities of the hedgehog antagonists patched 1 and Hhip1. *Development* **132**, 143–154.

Jia, J., Zhang, L., Zhang, Q., Tong, C., Wang, B., Hou, F., Amanai, K. and Jiang, J. (2005). Phosphorylation by double-time/CKIepsilon and CKIalpha targets cubitus interruptus for Slimb/beta-TRCP-mediated proteolytic processing. *Dev. Cell* **9**, 819–830.

Jia, J., Kolterud, Å., Zeng, H., Hoover, A., Teglund, S., Toftgård, R. and Liu, A. (2009). Suppressor of Fused inhibits mammalian Hedgehog signaling in the absence of cilia. *Dev. Biol.* **330**, 452–460.

Johnson, J. L. F. A., Hall, T. E., Dyson, J. M., Sonntag, C., Ayers, K., Berger, S., Gautier, P., Mitchell, C., Hollway, G. E. and Currie, P. D. (2012). Scube activity is necessary for Hedgehog signal transduction in vivo. *Dev. Biol.* **368**, 193–202.

Kawakami, Y., Marti, M., Kawakami, H., Itou, J., Quach, T., Johnson, a., Sahara, S., O'Leary, D. D. M., Nakagawa, Y., Lewandoski, M., et al. (2011). Islet1-mediated activation of the -catenin pathway is necessary for hindlimb initiation in mice. *Development* **138**, 4465–4473.

Khokha, M. K., Hsu, D., Brunet, L. J., Dionne, M. S. and Harland, R. M. (2003). Gremlin is the BMP antagonist required for maintenance of Shh and Fgf signals during limb patterning. *Nat. Genet.* **34**, 303–307.

Kim, Y. S., Lewandoski, M., Perantoni, A. O., Kurebayashi, S., Nakanishi, G. and Jetten, A. M. (2002). Identification of Glis1, a novel Gli-related, Kr??ppel-like zinc finger protein containing transactivation and repressor functions. *J. Biol. Chem.* **277**, 30901–30913.

Kim, J., Kato, M. and Beachy, P. A. (2009). Gli2 trafficking links Hedgehog-dependent activation of Smoothened in the primary cilium to transcriptional activation in the nucleus. *Proc. Natl. Acad. Sci. U. S. A.* **106**, 21666–21671.

Kinzler, K. W. and Vogelstein, B. (1990). The GLI gene encodes a nuclear protein which binds specific sequences in the human genome. *Mol. Cell. Biol.* **10**, 634–642.

Koressaar, T. and Remm, M. (2007). Enhancements and modifications of primer design program Primer3. *Bioinformatics* **23**, 1289–1291.

Kornberg, T. B. and Roy, S. (2014). Cytonemes as specialized signaling filopodia. *Development* **141**, 729–36.

Kovacs, J. J., Whalen, E. J., Liu, R., Xiao, K., Kim, J., Chen, M., Wang, J., Chen, W. and Lefkowitz, R. J. (2008). Beta-arrestin-mediated localization of smoothened to the primary cilium. *Science* **320**, 1777–1781.

Koziel, L., Kunath, M., Kelly, O. G. and Vortkamp, A. (2004). Ext1-dependent

heparan sulfate regulates the range of Ihh signaling during endochondral ossification. *Dev. Cell* **6**, 801–813.

Kumar, P., Franklin, S., Emechebe, U., Hu, H., Moore, B., Lehman, C., Yandell, M. and Moon, A. M. (2014). TBX3 Regulates Splicing In Vivo: A Novel Molecular Mechanism for Ulnar-Mammary Syndrome. *PLoS Genet.* **10**,.

Lance-Jones, C. and Landmesser, L. (1981). Pathway selection by chick lumbosacral motoneurons during normal development. *Proc. R. Soc. Lond. B. Biol. Sci.* **214**, 1–18.

Lanctôt, C., Moreau, A., Chamberland, M., Tremblay, M. L. and Drouin, J. (1999). Hindlimb patterning and mandible development require the Ptx1 gene. *Development* **126**, 1805–1810.

Lettice, L. a., Heaney, S. J. H., Purdie, L. a., Li, L., de Beer, P., Oostra, B. a., Goode, D., Elgar, G., Hill, R. E. and de Graaff, E. (2003). A long-range Shh enhancer regulates expression in the developing limb and fin and is associated with preaxial polydactyly. *Hum. Mol. Genet.* **12**, 1725–1735.

Lewandowski, J. P., Du, F., Zhang, S., Powell, M. B., Falkenstein, K. B., Ji, H. and Vokes, S. a. (2015). Spatiotemporal regulation of GLI target genes in the mammalian limb bud. *Dev. Biol.*

Li, D., Sakuma, R., Vakili, N. A., Mo, R., Puviindran, V., Deimling, S., Zhang, X., Hopyan, S. and Hui, C. chung (2014a). Formation of proximal and anterior limb skeleton requires early function of Irx3 and Irx5 and is negatively regulated by shh signaling. *Dev. Cell* **29**, 233–240.

Li, D., Sakuma, R., Vakili, N. a., Mo, R., Puviindran, V., Deimling, S., Zhang, X., Hopyan, S. and Hui, C. C. (2014b). Formation of proximal and anterior limb skeleton requires early function of Irx3 and Irx5 and is negatively regulated by shh signaling. *Dev. Cell* **29**, 233–240.

Liem, K. F., He, M., Ocbina, P. J. R. and Anderson, K. V (2009). Mouse Kif7/Costal2 is a cilia-associated protein that regulates Sonic hedgehog signaling. *Proc. Natl. Acad. Sci. U. S. A.* **106**, 13377–13382.

Litingtung, Y., Dahn, R. D., Li, Y., Fallon, J. F. and Chiang, C. (2002). Shh and Gli3 are dispensable for limb skeleton formation but regulate digit number and identity. *Nature* **418**, 979–983.

Liu, A., Wang, B. and Niswander, L. A. (2005). Mouse intraflagellar transport proteins regulate both the activator and repressor functions of Gli transcription factors. *Development* **132**, 3103–3111.

Logan, M. (2003). Finger or toe: the molecular basis of limb identity. *Development*

130, 6401–6410.

Logan, M. and Tabin, C. J. (1999). Role of Pitx1 upstream of Tbx4 in specification of hindlimb identity. *Science* **283**, 1736–1739.

Logan, M., Simon, H. G. and Tabin, C. (1998). Differential regulation of T-box and homeobox transcription factors suggests roles in controlling chick limb-type identity. *Development* **125**, 2825–2835.

Logan, M., Martin, J. F., Nagy, A., Lobe, C., Olson, E. N. and Tabin, C. J. (2002). Expression of Cre Recombinase in the developing mouse limb bud driven by a Prxl enhancer. *Genesis* **33**, 77–80.

Ma, Y., Erkner, A., Gong, R., Yao, S., Taipale, J., Basler, K. and Beachy, P. A. (2002). Hedgehog-mediated patterning of the mammalian embryo requires transporter-like function of dispatched. *Cell* **111**, 63–75.

Mann, R. K. and Beachy, P. A. (2004). Novel lipid modifications of secreted protein signals. *Annu. Rev. Biochem.* **73**, 891–923.

Marigo, V., Scott, M. P., Johnson, R. L., Goodrich, L. V and Tabin, C. J. (1996a). Conservation in hedgehog signaling: induction of a chicken patched homolog by Sonic hedgehog in the developing limb. *Development* **122**, 1225–1233.

Marigo, V., Johnson, R. L., Vortkamp, a and Tabin, C. J. (1996b). Sonic hedgehog differentially regulates expression of GLI and GLI3 during limb development. *Dev. Biol.* **180**, 273–283.

Martinelli, D. C. and Fan, C. M. (2007). Gas1 extends the range of Hedgehog action by facilitating its signaling. *Genes Dev.* **21**, 1231–1243.

Mas, C. and Ruiz i Altaba, A. (2010). Small molecule modulation of HH-GLI signaling: Current leads, trials and tribulations. *Biochem. Pharmacol.* **80**, 712–723.

Maurya, A. K., Ben, J., Zhao, Z., Lee, R. T. H., Niah, W., Ng, A. S. M., Iyu, A., Yu, W., Elworthy, S., van Eeden, F. J. M., et al. (2013). Positive and Negative Regulation of Gli Activity by Kif7 in the Zebrafish Embryo. *PLoS Genet.* **9**,.

McGlinn, E., Van Bueren, K. L., Fiorenza, S., Mo, R., Poh, A. M., Forrest, A., Soares, M. B., Bonaldo, M. D. F., Grimmond, S., Hui, C. C., et al. (2005). Pax9 and Jagged1 act downstream of Gli3 in vertebrate limb development. *Mech. Dev.* **122**, 1218–1233.

McLeskey Kiefer, S., Ohlemiller, K. K., Yang, J., McDill, B. W., Kohlhase, J. and Rauchman, M. (2003). Expression of a truncated Sall1 transcriptional repressor is responsible for Townes-Brocks syndrome birth defects. *Hum. Mol.*

Genet. **12**, 2221–2227.

McMahon, J. A., Takada, S., Zimmerman, L. B., Fan, C. M., Harland, R. M. and McMahon, A. P. (1998). Noggin-mediated antagonism of BMP signaling is required for growth and patterning of the neural tube and somite. *Genes Dev.* **12**, 1438–1452.

Mercader, N., Leonardo, E., Piedra, M. E., Martínez-A, C., Ros, M. a and Torres, M. (2000). Opposing RA and FGF signals control proximodistal vertebrate limb development through regulation of Meis genes. *Development* **127**, 3961–3970.

Min, H., Danilenko, D. M., Scully, S. a., Bolon, B., Ring, B. D., Tarpley, J. E., DeRose, M. and Simonet, W. S. (1998). Fgf-10 is required for both limb and lung development and exhibits striking functional similarity to Drosophila branchless. *Genes Dev.* **12**, 3156–3161.

Mo, R., Freer, a M., Zinyk, D. L., Crackower, M. a, Michaud, J., Heng, H. H., Chik, K. W., Shi, X. M., Tsui, L. C., Cheng, S. H., et al. (1997). Specific and redundant functions of Gli2 and Gli3 zinc finger genes in skeletal patterning and development. *Development* **124**, 113–123.

Morriss-Kay, G. M. and Sokolova, N. (1996). Embryonic development and pattern formation. *FASEB J. Off. Publ. Fed. Am. Soc. Exp. Biol.* **10**, 961–968.

Murillo-Ferrol, N. L. (1965). [Causal study of the earliest differentiation of the morphological rudiments of the extremities. Experimental analysis on bird embryos]. *Acta Anat. (Basel).* **62**, 80–103.

Nachtergaele, S., Mydock, L. K., Krishnan, K., Rammohan, J., Schlesinger, P. H., Covey, D. F. and Rohatgi, R. (2012). Oxysterols are allosteric activators of the oncoprotein Smoothened. *Nat. Chem. Biol.* **8**, 211–220.

Naiche, L. A. and Papaioannou, V. E. (2003). Loss of Tbx4 blocks hindlimb development and affects vascularization and fusion of the allantois. *Development* **130**, 2681–2693.

Nelson, C. E., Morgan, B. a, Burke, a C., Laufer, E., DiMambro, E., Murtaugh, L. C., Gonzales, E., Tessarollo, L., Parada, L. F. and Tabin, C. (1996). Analysis of Hox gene expression in the chick limb bud. *Development* **122**, 1449–1466.

Nguyen, L. K. and Kholodenko, B. N. (2015). Feedback regulation in cell signalling: Lessons for cancer therapeutics. *Semin. Cell Dev. Biol.*

Niederreither, K., Vermot, J., Schuhbaur, B., Chambon, P. and Dollé, P. (2002). Embryonic retinoic acid synthesis is required for forelimb growth and anteroposterior patterning in the mouse. *Development* **129**, 3563–3574.

Nieuwenhuis, E., Motoyama, J., Barnfield, P. C., Yoshikawa, Y., Zhang, X., Mo, R., Crackower, M. A. and Hui, C.-C. (2006). Mice with a targeted mutation of patched2 are viable but develop alopecia and epidermal hyperplasia. *Mol. Cell. Biol.* **26**, 6609–6622.

Nishimoto, S., Minguillon, C., Wood, S. and Logan, M. P. O. (2014). A combination of activation and repression by a colinear Hox code controls forelimb-restricted expression of Tbx5 and reveals Hox protein specificity. *PLoS Genet.* **10**, e1004245.

Nishimoto, S., Wilde, S. M., Wood, S. and Logan, M. P. O. (2015). RA Acts in a Coherent Feed-Forward Mechanism with Tbx5 to Control Limb Bud Induction and Initiation. *Cell Rep.* **12**, 879–891.

Nomura, N., Yokoyama, H. and Tamura, K. (2014). Altered developmental events in the anterior region of the chick forelimb give rise to avian-specific digit loss. *Dev. Dyn.* **243**, 741–752.

Nüsslein-Volhard, C. and Wieschaus, E. (1980). Mutations affecting segment number and polarity in Drosophila. *Nature* **287**, 795–801.

Ochi, H., Pearson, B. J., Chuang, P. T., Hammerschmidt, M. and Westerfield, M. (2006). Hhip regulates zebrafish muscle development by both sequestering Hedgehog and modulating localization of Smoothened. *Dev. Biol.* **297**, 127–140.

Oh, S., Kato, M., Zhang, C., Guo, Y. and Beachy, P. A. (2015). A Comparison of Ci/Gli Activity as Regulated by Sufu in Drosophila and Mammalian Hedgehog Response. *PLoS One* **10**, e0135804.

Ohta, K., Lupo, G., Kuriyama, S., Keynes, R., Holt, C. E., Harris, W. A., Tanaka, H. and Ohnuma, S. I. (2004). Tsukushi functions as an organizer inducer by inhibition of BMP activity in cooperation with chordin. *Dev. Cell* **7**, 347–358.

Ohuchi, H., Nakagawa, T., Yamamoto, a, Araga, a, Ohata, T., Ishimaru, Y., Yoshioka, H., Kuwana, T., Nohno, T., Yamasaki, M., et al. (1997). The mesenchymal factor, FGF10, initiates and maintains the outgrowth of the chick limb bud through interaction with FGF8, an apical ectodermal factor. *Development* **124**, 2235–2244.

Ohuchi, H., Takeuchi, J., Yoshioka, H., Ishimaru, Y., Ogura, K., Takahashi, N., Ogura, T. and Noji, S. (1998). Correlation of wing-leg identity in ectopic FGF-induced chimeric limbs with the differential expression of chick Tbx5 and Tbx4. *Development* **125**, 51–60.

Okada, I., Hamanoue, H., Terada, K., Tohma, T., Megarbane, A., Chouery, E., Abou-Ghoch, J., Jalkh, N., Cogulu, O., Ozkinay, F., et al. (2011). SMOC1 is

essential for ocular and limb development in humans and mice. *Am. J. Hum. Genet.* **88**, 30–41.

Pan, Y. and Wang, B. (2007). A novel protein-processing domain in Gli2 and Gli3 differentially blocks complete protein degradation by the proteasome. *J. Biol. Chem.* **282**, 10846–10852.

Panáková, D., Sprong, H., Marois, E., Thiele, C. and Eaton, S. (2005). Lipoprotein particles are required for Hedgehog and Wingless signalling. *Nature* **435**, 58–65.

Park, H. L., Bai, C., Platt, K. A., Matise, M. P., Beeghly, A., Hui, C. C., Nakashima, M. and Joyner, A. L. (2000). Mouse Gli1 mutants are viable but have defects in SHH signaling in combination with a Gli2 mutation. *Development* **127**, 1593–1605.

Parr, B. A. and McMahon, A. P. (1995). Dorsalizing signal Wnt-7a required for normal polarity of D-V and A-P axes of mouse limb. *Nature* **374**, 350–353.

Patro, R., Mount, S. M. and Kingsford, C. (2014). Sailfish enables alignment-free isoform quantification from RNA-seq reads using lightweight algorithms. *Nat. Biotechnol.* **32**, 462–4.

Pearse, R. V, Vogan, K. J. and Tabin, C. J. (2001). Ptc1 and Ptc2 transcripts provide distinct readouts of Hedgehog signaling activity during chick embryogenesis. *Dev. Biol.* **239**, 15–29.

Perler, F. B. (1998). Protein splicing of inteins and hedgehog autoproteolysis: Structure, function, and evolution. *Cell* **92**, 1–4.

Peters, H., Neubüser, A., Kratochwil, K. and Balling, R. (1998). Pax9-deficient mice lack pharyngeal pouch derivatives and teeth and exhibit craniofacial and limb abnormalities. *Genes Dev.* **12**, 2735–2747.

Pizette, S. and Niswander, L. (1999). BMPs negatively regulate structure and function of the limb apical ectodermal ridge. *Development* **126**, 883–894.

Putoux, A., Thomas, S., Coene, K. L. M., Davis, E. E., Alanay, Y., Ogur, G., Uz, E., Buzas, D., Gomes, C., Patrier, S., et al. (2011). KIF7 mutations cause fetal hydrolethalus and acrocallosal syndromes. *Nat. Genet.* **43**, 601–606.

Qu, S., Tucker, S. C., Ehrlich, J. S., Levorse, J. M., Flaherty, L. a, Wisdom, R. and Vogt, T. F. (1998). Mutations in mouse Aristaless-like4 cause Strong's luxoid polydactyly. *Development* **125**, 2711–2721.

R Development Core Team, R. (2011). R: A Language and Environment for Statistical Computing. *R Found. Stat. Comput.* **1**, 409.

Rainger, J., van Beusekom, E., Ramsay, J. K., McKie, L., Al-Gazali, L., Pallotta, R., Saponari, A., Branney, P., Fisher, M., Morrison, H., et al. (2011). Loss of the BMP antagonist, SMOC-1, causes Ophthalmo-acromelic (Waardenburg anophthalmia) syndrome in humans and mice. *PLoS Genet.* **7**,.

Rallis, C., Bruneau, B. G., Del Buono, J., Seidman, C. E., Seidman, J. G., Nissim, S., Tabin, C. J. and Logan, M. P. O. (2003). Tbx5 is required for forelimb bud formation and continued outgrowth. *Development* **130**, 2741–2751.

Rasband, W. (2008). *ImageJ 1997-2007*.

Raspopovic, J., Marcon, L., Russo, L. and Sharpe, J. (2014). Modeling digits. Digit patterning is controlled by a Bmp-Sox9-Wnt Turing network modulated by morphogen gradients. *Science* **345**, 566–70.

Ribes, V. and Briscoe, J. (2009). Establishing and interpreting graded Sonic Hedgehog signaling during vertebrate neural tube patterning: the role of negative feedback. *Cold Spring Harb. Perspect. Biol.* **1**,.

Riddle, R. D., Johnson, R. L., Laufer, E. and Tabin, C. (1993). Sonic hedgehog mediates the polarizing activity of the ZPA. *Cell* **75**, 1401–1416.

Riddle, R. D., Ensini, M., Nelson, C., Tsuchida, T., Jessell, T. M. and Tabin, C. (1995). Induction of the LIM homeobox gene Lmx1 by WNT7a establishes dorsoventral pattern in the vertebrate limb. *Cell* **83**, 631–640.

Rietveld, A., Neutz, S., Simons, K. and Eaton, S. (1999). Association of sterol- and glycosylphosphatidylinositol-linked proteins with Drosophila raft lipid microdomains. *J. Biol. Chem.* **274**, 12049–12054.

Rodriguez-Esteban, C., Schwabe, J. W., Peña, J. D., Rincon-Limas, D. E., Magallón, J., Botas, J. and Izpisúa Belmonte, J. C. (1998). Lhx2, a vertebrate homologue of apterous, regulates vertebrate limb outgrowth. *Development* **125**, 3925–3934.

Rohatgi, R., Milenkovic, L. and Scott, M. P. (2007). Patched1 regulates hedgehog signaling at the primary cilium. *Science* **317**, 372–376.

Ros, M. a, Dahn, R. D., Fernandez-Teran, M., Rashka, K., Caruccio, N. C., Hasso, S. M., Bitgood, J. J., Lancman, J. J. and Fallon, J. F. (2003). The chick oligozeugodactyly (ozd) mutant lacks sonic hedgehog function in the limb. *Development* **130**, 527–537.

Rosello-Diez, A., Ros, M. A. and Torres, M. (2011). Diffusible signals, not autonomous mechanisms, determine the main proximodistal limb subdivision. *Science* **332**, 1086–1088.

Rowe, D. A. and Fallon, J. F. (1982). The proximodistal determination of skeletal parts in the developing chick leg. *J. Embryol. Exp. Morphol.* **68**, 1–7.

Sanders, T. a, Llagostera, E. and Barna, M. (2013). Specialized filopodia direct long-range transport of SHH during vertebrate tissue patterning. *Nature* **497**, 628–32.

Sasaki, H., Nishizaki, Y., Hui, C., Nakafuku, M. and Kondoh, H. (1999). Regulation of Gli2 and Gli3 activities by an amino-terminal repression domain: implication of Gli2 and Gli3 as primary mediators of Shh signaling. *Development* **126**, 3915–3924.

Sauer, B. and Henderson, N. (1988). Site-specific DNA recombination in mammalian cells by the Cre recombinase of bacteriophage P1. *Proc. Natl. Acad. Sci. U. S. A.* **85**, 5166–5170.

Saunders, J. W. J. (1948). The proximo-distal sequence of origin of the parts of the chick wing and the role of the ectoderm. *J. Exp. Zool.* **108**, 363–403.

Saunders, J. W. and Gasseling, M. T. (1968). Ectodermal-mesenchymal interactions in the origin of limb symmetry. In *Epithelial Mesenchymal Interactions*, pp. 78–97.

Scherz, P. J., McGlinn, E., Nissim, S. and Tabin, C. J. (2007). Extended exposure to Sonic hedgehog is required for patterning the posterior digits of the vertebrate limb. *Dev. Biol.* **308**, 343–354.

Sekine, K., Ohuchi, H., Fujiwara, M., Yamasaki, M., Yoshizawa, T., Sato, T., Yagishita, N., Matsui, D., Koga, Y., Itoh, N., et al. (1999). Fgf10 is essential for limb and lung formation. *Nat. Genet.* **21**, 138–141.

Sharpe, J., Ahlgren, U., Perry, P., Hill, B., Ross, A., Hecksher-Sørensen, J., Baldock, R. and Davidson, D. (2002). Optical projection tomography as a tool for 3D microscopy and gene expression studies. *Science* **296**, 541–545.

Sheth, R., Marcon, L., Bastida, M. F., Junco, M., Quintana, L., Dahn, R., Kmita, M., Sharpe, J. and Ros, M. a (2012). Hox genes regulate digit patterning by controlling the wavelength of a Turing-type mechanism. *Science* **338**, 1476–80.

Sillibourne, J. E., Milne, D. M., Takahashi, M., Ono, Y. and Meek, D. W. (2002). Centrosomal anchoring of the protein kinase CK1?? mediated by attachment to the large, coiled-coil scaffolding protein CG-NAP/AKAP450. *J. Mol. Biol.* **322**, 785–797.

Smith, J. C. (1980). The time required for positional signalling in the chick wing bud. *J. Embryol. Exp. Morphol.* **60**, 321–328.

Soneson, C. and Delorenzi, M. (2013). A comparison of methods for differential expression analysis of RNA-seq data. *BMC Bioinformatics* **14**, 91.

Sowińska-Seidler, A., Socha, M. and Jamsheer, A. (2014). Split-hand/foot malformation - molecular cause and implications in genetic counseling. *J. Appl. Genet.* **55**, 105–115.

Stamataki, D., Ulloa, F., Tsoni, S. V., Mynett, A. and Briscoe, J. (2005). A gradient of Gli activity mediates graded Sonic Hedgehog signaling in the neural tube. *Genes Dev.* **19**, 626–641.

Stephens, T. D. and McNulty, T. R. (1981). Evidence for a metameric pattern in the development of the chick humerus. *J. Embryol. Exp. Morphol.* **61**, 191–205.

Stricker, S., Brieske, N., Haupt, J. and Mundlos, S. (2006). Comparative expression pattern of Odd-skipped related genes Osr1 and Osr2 in chick embryonic development. *Gene Expr. Patterns* **6**, 826–834.

Summerbell, D. (1974). A quantitative analysis of the effect of excision of the AER from the chick limb-bud. *J. Embryol. Exp. Morphol.* **32**, 651–660.

Suzuki, T., Takeuchi, J., Koshiba-Takeuchi, K. and Ogura, T. (2004). Tbx genes specify posterior digit identity through Shh and BMP signaling. *Dev. Cell* **6**, 43–53.

Suzuki, T., Hasso, S. M. and Fallon, J. F. (2008). Unique SMAD1/5/8 activity at the phalanx-forming region determines digit identity. *Proc. Natl. Acad. Sci. U. S. A.* **105**, 4185–4190.

Svärd, J., Henricson, K. H., Persson-Lek, M., Rozell, B., Lauth, M., Bergström, Å., Ericson, J., Toftgård, R. and Teglund, S. (2006). Genetic elimination of suppressor of fused reveals an essential repressor function in the mammalian hedgehog signaling pathway. *Dev. Cell* **10**, 187–197.

Sweeney, R. M. and Watterson, R. L. (1969). Rib development in chick embryos analyzed by means of tantalum foil blocks. *Am. J. Anat.* **126**, 127–149.

Taipale, J., Cooper, M. K., Maiti, T. and Beachy, P. A. (2002). Patched acts catalytically to suppress the activity of Smoothened. *Nature* **418**, 892–897.

Tamura, K., Nomura, N., Seki, R., Yonei-Tamura, S. and Yokoyama, H. (2011). Embryological evidence identifies wing digits in birds as digits 1, 2, and 3. *Science* **331**, 753–757.

te Welscher, P., Zuniga, A., Kuijper, S., Drenth, T., Goedemans, H. J., Meijlink, F. and Zeller, R. (2002a). Progression of vertebrate limb development through SHH-mediated counteraction of GLI3. *Science* **298**, 827–830.

te Welscher, P., Fernandez-Teran, M., Ros, M. A. and Zeller, R. (2002b). Mutual genetic antagonism involving GLI3 and dHAND prepatterns the vertebrate limb bud mesenchyme prior to SHH signaling. *Genes Dev.* **16**, 421–426.

Tenzen, T., Allen, B. L., Cole, F., Kang, J. S., Krauss, R. S. and McMahon, A. P. (2006). The Cell Surface Membrane Proteins Cdo and Boc Are Components and Targets of the Hedgehog Signaling Pathway and Feedback Network in Mice. *Dev. Cell* **10**, 647–656.

Thérond, P. P. (2012). Release and transportation of Hedgehog molecules. *Curr. Opin. Cell Biol.* **24**, 173–180.

Tian, H., Jeong, J., Harfe, B. D., Tabin, C. J. and McMahon, A. P. (2005). Mouse Disp1 is required in sonic hedgehog-expressing cells for paracrine activity of the cholesterol-modified ligand. *Development* **132**, 133–142.

Tickle, C. (1981). The number of polarizing region cells required to specify additional digits in the developing chick wing. *Nature* **289**, 295–298.

Tickle, C. (1995). Vertebrate limb development. *Curr. Opin. Genet. Dev.* **5**, 478–484.

Tickle, C., Summerbell, D. and Wolpert, L. (1975). Positional signalling and specification of digits in chick limb morphogenesis. *Nature* **254**, 199–202.

Tickle, C., Alberts, B., Wolpert, L. and Lee, J. (1982). Local application of retinoic acid to the limb bond mimics the action of the polarizing region. *Nature* **296**, 564–566.

Touahri, Y., Escalas, N., Benazeraf, B., Cochard, P., Danesin, C. and Soula, C. (2012). Sulfatase 1 promotes the motor neuron-to-oligodendrocyte fate switch by activating Shh signaling in Olig2 progenitors of the embryonic ventral spinal cord. *J. Neurosci.* **32**, 18018–34.

Towers, M. and Tickle, C. (2009). Growing models of vertebrate limb development. *Development* **136**, 179–190.

Towers, M., Mahood, R., Yin, Y. and Tickle, C. (2008). Integration of growth and specification in chick wing digit-patterning. *Nature* **452**, 882–886.

Towers, M., Signolet, J., Sherman, A., Sang, H. and Tickle, C. (2011). Insights into bird wing evolution and digit specification from polarizing region fate maps. *Nat. Commun.* **2**, 426.

Tukachinsky, H., Lopez, L. V. and Salic, A. (2010). A mechanism for vertebrate Hedgehog signaling: Recruitment to cilia and dissociation of SuFu-Gli protein complexes. *J. Cell Biol.* **191**, 415–428.

Tukachinsky, H., Kuzmickas, R. P., Jao, C. Y., Liu, J. and Salic, A. (2012). Dispatched and Scube Mediate the Efficient Secretion of the Cholesterol-Modified Hedgehog Ligand. *Cell Rep.* **2**, 308–320.

Turing, a M. (1952). The Chemical Basis of Morphogenesis THE CHEMICAL BASIS OF MOKPHOGENESIS. *Society* **237**, 37–72.

Tuson, M., He, M. and Anderson, K. V. (2011). Protein kinase A acts at the basal body of the primary cilium to prevent Gli2 activation and ventralization of the mouse neural tube. *Development* **138**, 4921–4930.

Untergasser, A., Cutcutache, I., Koressaar, T., Ye, J., Faircloth, B. C., Remm, M. and Rozen, S. G. (2012). Primer3-new capabilities and interfaces. *Nucleic Acids Res.* **40**,.

van den Heuvel, M. and Ingham, P. W. (1996a). Smoothened Encodes a Receptor-Like Serpentine Protein Required for Hedgehog Signalling. *Nature* **382**, 547–551.

van den Heuvel, M. and Ingham, P. W. (1996b). smoothened encodes a receptor-like serpentine protein required for hedgehog signalling. *Nature* **382**, 547–551.

Vargesson, N., Clarke, J., Vincent, K., Coles, C., Wolpert, L. and Tickle, C. (1997a). Cell fate in the chick limb bud and relationship to gene expression. **1918**, 1909–1918.

Vargesson, N., Clarke, J. D., Vincent, K., Coles, C., Wolpert, L. and Tickle, C. (1997b). Cell fate in the chick limb bud and relationship to gene expression. *Development* **124**, 1909–1918.

Veitch, E., Begbie, J., Schilling, T. F., Smith, M. M. and Graham, A. (1999). Pharyngeal arch patterning in the absence of neural crest. *Curr. Biol.* **9**, 1481–1484.

Vincent, S. D., Dunn, N. R., Sciammas, R., Shapiro-Shalef, M., Davis, M. M., Calame, K., Bikoff, E. K. and Robertson, E. J. (2005). The zinc finger transcriptional repressor Blimp1/Prdm1 is dispensable for early axis formation but is required for specification of primordial germ cells in the mouse. *Development* **132**, 1315–1325.

Vokes, S. A., Ji, H., McCuine, S., Tenzen, T., Giles, S., Zhong, S., Longabaugh, W. J. R., Davidson, E. H., Wong, W. H. and McMahon, A. P. (2007). Genomic characterization of Gli-activator targets in sonic hedgehog-mediated neural patterning. *Development* **134**, 1977–1989.

Vokes, S. a., Ji, H., Wong, W. H. and McMahon, A. P. (2008). A genome-scale

analysis of the cis-regulatory circuitry underlying sonic hedgehog-mediated patterning of the mammalian limb. *Genes Dev.* **22**, 2651–2663.

Vortkamp, A., Lee, K., Lanske, B., Segre, G. V, Kronenberg, H. M. and Tabin, C. J. (1996). Regulation of rate of cartilage differentiation by Indian hedgehog and PTH-related protein. *Science* **273**, 613–622.

Wall, N. a and Hogan, B. L. (1995). Expression of bone morphogenetic protein-4 (BMP-4), bone morphogenetic protein-7 (BMP-7), fibroblast growth factor-8 (FGF-8) and sonic hedgehog (SHH) during branchial arch development in the chick. *Mech. Dev.* **53**, 383–392.

Wang, C., Rüther, U. and Wang, B. (2007). The Shh-independent activator function of the full-length Gli3 protein and its role in vertebrate limb digit patterning. *Dev. Biol.* **305**, 460–469.

Wang, Y., Zhou, Z., Walsh, C. T. and McMahon, A. P. (2009). Selective translocation of intracellular Smoothened to the primary cilium in response to Hedgehog pathway modulation. *Proc. Natl. Acad. Sci. U. S. A.* **106**, 2623–2628.

Wang, Z., Young, R. L., Xue, H. and Wagner, G. P. (2011). Transcriptomic analysis of avian digits reveals conserved and derived digit identities in birds. *Nature* **477**, 583–586.

Wen, X., Lai, C. K., Evangelista, M., Hongo, J.-A., de Sauvage, F. J. and Scales, S. J. (2010). Kinetics of hedgehog-dependent full-length Gli3 accumulation in primary cilia and subsequent degradation. *Mol. Cell. Biol.* **30**, 1910–1922.

Wijgerde, M., Karp, S., McMahon, J. and McMahon, A. P. (2005). Noggin antagonism of BMP4 signaling controls development of the axial skeleton in the mouse. *Dev. Biol.* **286**, 149–157.

Wojcinski, A., Nakato, H., Soula, C. and Glise, B. (2011). DSulfatase-1 fine-tunes Hedgehog patterning activity through a novel regulatory feedback loop. *Dev. Biol.* **358**, 168–180.

Wolpert, L. (1969). Positional information and the spatial pattern of cellular differentiation. *J. Theor. Biol.* **25**, 1–47.

Wolpert, L. (1996). One hundred years of positional information. *Trends Genet.* **12**, 359–364.

Xu, X., Weinstein, M., Li, C., Naski, M., Cohen, R. I., Ornitz, D. M., Leder, P. and Deng, C. (1998). Fibroblast growth factor receptor 2 (FGFR2)-mediated reciprocal regulation loop between FGF8 and FGF10 is essential for limb induction. *Development* **125**, 753–765.

Xue, Y., Gao, X., Lindsell, C. E., Norton, C. R., Chang, B., Hicks, C., Gendron-Maguire, M., Rand, E. B., Weinmaster, G. and Gridley, T. (1999). Embryonic lethality and vascular defects in mice lacking the Notch ligand Jagged1. *Hum. Mol. Genet.* **8**, 723–730.

Yamada, M., Revelli, J. P., Eichele, G., Barron, M. and Schwartz, R. J. (2000). Expression of chick Tbx-2, Tbx-3, and Tbx-5 genes during early heart development: evidence for BMP2 indI'd loveuction of Tbx2. *Dev. Biol.* **228**, 95–105.

Yang, Y., Drossopoulou, G., Chuang, P. T., Duprez, D., Marti, E., Bumcrot, D., Vargesson, N., Clarke, J., Niswander, L., McMahon, a, et al. (1997). Relationship between dose, distance and time in Sonic Hedgehog-mediated regulation of anteroposterior polarity in the chick limb. *Development* **124**, 4393–4404.

Yu, J., Carroll, T. J. and McMahon, A. P. (2002). Sonic hedgehog regulates proliferation and differentiation of mesenchymal cells in the mouse metanephric kidney. *Development* **129**, 5301–5312.

Zakany, J. and Duboule, D. (2007). The role of Hox genes during vertebrate limb development. *Curr. Opin. Genet. Dev.* **17**, 359–366.

Zákány, J., Kmita, M. and Duboule, D. (2004). A dual role for Hox genes in limb anterior-posterior asymmetry. *Science* **304**, 1669–1672.

Zeller, R., López-Ríos, J. and Zuniga, A. (2009). Vertebrate limb bud development: moving towards integrative analysis of organogenesis. *Nat. Rev. Genet.* **10**, 845–858.

Zhu, J. and Mackem, S. (2011). Analysis of mutants with altered shh activity and posterior digit loss supports a biphasic model for shh function as a morphogen and mitogen. *Dev. Dyn.* **240**, 1303–1310.

Zhu, J., Nakamura, E., Nguyen, M. T., Bao, X., Akiyama, H. and Mackem, S. (2008). Uncoupling Sonic Hedgehog Control of Pattern and Expansion of the Developing Limb Bud. *Dev. Cell* **14**, 624–632.

Appendices

6 hours						12 hours						16 hours					
2nM		4nM		8nM		2nM		4nM		8nM		2nM		4nM		8nM	
1	GLI1	1	FOXC2	1	GLI1	1	AMER2	1	AMER2	1	PTCH2	1	APOD	1	PTCH2	1	PTCH2
2	AMER2	2	PTCH1	2	HS3ST2	2	GLI1	2	CNTFR	2	HHIP	2	KIRREL3	2	AMER2	2	HHIP
3	FOXC2	3	CNTFR	3	FOXC2	3	PTCH1	3	GLI1	3	OSR1	3	FIGF	3	GLI1	3	HOXD13
4	NTN1	4	FOXO6	4	PTCH1	4	FIGF	4	LHX6	4	CNTFR	4	FGF10	4	CNTFR	4	HOXD12
5	PTCH1	5	STRA6	5	NTN1	5	TRIB1	5	PTCH1	5	GLI1	5	IRK1	5	FOXD1	5	OSR1
6	STRA6	6	TRIB1	6	CNTFR	6	RHOJ	6	HAPLN1	6	LHX6	6	VTN	6	SMOC1	6	PTCH1
7	CNTFR	7	FIGF	7	FIGF	7	CDK6	7	EFEMP1	7	AMER2	7	GREM1	7	KCNH5	7	AMER2
8	FIGF	8	CASS4	8	TRIB1	8	IRK1	8	FOXC2	8	PTCH1	8	SALL1	8	HAPLN1	8	GLI1
9	CASS4	9	P2RY1	9	STRA6	9	ASB9	9	KCNH5	9	HS3ST2	9	FSTL4	9	APOD	9	CNTFR
10	HAPLN1	10	TMEM106C	10	CASS4	10	TSKU	10	CNGA3	10	FOXC2	10	ADAM23	10	LHX6	10	EFEMP1
11	P2RY1	11	GRAMD1C	11	FOXO6	11	ENC1	11	TRIB1	11	EFEMP1	11	CMTM8	11	FOXC2	11	HOXD11
12	na	12	B4GALT3	12	P2RY1	12	ELMO1	12	KIRREL3	12	SPRY4	12	HOXA7	12	KIRREL3	12	LHX6
13	TMEM106C	13	SOX9	13	HOXA10	13	PTPRZ1	13	STRA6	13	SPRY4	13	PLCD1	13	BMP2	13	BMP2
14	IRK1	14	GDAP1L1	14	THBD	14	GNPDA1	14	FIGF	14	TRIB1	14	FAM49A	14	HAS2	14	KCNH5
15	na	15	HES4	15	MORN5	15	KBTBD11	15	BMP2	15	KCNH5	15	PLCG1	15	STRA6	15	FOXD1
16	RNF122	16	EYA1	16	CPLX2	16	SLC38A6	16	IRK1	16	CNGA3	16	MMP11	16	FIGF	16	FOXC2
17	PALM	17	RNF122	17	RNF122	17	FGF10	17	HAS2	17	BMP2	17	LPIN1	17	IRK1	17	HAPLN1
18	SOX9	18	CAPN5	18	EPHB1	18	RIC3	18	ADAMTS9	18	FIGF	18	EPHB3	18	VTN	18	TRIB1
19	GDAP1L1	19	na	19	PIM1	19	MAP4K4	19	TSKU	19	P2RY1	19	na	19	FGF10	19	FOXL1
20	RAB11FIP4	20	SCPEP1	20	TMEM106C	20	HPGDS	20	SPATA13	20	STRA6	20	DDX31	20	SPRY4	20	KIRREL3
21	HES4	21	NUDT19	21	IRK1	21	PDE5A	21	MORN5	21	RHOJ	21	DNM1	21	SPRY4	21	NANOS1
22	B4GALT3	22	CDC42EP1	22	IL11RA	22	CXCL12	22	RHOJ	22	MORN5	22	KCTD1	22	PAMR1	22	APOD
23	TLE3	23	FAM92A1	23	RHOJ	23	TLL1	23	TMEM132D	23	FOXO6	23	COMMD5	23	C1QTNF5	23	FIGF
24	na	24	TM2D3	24	HES4	24	CD69	24	PTGS1	24	PTGS1	24	40057	24	ELMO1	24	IRK1
25	PREP2	25	SCCPDH	25	TSPO	25	GJA1	25	FOXO6	25	TSKU	25	MED24	25	MORN5	25	RAMP1
26	PRICKLE2	26	SLC25A22	26	C16orf59	26	AGPAT5	26	CDK6	26	IRF10	26	na	26	CDK6	26	SPRY4
27	ZNF704	27	PLCG1	27	na	27	C11ORF24	27	ELMO1	27	IRK1			27	IRF10	27	SPRY4
28	SCPEP1	28	ACBD6	28	KLHL17	28	na	28	PIM1	28	PAX1			28	SALL1	28	P2RY1
29	CDC42EP1	29	MRPS17	29	GNPDA1	29	CPED1	29	ENC1	29	PIM1			29	TMEM132D	29	TBX3
30	PLCG1			30	PRICKLE2	30	na	30	KBTBD11	30	DUSP26			30	RHOJ	30	STRA6
31	APBB2			31	TLE3	31	TUB	31	PODXL	31	na			31	SLC25A22	31	HAS2
32	TM2D3			32	PARP16	32	CTSD	32	NDNF	32	ADAMTS9			32	FAR-1	32	FGF1
33	SLC25A22			33	B4GALT3	33	ABCC3	33	PAMR1	33	HS3ST3A1			33	PTGS1	33	VTN
34	SCCPDH			34	CDC42EP1	34	ZNF521	34	EPHB1	34	LMCD1			34	FZD10	34	FGF10
				35	GDAP1L1	35	APBB2	35	CAPN5	35	EPHB1			35	SORBS1	35	IGF2
				36	WDR83OS	36	38596	36	TLL2	36	ASB9			36	CPED1	36	MORN5
				37	PLCG1	37	NOTCH2	37	GNPDA1	37	LMO7			37	SLC38A6	37	RSPO3
				38	CYB5D2	38	PARP16	38	ASB9	38	LRRC32			38	PODXL	38	PODXL
				39	SCPEP1	39	C7H2orf69	39	MAP4K4	39	KBTBD11			39	EYA1	39	ELMO1
				40	AGPAT5	40	SCPEP1	40	GDAP1L1	40	ABCG4			40	SNED1	40	SALL1
				41	RAB11FIP4	41	ZNHIT6	41	RIC3	41	NPY			41	GRAMD1C	41	VSTM2L
				42	SLC25A22	42	MSI2	42	EYA1	42	na			42	SDK2	42	RHOJ
				43	PREP2	43	GPHN	43	PRKD1	43	GBX2			43	EPHB1	43	CDK6
				44	TM2D3	44	SETD7	44	SLC25A22	44	FGF10			44	COL4A2	44	na
				45	APBB2	45	PLCG1	45	GRAMD1C	45	na			45	PLEKHH2	45	CASS4
				46	CRYM	46	UBE4A	46	SEMA6A	46	ELMO1			46	SDC3	46	TSKU
				47	ZNF740	47	na	47	na	47	GNPDA1			47	CPLX2	47	PTGS1
				48	DUSP14	48	PWP1	48	VEGFA	48	TMEM200B			48	CAMK2D	48	IRF10
				49	PFDN1	49	LRP5	49	PIGA	49	ENC1			49	APBB2	49	ABCC3
						50	ASNS	50	ABCC3	50	CAPN5			50	TMTC2	50	SIX1
						51	LANCL1	51	TLL1	51	na			51	ABCG4	51	FAR-1
						52	ELF2	52	SCPEP1	52	CDK6			52	PROM1	52	MYRF
						53	SURF2	53	HEY1	53	VEGFA			53	TSPAN9	53	FRAS1
						54	HSPA14	54	NID1	54	TLL2			54	TUB	54	KBTBD11
						55	HN1L	55	NET1	55	SEMA6A			55	FBXL7	55	SLC38A6
						56	LIMS1	56	SLC38A6	56	SORBS1			56	WDYHV1	56	PAMR1
						57	AKAP1	57	SDK2	57	CNR1			57	AGPAT5	57	GJB3
						58	HSD17B12	58	APBB2	58	FBRSL1			58	GNPDA1	58	CAPN5
						59	GEMIN4	59	AGPAT5	59	na			59	HES4	59	VCAN
						60	RFC1	60	SKAP2	60	ABCC3			60	CMTM8	60	UNC5D
						61	SETDB2	61	SOX9	61	SCPEP1			61	B4GALT3	61	PIM1
						62	EXOSC9	62	PDGF-A	62	HES4			62	PDGF-A	62	MSC
						63	RAPGEF1	63	na	63	SLC25A22			63	ARHGAP28	63	ENC1
						64	SART3	64	ARHGAP26	64	CD69			64	PIGA	64	REV3L
						65	XPO7	65	PLCG1	65	RFFL			65	SLC10A7	65	HAND2
						66	MYST2	66	IGSF3	66	LSAMP			66	VILL	66	ABCG4
						67	PRPF39	67	AP1S2	67	HEY1			67	LPIN1	67	SCNN1B
						68	MUDENG	68	FAM116A	68	SLC10A7			68	ACSL6	68	TLL2
								69	AGRN	69	AGPAT5			69	NID1	69	CPED1
								70	PARP16	70	MCC			70	PIK3IP1	70	PDZRN3
								71	FMNL2	71	PIGA			71	PLCG1	71	SLC25A22
								72	LRP5	72	C16orf59			72	DPYD	72	FZD10
								73	GPHN	73	EYA1			73	ZNF521	73	RFFL
								74	B9D1	74	B4GALT3			74	AP1S2	74	CPLX2
								75	NDUFA8	75	SDK2			75	RASA2	75	EYA1
								76	MSI2	76	NET1			76	SPSB4	76	GNPDA1
								77	PDCL	77	FMNL2			77	PDE8A	77	HOXD10
								78	CACHD1	78	PIK3IP1			78	GPRIN3	78	SORBS1
								79	CISD2	79	CDC42EP1			79	GPHN	79	RNF122
								80	CYB5B	80	APBB2			80	na	80	SDK2
										81	GPSM1			81	AMOT	81	HES4
										82	AP1S2			82	EPB41L5	82	EPHB1
										83	GFOD1			83	PLEKHG4	83	NET1
										84	EGFL7			84	FAM49A	84	SUPT3H
										85	SLC38A6			85	CACHD1	85	SCPEP1

Appendix 1 | (Linked to Table 3) Genes significantly upregulated by different Shh treatments in forelimb explants. Genes that are positively, differentially expressed in forelimb explants dosed with designated concentration of Shh morphogen for designated period of time, compared to control explants, as measured by normalised read counts. Gene lists are ordered by greatest difference in normalised read counts between explants under designated treatment and control explants. Novel, unnamed genes are described as "na". Significance determined by one-way ANOVA and Tukey's post hoc test, p= <0.05.

6 hours			12 hours				16 hours			
2nM	4nM	8nM	2nM	4nM	8nM		2nM	4nM		8nM	
					86	SKAP2		86	MOB1B	86	APBB2
					87	NDFIP1		87	EPHB3	87	COL4A2
					88	ARHGAP26		88	FITM2	88	MCC
					89	LIMS1		89	PCTP	89	PLEKHH2
					90	FAM116A		90	SNAI1	90	LIMS1
					91	PARP16		91	PLCD1	91	TLE1
					92	WDYHV1		92	TM2D3	92	HIF1A
					93	NDUFA8		93	DDX31	93	TSPAN9
					94	GPHN		94	CCNJ	94	AGPAT5
					95	MSI2		95	LRCH2	95	PDGF-A
					96	PLCG1		96	KCTD1	96	CYYR1
					97	PDCL		97	na	97	CMTM8
					98	CACHD1		98	CSGALNACT2	98	STXBP5
					99	VDAC3		99	SLC22A4	99	na
								100	DHTKD1	100	PLEKHA5
								101	C12ORF35	101	TMTC2
								102	ASCC1	102	ACER3
								103	COMMD5	103	PRICKLE2
								104	SUV39H2	104	TUB
								105	TTPAL	105	TSHZ2
								106	PPP2R5E	106	SLC10A7
								107	ZDHHC20	107	C16orf59
								108	FAM64A	108	CHRNA5
								109	EPB41L1	109	LRP5
								110	IL17RA	110	DOK4
								111	na	111	GPRIN3
								112	STK35	112	FLNB
								113	MAN2C1	113	IGFBP2
								114	ZFP64	114	GPHN
								115	FBXO7	115	ADORA2A
								116	FAM188A	116	B4GALT3
								117	CLTCL1	117	ITFG2
								118	40057	118	PARP16
								119	HSF3	119	NEK4
								120	MORC3	120	AGRN
								121	PCMT1	121	PIK3IP1
								122	SMS	122	SNAI1
										123	FMNL2
										124	LPIN1
										125	TM2D3
										126	ATAD2
										127	GCN1L1
										128	AP1S2
										129	NID1
										130	ZNF521
										131	SIK1
										132	AMOT
										133	LPCAT1
										134	HEMK1
										135	PLCG1
										136	ZMYM6NB
										137	EPHB3
										138	PCTP
										139	TFDP2
										140	SGMS1
										141	RASA2
										142	ASCC1
										143	C12ORF35
										144	ACTN4
										145	EPB41L5
										146	DOCK7
										147	CACHD1
										148	PPM1E
										149	AKAP10
										150	TOP2A
										151	FPGS
										152	NFKB1
										153	SEC24B
										154	KIF2A
										155	TBC1D8
										156	KCTD1
										157	PPP2R5E
										158	PNPLA8
										159	ZDHHC20
										160	DDX31
										161	WDR8
										162	SLC22A4
										163	BTBD10
										164	SF3B1
										165	BID
										166	MCAT
										167	EIF2B3
										168	HSF3
										169	GPI
										170	PCMT1

Appendix 1 Continued | (Linked to Table 3) Genes significantly upregulated by different Shh treatments in forelimb explants. Genes that are positively, differentially expressed in forelimb explants dosed with designated concentration of Shh morphogen for designated period of time, compared to control explants, as measured by normalised read counts. Gene lists are ordered by greatest difference in normalised read counts between explants under designated treatment and control explants. Novel, unnamed genes are described as "na". Significance determined by one-way ANOVA and Tukey's post hoc test, $p = <0.05$.

6 hours						12 hours						16 hours					
2nM		4nM		8nM		2nM		4nM		8nM		2nM		4nM		8nM	
1	APOA1	1	MYLK	1	APOA1	1	GSC	1	GSC	1	GSC	1	DKK-1	1	LHX9	1	LHX9
2	KRT15	2	ST3GAL1	2	MYLK	2	PTX3	2	ALX-4	2	ALX-4	2	LHX9	2	RASL11B	2	GSC
3	TGFB2	3	LHX2	3	LGR5	3	IRX5	3	MSX1	3	PTX3	3	FILIP1L	3	GAS1	3	PTX3
4	COL12A1	4	GPR137C	4	ST3GAL1	4	P4HA3	4	PTX3	4	BARX2B	4	RASL11B	4	FILIP1L	4	SOX8
5	MYLK	5	PLEKHA1	5	LHX2	5	CDON	5	RASL11B	5	MSX2	5	CCK	5	MERTK	5	RASL11B
6	LHX2	6	HEG1	6	DCN	6	na	6	HS6ST1	6	MSX1	6	MSX2	6	ALX-4	6	GAS1
7	PLEKHA1	7	LSP1	7	TSHZ1	7	PRRX1	7	CD82	7	WNT7B	7	ALX-4	7	MSX2	7	TOX
8	ORC6	8	RAB30	8	LSP1	8	LPAR2	8	LGR5	8	TMEM108	8	MSX1	8	CD82	8	CCK
9	RAB30	9	TPM1	9	HNRNPD	9	THSD7B	9	ZIC2	9	RASL11B	9	CD82	9	MSX1	9	ALX-4
				10	KIF5C	10	SOSTDC1	10	PRRX1	10	CD82	10	GAS1	10	CCK	10	FILIP1L
				11	TPM1	11	HS6ST1	11	BARX2B	11	TFAP2B	11	S100A16	11	na	11	PKP2
				12	DNM1L	12	na	12	GLCCI1	12	VIT	12	IRX5	12	SGK1	12	MERTK
				13	GDI2	13	LMO4	13	na	13	LHX2	13	MERTK	13	S100A16	13	GAS1
				14	GSPT1			14	LMO4	14	PRRX1	14	PTRF	14	PRRX1	14	CD82
				15	ARF5			15	CCRN4L	15	HS6ST1	15	HS6ST1	15	HS6ST1	15	MSX1
				16	YWHAQ			16	COL24A1	16	LGR5	16	SCNM1	16	IRX5	16	MSX2
								17	ALDH18A1	17	DACT2	17	PSMB3	17	STX18	17	IRX5
								18	CEP76	18	IRX5	18	SPCS1	18	PTRF	18	HS6ST1
								19	BMP7	19	PAK1	19	FEZ1	19	FEZ1	19	TMEM108
								20	COG1	20	GLCCI1	20	na	20	LLPH	20	PRRX1
								21	MRPL15	21	SOSTDC1	21	MYL4	21	POLR1D	21	DISP1
										22	RSPO2	22	SPRYD3	22	ASPG	22	SH3D19
										23	TMEM200A	23	na	23	LMO4	23	SGK1
										24	TP63	24	CHSAP18	24	SPCS1	24	OLFM1
										25	SLC25A29	25	CHMP1A	25	RAB20	25	RAB4A
										26	THSD7B	26	RNF41	26	PSMB3	26	ANGPT1
										27	PPFIBP2	27	ZNF740	27	SYNGR2	27	S100A16
										28	CEP76	28	SMAP2	28	RPL29	28	ADAM33
										29	ITFG1	29	NUDCD3	29	na	29	BMP4
										30	CCNDBP1			30	DAD1	30	GLCCI1
										31	LMO4			31	na	31	FEZ1
										32	IRF6			32	RPB6	32	BLOC1S4
										33	APLP2			33	TMA7	33	STX18
										34	na			34	MON1A	34	COQ10B
										35	na			35	ZNF740	35	na
										36	FBLN2			36	MRPL30	36	OTUD3
										37	PRDM10			37	na	37	LMO4
										38	BMP7			38	RNF41	38	ASPG
										39	ABHD12			39	RPL21	39	na
										40	BAHD1			40	TXN2	40	SHROOM4
										41	ACADL			41	RPL27	41	RAB20
										42	na					42	PBX3
										43	ZADH2					43	C16ORF5
										44	TWF1					44	PTRF
										45	AKR1A1					45	SPOCK2
										46	COG1					46	KHDRBS3
										47	ZNF330					47	ACAD8
										48	AAGAB					48	SLC7A6OS
										49	ACAD9					49	SPCS1
										50	PAPSS1					50	na
																51	na
																52	SCNM1
																53	SPRYD3
																54	DAD1
																55	FGFR1
																56	MON1A
																57	BASP1
																58	TMA7
																59	TNIP1
																60	RNF41
																61	C2ORF18
																62	TIMM22
																63	NUDCD3
																64	PSMD11
																65	TXN2
																66	SH3GL1

Appendix 2 | (Linked to Table 4) Genes significantly downregulated by different Shh treatments in forelimb explants. Genes that are negatively differentially expressed in forelimb explants dosed with designated concentration of Shh morphogen for designated period of time, compared to control explants, as measured by normalised read counts. Gene lists are ordered by greatest difference in normalised read counts between explants under designated treatment and control explants. Novel, unnamed genes are described as "na". Significance determined by one-way ANOVA and Tukey's post hoc test, p= <0.05.

6 hours						12 hours						16 hours					
2nM		4nM		8nM		2nM		4nM		8nM		2nM		4nM		8nM	
1	GPATCH3	1	MSC	1	SAMD11	1	SIX1	1	PTCH2	1	PTCH2	1	CNTFR	1	PTCH2	1	PTCH2
		2	MDM2	2	MAPK8IP2	2	ALDH1A2	2	GLI1	2	GLI1	2	GLI1	2	CNTFR	2	HHIP
		3	ZNF839	3	NRP1	3	BMP2	3	PTCH1	3	FOXF1	3	AMER2	3	HHIP	3	CNTFR
		4	EXD2	4	PRKD1	4	PIGG	4	BMP2	4	PTCH1	4	FIGF	4	OSR1	4	OSR1
		5	LSM14B	5	GAK	5	ADAMTS9	5	SIX1	5	HAPLN1	5	IRK1	5	FOXF1	5	EFEMP1
		6	ASXL1	6	PELO	6	FGFR4	6	DPYS	6	BMP2	6	STRA6	6	GLI1	6	HOXD13
		7	ODF2	7	F2RL2	7	PMP22	7	FIGF	7	FIGF	7	NGFR	7	HOXD13	7	FOXF1
		8	C5orf24	8	TSSC4	8	GRAMD1C	8	PODXL	8	SIX1	8	PTCH1	8	FIGF	8	PTCH1
				9	CNOT4	9	PKDCC	9	PAG1	9	IGF2	9	SCUBE3	9	BMP2	9	GLI1
				10	PTP4A3	10	MSANTD1	10	PIGG	10	ANO1	10	OPRM1	10	AMER2	10	BMP2
				11	SYT11	11	FZD10	11	NPR3	11	ALDH1A2	11	GDAP1L1	11	PTCH1	11	FIGF
				12	C5orf24	12	HOXD11	12	HAS2	12	PODXL	12	RASGEF1B	12	WT1	12	AMER2
						13	TBX3	13	SLC26A9	13	POSTN	13	PTPRU	13	HOXD12	13	HOXD12
						14	DNAJC12	14	GRAMD1C	14	HAS2	14	ELMO1	14	HAND2	14	FGF1
						15	KIAA1462	15	MSANTD1	15	LHX6	15	EYA1	15	LIX1	15	RASGEF1B
						16	TMEM106C	16	FRAS1	16	SLC26A9	16	RUNX1T1	16	CPXM2	16	na
						17	ZNF704	17	HOXA13	17	NPR3	17	na	17	PIGG	17	SIX1
						18	MANBA	18	P2RY1	18	PAG1	18	PODXL	18	FOXC2	18	SPRY4
						19	COL6A3	19	NCALD	19	TBX3	19	PTN	19	IRK1	19	SPRY4
						20	CD151	20	PLOD2	20	EMB	20	ASB9	20	VSTM2L	20	GJA4
						21	C10ORF11	21	HOXD11	21	GRAMD1C	21	LIMS1	21	HOXA13	21	HAND2
						22	na	22	DNAJC12	22	PIGG	22	na	22	TBX3	22	ENSGALG11911
						23	na	23	HES4	23	GDAP1L1	23	GRAMD1C	23	RASGEF1B	23	PIGG
						24	na	24	TLL2	24	ADAMTS9	24	COL4A2	24	PODXL	24	VTN
						25	PLOD2	25	TBX3	25	na	25	SLC38A6	25	RSPO3	25	TBX3
						26	NPNT	26	FABP5	26	VTN	26	TSKU	26	HOXD11	26	CPXM2
						27	SCPEP1	27	PKDCC	27	HOXD11	27	NEURL1B	27	GDAP1L1	27	HOXD11
						28	PIK3IP1	28	PDXK	28	HES4	28	CORTBP2	28	STRA6	28	HOXA13
						29	TOB	29	TMEM106C	29	MSANTD1	29	Unchar4	29	SCUBE3	29	VSTM2L
						30	ASB9	30	OLFM3	30	P2RY1	30	NR2F2	30	PDZRN4	30	ELMO1
						31	KIAA1715	31	GPRIN3	31	HOXA13	31	MSI1	31	TOX2	31	LMO1
						32	DEPDC1	32	KITLG	32	PLOD2	32	EPHB3	32	IRF10	32	ADAMTS9
						33	APP	33	PAWR	33	FGFR4	33	STXBP5	33	EYA1	33	KCNH5
						34	B4GALT3	34	ZNF704	34	PTGS1	34	SRR	34	RUNX1T1	34	PODXL
						35	AGA	35	SCPEP1	35	P4HA2	35	KLHL25	35	HEY1	35	IRK1
						36	RRAS2	36	PTGS1	36	NCALD	36	HOXA10	36	CYYR1	36	SCUBE3
						37	na	37	na	37	TLL2	37	ROR1	37	GRAMD1C	37	CASS4
						38	RAB11B	38	PIM1	38	TMEM200B	38	PCSK6	38	GNPDA1	38	EYA1
						39	KPNA2	39	SKAP2	39	PDXK	39	STRADB	39	SARM1	39	RSPO3
						40	RNF7	40	IGFBP2	40	DNAJC12	40	SCPEP1	40	SLC38A6	40	GDAP1L1
						41	PLK1	41	ASB9	41	HHIPL1	41	GPHN	41	FAM163A	41	SLC38A6
						42	CBX3	42	AP1S2	42	MORN5	42	DPYD	42	FAM101B	42	TOX2
						43	SAMM50	43	MTHFSD	43	SDK2	43	JDP2	43	ARAP3	43	IRF10
						44	ARPC1A	44	DCN	44	TMEM106C	44	AFAP1	44	FGF10	44	na
						45	BLCAP	45	TJP2	45	PPAPDC1A	45	LSM14B	45	NEURL1B	45	LIMS1
								46	GPSM1	46	ZNF704	46	MAP4K3	46	Unchar4	46	HAS2
								47	DEPDC1	47	PKDCC			47	LIMS1	47	GNPDA1
								48	PIK3IP1	48	OLFM3			48	HOXA11	48	IL13RA2
								49	CHST6	49	NELF			49	COL4A2	49	FGF10
								50	SNX6	50	SCPEP1			50	AGPAT5	50	PDZRN4
								51	RNF7	51	na			51	PIK3IP1	51	HES4
								52	KPNA2	52	AGRN			52	PIGA	52	CPED1
								53	BBS5	53	ASB9			53	TSPAN9	53	GRAMD1C
								54	TYMS	54	CNR1			54	EPHB3	54	HEY1
								55	CBX3	55	PIM1			55	SCPEP1	55	SARM1
								56	CCNB2	56	SKAP2			56	STXBP5	56	na
										57	GPRIN3			57	AP1S2	57	FAM101B
										58	IGFBP2			58	SRR	58	ASB9
										59	AP1S2			59	EXOC2	59	Unchar4
										60	FAM101B			60	HOXA10	60	HOXA11
										61	KLHL17			61	GGA.50396	61	CYYR1
										62	DCN			62	ITFG2	62	AGPAT5
										63	DEPDC1			63	GPHN	63	SLC25A30
										64	PLSCR4			64	MAP4K3	64	TMEM200B
										65	PIK3IP1			65	UHMK1	65	FAM163A
										66	B4GALT3					66	STXBP5
										67	DHCR7					67	RFFL
										68	RNF7					68	EXOC2
										69	na					69	IGFBP2
										70	CBX3					70	na
										71	AACS					71	C11ORF87
																72	SRR
																73	ABCC3
																74	TSKU
																75	EPHB3
																76	FAM107B
																77	PLEKHH2
																78	SNAI1
																79	PIGA
																80	NET1
																81	ABCG2
																82	DOK4
																83	ISOC1
																84	HIF1A
																85	ORAI1

Appendix 3 | (Linked to Table 5) Genes significantly upregulated by different Shh treatments in hindlimb explants. Genes that are positively, differentially expressed in hindlimb explants dosed with designated concentration of Shh morphogen for designated period of time, compared to control explants, as measured by normalised read counts. Gene lists are ordered by greatest difference in normalised read counts between explants under designated treatment and control explants. Novel, unnamed genes are described as "na". Significance determined by one-way ANOVA and Tukey's post hoc test, p= <0.05.

6 hours			12 hours			16 hours			
2nM	4nM	8nM	2nM	4nM	8nM	2nM	4nM	8nM	
								86	C16orf59
								87	SCPEP1
								88	SLC10A7
								89	TSPAN9
								90	AEN
								91	HOXA10
								92	B4GALT3
								93	GDPD2
								94	TM2D3
								95	CD151
								96	AP1S2
								97	ARHGAP26
								98	TLE1
								99	PIK3IP1
								100	SMAD6
								101	38596
								102	GGA.50396
								103	SIGMAR1
								104	DEPDC1
								105	ITFG2
								106	NDFIP1
								107	CHN1
								108	GARS
								109	GJA1
								110	MAD2L1BP
								111	DENND5A
								112	PLEKHA5
								113	MAP4K3
								114	PPP3CA
								115	PCSK6
								116	NT5C2
								117	GPHN
								118	SON
								119	DUSP10
								120	ATAD2
								121	SLC7A5
								122	VPS54
								123	TRIB2
								124	GPT2
								125	MAP3K4
								126	NUPL1
								127	PHLPP1
								128	COX18
								129	HYAL2
								130	SCCPDH
								131	SMAD1
								132	JDP2
								133	MOB3A
								134	KIF2A
								135	MCAT
								136	UHMK1
								137	FAM207A
								138	PPM1D

Appendix 3 continued | (Linked to Table 5) Genes significantly upregulated by different Shh treatments in hindlimb explants. Genes that are positively, differentially expressed in hindlimb explants dosed with designated concentration of Shh morphogen for designated period of time, compared to control explants, as measured by normalised read counts. Gene lists are ordered by greatest difference in normalised read counts between explants under designated treatment and control explants. Novel, unnamed genes are described as "na". Significance determined by one-way ANOVA and Tukey's post hoc test, $p = <0.05$.

6 hours			12 hours						16 hours					
2nM	4nM	8nM	2nM		4nM		8nM		2nM		4nM		8nM	
<empty>	<empty>	<empty>	1	na	1	Unchar7	1	LHX9	1	PTX3	1	CRABP-I	1	GLIS1
			2	Unchar1	2	na	2	Unchar1	2	MSX1	2	FGFBP1	2	LHX9
			3	LHX9	3	Unchar1	3	na	3	MSX2	3	LHX9	3	ALX-4
			4	FILIP1L	4	LHX9	4	MSX1	4	MT1	4	CHST9	4	PTX3
			5	MSX1	5	na	5	LHX2	5	LAD1	5	PTX3	5	MSX1
			6	MSX2	6	MSX1	6	MSX2	6	LGR5	6	SOD3	6	NBL1
			7	na	7	MSX2	7	FILIP1L	7	ID1	7	GAS1	7	CD82
			8	na	8	FILIP1L	8	PCDH8	8	DISP1	8	GAS1	8	MERTK
			9	ZIC2	9	LHX2	9	ZIC2	9	na	9	CALML3	9	MSX2
			10	C1orf53	10	na	10	na	10	CALML3	10	SERPINB5	10	GSC
			11	HS6ST1	11	na	11	TNFRSF6B	11	ID2	11	SLC40A1	11	FGFBP1
			12	HPSE2	12	PCDH8	12	GLIS1	12	GAS1	12	LAMB3	12	KAT6B
			13	CRABP-I	13	ZIC2	13	SESN2	13	GLIS1	13	MSX2	13	PRRX1
			14	PHLDA2	14	TNFRSF6B	14	HS6ST1	14	MT4	14	ITGA4	14	HS6ST1
			15	BTBD6	15	CSRP2	15	TFAP2A	15	KIFAP3	15	NBL1	15	PRKCD
			16	COMTD1	16	SESN2	16	CNNM1	16	DDT	16	LAMC2	16	DISP1
			17	TRIM35	17	HS6ST1	17	HPSE2	17	TMSB4X	17	SDC1	17	KIFAP3
			18	SMTN	18	CNNM1	18	PRRX1	18	RARRES2	18	DISP1	18	GLCCI1
			19	SNRPA1	19	GLIS1	19	C1orf53	19	YWHAH	19	MVD	19	CRISPLD1
			20	ING2	20	TFAP2A	20	CBX4	20	PSMB7	20	ID2	20	SERPINB5
			21	SCP2	21	PRRX1	21	BTBD6	21	ARF1	21	KRT19	21	PDGFRL
			22	RWDD4	22	HPSE2	22	TRIM35	22	COPS2	22	RFTN2	22	SOCS4
					23	BTBD6	23	GSDMA			23	HS6ST1	23	CALML3
					24	RGS3	24	PHLDA2			24	PLCD3	24	GAS1
					25	C1orf53	25	CRHOB			25	ITGA6	25	GNAL
					26	SOCS4	26	OTUD3			26	C1orf53	26	GAS1
					27	IRF2BP2	27	COMTD1			27	LMO4	27	FNDC4
					28	PHLDA2	28	SMTN			28	PBX3	28	KRT19
					29	TRIM35	29	GNPNAT1			29	LTF	29	LY6E
					30	PQLC2	30	HPCAL1			30	MSX1	30	STX18
					31	SMTN	31	CCDC101			31	BASP1	31	SERPINF1
					32	CRHOB	32	BAZ2A			32	DGCR6	32	OTUD3
					33	BAZ2A					33	PRKCD	33	na
					34	PCCA					34	TMSB4X	34	S100A16
					35	HPCAL1					35	IMPA2	35	HSP70
					36	TACC1					36	SERPINF1	36	LAMB3
											37	PQLC2	37	SDC1
											38	na	38	na
											39	AMT	39	TOX
											40	YBX3	40	MYO1E
											41	PSPC1	41	NDRG1
											42	SOCS4	42	SLC40A1
											43	NEK7	43	PLCD3
											44	STX18	44	CARHSP1
											45	na	45	NR2F2
											46	FAM134A	46	IMPA2
											47	CACTIN	47	SAT1
											48	CAPZB	48	YBX3
											49	PRRX1	49	CACTIN
											50	GNAL	50	DGCR6
											51	SLMO1	51	CRIP2
											52	HPSE2	52	DSP
											53	KAT6B	53	LSM1
											54	LAMB4	54	CAPZB
											55	KIFAP3	55	FAM134A
											56	MT4	56	RFTN2
											57	GLIS1	57	SRF
											58	HOXC9	58	CBY1
													59	LMO4
													60	MGST3
													61	IRX5
													62	ASNA1
													63	LSMD1
													64	AIDA
													65	HSBP1
													66	BASP1
													67	GNG5
													68	DNAJC1
													69	CORO1C
													70	TMA7
													71	CTSD
													72	CCNG2
													73	BERT
													74	RARRES2
													75	ID2
													76	CBX1
													77	na
													78	RARB
													79	SH3BGRL3
													80	METTL9
													81	TES
													82	TMSB4X
													83	FBLN2
													84	ITGA4
													85	TSHZ1
													86	CRABP-I

Appendix 4 |(Linked to Table 6) Genes significantly downregulated by different Shh treatments in hindlimb explants. Genes that are negatively differentially expressed in hindlimb explants dosed with designated concentration of Shh morphogen for designated period of time, compared to control explants, as measured by normalised read counts. Gene lists are ordered by greatest difference in normalised read counts between explants under designated treatment and control explants. Novel, unnamed genes are described as "na". Significance determined by one-way ANOVA and Tukey's post hoc test, p= <0.05.

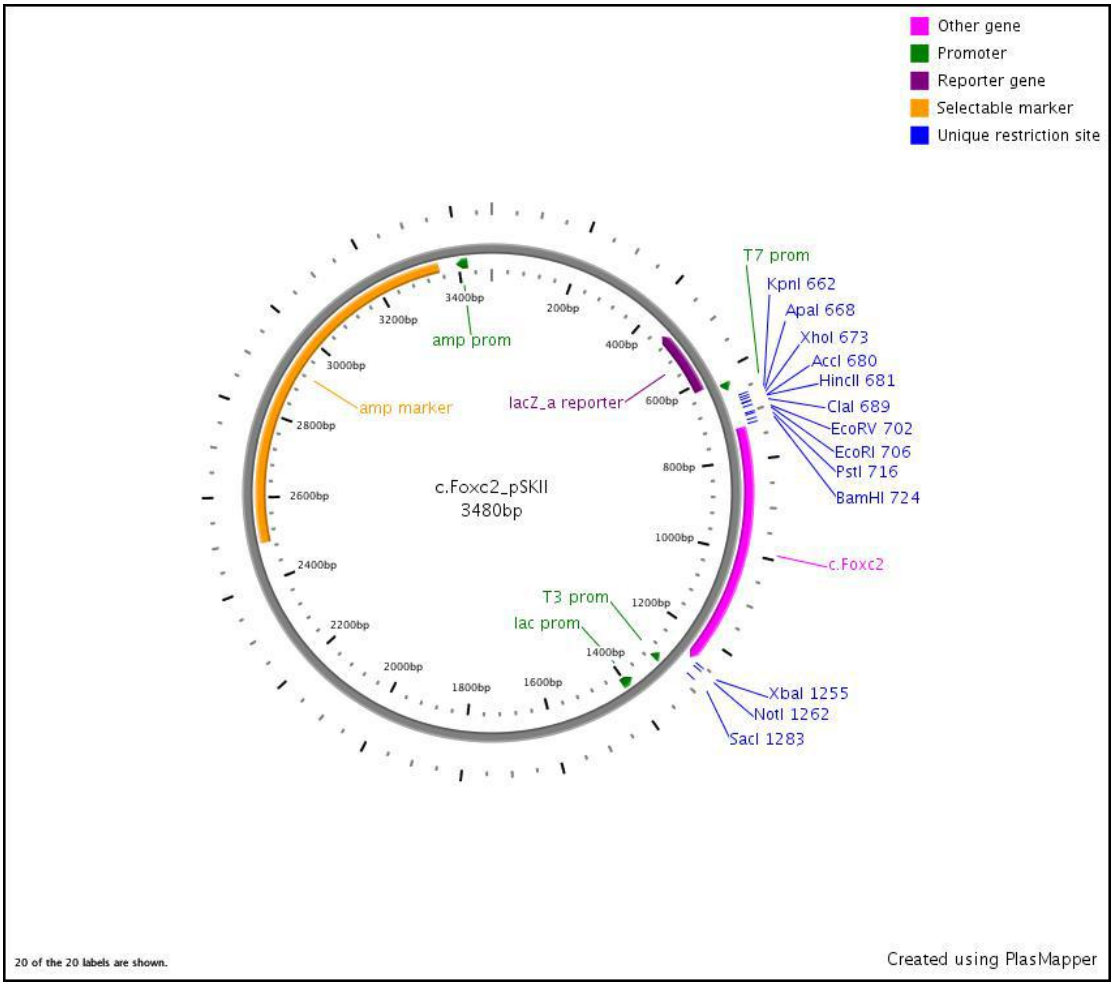

Appendix 5 | Plasmid map of *c.Foxc2*_pSK. (A) Schematic of cloning strategy. A 500bp region of chicken *Foxc2* cDNA was amplified from whole chicken cDNA with primers designed using Primer3 (Untergasser et al. 2012) - that had BamHI and SpeI sites added to 5' of forward and reverse primers respectively - and was cloned into a pBluescript SK II vector. Plasmid map was generated using PlasMapper 2.0 (Dong et al. 2004).

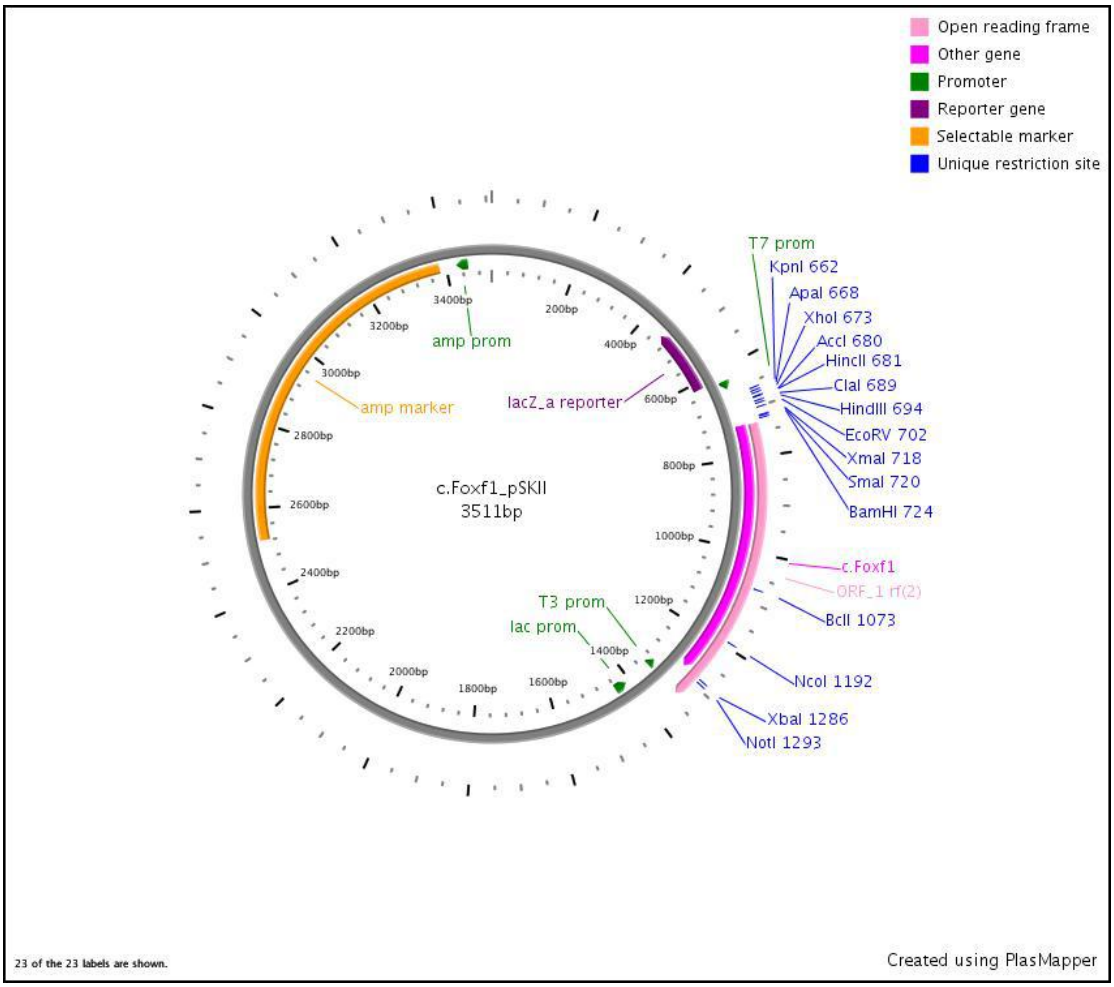

Appendix 6 | Plasmid map of *c.Foxf1*_pSK. A 500bp region of chicken *Foxf1* cDNA was amplified from whole chicken cDNA with primers designed using Primer3 (Untergasser et al. 2012) - that had BamHI and SpeI sites added to 5' of forward and reverse primers respectively - and was cloned into a pBluescript SK II vector. Plasmid map was generated using PlasMapper 2.0 (Dong et al. 2004).

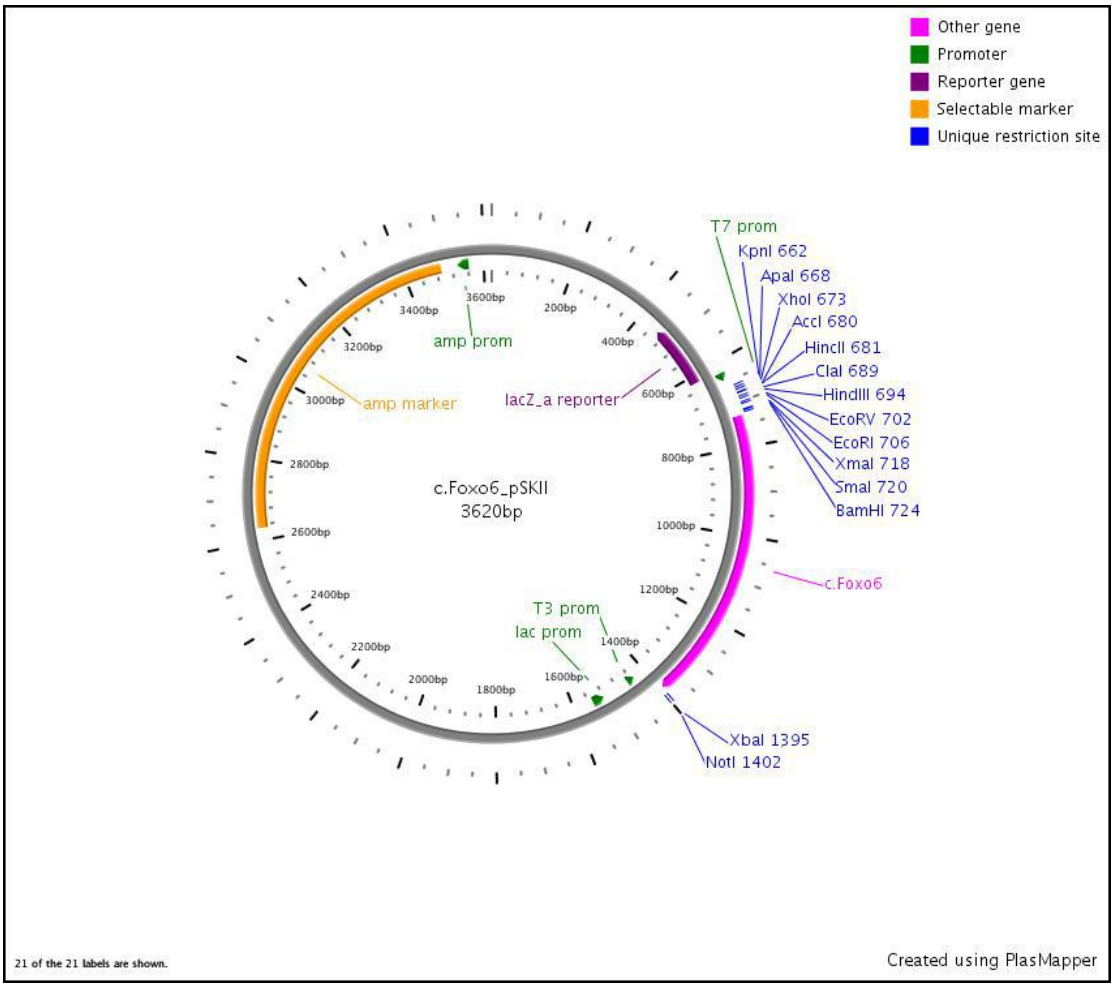

Appendix 7 | Plasmid map of *c.Foxo6*_pSK. A 500bp region of chicken *Foxo6* cDNA was amplified from whole chicken cDNA with primers designed using Primer3 (Untergasser et al. 2012) - that had BamHI and SpeI sites added to 5' of forward and reverse primers respectively - and was cloned into a pBluescript SK II vector. Plasmid map was generated using PlasMapper 2.0 (Dong et al. 2004).

Appendix 8 | R Scripts for generating statistically significant gene lists.

```
getwd()
list.files()
setwd("Desktop")
data<-read.csv("data_+1_allcells_anova.csv")
dim(data)
str(data)
head(data)

#Forelimb 6 hours, induced

on.fl<-subset (data, fl_sum >24)
fl.6.2nm<-on.fl[order(on.fl$FL_0nM_6hr/on.fl$FL_2nM_6hr ), ]
fl.6.2nm.induced<-subset(fl.6.2nm, fl.6.2nm$FL_2nM_6hr_sig >1)
fl.6.2nm.induced<-as.character(fl.6.2nm.induced$gene_name)
as.data.frame(fl.6.2nm.induced)

on.fl<-subset (data, fl_sum >24)
fl.6.4nm<-on.fl[order(on.fl$FL_0nM_6hr/on.fl$FL_4nM_6hr ), ]
fl.6.4nm.induced<-subset(fl.6.4nm, fl.6.4nm$FL_4nM_6hr_sig >1)
fl.6.4nm.induced<-as.character(fl.6.4nm.induced$gene_name)
as.data.frame(fl.6.4nm.induced)

on.fl<-subset (data, fl_sum >24)
fl.6.8nm<-on.fl[order(on.fl$FL_0nM_6hr/on.fl$FL_8nM_6hr ), ]
fl.6.8nm.induced<-subset(fl.6.8nm, fl.6.8nm$FL_8nM_6hr_sig >1)
fl.6.8nm.induced<-as.character(fl.6.8nm.induced$gene_name)
as.data.frame(fl.6.8nm.induced)

#Unique lists
fl.6.2nm.only<-as.character(fl.6.2nm.induced[! fl.6.2nm.induced
 %in% fl.6.4nm.induced & ! fl.6.2nm.induced %in%
 fl.6.8nm.induced])
as.data.frame(fl.6.2nm.only)
fl.6.4nm.only<-as.character(fl.6.4nm.induced[! fl.6.4nm.induced
 %in% fl.6.2nm.induced & ! fl.6.4nm.induced %in%
 fl.6.8nm.induced])
as.data.frame(fl.6.4nm.only)
fl.6.8nm.only<-as.character(fl.6.8nm.induced[! fl.6.8nm.induced
 %in% fl.6.2nm.induced & ! fl.6.8nm.induced %in%
 fl.6.4nm.induced])
as.data.frame(fl.6.8nm.only)

#Forelimb 12 hours, induced

on.fl<-subset (data, fl_sum >24)
fl.12.2nm<-on.fl[order(on.fl$FL_0nM_12hr/on.fl$FL_2nM_12hr ), ]
fl.12.2nm.induced<-subset(fl.12.2nm, fl.12.2nm$FL_2nM_12hr_sig
 >1)
fl.12.2nm.induced<-as.character(fl.12.2nm.induced$gene_name)
```

```
as.data.frame(fl.12.2nm.induced)

on.fl<-subset (data, fl_sum >24)
fl.12.4nm<-on.fl[order(on.fl$FL_0nM_12hr/on.fl$FL_4nM_12hr ), ]
fl.12.4nm.induced<-subset(fl.12.4nm, fl.12.4nm$FL_4nM_12hr_sig
 >1)
fl.12.4nm.induced<-as.character(fl.12.4nm.induced$gene_name)
as.data.frame(fl.12.4nm.induced)

on.fl<-subset (data, fl_sum >24)
fl.12.8nm<-on.fl[order(on.fl$FL_0nM_12hr/on.fl$FL_8nM_12hr ), ]
fl.12.8nm.induced<-subset(fl.12.8nm, fl.12.8nm$FL_8nM_12hr_sig
 >1)
fl.12.8nm.induced<-as.character(fl.12.8nm.induced$gene_name)
as.data.frame(fl.12.8nm.induced)

#Unique lists
fl.12.2nm.only<-as.character(fl.12.2nm.induced[!
 fl.12.2nm.induced %in% fl.12.4nm.induced & ! fl.12.2nm.induced
 %in% fl.12.8nm.induced])
as.data.frame(fl.12.2nm.only)
fl.12.4nm.only<-as.character(fl.12.4nm.induced[!
 fl.12.4nm.induced %in% fl.12.2nm.induced & ! fl.12.4nm.induced
 %in% fl.12.8nm.induced])
as.data.frame(fl.12.4nm.only)
fl.12.8nm.only<-as.character(fl.12.8nm.induced[!
 fl.12.8nm.induced %in% fl.12.2nm.induced & ! fl.12.8nm.induced
 %in% fl.12.4nm.induced])
as.data.frame(fl.12.8nm.only)

#Forelimb 16 hours, induced

on.fl<-subset (data, fl_sum >24)
fl.16.2nm<-on.fl[order(on.fl$FL_0nM_16hr/on.fl$FL_2nM_16hr ), ]
fl.16.2nm.induced<-subset(fl.16.2nm, fl.16.2nm$FL_2nM_16hr_sig
 >1)
fl.16.2nm.induced<-as.character(fl.16.2nm.induced$gene_name)
as.data.frame(fl.16.2nm.induced)

on.fl<-subset (data, fl_sum >24)
fl.16.4nm<-on.fl[order(on.fl$FL_0nM_16hr/on.fl$FL_4nM_16hr ), ]
fl.16.4nm.induced<-subset(fl.16.4nm, fl.16.4nm$FL_4nM_16hr_sig
 >1)
fl.16.4nm.induced<-as.character(fl.16.4nm.induced$gene_name)
as.data.frame(fl.16.4nm.induced)

on.fl<-subset (data, fl_sum >24)
fl.16.8nm<-on.fl[order(on.fl$FL_0nM_16hr/on.fl$FL_8nM_16hr ), ]
fl.16.8nm.induced<-subset(fl.16.8nm, fl.16.8nm$FL_8nM_16hr_sig
 >1)
fl.16.8nm.induced<-as.character(fl.16.8nm.induced$gene_name)
```

```
as.data.frame(fl.16.8nm.induced)

#Unique lists
fl.16.2nm.only<-as.character(fl.16.2nm.induced[!
 fl.16.2nm.induced %in% fl.16.4nm.induced & ! fl.16.2nm.induced
 %in% fl.16.8nm.induced])
as.data.frame(fl.16.2nm.only)
fl.16.4nm.only<-as.character(fl.16.4nm.induced[!
 fl.16.4nm.induced %in% fl.16.2nm.induced & ! fl.16.4nm.induced
 %in% fl.16.8nm.induced])
as.data.frame(fl.16.4nm.only)
fl.16.8nm.only<-as.character(fl.16.8nm.induced[!
 fl.16.8nm.induced %in% fl.16.2nm.induced & ! fl.16.8nm.induced
 %in% fl.16.4nm.induced])
as.data.frame(fl.16.8nm.only)

#Common to all fl lists @ 6hours
fl.6hr<-fl.6.2nm.induced[fl.6.2nm.induced %in% fl.6.4nm.induced &
 fl.6.2nm.induced %in% fl.6.8nm.induced]
as.data.frame(fl.6hr)

#Common to all fl lists @ 12hours
fl.12hr<-fl.12.2nm.induced[fl.12.2nm.induced %in%
 fl.12.4nm.induced & fl.12.2nm.induced %in% fl.12.8nm.induced]
as.data.frame(fl.12hr)

#Common to all fl lists @ 16hours
fl.16hr<-fl.16.2nm.induced[fl.16.2nm.induced %in%
 fl.16.4nm.induced & fl.16.2nm.induced %in% fl.16.8nm.induced]
as.data.frame(fl.16hr)

#Unique FL time lists
fl.6hr.only<-as.character(fl.6hr[! fl.6hr %in% fl.12hr & ! fl.6hr
 %in% fl.16hr])
as.data.frame(fl.6hr.only)
fl.12hr.only<-as.character(fl.12hr[! fl.12hr %in% fl.6hr & !
 fl.12hr %in% fl.16hr])
as.data.frame(fl.12hr.only)
fl.16hr.only<-as.character(fl.16hr[! fl.16hr %in% fl.6hr & !
 fl.16hr %in% fl.12hr])
as.data.frame(fl.16hr.only)

#Common to all forelimb lists
common_all_fl<-fl.16hr[fl.16hr %in% fl.6hr & fl.16hr %in%
 fl.12hr]
as.data.frame(common_all_fl)

#Hindlimb 6 hours, induced

on.hl<-subset (data, hl_sum >24)
hl.6.2nm<-on.hl[order(on.hl$HL_0nM_6hr/on.hl$HL_2nM_6hr ), ]
```

```
hl.6.2nm.induced<-subset(hl.6.2nm, hl.6.2nm$HL_2nM_6hr_sig >1)
hl.6.2nm.induced<-as.character(hl.6.2nm.induced$gene_name)
as.data.frame(hl.6.2nm.induced)

on.hl<-subset (data, hl_sum >24)
hl.6.4nm<-on.hl[order(on.hl$HL_0nM_6hr/on.hl$HL_4nM_6hr ), ]
hl.6.4nm.induced<-subset(hl.6.4nm, hl.6.4nm$HL_4nM_6hr_sig >1)
hl.6.4nm.induced<-as.character(hl.6.4nm.induced$gene_name)
as.data.frame(hl.6.4nm.induced)

on.hl<-subset (data, hl_sum >24)
hl.6.8nm<-on.hl[order(on.hl$HL_0nM_6hr/on.hl$HL_8nM_6hr ), ]
hl.6.8nm.induced<-subset(hl.6.8nm, hl.6.8nm$HL_8nM_6hr_sig >1)
hl.6.8nm.induced<-as.character(hl.6.8nm.induced$gene_name)
as.data.frame(hl.6.8nm.induced)

#Unique lists
hl.6.2nm.only<-as.character(hl.6.2nm.induced[! hl.6.2nm.induced
 %in% hl.6.4nm.induced & ! hl.6.2nm.induced %in%
 hl.6.8nm.induced])
as.data.frame(hl.6.2nm.only)
hl.6.4nm.only<-as.character(hl.6.4nm.induced[! hl.6.4nm.induced
 %in% hl.6.2nm.induced & ! hl.6.4nm.induced %in%
 hl.6.8nm.induced])
as.data.frame(hl.6.4nm.only)
hl.6.8nm.only<-as.character(hl.6.8nm.induced[! hl.6.8nm.induced
 %in% hl.6.2nm.induced & ! hl.6.8nm.induced %in%
 hl.6.4nm.induced])
as.data.frame(hl.6.8nm.only)

#Common to all hl lists @ 6hours
hl.6hr<-hl.6.2nm.induced[hl.6.2nm.induced %in% hl.6.4nm.induced &
 hl.6.2nm.induced %in% hl.6.8nm.induced]
as.data.frame(hl.6hr)

#Hindlimb 12 hours, induced

on.hl<-subset (data, hl_sum >24)
hl.12.2nm<-on.hl[order(on.hl$HL_0nM_12hr/on.hl$HL_2nM_12hr ), ]
hl.12.2nm.induced<-subset(hl.12.2nm, hl.12.2nm$HL_2nM_12hr_sig
 >1)
hl.12.2nm.induced<-as.character(hl.12.2nm.induced$gene_name)
as.data.frame(hl.12.2nm.induced)

on.hl<-subset (data, hl_sum >24)
hl.12.4nm<-on.hl[order(on.hl$HL_0nM_12hr/on.hl$HL_4nM_12hr ), ]
hl.12.4nm.induced<-subset(hl.12.4nm, hl.12.4nm$HL_4nM_12hr_sig
 >1)
hl.12.4nm.induced<-as.character(hl.12.4nm.induced$gene_name)
as.data.frame(hl.12.4nm.induced)
```

```
on.hl<-subset (data, hl_sum >24)
hl.12.8nm<-on.hl[order(on.hl$HL_0nM_12hr/on.hl$HL_8nM_12hr ), ]
hl.12.8nm.induced<-subset(hl.12.8nm, hl.12.8nm$HL_8nM_12hr_sig
 >1)
hl.12.8nm.induced<-as.character(hl.12.8nm.induced$gene_name)
as.data.frame(hl.12.8nm.induced)

#Unique lists
hl.12.2nm.only<-as.character(hl.12.2nm.induced[!
 hl.12.2nm.induced %in% hl.12.4nm.induced & ! hl.12.2nm.induced
 %in% hl.12.8nm.induced])
as.data.frame(hl.12.2nm.only)
hl.12.4nm.only<-as.character(hl.12.4nm.induced[!
 hl.12.4nm.induced %in% hl.12.2nm.induced & ! hl.12.4nm.induced
 %in% hl.12.8nm.induced])
as.data.frame(hl.12.4nm.only)
hl.12.8nm.only<-as.character(hl.12.8nm.induced[!
 hl.12.8nm.induced %in% hl.12.2nm.induced & ! hl.12.8nm.induced
 %in% hl.12.4nm.induced])
as.data.frame(hl.12.8nm.only)

#Common to all hl lists @ 12hours
hl.12hr<-hl.12.2nm.induced[hl.12.2nm.induced %in%
 hl.12.4nm.induced & hl.12.2nm.induced %in% hl.12.8nm.induced]
as.data.frame(hl.12hr)

#Hindlimb 16 hours, induced

on.hl<-subset (data, hl_sum >24)
hl.16.2nm<-on.hl[order(on.hl$HL_0nM_16hr/on.hl$HL_2nM_16hr ), ]
hl.16.2nm.induced<-subset(hl.16.2nm, hl.16.2nm$HL_2nM_16hr_sig
 >1)
hl.16.2nm.induced<-as.character(hl.16.2nm.induced$gene_name)
as.data.frame(hl.16.2nm.induced)

on.hl<-subset (data, hl_sum >24)
hl.16.4nm<-on.hl[order(on.hl$HL_0nM_16hr/on.hl$HL_4nM_16hr ), ]
hl.16.4nm.induced<-subset(hl.16.4nm, hl.16.4nm$HL_4nM_16hr_sig
 >1)
hl.16.4nm.induced<-as.character(hl.16.4nm.induced$gene_name)
as.data.frame(hl.16.4nm.induced)

on.hl<-subset (data, hl_sum >24)
hl.16.8nm<-on.hl[order(on.hl$HL_0nM_16hr/on.hl$HL_8nM_16hr ), ]
hl.16.8nm.induced<-subset(hl.16.8nm, hl.16.8nm$HL_8nM_16hr_sig
 >1)
hl.16.8nm.induced<-as.character(hl.16.8nm.induced$gene_name)
as.data.frame(hl.16.8nm.induced)

#Unique lists
hl.16.2nm.only<-as.character(hl.16.2nm.induced[!
```

```
 hl.16.2nm.induced %in% hl.16.4nm.induced & ! hl.16.2nm.induced
 %in% hl.16.8nm.induced])
as.data.frame(hl.16.2nm.only)
hl.16.4nm.only<-as.character(hl.16.4nm.induced[!
 hl.16.4nm.induced %in% hl.16.2nm.induced & ! hl.16.4nm.induced
 %in% hl.16.8nm.induced])
as.data.frame(hl.16.4nm.only)
hl.16.8nm.only<-as.character(hl.16.8nm.induced[!
 hl.16.8nm.induced %in% hl.16.2nm.induced & ! hl.16.8nm.induced
 %in% hl.16.4nm.induced])
as.data.frame(hl.16.8nm.only)

#Common to all hl lists @ 16hours
hl.16hr<-hl.16.2nm.induced[hl.16.2nm.induced %in%
 hl.16.4nm.induced & hl.16.2nm.induced %in% hl.16.8nm.induced]
as.data.frame(hl.16hr)

#Common to all hindlimb lists
common_all_hl<-hl.16hr[hl.16hr %in% hl.6hr & hl.16hr %in%
 hl.12hr]
as.data.frame(common_all_hl)

#Unique FL time lists
hl.6hr.only<-as.character(hl.6hr[! hl.6hr %in% hl.12hr & ! hl.6hr
 %in% hl.16hr])
as.data.frame(hl.6hr.only)
hl.12hr.only<-as.character(hl.12hr[! hl.12hr %in% hl.6hr & !
 hl.12hr %in% hl.16hr])
as.data.frame(hl.12hr.only)
hl.16hr.only<-as.character(hl.16hr[! hl.16hr %in% hl.6hr & !
 hl.16hr %in% hl.12hr])
as.data.frame(hl.16hr.only)

#Common to all forelimb and hindlimb lists

as.data.frame(common_all_fl[common_all_fl%in% common_all_hl])

#####################################################################
 #########
#NEGATIVELY REGULATED BY SHH SIGNALLING
#####################################################################
 #########

data<-read.csv("data_+1_allcells_anova.csv")

#Forelimb 6 hours, repressed

on.fl<-subset (data, fl_sum >24)
fl.6.2nm<-on.fl[order(on.fl$FL_2nM_6hr/on.fl$FL_0nM_6hr ), ]
fl.6.2nm.repressed<-subset(fl.6.2nm, fl.6.2nm$FL_2nM_6hr_sig_neg
 >1)
```

```
fl.6.2nm.repressed<-head(fl.6.2nm.repressed, 100)
fl.6.2nm.repressed<-as.character(fl.6.2nm.repressed$gene_name)
as.data.frame(fl.6.2nm.repressed)

on.fl<-subset (data, fl_sum >24)
fl.6.4nm<-on.fl[order(on.fl$FL_4nM_6hr/on.fl$FL_0nM_6hr ), ]
fl.6.4nm.repressed<-subset(fl.6.4nm, fl.6.4nm$FL_4nM_6hr_sig_neg
 >1)
fl.6.4nm.repressed<-head(fl.6.4nm.repressed, 100)
fl.6.4nm.repressed<-as.character(fl.6.4nm.repressed$gene_name)
as.data.frame(fl.6.4nm.repressed)

on.fl<-subset (data, fl_sum >24)
fl.6.8nm<-on.fl[order(on.fl$FL_8nM_6hr/on.fl$FL_0nM_6hr ), ]
fl.6.8nm.repressed<-subset(fl.6.8nm, fl.6.8nm$FL_8nM_6hr_sig_neg
 >1)
fl.6.8nm.repressed<-head(fl.6.8nm.repressed, 100)
fl.6.8nm.repressed<-as.character(fl.6.8nm.repressed$gene_name)
as.data.frame(fl.6.8nm.repressed)

#Forelimb 12 hours, repressed

on.fl<-subset (data, fl_sum >24)
fl.12.2nm<-on.fl[order(on.fl$FL_2nM_12hr/on.fl$FL_0nM_12hr ), ]
fl.12.2nm.repressed<-subset(fl.12.2nm,
 fl.12.2nm$FL_2nM_12hr_sig_neg >1)
fl.12.2nm.repressed<-head(fl.12.2nm.repressed, 100)
fl.12.2nm.repressed<-as.character(fl.12.2nm.repressed$gene_name)
as.data.frame(fl.12.2nm.repressed)

on.fl<-subset (data, fl_sum >24)
fl.12.4nm<-on.fl[order(on.fl$FL_4nM_12hr/on.fl$FL_0nM_12hr ), ]
fl.12.4nm.repressed<-subset(fl.12.4nm,
 fl.12.4nm$FL_4nM_12hr_sig_neg >1)
fl.12.4nm.repressed<-head(fl.12.4nm.repressed, 100)
fl.12.4nm.repressed<-as.character(fl.12.4nm.repressed$gene_name)
as.data.frame(fl.12.4nm.repressed)

on.fl<-subset (data, fl_sum >24)
fl.12.8nm<-on.fl[order(on.fl$FL_8nM_12hr/on.fl$FL_0nM_12hr ), ]
fl.12.8nm.repressed<-subset(fl.12.8nm,
 fl.12.8nm$FL_8nM_12hr_sig_neg >1)
fl.12.8nm.repressed<-head(fl.12.8nm.repressed, 100)
fl.12.8nm.repressed<-as.character(fl.12.8nm.repressed$gene_name)
as.data.frame(fl.12.8nm.repressed)

#Forelimb 16 hours, repressed

on.fl<-subset (data, fl_sum >24)
fl.16.2nm<-on.fl[order(on.fl$FL_2nM_16hr/on.fl$FL_0nM_16hr ), ]
fl.16.2nm.repressed<-subset(fl.16.2nm,
```

```
 fl.16.2nm$FL_2nM_16hr_sig_neg >1)
fl.16.2nm.repressed<-head(fl.16.2nm.repressed, 100)
fl.16.2nm.repressed<-as.character(fl.16.2nm.repressed$gene_name)
as.data.frame(fl.16.2nm.repressed)

on.fl<-subset (data, fl_sum >24)
fl.16.4nm<-on.fl[order(on.fl$FL_4nM_16hr/on.fl$FL_0nM_16hr ), ]
fl.16.4nm.repressed<-subset(fl.16.4nm,
 fl.16.4nm$FL_4nM_16hr_sig_neg >1)
fl.16.4nm.repressed<-head(fl.16.4nm.repressed, 100)
fl.16.4nm.repressed<-as.character(fl.16.4nm.repressed$gene_name)
as.data.frame(fl.16.4nm.repressed)

on.fl<-subset (data, fl_sum >24)
fl.16.8nm<-on.fl[order(on.fl$FL_8nM_16hr/on.fl$FL_0nM_16hr ), ]
fl.16.8nm.repressed<-subset(fl.16.8nm,
 fl.16.8nm$FL_8nM_16hr_sig_neg >1)
fl.16.8nm.repressed<-head(fl.16.8nm.repressed, 100)
fl.16.8nm.repressed<-as.character(fl.16.8nm.repressed$gene_name)
as.data.frame(fl.16.8nm.repressed)

#Hindlimb 6 hours, repressed

on.hl<-subset (data, hl_sum >24)
hl.6.2nm<-on.hl[order(on.fl$HL_2nM_6hr/on.fl$HL_0nM_6hr ), ]
hl.6.2nm.repressed<-subset(hl.6.2nm, hl.6.2nm$HL_2nM_6hr_sig_neg
 >1)
hl.6.2nm.repressed<-head(hl.6.2nm.repressed, 100)
hl.6.2nm.repressed<-as.character(hl.6.2nm.repressed$gene_name)
as.data.frame(hl.6.2nm.repressed)

on.fl<-subset (data, hl_sum >24)
hl.6.4nm<-on.hl[order(on.hl$HL_4nM_6hr/on.hl$HL_0nM_6hr ), ]
hl.6.4nm.repressed<-subset(hl.6.4nm, hl.6.4nm$HL_4nM_6hr_sig_neg
 >1)
hl.6.4nm.repressed<-head(hl.6.4nm.repressed, 100)
hl.6.4nm.repressed<-as.character(hl.6.4nm.repressed$gene_name)
as.data.frame(hl.6.4nm.repressed)

on.hl<-subset (data, hl_sum >24)
hl.6.8nm<-on.hl[order(on.hl$HL_8nM_6hr/on.hl$HL_0nM_6hr ), ]
hl.6.8nm.repressed<-head(hl.6.8nm.repressed, 100)
hl.6.8nm.repressed<-subset(hl.6.8nm, hl.6.8nm$HL_8nM_6hr_sig_neg
 >1)
hl.6.8nm.repressed<-as.character(hl.6.8nm.repressed$gene_name)
as.data.frame(hl.6.8nm.repressed)

#Hindlimb 12 hours, repressed

on.hl<-subset (data, hl_sum >24)
hl.12.2nm<-on.hl[order(on.fl$HL_2nM_12hr/on.fl$HL_0nM_12hr ), ]
```

```
hl.12.2nm.repressed<-subset(hl.12.2nm,
 hl.12.2nm$HL_2nM_12hr_sig_neg >1)
hl.12.2nm.repressed<-head(hl.12.2nm.repressed, 100)
hl.12.2nm.repressed<-as.character(hl.12.2nm.repressed$gene_name)
as.data.frame(hl.12.2nm.repressed)

on.fl<-subset (data, hl_sum >24)
hl.12.4nm<-on.hl[order(on.hl$HL_4nM_12hr/on.hl$HL_0nM_12hr ), ]
hl.12.4nm.repressed<-subset(hl.12.4nm,
 hl.12.4nm$HL_4nM_12hr_sig_neg >1)
hl.12.4nm.repressed<-head(hl.12.4nm.repressed, 100)
hl.12.4nm.repressed<-as.character(hl.12.4nm.repressed$gene_name)
as.data.frame(hl.12.4nm.repressed)

on.hl<-subset (data, hl_sum >24)
hl.12.8nm<-on.hl[order(on.hl$HL_8nM_12hr/on.hl$HL_0nM_12hr ), ]
hl.12.8nm.repressed<-subset(hl.12.8nm,
 hl.12.8nm$HL_8nM_12hr_sig_neg >1)
hl.12.8nm.repressed<-head(hl.12.8nm.repressed, 100)
hl.12.8nm.repressed<-as.character(hl.12.8nm.repressed$gene_name)
as.data.frame(hl.12.8nm.repressed)

#Hindlimb 16 hours, repressed

on.hl<-subset (data, hl_sum >24)
hl.16.2nm<-on.hl[order(on.hl$HL_2nM_16hr/on.hl$HL_0nM_16hr ), ]
hl.16.2nm.repressed<-subset(hl.16.2nm,
 hl.16.2nm$HL_2nM_16hr_sig_neg >1)
hl.16.2nm.repressed<-head(hl.16.2nm.repressed, 100)
hl.16.2nm.repressed<-as.character(hl.16.2nm.repressed$gene_name)
as.data.frame(hl.16.2nm.repressed)

on.hl<-subset (data, hl_sum >24)
hl.16.4nm<-on.hl[order(on.hl$HL_4nM_16hr/on.hl$FL_0nM_16hr ), ]
hl.16.4nm.repressed<-subset(hl.16.4nm,
 hl.16.4nm$HL_4nM_16hr_sig_neg >1)
hl.16.4nm.repressed<-head(hl.16.4nm.repressed, 100)
hl.16.4nm.repressed<-as.character(hl.16.4nm.repressed$gene_name)
as.data.frame(hl.16.4nm.repressed)

on.hl<-subset (data, hl_sum >24)
hl.16.8nm<-on.fl[order(on.hl$FL_8nM_16hr/on.hl$HL_0nM_16hr ), ]
hl.16.8nm.repressed<-subset(hl.16.8nm,
 hl.16.8nm$HL_8nM_16hr_sig_neg >1)
hl.16.8nm.repressed<-head(hl.16.8nm.repressed, 100)
hl.16.8nm.repressed<-as.character(hl.16.8nm.repressed$gene_name)
as.data.frame(hl.16.8nm.repressed)
```

Appendix 9 | R Scripts for generating gene lists based on transcriptional profiling

```
getwd()
list.files()
setwd("R")
data<-read.csv("data_+1_allcells_anova.csv")
data<-read.csv("transformed_sailfish_3.0.csv")
dim(data)
str(data)
summary(data)
head(data)

c<- data[which(data$FL_8nM_6hr >1.1 & data$FL_8nM_12hr >1.1 &
 data$FL_8nM_16hr >1.1 & data$FL_0nM_6hr <0.9 & data$FL_0nM_12hr
 <0.9 & data$FL_0nM_16hr <0.9 ), ] #To eliminate genes that show
 'flat' expression from transformed data
dim(c)

PTCH1_LIKE_FL

data<-read.csv("data_+1_allcells_anova.csv")
data<- subset (data, fl_sum>24)
ptch1_like_fl<- subset (data, data$FL_2nM_6hr >data$FL_0nM_6hr &
 data$FL_4nM_6hr >data$FL_0nM_6hr & data$FL_8nM_6hr
 >data$FL_0nM_6hr & data$FL_2nM_12hr >data$FL_0nM_12hr &
 data$FL_4nM_12hr >data$FL_0nM_12hr & data$FL_8nM_12hr
 >data$FL_0nM_12hr & data$FL_2nM_16hr >data$FL_0nM_16hr &
 data$FL_4nM_16hr >data$FL_0nM_16hr & data$FL_8nM_16hr
 >data$FL_0nM_16hr & data$FL_2nM_16hr <data$FL_2nM_12hr &
 data$FL_8nM_16hr >data$FL_4nM_16hr & data$FL_4nM_16hr
 >data$FL_2nM_16hr & data$FL_8nM_16hr > data$FL_8nM_6hr &
 data$FL_4nM_16hr > data$FL_4nM_6hr & data$FL_8nM_12hr
 >data$FL_2nM_12hr & data$FL_8nM_12hr >data$FL_4nM_12hr)

ptch1_like_fl <-ptch1_like_fl[order(ptch1_like_fl
 $FL_0nM_16hr/ptch1_like_fl $FL_8nM_16hr ), ]
ptch1_like_fl <-tail(ptch1_like_fl, 100)
ptch1_like_fl <-as.character(ptch1_like_fl $gene_name)
as.data.frame(ptch1_like_fl)

#ptch1_like_fl codes for A) induction by Shh at all
 concentrations and times.  B) to be graded by 16hr, C) for there
 to be accumulation at 8nM and 4nM between 6hr and 16hr,D) For
 there to be a characteristic dip in 2nM between 12hr and 16hr,
 E) for partial gradation (8nM greater than 4nM or 2nM) by 12
 hours and F) Ordered on greatest induction by 8nM at 16hr

Have not made 8nM 16hr higher than 8nM 12hr as this elimaintes
 false negatives like Hs3st2 and Osr1 that show a minor but non-
 significant dip between 12-16hr times.
```

```
HOXD13_LIKE_FL

data<-read.csv("data_+1_allcells_anova.csv")
data<- subset (data, fl_sum>24)
hoxd13_like_fl <- data[which(data$FL_2nM_6hr >data$FL_0nM_6hr &
 data$FL_4nM_6hr >data$FL_0nM_6hr & data$FL_8nM_6hr
 >data$FL_0nM_6hr & data$FL_2nM_12hr >data$FL_0nM_12hr &
 data$FL_4nM_12hr >data$FL_0nM_12hr & data$FL_8nM_12hr
 >data$FL_0nM_12hr & data$FL_2nM_16hr >data$FL_0nM_16hr &
 data$FL_4nM_16hr >data$FL_0nM_16hr & data$FL_8nM_16hr
 >data$FL_0nM_16hr & data$FL_8nM_16hr >data$FL_4nM_16hr &
 data$FL_8nM_16hr >data$FL_4nM_16hr), ]

hoxd13_like_fl <-hoxd13_like_fl[order(hoxd13_like_fl
 $FL_0nM_16hr/hoxd13_like_fl $FL_8nM_16hr ), ]
hoxd13_like_fl <-as.character(hoxd13_like_fl $gene_name)
hoxd13_like_fl <-head(hoxd13_like_fl, 100)
as.data.frame(hoxd13_like_fl)

#hoxd_like_fl codes for A) induction by Shh at all concentrations
 and times, B) specifies 8nM is highest at 16hr and C)  Ordered
 on greatest induction by 8nM at 16hr - but not a full graded
 response at end due to Hoxd lag. - Again have not made 8nM 16hr
 higher than 8nM 12hr as this elimaintes false negatives like
 Hs3st2 and Osr1 that show a minor but non-significant dip
 between 12-16hr times.


Hoxd only
Hoxd_like_only<-as.character(Hoxd_like_fl[! Hoxd_like_fl %in%
 ptch1_like_fl & !Hoxd_like_fl %in% foxc2_like_fl ])
as.data.frame(Hoxd_like_only)

all_posterior<-(ptch1_like_fl & hoxd13_like_fl)

FOXC2_LIKE_FL

data<-read.csv("data_+1_allcells_anova.csv")
data<- subset (data, fl_sum>24)
foxc2_like_fl<- data[which(data$FL_2nM_6hr >data$FL_0nM_6hr &
 data$FL_4nM_6hr >data$FL_0nM_6hr & data$FL_8nM_6hr
 >data$FL_0nM_6hr  & data$FL_2nM_12hr >data$FL_0nM_12hr &
 data$FL_4nM_12hr >data$FL_0nM_12hr & data$FL_8nM_12hr
 >data$FL_0nM_12hr & data$FL_2nM_16hr >data$FL_0nM_16hr &
 data$FL_4nM_16hr >data$FL_0nM_16hr & data$FL_8nM_16hr
 >data$FL_0nM_16hr & data$FL_8nM_12hr >data$FL_4nM_12hr &
 data$FL_4nM_12hr >data$FL_2nM_12hr & data$FL_8nM_16hr
 >data$FL_4nM_16hr & data$FL_4nM_16hr >data$FL_2nM_16hr &
 data$FL_8nM_12hr >data$FL_8nM_16hr & data$FL_4nM_12hr
 >data$FL_4nM_16hr & data$FL_2nM_12hr >data$FL_2nM_16hr), ]
```

```
foxc2_like_fl<-
 foxc2_like_fl[order(foxc2_like_fl$FL_0nM_12hr/foxc2_like_fl$FL_8
 nM_12hr ), ]
foxc2_like_fl<-tail(foxc2_like_fl, 100)
foxc2_like_fl <-as.character(foxc2_like_fl $gene_name)
as.data.frame(foxc2_like_fl)

#foxc2_like_fl codes for A) induction by Shh at all
 concentrations and times B) a graded response at 12 hours and 16
 hours and C) 12hr (2nM, 4nM and 8nM) are higher than at 16hr
 (2nM, 4nM and 8nM), D) ordered by greatest induction at 8nM_12hr
 to 0nM_12hr


SMOC1_LIKE_FL

data<-read.csv("data_+1_allcells_anova.csv")
data<- subset (data, fl_sum>24)
smoc1_like_fl<- data[which(data$FL_2nM_6hr >data$FL_0nM_6hr &
 data$FL_4nM_6hr >data$FL_0nM_6hr & data$FL_8nM_6hr
 >data$FL_0nM_6hr  & data$FL_2nM_12hr >data$FL_0nM_12hr &
 data$FL_4nM_12hr >data$FL_0nM_12hr & data$FL_8nM_12hr
 >data$FL_0nM_12hr & data$FL_2nM_16hr >data$FL_0nM_16hr &
 data$FL_4nM_16hr >data$FL_0nM_16hr & data$FL_8nM_16hr
 >data$FL_0nM_16hr & data$FL_4nM_12hr >data$FL_8nM_12hr &
 data$FL_4nM_12hr >data$FL_2nM_12hr & data$FL_4nM_16hr
 >data$FL_8nM_16hr & data$FL_4nM_16hr >data$FL_2nM_16hr), ]

smoc1_like_fl <-
 smoc1_like_fl[order(smoc1_like_fl$FL_0nM_16hr/smoc1_like_fl$FL_4
 nM_16hr ), ]
smoc1_like_fl <-head(smoc1_like_fl, 100)
smoc1_like_fl <-as.character(smoc1_like_fl $gene_name)
as.data.frame(smoc1_like_fl)

#smoc1_like_fl codes for A) induction by Shh at all
 concentrations and times, B) 4nM shows the peak response at 12hr
 and 16hr C) ordered by greatest induction 4nM_16h to 0nM_16hr

TWO_NM_PEAK_FL

data<-read.csv("data_+1_allcells_anova.csv")
data<- subset (data, fl_sum>24)
twonm_like_fl<- data[which(data$FL_2nM_6hr >data$FL_0nM_6hr &
 data$FL_4nM_6hr >data$FL_0nM_6hr & data$FL_8nM_6hr
 >data$FL_0nM_6hr  & data$FL_2nM_12hr >data$FL_0nM_12hr &
 data$FL_4nM_12hr >data$FL_0nM_12hr & data$FL_8nM_12hr
 >data$FL_0nM_12hr & data$FL_2nM_16hr >data$FL_0nM_16hr &
 data$FL_4nM_16hr >data$FL_0nM_16hr & data$FL_8nM_16hr
 >data$FL_0nM_16hr & data$FL_2nM_12hr >data$FL_4nM_12hr &
```

```
 data$FL_2nM_12hr >data$FL_8nM_12hr & data$FL_2nM_16hr
 >data$FL_4nM_16hr & data$FL_2nM_12hr >data$FL_8nM_16hr), ]

twonm_like_fl <-twonm_like_fl[order(twonm_like_fl
 $FL_0nM_16hr/twonm_like_fl $FL_2nM_16hr ), ]
twonm_like_fl <-as.character(twonm_like_fl$gene_name)
as.data.frame(twonm_like_fl)

#twonm_like_fl codes for A) induction by Shh at all
 concentrations and times, B) 2nM highest at 12hr and 16hr C)
 ordered on greatest induction by 2nM at 16hr

SIX_HOUR_LIKE_FL

data<-read.csv("data_+1_allcells_anova.csv")
data<- subset (data, fl_sum>24)
sixhour_like_fl<- data[which(data$FL_2nM_6hr >data$FL_0nM_6hr &
 data$FL_4nM_6hr >data$FL_0nM_6hr & data$FL_8nM_6hr
 >data$FL_0nM_6hr  & data$FL_2nM_12hr >data$FL_0nM_12hr &
 data$FL_4nM_12hr >data$FL_0nM_12hr & data$FL_8nM_12hr
 >data$FL_0nM_12hr & data$FL_2nM_16hr >data$FL_0nM_16hr &
 data$FL_4nM_16hr >data$FL_0nM_16hr & data$FL_8nM_16hr
 >data$FL_0nM_16hr & data$FL_8nM_12hr >data$FL_4nM_12hr &
 data$FL_4nM_12hr >data$FL_2nM_12hr & data$FL_8nM_16hr
 >data$FL_4nM_16hr & data$FL_4nM_16hr >data$FL_2nM_16hr &
 data$FL_8nM_6hr >data$FL_8nM_12hr & data$FL_8nM_12hr
 >data$FL_8nM_16hr), ]

sixhour_like_fl<-sixhour_like_fl[order(sixhour_like_fl
 $FL_0nM_6hr/sixhour_like_fl $FL_8nM_6hr ), ]
sixhour_like_fl <-tail(sixhour_like_fl, 100)
sixhour_like_fl <-as.character(sixhour_like_fl $gene_name)
as.data.frame(sixhour_like_fl)

#sixhour_like_fl codes for A) induction by Shh at all
 concentrations and times B) a graded response at 12 hours and 16
 hours and C) that values at 6hr (2nM, 4nM and 8nM) are higher
 than at 12 or 16hr (2nM, 4nM and 8nM), D) ordered by greatest
 induction at 8nM_6hr to 0nM_6hr


GREM1_LIKE_FL

data<-read.csv("data_+1_allcells_anova.csv")
data<- subset (data, fl_sum>24)
grem1_like_fl <- data[which (data$FL_2nM_6hr >data$FL_0nM_6hr &
 data$FL_2nM_6hr >data$FL_4nM_6hr & data$FL_2nM_6hr
 >data$FL_8nM_6hr & data$FL_2nM_12hr >data$FL_0nM_12hr &
 data$FL_2nM_12hr >data$FL_4nM_12hr & data$FL_2nM_12hr
 >data$FL_8nM_12hr & data$FL_2nM_16hr >data$FL_0nM_16hr &
 data$FL_2nM_16hr >data$FL_4nM_16hr & data$FL_2nM_16hr
```

```
>data$FL_8nM_16hr & data$FL_2nM_12hr >data$FL_2nM_6hr &
data$FL_4nM_12hr >data$FL_4nM_6hr), ]

grem1_like_fl<-grem1_like_fl[order(grem1_like_fl
$FL_0nM_12hr/grem1_like_fl $FL_2nM_12hr ), ]
grem1_like_fl <-as.character(grem1_like_fl $gene_name)
as.data.frame(grem1_like_fl)

#grem1_like codes for A) 2nM highest at all time points B)
Ordered on 2nM_12hr over 0nm_12hr


ALX4_LIKE_FL

data<-read.csv("data_+1_allcells_anova.csv")
data<- subset (data, fl_sum>24)
alx4_like_fl <- data[which(data$FL_0nM_12hr >data$FL_2nM_12hr &
data$FL_0nM_12hr >data$FL_4nM_12hr & data$FL_0nM_12hr
>data$FL_8nM_12hr & data$FL_2nM_12hr >data$FL_4nM_12hr &
data$FL_2nM_12hr >data$FL_8nM_12hr & data$FL_0nM_16hr
>data$FL_2nM_16hr & data$FL_0nM_16hr >data$FL_4nM_16hr &
data$FL_0nM_16hr >data$FL_8nM_16hr & data$FL_2nM_16hr
>data$FL_4nM_16hr & data$FL_2nM_16hr >data$FL_8nM_16hr &
data$FL_4nM_16hr >data$FL_8nM_16hr), ]

alx4_like_fl<-
alx4_like_fl[order(alx4_like_fl$FL_8nM_16hr/alx4_like_fl$FL_0nM_
16hr ), ]
alx4_like_fl<-head(alx4_like_fl, 100)
alx4_like_fl <-as.character(alx4_like_fl $gene_name)
as.data.frame(alx4_like_fl)

#alx4_like codes for A) 0nM highest at 12 hr and 16 hr, B) that
2nM is second highest at 12 hr C) that a reverse graded response
is observed at 16 hours


#################################################################
###############
HINDLIMB
#################################################################
###############

PTCH1_LIKE_HL

data<-read.csv("data_+1_allcells_anova.csv")
data<- subset (data, hl_sum>24)
ptch1_like_hl<- subset (data, data$HL_2nM_6hr >data$HL_0nM_6hr &
data$HL_4nM_6hr >data$HL_0nM_6hr & data$HL_8nM_6hr
>data$HL_0nM_6hr  & data$HL_2nM_12hr >data$HL_0nM_12hr &
data$HL_4nM_12hr >data$HL_0nM_12hr & data$HL_8nM_12hr
```

```
 >data$HL_0nM_12hr  & data$HL_2nM_16hr >data$HL_0nM_16hr &
 data$HL_4nM_16hr >data$HL_0nM_16hr & data$HL_8nM_16hr
 >data$HL_0nM_16hr & data$HL_8nM_16hr >data$HL_4nM_16hr &
 data$HL_4nM_16hr >data$HL_2nM_16hr & data$HL_8nM_12hr
 >data$HL_4nM_12hr & data$HL_8nM_12hr >data$HL_2nM_12hr &
 data$HL_2nM_16hr <data$HL_2nM_12hr & data$HL_4nM_16hr
 <data$HL_4nM_12hr & data$HL_8nM_16hr <data$HL_8nM_12hr &
 data$HL_8nM_12hr > data$HL_8nM_6hr & data$HL_4nM_12hr >
 data$HL_4nM_6hr & data$HL_2nM_12hr > data$HL_2nM_6hr)

ptch1_like_hl <-ptch1_like_hl[order(ptch1_like_hl
 $HL_0nM_16hr/ptch1_like_hl $HL_8nM_16hr ), ]
ptch1_like_hl <-head(ptch1_like_hl, 100)
ptch1_like_hl <-as.character(ptch1_like_hl $gene_name)
as.data.frame(ptch1_like_hl)

#ptch1_like_hl codes for A) induction by Shh at all
 concentrations and times.  B) to be graded at 16hr, C) for there
 to be accumulation at all concs betwen 6hr and 12 hrs D)for
 desensitisation between 12hr to 16hr in 2,4 and 8nM E) for
 partial gradation (8nM greater than 4nM or 2nM) by 12 hours and
 F) Ordered on greatest induction by 8nM at 16hr


HOXD13_LIKE_HL

data<-read.csv("data_+1_allcells_anova.csv")
data<- subset (data, hl_sum>24)
hoxd13_like_hl<- subset (data, data$HL_4nM_6hr >data$HL_0nM_6hr &
 data$HL_8nM_6hr >data$HL_0nM_6hr  & data$HL_2nM_12hr
 >data$HL_0nM_12hr & data$HL_4nM_12hr >data$HL_0nM_12hr &
 data$HL_8nM_12hr >data$HL_0nM_12hr  & data$HL_2nM_16hr
 >data$HL_0nM_16hr & data$HL_4nM_16hr >data$HL_0nM_16hr &
 data$HL_8nM_16hr >data$HL_0nM_16hr & data$HL_8nM_16hr
 >data$HL_4nM_16hr & data$HL_4nM_16hr >data$HL_2nM_16hr &
 data$HL_2nM_16hr<data$HL_2nM_12hr & data$HL_8nM_16hr >
 data$HL_8nM_6hr  & data$HL_4nM_16hr > data$HL_4nM_6hr &
 data$HL_8nM_12hr >data$HL_4nM_12hr & data$HL_8nM_12hr
 >data$HL_2nM_12hr)

hoxd13_like_hl <-
 hoxd13_like_hl[order(hoxd13_like_hl$HL_0nM_16hr/hoxd13_like_hl$H
 L_8nM_16hr ), ]
hoxd13_like_hl <-as.character(hoxd13_like_hl $gene_name)
hoxd13_like_hl <-head(hoxd13_like_hl, 100)
as.data.frame(hoxd13_like_hl)

#hoxd_like_hl codes for A) induction by Shh at all concentrations
 and times. B) For a graded response at 16h C) for
 desensitisation in 2nM between 12hr and 16hr D) accumulation
 from 8nM/4nM_6hr to 8nM/4nM_16hr E) 8nM is highest at 12hr
```

FOXC2_LIKE_HL

```
data<-read.csv("data_+1_allcells_anova.csv")
data<- subset (data, hl_sum>24)
foxc2_like_hl<- data[which(data$HL_2nM_6hr >data$HL_0nM_6hr &
 data$HL_4nM_6hr >data$HL_0nM_6hr & data$HL_8nM_6hr
 >data$HL_0nM_6hr  & data$HL_2nM_12hr >data$HL_0nM_12hr &
 data$HL_4nM_12hr >data$HL_0nM_12hr & data$HL_8nM_12hr
 >data$HL_0nM_12hr & data$HL_2nM_16hr >data$HL_0nM_16hr &
 data$HL_4nM_16hr >data$HL_0nM_16hr & data$HL_8nM_16hr
 >data$HL_0nM_16hr & data$HL_8nM_12hr >data$HL_4nM_12hr &
 data$HL_4nM_12hr >data$HL_2nM_12hr & data$HL_8nM_16hr
 >data$HL_4nM_16hr & data$HL_8nM_16hr >data$HL_2nM_16hr &
 data$HL_8nM_12hr >data$HL_8nM_16hr & data$HL_4nM_12hr
 >data$HL_4nM_16hr & data$HL_2nM_12hr >data$HL_2nM_16hr), ]

foxc2_like_hl<-
 foxc2_like_hl[order(foxc2_like_hl$HL_0nM_12hr/foxc2_like_hl$HL_8
 nM_12hr ), ]
foxc2_like_hl<-tail(foxc2_like_hl, 100)
foxc2_like_hl <-as.character(foxc2_like_hl $gene_name)
as.data.frame(foxc2_like_hl)

#Foxc2_like_hl codes for A) induction by Shh at all
 concentrations and times B) a partial graded response at 12
 hours and fully at 16 hours and C) that values at 12hr (2nM, 4nM
 and 8nM) are higher than at 16hr (2nM, 4nM and 8nM)
```

SMOC1_LIKE_HL

```
data<-read.csv("data_+1_allcells_anova.csv")
data<- subset (data, hl_sum>24)
smoc1_like_hl<- data[which(data$HL_2nM_6hr >data$HL_0nM_6hr &
 data$HL_4nM_6hr >data$HL_0nM_6hr & data$HL_8nM_6hr
 >data$HL_0nM_6hr  & data$HL_2nM_12hr >data$HL_0nM_12hr &
 data$HL_4nM_12hr >data$HL_0nM_12hr & data$HL_8nM_12hr
 >data$HL_0nM_12hr & data$HL_2nM_16hr >data$HL_0nM_16hr &
 data$HL_4nM_16hr >data$HL_0nM_16hr & data$HL_8nM_16hr
 >data$HL_0nM_16hr & data$HL_4nM_12hr >data$HL_8nM_12hr &
 data$HL_4nM_12hr >data$HL_2nM_12hr & data$HL_4nM_16hr
 >data$HL_8nM_16hr & data$HL_4nM_16hr >data$HL_2nM_16hr), ]

smoc1_like_hl <-
 smoc1_like_hl[order(smoc1_like_hl$HL_0nM_16hr/smoc1_like_hl$HL_4
 nM_16hr ), ]
smoc1_like_hl <-head(smoc1_like_hl, 100)
smoc1_like_hl <-as.character(smoc1_like_hl $gene_name)
```

```
as.data.frame(smoc1_like_hl)

#smoc1_like_fl codes for A) induction by Shh at all
 concentrations and times, B) 4nM shows the peak response at 12hr
 and 16hr C) ordered by greatest induction 4nM_16h to 0nM_16hr


TWO_NM_PEAK_HL

data<-read.csv("data_+1_allcells_anova.csv")
data<- subset (data, hl_sum>24)
twonm_like_hl<- data[which(data$HL_2nM_6hr >data$HL_0nM_6hr &
 data$HL_4nM_6hr >data$HL_0nM_6hr & data$HL_8nM_6hr
 >data$HL_0nM_6hr  & data$HL_2nM_12hr >data$HL_0nM_12hr &
 data$HL_4nM_12hr >data$HL_0nM_12hr & data$HL_8nM_12hr
 >data$HL_0nM_12hr & data$HL_2nM_16hr >data$HL_0nM_16hr &
 data$HL_4nM_16hr >data$HL_0nM_16hr & data$HL_8nM_16hr
 >data$HL_0nM_16hr & data$HL_2nM_12hr >data$HL_4nM_12hr &
 data$HL_2nM_12hr >data$HL_8nM_12hr & data$HL_2nM_16hr
 >data$HL_4nM_16hr & data$HL_2nM_12hr >data$HL_8nM_16hr), ]

twonm_like_hl <-twonm_like_hl[order(twonm_like_hl
 $HL_0nM_16hr/twonm_like_hl $HL_2nM_16hr ), ]
twonm_like_hl <-as.character(twonm_like_hl$gene_name)
as.data.frame(twonm_like_hl)

#twonm_like_fl codes for A) induction by Shh at all
 concentrations and times, B) 2nM highest at 12hr and 16hr C)
 ordered on greatest induction by 2nM at 16hr


SIX_HOUR_LIKE_HL

data<-read.csv("data_+1_allcells_anova.csv")
data<- subset (data, hl_sum>24)
sixhour_like_hl<- data[which(data$HL_2nM_6hr >data$HL_0nM_6hr &
 data$HL_4nM_6hr >data$HL_0nM_6hr & data$HL_8nM_6hr
 >data$HL_0nM_6hr  & data$HL_2nM_12hr >data$HL_0nM_12hr &
 data$HL_4nM_12hr >data$HL_0nM_12hr & data$HL_8nM_12hr
 >data$HL_0nM_12hr & data$HL_2nM_16hr >data$HL_0nM_16hr &
 data$HL_4nM_16hr >data$HL_0nM_16hr & data$HL_8nM_16hr
 >data$HL_0nM_16hr & data$HL_8nM_12hr >data$HL_4nM_12hr &
 data$HL_4nM_12hr >data$HL_2nM_12hr & data$HL_8nM_16hr
 >data$HL_4nM_16hr & data$HL_4nM_16hr >data$HL_2nM_16hr &
 data$HL_8nM_6hr >data$HL_8nM_12hr & data$HL_8nM_12hr
 >data$HL_8nM_16hr), ]

sixhour_like_hl<-sixhour_like_hl[order(sixhour_like_hl
 $HL_0nM_6hr/sixhour_like_hl $HL_8nM_6hr ), ]
sixhour_like_hl <-tail(sixhour_like_hl, 100)
sixhour_like_hl <-as.character(sixhour_like_hl $gene_name)
```

```
as.data.frame(sixhour_like_hl)

#sixhour_like_fl codes for A) induction by Shh at all
 concentrations and times B) a graded response at 12 hours and 16
 hours and C) that values at 6hr (2nM, 4nM and 8nM) are higher
 than at 12 or 16hr (2nM, 4nM and 8nM), D) ordered by greatest
 induction at 8nM_6hr to 0nM_6hr


GREM1_LIKE_HL

data<-read.csv("data_+1_allcells_anova.csv")
data<- subset (data, fl_sum>24)
grem1_like_hl <- data[which (data$HL_2nM_6hr >data$HL_0nM_6hr &
 data$HL_2nM_12hr >data$HL_0nM_12hr & data$HL_2nM_12hr
 >data$HL_4nM_12hr & data$HL_2nM_12hr >data$HL_8nM_12hr &
 data$HL_2nM_16hr >data$HL_0nM_16hr & data$HL_2nM_16hr
 >data$HL_4nM_16hr & data$HL_2nM_16hr >data$HL_8nM_16hr &
 data$HL_4nM_16hr >data$HL_8nM_16hr & data$HL_4nM_16hr
 >data$HL_0nM_16hr & data$HL_4nM_12hr >data$HL_8nM_12hr &
 data$HL_4nM_12hr >data$HL_0nM_12hr & data$HL_2nM_12hr
 >data$HL_2nM_6hr), ]

grem1_like_hl<-grem1_like_hl[order(grem1_like_hl
 $HL_0nM_16hr/grem1_like_hl $HL_2nM_16hr ), ]
grem1_like_hl <-as.character(grem1_like_hl $gene_name)
as.data.frame(grem1_like_hl)

#grem1_like codes for A) 2nM highest at 12hr and 16hr B) 4nM
 second highest at 16hr C) 2nM 12hr higher than 2nM 6hr D)
 Ordered on 2nM_16hr over 0nm_16hr


ALX4_LIKE_HL

data<-read.csv("data_+1_allcells_anova.csv")
data<- subset (data, fl_sum>24)
alx4_like_hl <- data[which(data$HL_0nM_12hr >data$HL_2nM_12hr &
 data$HL_0nM_12hr >data$HL_4nM_12hr & data$HL_0nM_12hr
 >data$HL_8nM_12hr & data$HL_2nM_12hr >data$HL_4nM_12hr &
 data$HL_2nM_12hr >data$HL_8nM_12hr & data$HL_0nM_16hr
 >data$HL_2nM_16hr & data$HL_0nM_16hr >data$HL_4nM_16hr &
 data$HL_0nM_16hr >data$HL_8nM_16hr & data$HL_2nM_16hr
 >data$HL_4nM_16hr & data$HL_2nM_16hr >data$HL_8nM_16hr &
 data$HL_4nM_16hr >data$HL_8nM_16hr), ]

alx4_like_hl<-
 alx4_like_hl[order(alx4_like_hl$HL_8nM_16hr/alx4_like_hl$HL_0nM_
 16hr ), ]
alx4_like_hl<-head(alx4_like_hl, 100)
alx4_like_hl <-as.character(alx4_like_hl $gene_name)
```

```
as.data.frame(alx4_like_hl)

#alx4_like codes for A) 0nM highest at 12 hr and 16 hr, B) that
 2nM is second highest at 12 hr C) that a reverse graded response
 is observed at 16 hours



#####################################################################
 ###############
GRAPH TEMPLATE
#####################################################################
 ###############

data<-read.csv("data_+1_allcells_anova.csv")

x<-c(0, 6, 12, 16)
zero<- c(3,4,8,12)
two<-c(3,5,9,13)
four<-c(3,6,10,14)
eight <-c(3,7,11,15)

k<-6258
y1<-data[k, zero]
y2<-data[k, two]
y3<-data[k, four]
y4<-data[k, eight]


plot(x,y1, type= "o", main="Dlx5", font.main=4, col="black",
 xlab= "Time (hours)", ylab="Normalised read counts", pch=16,
 ylim=c(0,250), lwd=2.5)
lines(x,y2, type= "o",col="red", pch=15, lwd=2.5)
lines(x,y3, type= "o",col="139", pch=17, lwd=2.5)
lines(x,y4, type= "o",col="blue", pch=15, lwd=2.5)

legend(0,250, c("0nM", "2nM", "4nM", "8nM"), lty=c(1,1,1,1),
 lwd=c(2.5,2.5,2.5,2.5), col=c("black", "red", "139", "blue"),
 pch= c(16,15,17,15))
```